Stony Brook University

Tumors as Wounds that Never Heal:

Signaling Modalities Governing Lung Epithelial Repair and Tumor Heterogeneity

A Dissertation Presented

By

Matthew Camiolo

to

The Graduate School

in Partial Fulfillment of the

Requirements

for the Degree of

Doctor of Philosophy

in

Genetics

Stony Brook University

August 2012

Stony Brook University

The Graduate School

Matthew Joseph Camiolo

We, the dissertation committee for the above candidate for the

Doctor of Philosophy degree, hereby recommend

acceptance of this dissertation.

Raffaella Sordella
Associate Professor, Cold Spring Harbor Laboratory

Scott Lowe
Professor, Cancer Biology & Genetics Program, Sloan Kettering Insititute

Linda Van Aelst
Professor, Cold Spring Harbor Laboratory

Markus Seeliger
Assistant Professor, Department of Pharmacology, Stony Brook University

Andrew Jess Dannenberg

Henry R. Erle, MD-Roberts Family Professor of Medicine, Weill Cornell Medical College

This dissertation is accepted by the Graduate School

Charles Taber
Interim Dean of the Graduate School

Abstract of the Dissertation

Tumors as Wounds that Never Heal:

Signaling Modalities Governing Lung Epithelial Repair and Tumor Heterogeneityby

Matthew Joseph Camiolo

Doctor of Philosophy

in

Genetics

Stony Brook University

2012

The attrition of cells within organs necessitates replenishment from tissue resident progenitor populations. Study of the murine lung has suggested a number of niches present at different levels of the airways along the proximal-distal axis responsible for steady state epithelial turnover as well as response to catastrophic injury. Within the distal most bronchiole airspaces, injury resistant cells termed bronchioalveolar stem cells (BASCs) have been reported to reside at the bronchioalveolar duct junction (BADJ).

Since the initial reporting of BASCs, controversy over their true nature has confounded progress towards useful application of insights from their biology towards new therapeutic modalities. We report that additional stratification of the Sca-1+, Pecam-, CD45- lung population with the surface marker CD24 yields to the identification of BASC cells in multiple cell populations. Among them, CD24high cells possess characteristics of stem/progenitor cells. Not only do these cells express molecular markers associated with embryonic pluripotency, but harbor self-renewal capacity and the potential to differentiate into multiple bronchial epithelium cell components when orthotopically transplanted in recipient mice.

Transcriptional analysis of this cell population revealed activation of specific signaling pathways and the expression of distinct surface markers that unlike Sca-1 have human ortholog, thereby making them potentially useful in a clinical setting. We confirmed the serotonin receptor isoform 2B (HTR2B) was highly expressed and HTR2B axis components to be activated after naphthalene induced Clara cell ablation. Chemical inhibition of HTR2B manifests as a reduction in mitotic cells after injury and a deficit in re-epitheliazation. Hence, HTR2B signaling is a novel component of the intricate signaling network regulating the homeostasis of bronchial epithelial progenitor of the distal airway. In principle, deregulation of HTR2B might be involved in the promotion of pathological conditions such as COPD, idiopathic fibrosis and NSCLC.

Table of Contents

Table of Figures

Acknowledgements

The work that follows would not be possible without the support of my family and friends. For the countless times they've picked me up over the past four years, these pages are dedicated to my parents, my sister and to Nilgun.

My time at Cold Spring Harbor has been challenging and rewarding, and I owe the experience to my advisor, Raffaella. She is never afraid to try new ideas and finds inspiration from every facet of biology. She once told me I have to be more precise, and she was right. But my favorite advice from her: science should be fun. If a marrow derived lung cancer ever shows up, I'll be back at the Blackford bar to collect my beer.

Chapters 3 and 4 feature work done in collaboration with my labmates: Trine Lindsted performed the careful analysis of mir335 expression and regulation in countless cell lines, Zhan Yao serendipitously discovered (and then diligently characterized) p53Ψ, and Serif Senturk provided the final push needed to bring the story to conclusion. I owe them all a debt of gratitude. It has been a pleasure to work together with such talented people.

I would like to thank my thesis committee members for making time in their schedule to offer help and guidance: Scott Lowe, who selflessly agreed to chair, Linda Van Aelst, who has been there countless times for conversation in the hallways of Demerec, Andrew Dannenberg, who generously agreed to take part, and Markus Seeliger, who stepped in on short notice to provide support and advice.

I would also like to thank Kate Bell and Turhan Canli of the Stony Brook Genetics program and Carron Kaufman and Mike Frohman of the Medical Scientist Training Program for all their effort and patience.

My time here would not have been nearly as enjoyable without my Sordella labmates, past and present. I look forward to seeing them all again.

Much of my thesis relied on Cold Spring Harbor's shared resources, so I would be remiss not to thank Stephen Hearn for maintaining the microscopes and Pam Moody for keeping the flow cytometers running.

Finally, I would like to thank David Spector, who gave me my first opportunity to work at the lab, and was my first mentor in science. The lessons I learned while working with him are reflected in every figure of this dissertation.

Chapter 1

Introduction

Chapter 1: Introduction

The human body is composed of an almost staggering amount of diverse and highly specialized cell types that are arranged into functional units to form our various organ systems. During the actions of everyday life, our organs are exposed to noxious stimuli and gross insult that can result in tissue damage. To meet the challenges of normal attrition and to maintain proper function, whether it be a keratinocyte of the skin, a hepatocyte of the liver, or type I pneumocyte of the lung, these cellular components must be replenished every so often as the hazards of their "jobs" may render them unable to function at a suitable level. To ensure homeostasis is maintained, tissues must coordinate a wound healing process as well as activate resident cells capable of replenishing those lost to insult (Arwert, Hoste, & Watt, 2012). Because maintaining the correct number of differentiated cells with a certain tissue/organ is critical to ensuring proper function, dysfunction of homeostatic control mechanisms within progenitor populations underlie a vast array of pathologies (Chilosi, Poletti, & Rossi, 2012; C. F. Kim & Dirks, 2008). Gaining understanding of the biological processes that underlie compensatory growth and regeneration is thus of central importance and may potentially lead to development of novel therapeutics. This is particularly evident in the case of the lung.

Pathologies of the lung constitute a major source of morbidity and mortality worldwide (Hurd, 2000; Jemal et al., 2011; Punturieri, Szabo, Croxton, Shapiro, & Dubinett, 2009). While structures such as the colonic crypt and hair bulge enjoy a renaissance of scientific discovery, the biology underlying lung epithelium is still much less understood (Fuchs, 2009; L. Li & Clevers, 2010). The past decade has seen a number of advances in our understanding of lung progenitor biology, but there are still many unanswered questions (Weiss et al., 2011). As of yet, it is unknown whether a universal lung progenitor cell exists. Can we trace a single fate hierarchy from this progenitor down to the nearly 40 distinct lung resident cell types? Do multiple autonomous progenitor trees co-exist? If so, do they obey similar or divergent rules? In this chapter I will review current concepts salient to lung epithelial regeneration, spanning topics from general wound healing mechanisms to the biology of lung resident stem and progenitor cells, as well as signaling modalities thought to govern them. Lastly I will discuss how deregulation in these systems could lead to the development of pathologies such as fibrosis and cancer.

Before I progress deeper into these issues, however, I will first briefly overview the principles of lung anatomy and morphogenesis.

1.2 Lung Anatomy and Morphogensis

The conducting airways of the respiratory system consist of the naso- and oro- pharynx, larynx, trachea, bronchii and terminal bronchioles (Armstrong & Netterville, 1995). No gas exchange occurs within these structures. The trachea divides at the carina into the right and left mainstem bronchi, which branch into lobar bronchi (three on the right, two on the left in humans), segmental bronchi, and then an extensive system of sub-segmental and smaller bronchi. These conducting airways will subdivide 15 to 20 times as they arborize out towards the level of terminal bronchioles, which are the smallest unit not participating in gas exchange (Warburton et al., 2010).

Beyond the terminal bronchioles, further divisions include the respiratory bronchioles, alveolar ducts and alveoli. Portions of the lung from the respiratory bronchiole on participate in gas exchange, allowing oxygen to enter capillary beds and carbon dioxide to exit. These structures are termed the respiratory unit, or acinus. The massively parallel network of acini create a tremendous surface for gas exchange—the average human possesses close to 70 square meters of alveolar surface, comprised of 300 million respiratory units (Scarpelli, 2003).

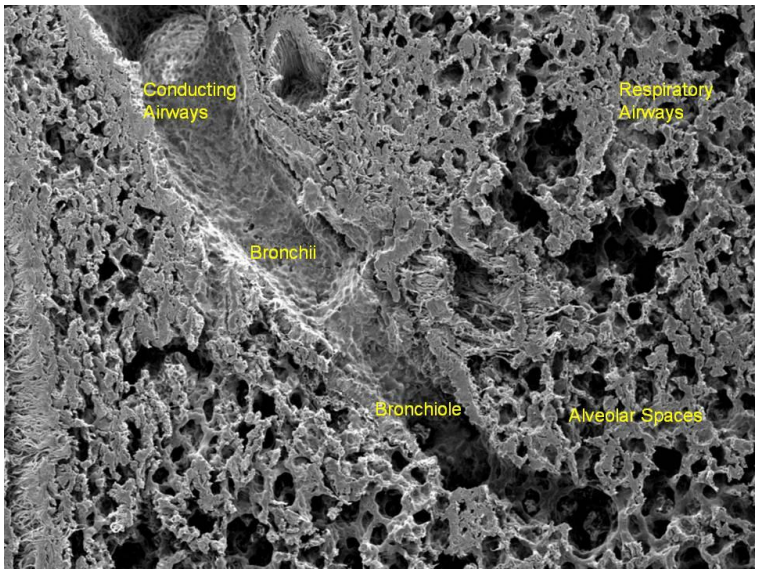

Figure 1.1 Topology of the Lung. SEM of the mouse lung illustrates branching of the respiratory tree. Gas is carried through the bronchii and bronchioles of the conducting airways into terminal respiratory units of alveoli and respiratory bronchioles.

At the cellular level, a great amount of heterogeneity comprising over 40 different cell types is seen between the different lung compartments (Sorokin, 1970). The large conducting airways are lined by pseudostratified columnar epithelium comprised of four basic cell types: ciliated, goblet, brush and basal. Interspersed among these cells are secretory cells that express Clara cell secretory protein (CCSP, CC10) (Reynolds & Malkinson, 2010).

At the level of the terminal bronchiole, the epithelium takes on a simple columnar morphology, lacks mucus producing goblet cells and is predominantly composed of ciliated cells (Stripp, 2008). As we enter the respiratory unit, epithelial cells are now mostly simple cuboidal in morphology. Ciliated and non-ciliated Clara cells predominate in this region. Although the Clara cells of this region display certain common features to those of the upper respiratory tract, lineage tracing analysis has indicated that the two do not originate from a common ancestor (Reynolds & Malkinson, 2010). This region transitions towards the alveolar airspaces that are composed of type I pneumocytes of squamous morphology that form the inner lining of the saccuole and type II pneumocytes that reside adjacent to capillaries within alveolar septae. A significant amount of the cellularity of the lung at this level can be attributed to capillary endothelial cells as well as tissue resident leukocytes (Schaible, Schaffer, & Taylor, 2010; T. Stevens, 2011).

Development of the respiratory tree begins around 9.5 days post coitum (dpc) when the lung primordium arises from the ventral foregut endoderm as a primitive trachea and two primary buds (Morrisey & Hogan, 2010). Commitment to the lung lineage is dependent upon expression of thyroid transcription factor 1 (Ttf1 or Nkx2.1 in humans). Ttf1 null mice form highly abnormal lungs comprised of airway epithelium that express no markers of lung cell fate (Minoo, Su, Drum, Bringas, & Kimura, 1999). At 10.5 dpc, lateral branching of the primary buds gives rise to five secondary buds; four on the right side, which will become the lobes of the mature right lung, and one on the left (Cardoso & Lü, 2006). This process varies between species—humans have three lobes on the right and two on the left. As morphogenesis continues, the airways undergo dichotomous branching at the tip of each duct, causing a rapid and dramatic increase in lung epithelium. This process does not appear to differ between individuals, indicating a hardwired, genetic program (Morrisey & Hogan, 2010).

Crucial to the progression of branching are reciprocal interactions between the emerging epithelium and the underlying mesenchyme. The fibroblast growth factor (FGF), Hedgehog (Hh), wingless (Wnt) and transforming growth factor-beta (TGF-β) pathways have all been identified as key mediators of the process (Shu et al., 2005).

Patterning beyond secondary branching appears to be governed by TGF-β, Wnt, platelet derived growth factor (PDGF) and epidermal growth factor (EGF) as demonstrated by genetic ablation and/or overexpression experiments (Ramasamy et al., 2007). Studies using vitamin A deficient animal models have shown that deficit in retinoic acid disrupts Fgf 10 and TGF-β signaling, resulting in lung agenesis (F. Chen et al., 2007). The transcriptional networks underlying alveolarization and sacculation of the

developing epithelium include those governed by NfatC3, Nf-, C/EBPα, Foxa2, Etv5 and Gata6 (Maeda, Davé, & Whitsett, 2007). These have each been shown to control differentiation of alveolar epithelium and are critical for normal formation of the alveolar region as well as surfactant production, which lowers airway surface tension preventing spontaneous collapse. Pulmonary vasculogenesis has been shown to be dependent on expression of Foxf1 in the splanchnic mesenchyme and is governed by paracrine signaling from respiratory epithelium, which directs nascent precursor cells into the lung (Kalinichenko et al., 2001).

1.3 Wound Healing

Catastrophic insult to a tissue or organ can result in perturbations of homeostasis that require active intervention to correct. In these instances, effective surveillance and rapid resolution of tissue damage became tantamount to survival. Among the most important components of this processes are: hemostasis, inflammation, cellular migration and proliferation of fibroblasts and endothelial cells, wound contraction, and remodeling (Monaco & Lawrence, 2003).

Figure 1.2 Schematic of Wound Healing Progression

1.3.1 Hemostasis

One critical yet often forgotten component of the healing process is hemostasis, as tissue repair may not proceed until the discontinuation of bleeding and blood vessel integrity is returned. This is accomplished by vasoconstriction of nearby arterioles to limit hydrostatic pressure, and by the formation of a clot through platelet aggregation and fibrin deposition (Lawrence, 1998). This early provisional wound matrix prevents fluid loss, limits contamination from the outside environment, and

provides a scaffold for fibroblasts, leukocytes and other critical cellular components that contribute later on to the tissue repair.

To initiate the process of clot formation (primary hemostasis), platelets adhere to the damaged sub-endothelial cell layer as well as Von Willebrand factor (VWF) and collagen I of exposed basement membranes to form a platelet plug (Sumitran-Holgersson & Holgersson, 2001). Primary hemostasis is then followed by degranulation in which dense bodies and lysosomes from the cytosol, called alpha granules, are expelled from activated platelets. This process introduces a number of cytokines and signaling molecules into the local environment, including adenosine diphosphate (ADP), serotonin (5HT), thromboxane A2, transforming growth factor-beta (TGF-β), plasma-derived growth factor (PDGF), fibroblast growth factor-2 (FGF-2) and vascular endothelial growth factor (VEGF) (Costa, 1977). This elicits a self-propagating forward feedback loop that ensures sufficient platelets are recruited to the site of injury to mitigate vessel patency and the transformation of the nascent extracellular matrix (ECM) to a more rigid and structurally sound form. This later process, known as secondary hemostasis, involves the enzymatic conversion of fibrinogen that has been secreted by the degranulated platelets to fibrin by the serine protease thrombin (Stiernberg, Redin, Warner, & Carney, 1993). Thrombin is produced in its active form through cleavage by serum derived clotting factors that themselves are activated by exposure to damaged tissue. The polymerized fibrin clot works as a nucleation factor, becoming coated with serum and platelet derived vitronectin, itself facilitating fibronectin accumulation. While fibrin supplies structural rigidity, the fibronectin via numerous cellular interaction domains facilitates adhesion of cells and cellularization of the clot (Grinnell, 1984). Additionally, the fibrin-fibronecting matrix serves to trap cytokines that play integral roles in signaling throughout the healing (Blatti, Foster, Ranganathan, Moses, & Getz, 1988).

1.3.2 Inflammation

During the degranulation process, activated thrombin and secreted signaling molecules such as histamine, kinins and prostaglandins act in concert with the complement system, a series of proteins involved in innate immunity, to cause capillary leak in areas proximal to the wound and to facilitate leukocyte extravasation (Vestweber, 2012). This increase in vascular permeability, as well as the expression of key molecules on endothelial cells, creates a permissive environment for the migration of inflammatory cells. Immune cells are attracted to a site of injury via numerous signaling modalities, including collagen and elastin breakdown products, complement factors, cytokines such as TGF-β,

interleukin-1 (Il-1), PDGF, leukotriene B4 and tumor necrosis factor alpha (TNF-α) (Bhatia, Zemans, & Jeyaseelan, 2012).

1.3.3 Margination

Margination, or invasion of tissue by migrating white blood cells, is accomplished through rolling along the endothelial surfaces of the neighboring post-capillary venuoles via attachment to p-selectin and e-selectin present on the membranes of these cells (Almaraz, Mathew, Tan, & Yarema, 2012). This process allows for localized homing of circulating immune cells and is mediated by cytokine activation of the endothelium. Once slowed by the rolling process, leukocytes utilize interaction with specific integrins to facilitate tissue entry via a process known as diapedesis. The early vasoconstriction gives way to vasodilation caused by leukotrienes, prostaglandins and histamine acting on endothelial cells and causing remodeling of cell-cell adhesions (Ando & Kamiya, 1993). Within the first 48 hours, the earliest leukocytes to arrive are typically neutrophils and monocytes. The latter will then transform to become macrophages—a process mediated by factors within the ECM such as fibronectin (Burgess, 2009).

One of the functions of leukocyte invasion is to provide a means to eliminate dying cells as well as damaged ECM. Indeed, these early arrivals at the scene of injury are responsible for wound debridement via phagocytosis of debris. The ability to do so is entirely contingent upon activation via paracrine stimulation through Il-2 and interferon-γ (INF-γ) (Adamson, 2009). Additionally, macrophages are also responsible for tissue breakdown via the secretion of matrix metalloproteinases (MMPs) such as collagenase and elastase (Belvisi & Bottomley, 2003). Yet, the role of macrophages in wound resolution is much more complex and extends to numerous other processes including angiogenesis, fibroblast migration and proliferation, collagen production and immunomodulation via secretion of cytokines (Murray & Wynn, 2011).

As the wound matures, lymphoid cells will come to supplant myeloid cells as the most numerous cellular component of the immune response. Both CD4+ T-helper cells and CD8+ cytotoxic T-cells peak in concentration between 5 and 7 days post-injury (Nielson, Phillips, & Jimenez, 1982). Macrophages and lymphocytes persist until around 7 days after damage induction, at which point they will gradually diminish in number. This is, of course, provided that cues for chronic inflammation are absent and any persistent stimuli can be encapsulated in a sort of physiologic cellular quarantine. This process, known

as the foreign body response, is mediated by fibroblast recruitment, TGF-β signaling and interaction with T-cells (Murray & Wynn, 2011).

1.3.4 Fibroblasts and Endothelial Migration

As the inflammatory phase continues toward conclusion, the next stage of wound healing will be carried out predominantly by fibroblasts and endothelial cells. For "activated" fibroblasts, migration towards the site of the wound is accomplished via travel along integrin molecules, which are in turn induced by the very cytokines that are chemotactic for these cells—PDGF, EGF, fibronectin and TGF-β (Albini, Adelmann-Grill, & Muller, 1985). There is also evidence that tenascin C deposition at the margin of the wound provides cues for migrating fibroblasts as to the whereabouts of the injury (Mackie, Halfter, & Liverani, 1988). Once at the proper location, PDGF, TGF-β and insulin-like growth factor (IGF) act in concert to stimulate fibroblast proliferation (Cho, Lin, & Genco, 1995).

Fibroblasts that have migrated into the wound are responsible for the *de novo* synthesis of proteins meant to contribute mechanical strength and facilitate closure. As wound healing progresses, synthesis of collagen, which comprises more than 50% of the protein in scar tissue, as well as other constituents of the evolving matrix becomes an important facet of the process (Nimni, 1974). Protein synthesis and deposition occurs 4 to 5 days after injury and continues at maximal rate for 2 to 4 weeks before slowing and ceasing (Monaco & Lawrence, 2003). During this time, secreted procollagen molecules are cleaved by extracellular procollagen proteinases in a process that decreases solubility and facilitates fibril formation via electrostatic interactions (Veis & Anesey, 1965). The enzyme lysyl oxidase creates covalent cross-linking between adjacent fibrils, thus stabilizing them and increasing the rigidity of the tissue (Xiao & Ge, 2012). Other ECM components of note within the evolving scar include dermatan sulfate, a proteoglycan that helps orient collagen to facilitate fibril formation, and hyaluronan, a contributor of elasticity and modulator of cell migration (Plichta & Radek, 2012).

Occurring concomitantly with the synthesis and deposition of new matrix proteins is the contraction of the scar tissue. This is carried out by fibroblasts within the scar tissue as well as myofibroblasts located at the wounds periphery (Phan, 2012). These cells typically appear between 4 and 6 days after injury, persist for several weeks and are noted for possessing smooth muscle actin rich filaments in the cytoplasm and multi-lobulated nuclei. Proper wound healing resolves with the

clearance of myofibroblasts, and persistence of these cells is a sign of fibrotic change within the damaged tissue (Willis & Borok, 2007).

Several cues within the microenvironment of a wound—including elevated lactate levels, acidic pH and decreased oxygen tension—create an impetus for neo-vascularization by way of angiogenesis (Otrock, Mahfouz, Makarem, & Shamseddine, 2007). This process involves the sprouting off of new capillaries from existing vessels that will invade the fibrin-fibronectin matrix created during clotting via binding of integrin domains in a manner similar to fibroblasts (Grinnell, 1984). The cytokines FGF-2 (with heparin as co-factor) and VEGF play critical roles in this process, which involves a proliferative component as well (Plouet, Schilling, & Gospodarowicz, 1989). As angiogenesis proceeds, cell migration is accomplished via MMP breakdown of ECM and eventually the new endothelial sprouts will meet to form interconnected capillaries (Papetti & Herman, 2002). The vascularization process leads to a decrease in local cytokine concentrations, which is thought to contribute to vessel maturation.

1.3.5 Re-Epitheliazation

During the early stages of wound healing, re-establishment of the barrier that limits interface between internal and external environments is crucial for preventing infection and restoring the milieu. This process of re-epitheliazation begins between 24 and 48 hours after injury depending on the size and extent of injury (Nanney, Magid, Stoscheck, & King, 1984). Epithelial cells at the margin of the wound will migrate across the denuded surface seeking to recreate continuity, while nearby progenitors will proliferate to contribute new cells to the emerging monolayer. Epithelial cell migration first requires the dissolution of desmosomes that link neighboring cells as well as the hemidesmosomes that tether them to the basement membrane before subsequent migration to the site of injury (Windoffer, Borchert-Stuhltrager, & Leube, 2002). This process is stimulated by a number of cytokines including epidermal growth factor (EGF), TGF-α, and keratinocyte growth factor (KGF) and it is dependent on the presence of intact basement membrane; should this structure be damaged, cells must regenerate it before continuing onward (Snyder, Zemke, & Stripp, 2009). Proliferation and migration over the surface of a wound reaches resolution with contact inhibition of the outgrowing monolayer (McClatchey & Yap, 2012). At this point, cell-cell adhesions are restored and focus now shifts towards restoring the physical and functional properties of normal epithelium.

1.3.6 Scar Remodeling

As a wound approaches three weeks in age, focus of cellular activities turns towards the active remodeling of the scar. This involves the down regulation of collagen synthesis, which is induced by interferon-γ and TNF-α signaling as well as by the collagen matrix itself (Varkey, Ding, & Tredget, 2011). The remodeling process focuses on restoring mechanical strength to the damaged area as well as normalizing ECM components to physiologic levels. This is highly dependent upon the action of MMPs as well as their inhibitors, the tissue inhibitors of metallo-proteinases (TIMPs), which regulate enzymatic activity and thus balance ECM turnover (Steffensen, Hakkinen, & Larjava, 2001).

1.4 Tissue Regeneration

The goal of wound repair process is to acutely respond to an injury that has caused a disruption in normal tissue physiology. Speed of response is crucially important, as restoration of barrier function is critical in protecting neighboring cells from the external environment. This process is distinct from true tissue regeneration, which instead involves complete morphological and functional restoration of the initial tissue lost to insult (Eming, Hammerschmidt, Krieg, & Roers, 2009). While such repair processes are common in amphibians, mammalian organisms seem to have limited capacity for true tissue regeneration (Brockes & Kumar, 2008). Hence, during post-natal life, the reparative response in most mammalian animals results in scar formation with partial loss of organ function.

One possible explanation for the compromised ability to accomplish true tissue regeneration in mammalian animals is the strength and duration of the immune response (Godwin & Brockes, 2006). It has been demonstrated that the repair during early fetal life is fully regenerative and totally lacking inflammation (Colwell, Longaker, & Lorenz, 2003). Similar correlations have been drawn between tissue regeneration and immune regulation in Zebrafish, Salamander, and Xenopus model organisms. Yet paradoxically, depletion of macrophages in mammals or defects in leukocyte homing via abrogation of selectin binding on endothelial cells results in delayed wound healing (Nagaoka et al., 2000). Much work now focuses on interventions meant to reign in the immune response, with hope that decreasing inflammation without eliminating it completely will facilitate regrowth of functional tissue after injury.

At the opposite end of the spectrum from tissue regeneration is chronic inflammation—one of the most common and disabling of human diseases (Cottam et al., 2004; Grisham, Jourd'heuil, & Wink,

2000). It may occur as a result of persistent infection, prolonged exposure to toxic agents or foreign bodies, and in some cases, autoimmunity (Ueha, Shand Francis, & Matsushima, 2012). Chronic inflammation involves the persistence of lymphocyte-monocyte interactions as well as myofibroblasts that sustain the synthesis of growth factors (e.g. PDGF, FGF and TGF-β) and fibrogenic cytokines (e.g. TNF, Il-1, Il-4 and Il-13) while decreasing MMP activity (Phan, 2012). The net effect of these processes is the persistence of cytokine secretion and increase in collagen deposition that compromises proper organ function.

As mentioned earlier, for tissue regeneration to occur, proper restoration of morphological and physiological function must be accomplished through generation of cell mass that mirrors the phenotypic diversity of the pre-injured state. This task is complex and difficult; it requires acute wound resolution, proper wound remodeling, and the elaboration of a potential myriad different cell types all without compromise of surrounding normal tissue. This final point has been and remains an intensely researched topic. What are the cells that home to sites of injury and restore organ function? Are they locally or systemically derived? What is the threshold for triggering their action, and at what point will their regenerative capacity by overwhelmed? While many questions remain unanswered, studies of the cellular biology of tissue generation and regeneration have begun to shed light on these issues.

Cells of the embryionic epiblast are considered pluripotent due to their ability to contribute to all three germ layers: endoderm (interior stomach lining, gastrointestinal tract and lungs), mesoderm (muscle, bone, blood and urogenital system) and ectoderm (epidermal tissues and nervous system) (Evans, 2011). As these cells progress towards their terminally differentiated fates, they lose ability to form the full diversity of structures and become relegated in their fate to an increasingly narrow spectrum of cell types. Although evidence has suggested the persistence of immature cell types in the adult organism, it is not clear whether these cells are carryovers from fetal life or committed/differentiated cells that have acquired stem cells features (X. Wang et al., 2011).

The discovery of induced pluripotent stem cell (iPSC) reprogramming via expression of the transcription factors Oct4, Nanog, Klf-4 and c-Myc suggests the intriguing possibility that differentiated cells in adult tissues may be epigenetically reprogrammed and thus contribute to the generation of stem cell niches (Takahashi & Yamanaka, 2006). Yet, evidence of pluripotency in mammalian organisms remains controversial (Berg & Goodell, 2007; Kajstura et al., 2011; Lengner et al., 2007; Lengner, Welstead, & Jaenisch, 2008). Works utilizing markers of pluripotency, such as expression of pluripotency inducing transcription factors, have refuted the idea that such cells exist in the adult

organism (Lengner et al., 2007). Other studies, however, have detected expression of pluripotency markers in both tissue injury and tumors (Kajstura et al., 2011; X. Li et al., 2012; Santini et al., 2012). Intriguingly, evidence suggests that progenitor cells in a mature animal may lie closer to the pluripotent state than other cell types (J. B. Kim et al., 2008).

The cellular contribution of circulating cells to solid organs has been noted in both human transplantation surgery and animal models of injury and suggests a number of different niches may be responsible for maintaining tissues of the body in normal and pathologic states (Jones & Rankin, 2011; Krause, 2008; Lama et al., 2007). While much work is focused on identifying, characterizing and applying marrow derived, non-hematopoietic stem cells to human therapeutics, success has remained elusive.

1.5 Adult Tissue Progenitor/Stem Cells

1.5.1 General Concepts

In all organ systems of the body, differentiated cells are lost due to damage by exogenous agents as well as endogenously generated hazards and must be replenished. In order to accomplish this, adult stem cells are endowed with the ability to self-renew as well as give rise to differentiated progeny able to perform the daily tasks required for organ function.

The lifespan of specialized, terminally differentiated cells varies greatly between different tissues of the body. In general, however, it is possible to broadly group tissues into two classes based on basal rate of cellular turnover and response to injury (Stripp, 2008). The hematopoietic and gastrointestinal systems are classic examples of quickly regenerating systems. Within the small intestine and colon, for instance, epithelium is replaced every 5 days (van der Flier & Clevers, 2009). In addition to a high steady state turnover rate, both of these systems share similarity in their ability to respond to acute injury. Perturbations to epithelium are not typically associated with drastic increases in cycling cells. Although the hematopoietic system does possess the ability to adapt to insult, regeneration can become saturated in the face of dramatic blood loss .

Epithelial structures of foregut-derived organs, such as the thymus, pancreas, liver and lung, on the other hand, display different steady state kinetics with regard to turnover as a result of natural wear. These tissues show low levels of spontaneous proliferation during non-pathological conditions, with drastic change during acute injury (Fuchs, 2009). The duration of this heightened proliferative state

may vary depending on the magnitude and duration of injury, with chronic insult leading to the adaptation of a new steady state regenerative frequency (Snyder et al., 2009).

More recent studies of the "fast cycling" intestinal epithelium and hair follicle indicate the existence of multiple stem cell populations with different intrinsic cycling speeds (Barker, Bartfeld, & Clevers, 2010). The co-existence of fast and slow cycling multi-potent cells within structures historically noted for having high steady state turnover raises many interesting questions as what is the functional role of these different stem cell compartments. The presence of a reserve pool of quiescent stem cells would provide mechanism for increasing the longevity of adult tissue stem cells as well as protecting the organism from deleterious effects of constant progenitor cycling. By avoiding mitosis, long-lived stem cells would then be kept safe from accumulating potentially tumorigenic mutations during replication. In addition, the ability to replenish a niche would no longer require self-renewal at the single cell level. Interestingly, induction of Wnt signaling appears to be a conserved feature between fast cycling progenitors of these tissues, and the maintenance of a Wnt inhibitory microenvironment seems to be necessary to maintain quiescent cells in each these cases (L. Li & Clevers, 2010).

For a variety of reasons, stem cells of rapidly renewing organ systems have been thus far more amenable to study. This research has yielded the "classical" stem cell hierarchy, where a multi- or pluri-potent stem cell, capable of self-renewal, gives rise to a transit amplifying population that goes on to form the majority of the cellular mass. These transit amplifying cells will undergo a certain number of replications before reaching terminal differentiation, and along this course lose multi-potency and become lineage committed.

Much of the early work done to identify the cells that sit atop the hierarchy trees of cell fate within solid organs of the body took advantage of labeled nucleotide incorporation and retention within target cells (Raiser et al., 2008). These experiments were performed based on the assumption that stem cells possess the quality of relative quiescence, and as such would retain a nucleotide label while rapidly dividing cells would effectively dilute out signal via subsequent mitosis (Rawlins & Hogan, 2006). Histological examination of tissues after labeled nucleotide incorporation allows for anatomic description of prospective stem cell harboring structures without any further phenotypic data pertaining to the population.

The development of fluorescence assisted cell sorting (FACS) ushered in a wave of discovery to the stem cell field. This was particularly true for the hematopoietic system, where ease of preparation

facilitated sorting of cells for subsequent clonogenecity assay to identify immunophenotypes associated with increased colony forming capacity (Little & Storb, 2002). This work could then be validated using reconstitution experiments into lethally irradiated hosts to identify long term hematopoietic stem cells (Rossi, Challen, Sirin, Lin, & Goodell, 2011).

Study of tissues with lower rates of epithelial turnover have similarly employed label retention and sorting by immune-phenotypic characteristics. Unlike fast cycling organs, identifying stem or progenitor cells in these tissues requires niche activation by injury (T. P. Stevens, McBride, Peake, Pinkerton, & Stripp, 1997). Protocols involving chemical injury or sub-lethal irradiation are used to cause cell death which in turn leads to activation of quiescent progenitors. FACS sorting of progenitors followed by transplant or *in vitro* culture has also allowed for investigation lineage contributions and determining differentiation capacity of prospective stem or progenitor cell populations.

1.5.2 Lung Resident Adult Stem Cells

The mature lung is notably quiescent in the resting state (Rawlins & Hogan, 2008). Resident cells have relatively long life spans in comparison to those of fast cycling structures such as the colonic epithelium. While steady state rate of mitosis is low, response to injury, infection, inflammation or toxin exposure may result in a rapid and extensive proliferative response (Cole et al., 2010; Reynolds, Hong, et al., 2000).

Questions as to how the hierarchy tree of stem/progenitor cells may be organized or if a hierarchy tree in the lung even exists remain murky. Induced injury and label retention paradigms have shed some light on these issues, but it is clear that much has yet to be learned about adult stem cells in the lung. Literature in the field has suggested a diversity of regenerative mechanisms, ranging from marrow derived contributions to local growth of facultative progenitors (Jones & Rankin, 2011; Reynolds et al., 2004). Observations of the lung during regeneration have fostered the concept that discrete anatomic regions harbor injury resistant progenitors that are capable of restoring the diverse cell types present within their local environment (H. Chen et al., 2012).

What is currently known about cellular reparative mechanisms in lung epithelia will be detailed below, beginning with an overview of the injury protocols used to identify them.

There are a number of methods described in literature for injuring the murine lung (See table below). Oleic acid, LPS and hyperoxia mimic acute respiratory distress syndrome in humans by

increasing alveolar permeability and causing diffuse transudative fluid accumulation (H. M. Wang, Bodenstein, & Markstaller, 2008). As such, they are particularly effective in causing damage to the small, distal airways. Bleomycin, saline lavage and sulfur dioxide cause direct injury with no selectivity for different cell types (Ghanei & Harandi, 2011; Rock, Barkauskas, et al., 2011). The mechanism for action varies between these substances—bleomycin causes delayed fibrotic change and diffuse apoptotic cell death, whereas sulfer dioxide acts quickly to primarily denude the upper airways via direct necrotic toxicity (Hong, Reynolds, Watkins, Fuchs, & Stripp, 2004a). Saline lavage, on the other hand, causes mechanical damage to the lung by stripping away pulmonary surfactants that lower alveolar surface tension and prevent saccule collapse. A variety of pathogenic agents have also been employed to cause diffuse damage within proximal and distal airspaces.

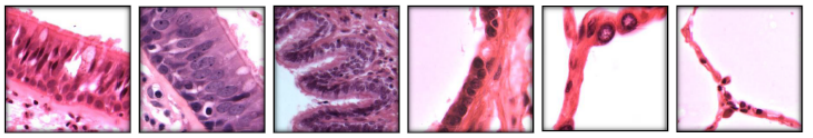

	Trachea	Bronchii	Terminal Bronchiole	Respiratory Bronchiole	Alveolar Septae	Alveoli
Oleic Acid			+	+	+++	+++
LPS			+	+	+++	+++
Hyperoxia	+	+	++	++	+++	+++
Bleomycin			+	+	+++	+++
Saline Lavage				+	+	+
Sulfer Dioxide	+++	+++	+++	+++	+++	+++
Napthalene			++	+++		

Table 1.1 Currently Used Lung Injury Protocols

Unlike these methods, intra-peritoneal naphthalene administration specifically induces death in Clara cells, which serve as xenobiotic metabolizers of inhaled chemicals and as such express a host of microsomal enzymes (Reynolds, Hong, et al., 2000). One of these enzymes, Cyp2F2, converts normally inert naphthalene into a reactive epoxide species that quickly leads to necrotic exfoliation of affected epithelia (Buckpitt et al., 2002). This injury is not fatal to the animal and the airway is regenerated by outgrowth of naphthalene resistant progenitor populations (Hong, Reynolds, Giangreco, Hurley, & Stripp, 2001; Reynolds, Hong, et al., 2000).

Use of these models has led to the prospective identification of populations within the murine lung that have the ability to enter the cell cycle in response to local tissue damage and may thus be considered facultative progenitor cells: basal and Clara-like cells of the proximal conducting bronchioles, Clara, pulmonary neuroendocrine and variant Clara cells of the distal bronchioles, and alveolar type 2

cells of the respiratory airspaces (Cole et al., 2010; Hong et al., 2001; Liu et al., 2011). Data suggests that much of the steady state epithelial turnover is accomplished by facultative progenitors—cells that exhibit differentiated features when in a quiescent state but have the capacity to proliferate for normal tissue maintenance and in response to injury. Lineage tracing analysis has suggested that clonal outgrowth of stem like populations occurs primarily in cases of catastrophic injury (Giangreco et al., 2009).

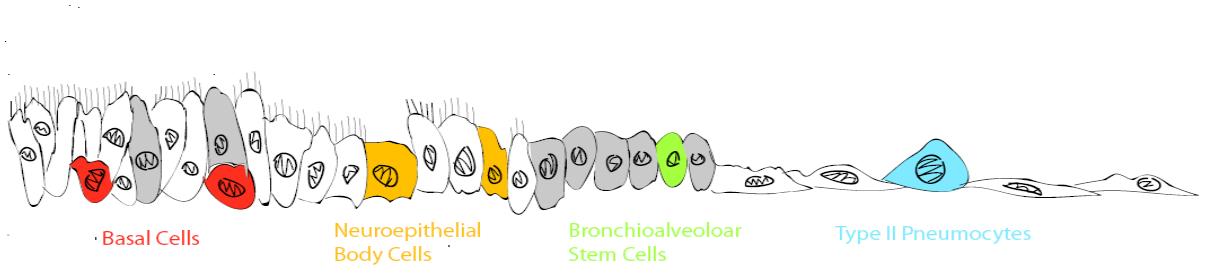

Figure 1.3 Previously Described Progenitor Niches Within the Lung. Basal cells (colored red) of the proximal airway give rise to ciliated epithelium (colored white) as well as non-ciliated Clara cells (colored gray) of the lower trachea and primary bronchii. Variant Clara cells of the neuroepithelial body (colored yellow) as well as bronchio-alveolar stem cells (colored green) give rise to ciliated and non-ciliated cells of the smaller bronchioles. Type II pneumocytes have been shown to give rise to Type I pneumocytes of the alveoli, where gas exchange occurs.

The distinction between Clara cells, Clara-like cells and variant-Clara cells highlight the limitations to our current understanding of progenitor cells in the lung. While it is clear that all three populations express Clara cell secretory protein (CCSP, CC10, Scgb1a1) and have ultra-structures consistent with secretory epithelium, there appear to be several key differences between the groups (Reynolds & Malkinson, 2010). Clara-like cells reside in the tracheo-bronchial epithelium of the upper airway, whereas both Clara and variant-Clara cells are found exclusively in terminal and respiratory bronchioles (Weiss et al., 2011). Additionally, while all populations express CCSP, studies have found divergence in the repertoire of factors otherwise secreted by the Clara-like and Clara cells. Finally, and perhaps most significantly, it has been shown that CCSP+ cells of the upper airway are derived from a different progenitor than those of the distal airspace (Rock, Gao, et al., 2011).

Perhaps the best characterized niche in the lung is the tracheo-bronchiole airspace. Studies using detergent application, sulfer dioxide and naphthalene administration have illustrated a number of

lineage relationships between the cell types found therein. The basal cells, typified by their distinct morphology, label retention after injury, and expression of cytokeratins 5 or 14, have been shown to have the capacity to regenerate all lineages of the upper airway after injury (Hong, Reynolds, Watkins, Fuchs, & Stripp, 2004b). Clara-like cells, on the other hand, seem incapable of reconstituting all differentiated cell types (Hong et al., 2004a). In the steady-state, it appears that these cell types operate semi-autonomously in the maintenance of their respective niches. Although Clara-like cells do not have qualities of true adult tissue stem cells, they are able to self renew as well as give rise to ciliated cells in the uninjured animal (Smith, Koch, & Reynolds, 2012).

As we progress along the proximal-distal axis towards the smaller bronchioles, the relationship between putative progenitors and differentiated cells becomes a bit more controversial. A point of note that warrants mention is the variation between species in anatomic structure of the distal bronchiole tree—human beings transition from terminal bronchiole to alveolar saccuole with little to no intervening respiratory bronchiole (Rock, Gao, et al., 2011). As such, cells that are typically found in this region such as Clara and variant-Clara occur with relatively lesser abundance than in animals such as the mouse or rat.

Interspecies variation is not the only controversy surrounding distal bronchiole epithelial progenitors. There has been much debate over the potential lineage contributions and physiologic significance of in vitro studies of prospective adult stem cell populations from this region (H. Chen, Matsumoto, & Stripp, 2009). These different cell groups were identified more than a decade ago according to their differential sensitivity to naphthalene (Giangreco, Reynolds, & Stripp, 2002; Reynolds, Hong, et al., 2000). It has been postulated that progenitors of Clara cells would not express the microsomal enzymes that confer naphthalene sensitivity, as doing so would place them at risk for genomic alteration during xenobiotic metabolism.

Similar to Clara-like cells of the upper airway, it appears that true Clara cells are able to self-renew and generate ciliated epithelium in the steady state. However, in cases of catastrophic injury, their lineage potential is constrained and they are unable to act as tissue stem cells (Wong, Keating, & Waddell, 2009). Naphthalene resistance Clara cell progenitors, termed variant-Clara cells, were found to reside at two locations: the bifurcation of bronchioles, adjacent to pulmonary neuro-epithelial bodies, and the bronchioalveolar duct junction (BADJ), where respiratory bronchioles converge with alveoli (H. Chen et al., 2012). These naphthalene resistant variant-Clara cells at the bronchio-alveolar duct junction express surfactant protein-c (SPC, Sftpc) in addition to CCSP. Although dual positive cells do not seem

to have the canonical stem cell property of label retention during genetic lineage tracing experiment, purification of these cells from whole tissue homogenate by FACS showed that this population could give rise to CCSP+, SPC, and aquaporin Q5 positive colonies when grown in matrigel (C. F. Kim et al., 2005; Rawlins et al., 2009). As a result, they were given the name bronchio-alveolar stem cells (BASCs) to denote their possible contribution to diverse epithelial lineages in the distal lung. However, using the same FACS algorithm reported in the identification of BASCs, subsequent studies have shown that purified cells kept in vitro are predominantly mesenchymal in nature (McQualter et al., 2009; Teisanu et al., 2011). Additional evidence questioning the stem like nature of variant Clara cells was provided by use of Scgb1a1 (CCSP) transgenic lineage tracing mice, which demonstrated autonomy between bronchiole and alveolar domains in the steady state and in cases of bronchial injury (Rawlins et al., 2009). It is worth noting that the efficiency of Cre mediated GFP recombination was reported to be 85% of all CCSP+ cells by co-staining immunofluorescence. Subsequent work from the same laboratory has shown the generation of peripheral alveolar epithelium from Scgb1a1 expressing cells (Rock, Barkauskas, et al., 2011).

Despite these contradictory findings, a number of intriguing results supports the relevance of CCSP+ cells at the BADJ. Pulmonary progenitors in neonatal mice have been shown to co-express CCSP and Sca-1 and dual positive CCSP/SPC cells expand in number after naphthalene injury in a manner that is corroborated by FACS analysis (C. F. Kim et al., 2005; Ling et al., 2006). This hyperplasia of CCSP+ cells is seen in other injury models including unilateral pneumonectomy (Nolen-Walston et al., 2008). Altogether this evidence suggests that a relatively quiescent progenitor able to replenish cells lost to catastrophic injury to a number of different niches of lung epithelium does in fact reside in this region.

1.5.3 Contribution of Marrow Derived Cells To Lung Repair

In addition to resident progenitor/ stem cells, recent evidences also suggest a possible contribution of circulating marrow derived cells to lung epithelia in the steady state. Engraftment potential of different purified populations by either hematogenous dissemination or intra-tracheal instillation has been observed (Weiss et al., 2011). Much of this work utilized integrated transgene labeling of donor cells into wild type hosts followed by histologic analysis of lung tissue. The results have been mixed, and positive findings often called into question for matters of technique, including improper interpretation of auto-fluorescence, lack of co-labeling with specific cell fate identifiers as well

as the tendency of bone-morrow derived cells of fuse with other cells (Herzog & Krause, 2006; Herzog, Van Arnam, Hu, & Krause, 2006; Van Arnam et al., 2005). In spite of these criticisms, it appears there may be optimism that engraftment is in fact possible.

Findings that directly link endogenously generated, marrow derived cells to lung regeneration have been less numerous. Evidence of marrow derived contribution to lungs injured by Bleomycin administration is fairly convincing, but it is not clear whether these cells can generate normal epithelium or are relegated to fibrotic interstitial fates (Ortiz et al., 2003). Marrow derived CD45+/CXCR4+/cytokeratin+ cells have been shown to re-epithelialize denuded tracheal explants (Dupuit et al., 2000).

Circulating endothelial progenitor cells (EPCs) also appear to play a role in a diverse number of lung pathologies, including pulmonary hypertension, fibrosis, asthma, chronic obstructive pulmonary disease (COPD), acute lung injury, carcinoma and broncho-pulmonary dysplasia (Ding et al., 2011; Duong, Erzurum, & Asosingh, 2011; Yeager, Frid, & Stenmark, 2011).

Perhaps the most encouraging evidence of marrow derived lung progenitors comes from a recent finding that CCSP+ cells exist in adult bone marrow, and when engrafted into CCSP deficient mice by either hematogenous or intra-tracheal routes, are able to form CCSP+ epithelium within the host lungs (Wong, Keating, Lu, et al., 2009). This raises the possibilities that CCSP+ lung cells may have at least a partial origin from bone marrow, or that lung resident stem cells may enter into circulation in a manner similar to hematopoetic stem cells. In vitro studies have demonstrated that soluble factors released from lung epithelia or injured lung homogenates are able to induce expression of markers of lung epithelium in marrow derived cells (Van Vranken et al., 2005). This raises the third possibility that marrow derived MSCs or HSCs may become exposed to paracrine signals while transiting out of the bone marrow that cause them to differentiate along specific lineages.

1.6 Signaling Mechanisms Regulating Tissue Homeostasis in Normal and Injured Lung

The ability of a given organ system to respond to noxious stimuli or insult is contingent upon the convergence of a number of different factors, some touched on earlier in the discussion of general wound healing. Challenges to homeostasis are perceived by a surveillance system within the local

microenvironment, which cause the secretion of cytokines and growth factors that act on cells capable to transducing these signals to stimulate growth and differentiation.

Data gleamed from acute and chronic injury indicates a large number of soluble factors can be provided from a number of different sources, including neighboring epithelium, endothelial cells, marrow-derived white blood cells and mesenchymal cell population during injury. These include growth factors such as TGF-α and –β, VEGF, EGF, PDGF, FGF-2 and -7, and IGF (Crosby & Waters, 2010). In addition, cell-to-cell and cell-ECM interactions may mediate critical components of injury response as well. This description is of course a gross over-simplification, as the array of sensors as well as the signals they elaborate is much more complex than what is described above.

Taken together, these stimuli are involved in important aspects of the wound healing response such as cell fate specification, activation of quiescent populations, proliferation, motility and modulation of soluble factor signaling. As often in biology, while each represents an independent signaling axis, there is convergence and cross talk between them.

Just as important to the act of wound healing is the cessation of these growth related processes; failure to accomplish this may lead to a number of pathologies ranging from fibrotic change to neoplastic growth. The attenuation of pro-repair signals may be accomplished through simple diminution of secreted factors, or by the activation of antagonizing systems that limit proliferation, favor differentiation or force the cell into a quiescent state. In this regard, recent studies highlighting the role of senescence in limiting wound healing are of particular interesting.

1.7 The Role of Senescence in Controlling Wound Healing

Senescence was first described in the context of cell replication (Hayflick & Moorhead, 1961). Telomere attrition imbues a definite replicative potential upon most cells (Cristofalo & Pignolo, 1993). The stress of critical telomere shortening after repeated mitosis leads permanent cell cycle arrest known as the senescence phenotype. This state is typified by several common characteristics including flat, enlarged morphology, induction of senescence associated beta-galactosidase activity (SA-beta-Gal) and appearance of senescence associated heterochromatic foci (Pazolli & Stewart, 2008). Telomere shortening, however, is not the only way a cell may reach the endpoint of senescence. There are, in fact, many additional cues that may play a role in inducing cellular senescence (Kuilman, Michaloglou,

Mooi, & Peeper, 2010). Some of them are directly linked to the inflammatory response, such as reactive oxygen species (ROS) generation, pro-inflammatory cytokines, and unbalanced strong mitogenic signaling (Ferbeyre et al., 2002; Krizhanovsky, Xue, et al., 2008).

It has been recently been proposed that cellular senescence itself may be an active contributor to wound resolution, rather than just a consequence of the injury response (Krizhanovsky, Yon, et al., 2008). Studies have shown that cells driven to senescence by genotoxic stress secrete multiple factors associated with immune response, inflammation and cancer. These factors include Il-1, Il-6, Il-8, MCP-2, FGF, EGF, VEGF, several MMPs and nitric oxide and together constitute what has been called the senescence associated secretory phenotype (SASP) (Coppe et al., 2008). The functions of these secreted factors are topic of intense investigation but evidence suggest that they can contribute to the wound healing process either by inducing the proliferation of epithelial cells or through the recruitment of immune cells (Krizhanovsky, Yon, et al., 2008). This has been demonstrated using injury paradigms such as carbon tetrachloride (CCl4) induced liver toxicity. In this work, evasion of cellular senescence via suppression of p53 signaling was shown to diminish SASP secretion, abrogating immune clearance of damaged cells by Natural Killer cells and causing fibrosis.

At the molecular level, studies have reported the importance of signaling via nuclear factor kappa-light-chain-enhancer of activated B cells (NF-κB) in the induction of senescence and SASP (Salminen, Kauppinen, & Kaarniranta, 2012). This is particularly intriguing as this pathway is an important, evolutionarily conserved sensor mechanism protecting against oxidative and genotoxic stresses (Campisi, 2005). NF-κB is in fact constitutively expressed and acts as a first response transducer of stress. It is kept in an inactive state via binding by the IκB family of proteins that sequester it to the cytosol. Phosphorylation of the IκB proteins by a number of upstream kinases, the most important of which being canonical signaling partner IKKα/β, causes dissociation and degradation of IκB which allows NF-κB to translocate to the nucleus and act as a sequence specific transcription factor (Gilmore, 2006). The IKKγ subunit, generally called NEMO (a contraction of NF-κB essential modulator), is a crucial mediator of NF-κB system, as IKKα/β dependent degradation of IκB relies upon this regulatory molecule (Salminen, Suuronen, Huuskonen, & Kaarniranta, 2008). In the case of DNA damage, ataxia telangiectasia mutated (ATM) kinase, which is activated by DNA double-strand breaks, phosphorylates NEMO leading to a variety of modifications that ultimately result in its translocation from nucleus to cytoplasm, where it can initiate NF-κB signaling by degrading IκB via interaction with IKKα/β (Yang et al., 2011).

Activation of NF-κB has several important consequences for a cell that are highly cell context dependent. In addition to its role in cellular senescence, it may act as either an enhancer or suppressor of programmed cell death via apoptosis (Bharti & Aggarwal, 2002; W. Chen, Li, Bai, & Lin, 2011). Interestingly, while NF-κB is able to directly induce expression and secretion of SASP, NF-KB activation per se' is not sufficient for the induction of senescence as p53 deficient cells fail to undergo senescence in response to NF-κB activation (McDuff & Turner, 2011).

Direct NF-κB activation does not appear to be the only means for a cell to produce SASP. Signaling by p38 mitogen-activated protein kinase (p38MAPK) in response to metabolic, oxidative and endoplasmic reticulum stresses as well as DNA damage and heat shock appears to also play an important role in the induction of senescence as well (Freund, Patil, & Campisi, 2011). Expression of a constitutively active p38MAPK in human fibroblasts induces senescence and increased SASP in a manner independent on DNA damage induction or ATM activation (Freund et al., 2011). Evidences suggest that p38MAPK may potentiate NF-κB signaling via activation of mitogen- and stress-activated protein kinases (MSK1 and 2) through the phosphorylation of the p65 subunit of NF-κB at Ser276 (Kefaloyianni, Gaitanaki, & Beis, 2006; Vermeulen, De Wilde, Van Damme, Vanden Berghe, & Haegeman, 2003). It appears that this interaction may thus contribute to the senescence associated secretory phenotype.

How NF-κB is activated in the context of senescent cells is still an open question. Interestingly, we and others have shown TGF-β to be able to activate the NF-κB pathway. Canonical TGF-β signaling utilizes receptors specific for the secreted factor that phosphorylate the SMAD family proteins, leading to their nuclear translocation and activation as transcription factors (Derynck & Zhang, 2003). In the case of NF-κB activation, however, signal transduction is accomplished via non-SMAD mediated interaction between TRAF6, TGF-β activated kinase-1 (TAK1) and p38MAPK (Yang et al., 2011).

The activation of the NF-κB pathway by TGF-β is of particular interest in the context of senescence as TGF-β is one of the main factors secreted during wound healing to impact epithelial growth dynamics and suppress spurious hyper-proliferation (Laiho, DeCaprio, Ludlow, Livingston, & Massague, 1990). As we describe later, we have uncovered a novel alternative splicing event of p53 (dubbed p53-Ψ) that is induced by TGF-β during tissue injury/repair. This isoform of p53 lacks the ability to trans-activate canonical targets associated with cell cycle arrest. Cells expressing p53-psi exhibit the SASP through activation of p38 MAPK and NF-KB but do not undergo senescence. Intriguingly, ectopic expression of full length p53 is able to rapidly induce their senescence. Hence the regulation of p53-

Ψcould in principle allow for the activation of NF-κB signaling and SASP independently of cell cycle arrest or senescence.

1.8 Deregulation in Molecular Mechanisms of Tissue Homeostasis Leads to Fibrosis

Proper lung function requires a highly elastic parenchyma, and as such, disorders marked by varying degrees of inflammation and fibrosis are particularly detrimental. Among them, Idiopathic Pulmonary Fibrosis (IPF)/usual interstitial pneumonitis stands out as the most common diagnosed form of still unknown origin (Navaratnam et al., 2011; Raghu, Weycker, Edelsberg, Bradford, & Oster, 2006). Presenting symptoms include shortness of breath, radiographically evident diffuse pulmonary infiltrates, and varying degrees of inflammation, fibrosis, or both on biopsy ("Idiopathic Pulmonary Fibrosis: Diagnosis and Treatment," 2000). Median survival after time of diagnosis ranges from 2 to 3 years, making IPF a particularly insidious disease (Walter, Collard, & King, 2006). A 2006 study estimated a prevalence ranging from 14 to 42.7 and incidence ranging from 6.8 to 16.3 cases per 100,000 persons (Raghu et al., 2006).

IPF is characterized by a number of pathological changes to the lung parenchyma, including fibrotic zones with associated honeycombing, interstitial inflammation and alternating regions showing relatively unaffected tissue ("American Thoracic Society/European Respiratory Society International Multidisciplinary Consensus Classification of the Idiopathic Interstitial Pneumonias," 2002). The physical distribution of change is believed to allay itself with the natural history of the disease. In the acute phase, focal zones of fibroblast and myofibroblast proliferation from recent alveolar injury are readily observable (Gharaee-Kermani, Gyetko, Hu, & Phan, 2007). Failed alveolar re-epithelialization within these foci results in excessive deposition of collagen and other extracellular matrix (ECM) components, leading to irreversible loss of function.

Despite efforts within the field, questions as to the precise cellular and molecular mechanism underlying this process remain unanswered. There appears to be some genetic susceptibility to IPF, as up to three percent of cases appear to cluster in families. Within these cohorts, polymorphisms of the interleukin-1–receptor antagonist, tumor necrosis factor, and major-histocompatibility-complex loci have been detected (Lee et al., 2005). In addition, defects in the processing of surfactant protein within alveolar type II cells have been implicated in IPF (Thomas et al., 2002). However, as of yet there is no clear evidence of a genetic basis for IPF.

Current available therapies offer little to patients with IPF, as anti-inflammatory and immune suppressive treatments such as prednisone, azathioprine, or cyclophosphamide have shown little ability to modify the course of the disease (Walter et al., 2006). Findings using model systems for IPF such as rats over-expressing transforming growth factor (TGF)-β1 suggest that treatments aimed at resolving inflammation may be neglecting the true cause of the disease; fibrosis is still able to progress even in the absence of a chronic inflammatory component (Sime, Xing, Graham, Csaky, & Gauldie, 1997). The fact that inflammation alone is not sufficient as cause of IPF is highlighted by the observation that αvβ6 integrin knockout mice, unable to activate TGF-β1, may develop and exaggerated inflammatory response to bleomycin with near-complete attenuation of the fibrotic response (Munger et al., 1999). Some groups have suggested that inflammation associated with IPF is in fact a result of the initial insult, which involves epithelial cell injury and abnormal wound repair in the absence of a chronic inflammatory response.

Although questions remain concerning the cause of IPF, it is clear that the presence of dysplastic foci are critical to pathogenesis. Increased numbers of foci are associated with disease progression and reflect a worsened prognosis (King et al., 2001). Foci consist of fibroblasts and myofibroblasts, which together are responsible for deposition of excessive ECM and likely remodeling of the lung.

In the resting state, fibroblasts are the principal structural component of the mesenchyme and are responsible for the baseline secretion of proteins such as collagen that contribute to the normal turnover of ECM within airways. Myofibroblasts have been classically viewed as morphological intermediates of fibroblasts and smooth muscle cells and are more biosynthetic in nature than the fibroblasts. Although typically only a transient cell type within the lung, they may become drastically over represented in fibro-proliferative disorders (Schurch, Seemayer, & Gabbiani, 1998). Myofibroblasts are characterized by spindle or stellate morphology and possess specific intra-cytoplasmic stress fibers that confer a highly contractile phenotype. It is believed that the myofibroblast lies at the core of the IPF disease process due to their predominant role in ECM deposition, structural remodeling and destruction of alveoli during and after lung injury (Phan, 2012). As such, delineating the origin of the cell is of crucial importance, as this may gleam new insights as to the regulatory mechanisms that have gone awry during fibrotic progression. There are currently three competing theories within the field as to the origin of the myofibroblasts seen at fibroelastic foci. It is worth noting that these theories are not mutually exclusive, and the actual pathogenesis of IPF may involve contributions from each of the following mechanisms.

The first theory, which postulates that myofibroblasts are derivative of resident intrapulmonary fibroblasts that have undergone trans-differentiation in response to stimuli, has been historically held as correct during much of the study of IPF (Phan, 2002). These fibroblasts, which are derived from the adventitia of peri-vascular and peri-bronchial areas are believed to migrate and differentiate under the influence of the pro-fibrotic microenvironment (K. Zhang, Rekhter, Gordon, & Phan, 1994). Observation based on the bleomycin model of lung fibrosis in rats suggests that initial myofibroblasts indeed arise in the adventia of the distal airways from peri-bronchiolar and peri-vascular fibroblasts. This view is supported by evidence that TGF-β1 may induce trans-differentiation of fibroblasts to myofibroblasts in vivo via a Smad-3 dependent mechanism (Hu, Wu, & Phan, 2003).

As an alternative explanation to the origin of myofibroblasts, some groups have suggested a contribution by cells not endogenous to the lung. This view posits that the mesenchymal cells patho-gnomonic to IPF may in fact be derived from circulating bone marrow-derived progenitors. These progenitors, termed fibrocytes, were originally identified by Bucala et. al as collagen I+/CD34+/CD45+, circulating precursors important for tissue repair (Bucala, Spiegel, Chesney, Hogan, & Cerami, 1994). Several cytokines including stromal derived factor-1 (SDF-1) and the CCR2 and CCR5 axis have been shown responsible for homing of circulating fibrocytes (Gomperts & Strieter, 2007). Blocking tissue ingress of these cells has been shown to be protective against bleomycin induced fibrosis. Studies in wild-type irradiated mice transplanted with green fluorescent protein (GFP)-positive marrow indicated that twenty to fifty percent of cells constituting fibrotic areas of the lung were indeed graft derived (Ortiz et al., 2003). A caveat to this result was the lack of α-SMA expression in marrow derived fibroblasts and resistance of these cells to TGF-β induced trans-differentiation, indicating an inability to assume the myofibroblast lineage.

Recent work has elucidated another possible explanation for the derivation of myofibroblasts during fibro-proliferative disease processes. Alveolar epithelial cells (AECs) have been shown to be capable of assuming a mesenchymal phenotype after chronic exposure to TGF-β, suggesting the possibility that myofibroblasts are derived from AECs (Willis et al., 2005). The process by which this change occurs is termed epithelial to mesenchymal transition (EMT), and has long been known to play a role in cellular differentiation during development and tumor invasion.

EMT is characterized by loss of polarity, cytoskeletal reorganization, transition to spindle shaped morphology, and changes in gene expression program (Kalluri & Weinberg, 2009). These changes in gene expression include loss of epithelial markers such as E-cadherin, cytokeratins and zonula

occludens-1 with concomitant increase of mesenchymal marker expression including α-SMA and vimentin.

During development, EMT enables the production of mesoderm from epithelial precursors during gastrulation, thus playing a crucial role in the formation of endocardial cushions, the atrio-ventricular canal, and the palate (Boyer et al., 1999; Nawshad, LaGamba, & Hay, 2004). In addition to its known roles in organogenesis, EMT has been implicated in the acquisition of a migratory phenotype by tumor cells, thus increasing invasiveness. TGF-β-mediated Smad2 and 3 signaling have been demonstrated in EMT associated with tumor progression and development using different model systems (Gomes, Terra, Sogayar, & Labriola, 2011). EMT has also been described in a number of pathological fibroproliferative disorders, including injury to lens epithelial cells and renal fibrosis (Winbanks et al., 2011).

Although AECs have been shown capable of EMT, the precise role of this process in pathological fibrosis of the lung is still unclear. Interrogation of lung tissue from patients with IPF has revealed interesting evidence that cellular constituents of fibroelastic foci may in fact be derived from epithelial lineages (Willis & Borok, 2007). Co-localization analysis of hyperplastic epithelial cells overlying fibroblastic foci in biopsies displayed markers of both epithelial and mesenchymal lineages such as α-SMA. These data are supported by further observation that the epithelial marker pro-surfactant protein C and mesenchymal marker N-cadherin co-localize within IPF lung tissue. Perhaps the most compelling evidence of an epithelial origin to mesenchymal cells present after fibrotic resolution to injury is provided by Cre-Lox lineage tracing study wherein type II pneumocytes (AT2 cells) were labeled with β-galactosidase prior to TGF-β1 induced fibrosis (K. K. Kim et al., 2006). These cells proved to constitute the overwhelming majority of vimentin positive cells within the injured lung, thus proving an epithelial origin. Although indirect, these evidence strongly support the possibility that EMT plays an important role in IPF. This is reinforced by links between signaling pathways (e.g. TGF-β) known to induce both fibrosis and EMT in mouse model systems of IPF and in human patients.

1.9 Persistent Lung Wounding and its Role in Neoplasia

While the exact mechanisms underlying IPF have yet to be elucidated, it is clear that prolonged injury is capable of imparting profound variation on the structure and function of the lung. As mentioned above, there appears to be specific signaling pathways that underlie fibrosis that are distinct

from those of the general inflammatory process. Conceptually, we may consider these changes as part of a spectrum of outcomes resulting from chronic, unresolved and sometimes spurious wound healing. In addition to fibrotic conditions, it is now appreciated that cancerous growth and the process of wound healing are intrinsically linked. This association was first proposed more than a century ago and remains an intense area of research today.

Rudolf Virchow postulated that chronic irritation and previous injuries are a precondition for tumorigenesis in a classic study published in 1863 (Schafer & Werner, 2008). Almost 150 years later, we are still exploring how the two phenomena are related. Examples include hepatitis C induced hepatocellular carcinoma, H. pylori induced gut-associated lymphoid tissue lymphoma, and inflammatory bowel disease induced carcinoma of the colon. In the lung, anecdotal incidence of tumor formation in peripheral areas of scar tissue was first reported by Friedrich in 1939 (Bobba, Holly, Loy, & Perry, 2011). These so called scar carcinomas are typically located in sub-pleural areas and involve extensive formation of fibrous tissue surrounding nests of epithelial structures with adenomatous morphology (Bakris et al., 1983). Ongoing work is aimed at addressing the relationship between neoplastic growth and the surrounding mesenchymal tissue.

Perhaps the greatest source of chronic wounding of lung tissue worldwide is cigarette smoking. About 50% of lifetime smokers will develop chronic obstructive pulmonary disease (COPD), a disease state comprised of two distinct processes: emphysema and chronic bronchitis (Kelly, 2002). The underlying pathology to emphysema involves destruction of alveolar septae leading to structural failure of the respiratory unit during exhalation. Chronic bronchitis, on the other hand, involves remodeling of the small conducting airspaces to decrease luminal volume as well as over-secretion of mucus into the air space. COPD is a very strong risk factor for development of lung cancer, as well as a significant detriment to quality of life for effected patients (Hurd, 2000; Punturieri et al., 2009; Raviv, Hawkins, DeCamp, & Kalhan, 2011). Inflammation is believed to mechanistically underlie the changes of COPD and may play a part in the advancement to carcinoma. Interestingly, it has been shown that glucocorticoid anti-inflammatory drugs are able to decrease incidence of lung cancer in COPD patients (Parimon et al., 2007).

The ways by which fibrotic lesions may promote cancer within a tissue are many, and include the disruption of cell polarity, stimulation of cell proliferation and induction of inflammation. The fibrin matrix that develops during the wounding response is a fantastic reservoir for cytokines and growth factors that trigger proliferation of neighboring cells.

Among the many studies linking tissue injury and neoplasia, I found the older works by Mina Bissell's group to be particularly fascinating. These studies showed that chickens inoculated with rous sarcoma virus only experienced tumors when the limb contralateral to the injection site was injured (Dolberg, Hollingsworth, Hertle, & Bissell, 1985). This data suggests that localized activation of a sensitized cell is necessary to tumor initiation. One could easily extend this to involve a cell harboring significant genomic alteration to allow for continuous growth that remains quiescent until given pro-growth signals from a local injury.

The myofibroblast—pathognomonic marker cell of fibrosis—is also largely present in cancer. Many carcinomas provoke a desmoplastic response in which the body attempts to encapsulate a growing tumor that way it might a trapped foreign body (Akashi et al., 2005; Colby, 1995; Conti et al., 2008). The physical matrix created by this process, supported by the myofibroblast cell, has important consequence on the epithelial cells of a growing neoplasm. For instance, remodeling initiated by myofibroblasts has been shown to support invasion of squamous cell carcinoma cell in organotypic culture (Lewis et al., 2004). In addition, structural rigidity due to ECM components has been shown to foster invasion and metastasis in murine models of breast cancer (Egeblad, Nakasone, & Werb, 2010). Importantly, changes to the local microenvironment caused by myofibroblasts and tumor associated fibroblasts may help contribute to tumor heterogeneity by secreting soluble factors and providing integrin components of the ECM.

Changes in cellular signaling dependencies may have important consequence on a vast array of phenotypes for a given cancer. These may include sensitivity to chemotherapeutics or radiation, growth rate, constitutional effects (e.g. cachexic wasting), proclivity for metastasis and propensity for local invasion. In the case of cancers that are treated with molecular targeted therapies, this may even render a cancer insensitive to drug therapy (Garofalo et al., 2012; Yoshida et al., 2010). Growing evidence implicates factors associated with the wound healing process as central players in tumor evolution. Studies of lung cancer have shown that tumors baring signatures enriched for injury-repair genes typically have worse prognosis, linked to an increased likelihood of metastasis. This may be attributed to induction of EMT in a subset of tumor cells that acquire a "metastatic phenotype" and develop a diversity of growth signaling dependencies (Barr et al., 2008; Thomson et al., 2005). Interestingly, cytokines such as TGF-β and Il-6 also seem to play an important role in fostering paracrine changes to tumor cells. Response of lung cancer cells baring sensitizing mutations in the EGFR to the RTK inhibitor Erlotinib is mitigated by Il-6 (Yao et al., 2010). In addition, secreted Il-6 originating from

thymic endothelial cells protects leukemic white blood cells from radiation induced apoptosis in a murine model of lymphoma (Gilbert & Hemann, 2010).

1.10 Expansion of Progenitor Populations and Cancer Initiation

Manipulation of the murine genome to cause activation of oncogenic signaling pathways is an invaluable tool for modeling tumorigenesis. Around the same time that naphthalene resistant progenitors of the distal bronchioles were being reported, characterization of a mouse model of lung carcinoma that utilized conditional expression of a constitutively active KRAS G12D was being performed (Jackson et al., 2001). This system utilized inhaled adenovirus expressing Cre recombinase to excise a stop codon from the mutant KRAS allele. Activation of oncogenic KRAS leads to the formation of hyperplastic lesions, adenomas and adenocarcinomas in the lungs of effected mice. Interestingly, the earliest stages of disease appeared to involve hyperplasia at the BADJ; the exact location thought to harbor BASCs. Subsequent work has demonstrated that expansion of CCSP+/SPC+ dual positive cells is detectable in human and mouse tumors (Yatabe, Kosaka, Takahashi, & Mitsudomi, 2005). Interestingly, individual signaling components of the RAS pathway seem to differently contribute to the regulation of the BASC population. In the case of B-raf, one its most immediate downstream targets, a mouse model recapitulating oncogenic mutations found in in 3% of non-small cell lung cancer (NSCLC) (V600E mutation) gave a striking phenotype (Haigis, Wistuba, & Kurie, 2007). While these animals readily developed hyperplasia and papillary adenomas that were histologically similar to Kras G12D transduced lungs, they were notably unable to progress to full blown adenocarcinoma without concomitant loss of function of p53 or p16Ink4a/p19Arf. Instead, lesions exhibited growth arrest and a senescence-like phenotype.

Other work demonstrating the pre-cancerous expansion of cells at the BADJ upon activation of phosphatidylinositol 3-kinase (PI3K) signaling, which produces phosphatidylinositol (3,4,5)-trisphosphate (PIP3) from phosphatidylinositol (4,5)-bisphosphate (PIP2) (Morgensztern & McLeod, 2005). The membrane bound product of this reaction then recruits the protein kinase Akt via its pleckstrin homology domain to the internal surface of the plasma membrane where it becomes partially activated by phosphorylation from phosphoinositide-dependent protein kinase 1 (PDK1) on threonine 308 . Full activation of AKT occurs upon phosphorylation of serine 473 by the TORC2 complex of the mTOR protein kinase, a critical downstream effector of the PI3K/Akt pathway that facilitates cell survival and growth by increasing protein synthesis and blocking apoptotic pathways. Chemical inhibition of PI3K has been shown to abrogate tumorigenesis in the conditional Kras G12D model of lung adenocarcinoma (Yang et

al., 2008). Interestingly, this includes interfering with stages of precancerous growth in which BASCs expand in number but also move out of their normal physiologic niche at the bronchio-alveoloar duct junction (BADJ). The tumor suppressor phosphatase and tensin homolog (PTEN) opposes this pathway by catalyzing the dephosphorylation of PIP3 thus preventing juxtaposition of Akt with the plasma membrane. Targeted loss of PTEN in SPC expressing cells of the murine lung causes neonatal cellular hyperproliferation as well as expansion of the BASC population and increased tumor incidence in response to urethane administration when compared to wild-type littermates (Yanagi et al., 2007). Interestingly, alveolar septal thickening in neonates was attributed to an increase in α-SMA positive cells, indicating an interstitial fibrosis-like phenotype.

Protein kinase C iota (PKCι) was proven necessary for BASC expansion in vivo by gene knockout (Regala et al., 2009). Pharmacological inhibition of PKCι using the small molecule aurothiomalate also decreased in vitro colony forming capacity of cells isolated from Kras G12D transduced lungs. The authors suggest that aurothiomalate accomplishes this by blocking interaction between PKCι and the cell polarity protein Par6, causing diminished signaling to downstream target Rac1. Perturbations in this axis have been previously shown to be growth inhibitory to mutant KRAS cell lines (Scotti, Bamlet, Smyrk, Fields, & Murray, 2010).

Another possible downstream effector of PKCι signaling in Kras G12D transformed lung epithelia is the NF-κB pathway. Interaction between the protein kinase C family, in particular the atypical members, has been associated with NF-κB dependant transcriptional activity (Sajan et al., 2009). Multiple studies have now confirmed the importance of NF-κB activation in Kras G12D transduced tumorigenesis. Expression of a dominant-negative form of IkBa (encoded by Nfkbia; super repressor, IkB-SR) within the lungs of Kras G12D activated mice greatly diminishes tumor volume in a p53 dependent manner, such that cells that have lost wt p53 function require persistent NF-κB activation to remain viable (Meylan et al., 2009). A recent report demonstrated that Gata2 dependent NF-κB activity was required in solid tumor formation within lungs of Kras G12D transduced animals (Kumar et al., 2012). In its absence, nodules were nearly absent and the apoptosis marker cleaved caspase-3 was greatly increased within whole lung lysates.

Reports from the literature have also provided evidence that other signaling pathways may favor tumorigenesis through expansion of the BASC population. Studies utilizing inducible genomic loss of p38αMAPK have for example indicated a BASC specific role for this pathway (Ventura et al., 2007). Homozygous deletion mice experience alveolar septal thickening with reduced expression levels of the

epithelial cell marker E-Cadherin, evocative of the phenotype occurring from PTEN loss. Global proliferation levels and total number of type II pneumocytes were both increased in these mice, with concomitant gains in EGFR expression and decrease in Sprouty2, a negative regulator to RTK signaling in lung cells. The presence of CCSP+/SPC+ BASCs increased in the lungs of transgenic mice, and most interestingly, these cells were shown to have increased residence in the cell cycle when compared to SPC+ cells, which were mostly found in G0/G1 arrest. These data suggest that BASCs are pushed towards proliferation in the absence of differentiation signals from p38αMAPK, and that this proliferation results in a downstream accumulation of type II pneumocytes and eventual adenocarcinoma. Most strikingly, although BASCs were originally identified as injury resistant CCSP+ bronchial epithelial progenitors, neither PTEN nor p38αMAPK loss results in an increase in lower airway Clara cells despite increasing numbers of BASCs themselves.

Studies using expression of a mutated form of the cell cycle inhibitor p27Kip1 that is unable to associate with cyclins and cyclin-dependant kinases (CDKs) showed BASC expansion, lung epithelial hyperplasia and formation of spontaneous adenocarcinoma (Besson et al., 2007). Similar results have been obtained with DOK2 knockout (Berger et al., 2010). Additionally, loss of Gata6 expression causes BASC compartment expansion via increased Wnt signaling (Y. Zhang et al., 2008).

Interestingly, genetic changes to BASCs result not only in their numerical increase but may also act to define the phenotypes of tumors they give rise to. Targeted loss of the p18 and Men1 genes not only cooperate to cause BASC expansion and tumor formation, but also generate neoplasias that, unlike those of other genetic backgrounds, bared strongest resemblance to neuro-epithelial tumors as opposed to typical adenocarcinoma (Pei, Bai, Smith, & Xiong, 2007). While it has not been definitively proven that the cell of origin was the same for these tumors, the data does suggest that in principle different genotypes may result in the commitment of stem cells toward different cell lineages.

Chapter 2

Regulation of Bronchial Epithelial Progenitors of the Distal Airway by HTR2B

Chapter 2: Regulation of Bronchial Epithelial Progenitors of the Distal Airway by HTR2B

Summary

The attrition of cells within organs necessitates replenishment from tissue resident progenitor populations. Study of the murine lung has suggested a number of niches along the proximal-distal axis of the airway responsible for epithelial regeneration in the steady state and during injury repair (H. Chen et al., 2012). Within the distal most bronchioles, injury resistant cells termed bronchioalveolar stem cells (BASCs) have been reported to reside at the bronchioalveolar duct junction (Giangreco et al., 2002; C. F. Kim et al., 2005). Since the initial description of cytological markers for these cells, controversy over their true nature has impeded progress towards application of their biology towards new therapeutics (Raiser & Kim, 2009). We report that additional stratification of the Sca-1+/CD45-/Pecam- lung population yields cells with characteristics of true bronchial progenitors. These cells express genes associated with pluripotency and stem cell state and are able to generate differentiated bronchiole epithelium upon orthotopic transplant. Transcriptional analysis revealed expression of novel surface markers that unlike Sca-1 have human orthologs, making them potentially useful in a clinical setting. In particular, the serotonin receptor isoform 2B (HTR2B) was highly expressed after injury and its activation was required for re-epithelialization. Our work suggests a role for autocrine serotonin production in the maintenance of the progenitor niche residing at the bronchioalveolar duct junction.

Highlights

- Stratification of the Sca-1+/CD45-/Pecam- lung population with CD24 yields cells that express cytological markers of progenitors at the BADJ that respond to local injury.
- CD24high cells display molecular and phenotypic characteristics of lung progenitor/stem cells
- Transcriptional profiling revealed expression of distinct cell surface receptors such as HTR2B, Lifr, Lgr8 and Drd5
- Functional validation of HTR2B revealed serotonin receptor signaling to be important for progenitor cell activation and epithelial cell regeneration.

Introduction

The attrition of cells within organs necessitates a continuous replenishment in order to maintain proper structure and function of tissues. This is achieved mainly through the expansion and differentiation of tissue resident progenitor populations (Arwert et al., 2012). Study of the murine lung has suggested a number of niches present at different levels of the airways along the proximal-distal axis to be responsible for steady state epithelial turnover as well as response to catastrophic injury (See Chapter I). Within the distal most bronchiole airspaces, injury resistant progenitor/stem cells have been reported to reside at the bifurcation of bronchioles as well as the bronchioalveolar duct junction (BADJ) (Giangreco et al., 2002; C. F. Kim et al., 2005).

The initial reporting of these cells, then referred to as variant-Clara cells, was based on their differential sensitivity to the drug naphthalene. Normal Clara cells of the lung perform many tasks including generation of ciliated cells, secretion of lubricants (e.g. secretoglobin family proteins), and xenobiosis of inhaled chemicals (Reynolds & Malkinson, 2010; Reynolds et al., 2007; Wong, Keating, & Waddell, 2009). This last quality renders typical Clara cells sensitive to naphthalene due to expression of the microsomal enzyme Cyp2F2, which converts the drug to a reactive and toxic epoxide species (Buckpitt et al., 2002). This injury paradigm has been crucial in delineating the adult stem cell population, as exposure to naphthalene causes rapid denudation of sensitive cells and activation of their nearby progenitors.

Niches of naphthalene resistant progenitor cells that replicate in response to injury have been reported next to the neuroepithelial body (neuroepithelial body cells, NEBs) as well as at the BADJ (Reynolds, Giangreco, Power, & Stripp, 2000). This latter population has been shown to express the mature Clara cell marker Clara cell secretory protein (CCSP) as well as the type II pneumocyte marker surfactant protein C (SPC) (C. F. Kim et al., 2005). CCSP+/SPC+ cells were enriched in the Sca-1+/CD45-/Pecam- fraction of lung homogenate when purified by fluorescence assisted cell sorting (FACS). *In vitro* culture of these cells yielded colonies expressing markers of multiple cell types present in the respiratory airways, including type 1 and 2 pneumocytes as well Clara cells. As such, these cells were termed bronchioalveolar stem cells(BASCs) due to their ability to self renew as well as generate daughters with characteristics of both bronchial and alveolar epithelium. Subsequent work has asserted that FACS purification of the Sca-1+/CD34+/CD45-/Pecam- fraction yields colonies with mesenchymal type morphology (McQualter et al., 2009). Additionally, lineage tracing utilizing genomic techniques has called into question the ability of CCSP expressing cells to contribute to epithelia within the alveolar airways (Rawlins et al., 2009).

Despite the controversy surrounding BASCs, studies using animal models of lung injury have supported the idea that proliferation of this population precedes post-exfoliative re-epitheliazation as well as compensatory lung hypertrophy in response to unilateral pneumonectomy (Nolen-Walston et al., 2008). Cases of catastrophic damage to bronchiole epithelium also clearly resulted in clonal outgrowth emanating from the BADJ, further corroborating the significance of cells within this region (Giangreco et al., 2009). But perhaps the most intriguing evidence indicating the importance of injury resistant progenitors at the BADJ has been provided by animal models of lung cancer, which have consistently shown that hyperplastic change in this specific population precedes frank carcinoma formation (Jackson et al., 2001; Pacheco-Pinedo et al., 2011; Regala et al., 2009).

A possible explanation to resolve the variation seen by FACS using the current purification algorithm is population heterogeneity within the Sca-1+/CD34+/CD45-/Pecam- fraction of the lung. To test this hypothesis, we interrogated multiple candidates from the literature for their ability to identify novel sub-fractions. Consistent with reports from other organ systems, we found the surface marker CD24 was able to stratify the previously described BASC population (Sca-1+/CD45-/Pecam-) into four sub-fractions. Among these groups, cells with the highest level of CD24 showed expression of cytological markers of progenitors at the BADJ, proliferate in response to injury, and express markers of pluripotency (e.g. Nanog and Oct4) (Lengner et al., 2008). Consistent with this population acting as a bronchial progenitor, orthotopic transplant of FACS purified cells resulted in engraftment and generation of differentiated epithelium.

Our findings thus suggest that much of the conflicting data regarding the nature of BASCs may be attributed to limitations of the algorithm adopted for their purification. Further molecular characterization of these cells yielded novel surface markers that unlike Sca-1 have human ortholog, thereby making them potentially useful in a clinical setting. In particular, the serotonin receptor isoform 2B (HTR2B) was highly expressed after naphthalene induced Clara cell ablation within cells previously identified as injury resistant progenitors at the bronchioalveolar duct junction. We show that these cells produce serotonin during injury, suggesting a possible role in autocrine or paracrine regulation. Chemical inhibition of HTR2B leads to decreased proliferation after injury that manifests as deficit in re-epitheliazation.

Results

Identification of a Novel Putative Lung Epithelial Progenitor/Stem Cell

In order to isolate a putative lung resident progenitor within the lower respiratory tract, we sought to identify a non-endothelial, non-marrow derived cell that persists through, as well as expands after, tissue injury. Because similar molecular features have been shown to characterize stem/progenitor cells independently of tissue of origin , we reasoned that candidates for surface markers may already have application in studying stem-like populations in other organs (Hombach-Klonisch et al., 2008). Towards this end, we tested the surface markers CD24, used for sorting of prostate, breast and colon adult stem cells, CD34, used for sorting skeletal muscle stem cells as well as endothelial and hematopoetic progenitors, CD44, label of breast, prostate and bladder cancer stem cells, and the colonic and neural progenitor marker CD133 (Marhaba et al., 2008; Shackleton et al., 2006; Uchida et al., 2000).

To direct our study at cells of the lower airway, we utilized the naphthalene injury paradigm, which rapidly induces Clara cell-specific necrosis via conversion of the drug to a reactive and toxic arene species by the Cyp2F2 microsomal enzyme. Efficacy of necrotic Clara cell exfoliation was determined by cytological changes seen upon transmission electron microscopy of lung tissue harvested at varying time points after intra-peritoneal naphthalene injection (Figure 2.1). Vacuolization of the cytoplasm and irreversible change was apparent as early as 24 hours after injection. By 48 hours post injury, the terminal and respiratory bronchiole airways were nearly absent of cells with non-ciliated secretory morphology, indicating successful Clara cell ablation. These results were corroborated by immunofluorescence microscopy against Clara cell secretory protein (CCSP) (Figure 2.1). CCSP+ cells were detected at both the bifurcation of bronchioles and the bronchioalveolar duct junction at 48 hours post injection. We observed restoration of CCSP signal to near pre-injury levels by 120 hours after naphthalene administration, suggesting expansion of the CCSP cells. Based on these dynamics, we choose 48 and 72 hours post injection as time points for our study, as this corresponds to periods when only injury resistant CCSP+ cells are present and when these cells should be mitotically active, respectively.

Of the markers tested, CD24 was able to successfully delineate four previously undescribed populations all having the immune-phenotype of Sca-1+/CD34+/CD45-/Pecam- (Figure 2.2). Based on the relative CD24 expression, we termed these groups CD24(-), CD24low, CD24mid and CD24high. The

abundance of these populations changed with time after injury, with an approximate three-fold increase of CD24 high cells at 72 and 96 hours (Figure 2.2). When these four populations were sorted and analyzed by RT-PCR we found that both CD24mid and CD24high cells were found to express CCSP, albeit at different levels. CD24high cells were almost 10-fold enriched for CCSP expression over the Sca-1 only selected population of CD45-/Pecam- cells. The CD24mid population showed a more modest increase. Expression of SPC was comparable between these two groups but undetectable in CD24low or CD24(-) fractions. Notably, CD24high cells also expressed elevated levels of the epithelial cell marker Epcam and lower levels of the enzyme that confers naphthalene sensitivity, Cyp2F2, than CD24mid cells (Figure 2.3). It is possible that of the two populations positive for CCSP expression, the CD24high cells represent Clara cell progenitors of the epithelial lineage within the Sca-1+ fraction of the lung, while CD24mid cells may be their recent daughters or a heterogeneous mix of cells.

To confirm these observations we sorted the CD24 subgroups of the Sca-1+/CD45-/Pecam- fraction from uninjured mice and analyzed them by immunofluorescence using a CCSP specific antibody. Approximately 85% of the CD24high subgroup were found CCSP+, compared to 30% of CD24mid cells, 4% of CD24low cells and >1% of CD24(-)(Figure 2.5). In general, all groups demonstrated relative quiescence in the steady-state, evidenced by very little immunoreactivity to the mitosis label phospho-histone H3 (ph-HH3). In cells collected 72 hours after injury, however, this number increased dramatically, with 56% of CD24high cells staining positive for ph-HH3 (Figure 2.5). These data indicates that CCSP+ cells found cycling after injury are found almost exclusively within the CD24high sub-fraction of Sca-1+/CD45-/Pecam- lung cells.

Injury resistant Clara cell progenitors of the lower airway have been reported to reside at the bifurcation of bronchioles as well as the bronchioalveolar duct junction (BADJ). Consistent with the hypothesis that CD24high/Sca-1+/CD45-/Pecam- cells are lower airway progenitors, we observed bright staining for CD24 in the proximity of the bronchioalveolar duct junction in uninjured and injured mice (Figure 2.4). These cells were CCSP+ in both injured and uninjured animals (Figure 2.4)

CD24high/Sca-1+/CD45-/Pecam- Cells Display Features of Lung Progenitor/Stem Cells

To further characterize these cells and evaluate their potential function as true progenitor/stem cells, we first determined mRNA expression levels of the common markers of embryonic pluripotency Oct4, Sox2 and Nanog in RNA isolated from the respective CD24 subfractions (Figure 2.6). As negative

expression control, we employed embryonic stem cells (ESCs) expressing an inducible Oct4 targeted shRNA which causes rapid differentiation and as a positive control, ESCs expressing luciferase targeted shRNA. Levels of SOX2, Nanog and OCT4 transcript were normalized to B2M. Intriguingly, CD24high cells are characterized by expression levels of the pluripotency initiating factor Oct4 that are comparable those observed in undifferentiated ESCs. Although to a lesser extent, CD24mid cells also showed elevated levels of Oct4. These results were mirrored by increase in NANOG expression, a transcription factor necessary for maintaining the pluripotent ground state in ESCs. Consistent with a lower respiratory tract origin, all of the CD24 sub-fractions expressed low levels of Sox2, with appreciable transcript detected only in the CD24low population (Tompkins et al., 2011).

To verify the expression results, we next employed use of an Oct4-GFP reporter mouse, which expresses a fusion protein under the control of the endogenous Oct4 locu allowing the expression of Oct4 to be easily traced by immunostaining or FACS. When lungs from uninjured mice were harvested and analyzed by flow cytometry we observed GFP+ signal when compared to control wt C57Bl/6 animals (Figure 2.7). Oct4-GFP+ cells were present in both the CD45+ and CD45- fractions, but not in the Pecam+ fraction. Both marrow-derived and non-marrow derived cell populations are enriched by injury, evidenced by increased count 48 hours after naphthalene injection. When we looked at the four CD24 sub-fractions of Sca-1+/CD45-/Pecam- cells, we found increased Oct4-GFP reporter activity in all populations when compared to Sca-1(-) cells, with CD24high cells displaying the highest GFP signal (Figure 2.7).

To provide functional evidence that CD24high/Sca-1+/CD45-/Pecam- cells were indeed a bronchial progenitor population, we next decided to test their ability to engraft into syngenic hosts. To this end, we utilized C57BL/6-Tg(CAG-EGFP)131Osb/LeySopJ mice, referred to simply as EGFP mice from herein, that express eGFP cDNA from the chicken beta-actin promoter with cytomegalovirus enhancer . The transgene is homozygous lethal, so mating with wt C57Bl/6 produce fluorescent and non-fluorescent littermates in approximately equal numbers. Cells were harvested from EGFP mice injured 48 hours prior with naphthalene and sorted based on surface marker expression. Equal number of cells from each of the CD24 subfractions, in totals ranging from 10,000 to 100,000, was introduced to wild-type non-fluorescence littermate hosts via intra-tracheal instillation.

Mice were sacrificed three months after surgery and engraftment success was determined by immunofluorescence microscopy (Figure 2.8). Successful engraftment was detected within recipient lungs of mice transplanted by each of the CD24 sub-fractions, with the CD24high fraction being most

efficient in doing so. To determine whether transplanted cells were able to generate differentiated epithelium, we stained for CCSP and SPC expression. Evidence of CCSP+/GFP+ cells within the bronchial airspace of animals receiving both CD24mid and CD24high cells was readily apparent. Donor derived Clara cells constituted the majority of CCSP+ cells in mice receiving CD24high transplants and a smaller but significant amount in CD24mid transplants. In both cases, GFP+ cells occurred in contiguous areas of the airway, rather than interspersed patches. SPC+/CCSP-/GFP+ cells were detected within the peripheral airways of CD24mid and CD24high cells, indicating that both are able to generate differentiated Type 2 pneumocytes although at diminished efficacy compared to their contribution to CCSP+ cells. These data suggest preferential growth within the region of lung from which they are derived.

Molecular Characterization of CD24high/Sca-1+/CD45-/Pecam- Cells

In order to gain insight into the biology and molecular characteristics of the different sub-populations of Sca-1+/CD45-/Pecam- lung cells, we performed gene expression analysis on samples sorted from animals injured with naphthalene 48 hours before sacrifice. We chose this time after injection because it corresponded with the point at which only injury resistant progenitors are present within the lung.

RNA was extracted from 10,000 FACS purified cells according to the specifications of the Miltenyi SuperAmp protocol and hybridization carried out on the Agilent whole genome 44K array. Probe intensity data was furnished by Miltenyi. Comparative gene ratios were calculated by establishing the minimum value across data sets as baseline for a gene identifier. Log ratios were constructed and values falling below a 3-fold increase over baseline were excluded (Figure 2.9). As the method employed for RNA amplification in this experiment is tailored for small sample material, it is notoriously error prone. We chose the 3-fold cutoff point to limit false discovery, as most stochastic variation occurs in instances of small variation. From this data set, we then constructed a list of 10-fold increased genes for pathway analysis and a biomarker candidate list based on probe intensity and specificity to one CD24 sub-fraction.

Similar to what we observed in our initial characterization of the CD24 fractions of Sca-1+/CD45-/Pecam- cells, analysis of lung epithelial lineage markers from the microarray data set indicates that CD24high cells express both CCSP and SPC (Figure 2.10) While CD24mid cells also expressed CCSP, they

showed high levels of Cyp2f2, the enzyme that confers naphthalene sensitivity. CD24low cells expressed none of these markers, but were instead typified by increased FoxJ1 expression, indicating possible identity as ciliated cells. None of the epithelial lineage markers we interrogated were expressed at appreciable levels in the CD24(-) cells. Intriguingly, CD24high cells expressed high levels of Krt5, previously thought to specifically label basal cells of the large airways. For an expanded view of marker expression, please refer to the heatmap in Figure 2.10.

Having already obtained evidence of pluripotency factor expression in putative bronchial progenitor cells, we sought to further investigate similarities to known stem cell transcriptomes. 10-fold up-regulated transcripts from each of the CD24 sub-fractions were first compared for overlap with curated gene ontology gene sets within the Broad Institute Molecular Signature Database (Figure 2.11). Surprisingly, signatures from each of the sub-fractions appeared to have overlap with gene groups from stem cell populations.

To better understand the molecular features of the different CD24 sub-fractions we next performed pathway analysis using the Ingenuity software (Figure 2.12). The top hits for canonical pathway activation varied greatly between data sets, suggesting different biological processes occurring in these cells at 48 hours after naphthalene treatment. CD24high cells showed increased activation of Rac, ERK5, MAPK and PI3K/Akt as well as enrichment for cAMP mediated and G-coupled protein signaling. In contrast, CD24mid cells displayed evidence of JAK/Stat, Il-6 and Il-8 activation as well as pathways associated with hepatic fibrosis and stellate cell activation. Previous reports have demonstrated that Il-6, Stat3 and Gp130 are required for epithelial regeneration after naphthalene induced Clara cell toxicity (Kida et al., 2008). It is tempting to speculate that these cells are the migrating daughters of injury resistant progenitors. Further work is needed to confirm this hypothesis.

Identifying a Novel Marker of Bronchial Progenitors

The surface marker Sca-1 has found much utility in the enrichment of cells displaying progenitor or stem cell behaviors in the adult tissues and hematopoetic system of the mouse (Hombach-Klonisch et al., 2008). While aspects of it function promoting GPI-anchored protein signaling within lipid rafts can now be appreciated, there is no human ortholog of the ly6a gene and as such it cannot be used with human specimens (Bradfute, Graubert, & Goodell, 2005). Hence, we sought to uncover new surface markers that could be used to enrich for the newly described putative lung stem cell population.

To this end, we assembled a list of genes that were at least five-fold up-regulated in the CD24high sub-fraction, scored in the top quartile of probe intensity, were classified as plasma membrane proteins by gene ontology and had human ortholog (Figure 2.13). Among these candidate genes, expression of the leukemia inhibitory factor receptor (Lifr), dopamine receptor D5, Leucine-rich repeat-containing G-protein coupled receptor 8 and serotonin receptor 2B were of particular interest to us. The LIFR has had a long standing role in stem cell biology(Kimber et al., 2008). It forms a complex with gp130 and responds to specific ligand binding by signaling via the JAK/Stat pathway. The dopamine receptor D5 (Drd5) was recently described as a marker of cancer stem cells in both solid and hematogenous cancers, as well as Oct4 expressing malignant teratoma cells (Sachlos et al., 2012). Leucine-rich repeat-containing G-protein coupled receptor 8 (Lgr8, or relaxin/insulin-like family peptide receptor 2, Rxfp2) belongs to the same family of receptors as known adult stem cell marker Lgr5 (van der Flier & Clevers, 2009).

HTR2B is a Gq family, G-protein coupled receptor that signals to downstream targets via activation of phospholipase C (Schmuck, Ullmer, Engels, & Lubbert, 1994). Stimulation of HTR2B has been shown to activate the MAPK and NF-κB pathways (Matsuda et al., 2003). Previous reports have demonstrated that homozygous loss of HTR2B renders mice insensitive to hypoxia induced right ventricular failure (Launay et al., 2002). As such, we reasoned that signaling via this receptor might be an important paradigm for hypertrophic change and tissue remodeling responses within the lung. Naphthalene resistant CCSP+ cells have been reported in the proximity of the neuroepithelial body, which itself has been shown to produce high levels of serotonin (Lauweryns, de Bock, Verhofstad, & Steinbusch, 1982). These data underscore a probable importance of HTR2B in regulating the interaction of different components of the stem cell niche. QPCR analysis on extracts of cells sorted from murine lungs before and 48 hours after injury validated expression of HTR2B and Lifr within the CD24high population (Figure 2.14).

When we next analyzed expression of HTR2B by immunofluorescence we detected immune-reactivity in large and medium sized blood vessels, as well as on some CCSP+ cells of the bronchial epithelium (Figure 2.15). Signal intensity varied between cells in the uninjured animal—there were brightly staining cells present at the bronchioalveolar duct junction (BADJ), and occasionally more dimly staining cells within interior regions of the respiratory bronchiole. We found that CCSP+ injury resistant progenitors at the BADJ were brightly stained for HTR2B at 48 hours post naphthalene injection. HTR2B

staining was also found increased within patches of CCSP+ cells at later time points after injury (Figure 2.16).

Based on the current literature, we reasoned that platelets or the NEB would be likely candidates for sources of serotonin (5HT) during the injury process. While the former could regulate progenitor activation during injury, the latter could control replication in the steady state. When we checked for 5HT production in the murine lung, we found little production within or around the bronchiole epithelium (Figure 2.17). It was notably absent from the BADJ, where HTR2B+ cells are found before and after injury. Yet, surprisingly, within 48 hours of injury, large amounts of 5HT could be detected within the cytoplasm of HTR2B+ cells at the BADJ (Figure 2.18). These signals persisted through 96 hours after injury, when a larger patch of cells could be stained for both 5HT and HTR2B. These data indicate a possible autocrine or paracrine signaling axis responsible for regulating progenitor cells responding to naphthalene induced Clara cell ablation. Previous reports have indeed indicated that HTR2B inhibition can mitigate serotonin release in response to a variety of stimuli, presumptively through regulation of the serotonin transporter (Callebert et al., 2006; Diaz & Maroteaux, 2011). Further studies are needed to confirm the mechanism behind the observed increase in 5HT levels upon injury.

HTR2B Signaling is Required for Lung Re-Epitheliazation

Based on these evidence, we reasoned that deregulation of HTR2B activity could impact post injury re-epitheliazation. To test the functional role of this receptor in lung repair, we optimized a treatment protocol for the HTR2B small molecule inhibitor SB-204741 (Forbes, Jones, Murphy, Holland, & Baxter, 1995). Dosing strategies were designed to minimize morbidity associated with co-administration of naphthalene. To determine the effect of HTR2B inhibition, lung tissues were harvested at different points after naphthalene injection; slides were prepared from three planes of sectioning and examined by immunofluorescence.

HTR2B is believed to signal through the Gq coupled pathway, causing an increase in PKC activation that leads to stimulation of the MAPK and NF-KB pathways. Hence phosphorylation of p44/p42 MAPK was used as an indirect read-out for HTR2B activity (B. Li, Zhang, Li, Hertz, & Peng, 2010). Phosphorylated p44/p42 MAPK (ph-Erk1/2) was readily detected within HTR2B+/5HT+cells of vehicle treated animals at 48 and 96 hours post injection (Figure 2.18). This signal was markedly reduced within HTR2B+ cells of SB-204741 treated animals, indicating that inhibitor treatment was successful.

Staining against ph-HH3 indicated that SB-204741 treatment resulted in 4-fold reduction in the number of mitotically active cells at the BADJ 96 hours after naphthalene injection when compared to animals receiving vehicle only (Figure 2.19). This decrease in proliferating cells was accompanied by a greater than 50% reduction in the ratio of CCSP to DAPI staining area measured in the lungs of SB-204741 treated animals compared to vehicle alone (Figure 2.19). Immunofluorescence studies of lungs from animals receiving either SB-204741 or vehicle only revealed a profoundly decreased presence of 5HT in HTR2B+ cells of the BADJ in animals treated with inhibitor (Figure 2.18). This supports the notion that HTR2B stimulation leads to enhanced 5HT production by bronchial progenitors. Further analysis is needed to determine whether the decrease in CCSP+ cells within the bronchial epithelium is due to a deficit of proliferation or increased cell death. Preliminary data in cell culture setting suggest the former to be the most likely explanation.

Discussion

Since the initial reporting of bronchioalveolar stem cells (BASCs), controversy over their true nature has confounded progress towards useful application of insights from their biology towards new therapeutic modalities. Our data sheds light on the conflicting reports concerning BASCs by providing evidence that the Sca-1+/CD45-/Pecam- population of lung cells is in fact highly heterogeneous. We report that additional stratification of the Sca-1+, Pecam-, CD45- lung population yields cells with characteristics of progenitor/stem cells. These cells are characterized by high expression of the cell surface marker CD24 and of genes associated with pluripotency. When transplanted into recipient mice, they not only engraft but also yield differentiated bronchial epithelium. Transcriptional analysis of the putative bronchial progenitor population revealed expression of novel surface markers that unlike Sca-1 have human orthologs, making them potentially useful in a clinical setting. In particular, the serotonin receptor isoform 2B (HTR2B) was highly expressed after injury. Our work suggests a role for autocrine/paracrine serotonin signaling in the regulation of the progenitor niche at the bronchioalveolar duct junction during injury repair.

The finding that Oct4 and NANOG are expressed by an epithelial adult stem cell population within the lung is of particular interest as it adds another wrinkle to the body of work teasing apart if and how these factors may have a role in regulating cells in adult tissue. Since the initial report that Oct4 was not necessary for maintaining adult somatic tissue, multiple groups have come forward presenting evidence otherwise (Lengner et al., 2007). Oct4 and NANOG have been detected in cultured mesenchymal stem cells as well as lung derived populations that display stem cell characteristics

(Kajstura et al., 2011; Tsai, Su, Huang, Yew, & Hung, 2012) In both cases, experimental preparation required an in vitro selection process which could have favored cells with stochastic reactivation of those loci or induced population-wide changes in gene expression. In our study, cells have gone as directly from whole tissue to analysis as possible.

Recent trends in the study of colon and hair follicle epithelium have suggested that multiple stem cells exist in adult organs, comprising both an active and latent pool (L. Li & Clevers, 2010). There appears to be evidence that these latent cells represent a reserve pool of adult progenitors. Both of these tissues represent fast cycling organs with high steady state levels of epithelial turnover. The lung, on the other hand, is relatively quiescent at ground state but can be induced to rapidly proliferate after injury. It is tempting to speculate that Clara cells, as facultative progenitors, represent the fast cycling stem cell in a slow cycling organ. This in turn implies that the CD24high/HTR2B+ cells described above, able act as Clara cell progenitors, are akin to the latent or reserve pool in other tissues. It should then be interesting to generalize data gleamed from the lung into other slow cycling, foregut derived organ systems.

As for the role of HTR2B and serotonin signaling in bronchial epithelium, our data highlight it as an important axis in the regulation of putative adult stem cell populations. The body's largest serotonin store is within circulating platelets, suggesting that post injury changes in vascular permeability may sit on top of a process involving platelet de-granulation and activation of latent epithelial progenitors. HTR2B has also been shown to mediate serotonin release, suggesting that cells expressing it may in fact be paracrine coordinators of the proximal niche. Initial excitatory events may lead to a feed-forward impetus for serotonin release causing changes to progenitor and daughter cells nearby. Data indicating serotonin as a mediator in the bronchial hyperplasia of chronic bronchitis reinforce the concept of this molecule as homeostatic regulator of epithelium in these airways (Lau et al., 2012). We are currently investigating a possible role of platelets and NEBs in mediating regulation of the CD24high positive cells.

Hyperplasia at the BADJ is seen frequently in mouse models of lung adenocarcinoma and evidence suggests that transplant of cells from Sca-1+ fraction can recapitulate disease in a genotype dependant manner (Curtis et al., 2010). Our data suggests that cells forming early hyperplastic lesions may bare strong resemblance to the CD24high/Sca-1+/CD45-/Pecam- cells we have identified as injury responsive bronchial progenitors. In principle, these cells may be governed by similar signaling processes as normal progenitors, making HTR2B and other CD24high specific targets potentially useful in the study of tumor onset and progression.

While all of our experiments have thus far been conducted using cells of murine origin, we are now expanding these studies to human tissue. We are compelled to investigate changes that putative progenitor populations may undergo in conditions such as bronchial hyperplasia, COPD or idiopathic pulmonary fibrosis. Given the standing connection between serotonin signaling and each of these diseases, it is likely that HTR2B+ cells are profoundly impacted and may even play a mechanistic role in pathogenesis. We are also particularly interested in exploring how this population may be related to tumorigenesis in NSCLC. Preliminary data has suggested the existence of cells baring molecular features of CD24high/HTR2B+ cells within certain tumor-derived cell lines. Manipulation of serotonin signaling resulted in dramatic changes to cell fate. One may speculate that the CD24high population could represent the cancer cell of origin for a subset of non-small cell lung carcinomas characterized by neuro-epithelial features.

Experimental Procedures

Maintenance and Breeding of Mice

All animals were housed in a clean, monitored, environmentally controlled environment with access to food and water ad libidum. Wildtype C57Bl/6 mice were obtained from Charles River (Wilmington, MA, USA). C57BL/6-Tg(CAG-EGFP)131Osb/LeySopJ mice were purchased from Jackson Labs (Bar Harbor, ME, USA) and bred to wildtype C57Bl/6 mice. As the transgene is homozygous lethal, genotype was scored by presence or absence of fluorescence in skin and retinal tissue. B6;129S4-Pou5f1tm2Jae/J (Oct4-GFP reporter mice) were obtained from Jackson Labs (Bar Harbor, ME, USA) as a homozygous breeding pair. All breeding was within genotype to retain homozygosity of the line.

Animal experiments were performed following approval of Institutional Animal Care and Use Committees (IACUC). Procedures designed to assure that discomfort and injury to animals was limited were employed. Analgesic, anesthetic, and tranquilizing drugs were used where to minimize discomfort and pain to animals.

Naphthalene Injury

Female mice aged 4-8 weeks were administered a single dose of naphthalene (Sigma-Alrich, St. Louis, MO, USA) suspended in vegetable oil via intraperitoneal injection at 8 AM. Volume of naphthalene solution administered was adjusted to deliver a mass of 225 mg naphthalene per kilogram mouse. Afterwards, mice were housed with Dietgel Recovery food (ClearH2O, Portland, Me, USA) and monitored for treatment efficacy and animal discomfort.

HTR2B Inhibitor Treatment

SB204741 (Tocris Pharmaceuticals) was suspended in sterile DMSO and administered to mice by intra-peritoneal injection at a dosage of 1 mg/kg, 12 hours before naphthalene administration. Mice were continued on a .5 mg/kg dosage schedule every 24 hours, starting 12 hours after naphthalene administration.

Non-surgical Preparation for Transplant

Offspring from mating of C57BL/6-Tg(CAG-EGFP)131Osb/LeySopJ with wildtype C57Bl/6 mice were genotyped with transgene baring mice utilized as donor and non-transgenic littermate serving as recipient for transplant surgery. 48 hours prior to donor mouse sacrifice, donor mice were injured with naphthalene as described. The day of surgery, mice were sacrificed using carbon dioxide asphyxiation and cervical dislocation.

Generation of Lung Cell Suspension

After sacrifice, mice were dissected to allow for clear access to the thoracic cavity. The brachial arteries and aorta were severed and phosphate buffered saline (PBS) pH 7.2 instilled into the right ventricle of the heart by peristaltic pump to flush red blood cells from lung vasculature. Once clearing had been accomplished, digestion solution made of collagenase IA (Sigma-Alrich, St. Louis, MO, USA) and hyaluronidase (Sigma-Alrich, St. Louis, MO, USA) suspended in DMEM supplemented with penicillin streptomycin was instilled into the trachea. Lungs were removed, the trachea, bronchii, and hilar lymph

nodes dissected away and the remaining tissue minced into 1 mm pieces. Digestion was carried out for 1 hour at 37 degrees Celsius with periodic agitation by vortexing.

FACS and Flow Cytometry of Lung Tissue

Once lung tissue had been digested, samples were washed in complete DMEM media, filtered through 100 micron mesh, pelleted and washed again with cold PBS. Red blood cells were lysed using hypotonic ammonium chloride lysis buffer, and cells washed twice more with cold PBS. Cells were incubated with directly fluorescent conjugated antibodies to the desired antigens for 20 minutes on ice. Flow cytometry was perfomed using the LSRII running FACS Diva software. Single channel gating eliminated all cells expressing the surface antigen CD31, which labels endothelial cells, and CD45, which labels marrow-derived cells. Sorting experiments were performed using the BD Aria II.

Trans-thyroidal Surgery

Animals were anesthetized using a combination of Ketamine and medetomidine at 75 and 1 mg/kg, respectively. The area between the mandibular margin and the top of the rib cage was shaved and seventy percent ethanol was used for anti-septic prior to surgery. All tools were autoclaved and kept sterile before transplant, and sterilized using the Germinator dry sterilization system (Roboz, Gaithersburg, MD, USA) in between mice. Approach to the trachea was directed at the most avascular region of the thyroid to avoid bleeding. Incision into the trachea was limited in size to the smallest opening that would accommodate the transplant delivery. Cells were delivered suspended in PBS pH 7.2 supplemented with 2 mM EDTA and .05 % BSA. Afterwards, animals were shut using resorbable sutures and wounds were dressed with sulfonamide antibiotics. Recipient mice were monitored for recovery from anesthesia, then placed in individual housing with Dietgel Recovery food (ClearH2O, Portland, Me, USA).

Immunofluorescence

Whole tissue sections were prepared from animals sacrificed and exsanguinated using PBS flushing. Lungs were removed, washed and fixed in 4% formaldehyde/PBS overnight. Processing and

embedding was performed by RADIL (University of Missouri) and the CSHL histology core facility, sections were cut at a thickness of 5 um. Slides were heated to 65 degree Celsius for 30 minutes to remove excess paraffin then cleared using Histoclear and rehydrated in stepwise graded alcohol. After washing in PBS, slides were treated with H2O2 to limit autofluorescence. Following another round of washes, slides were boiled in citrate antigen retrieval buffer for 20 minutes.

Alternatively, fresh frozen sections were prepared by snap freezing of exsanguinated lungs instilled with OCT/buffered sucrose mixture to maintain architecture and mounted in OCT blocks. Tissue was sectioned by cryostat at a thickness of 5 microns. Slides were dried for 15 minutes at room temperature then washed briefly in PBS and fixed using neutral buffered formalin.

Permeabilization was accomplished with 0.5% triton x-100 in PBS with 2% BSA, followed by washing with 1% BSA in PBS. Slides were incubated with primary antibody at 4 degrees Celsius overnight. Secondary antibody labeling was performed with the species appropriate fluorescent conjugate for one hour at room temperature the next day. DAPI was used to label nuclei. All slides were mounted using p-Phenylenediamine anti-fade media. Imaging was performed on the Zeiss 710 confocal microscrope running Zen software.

Quantification of CCSP and DAPI Immunofluorescence

To quantify area of staining for CCSP and DAPI in IF mounts of mouse lung, tissue was prepared and stained as described. Slides were scanned on the Aperio Scanscope FL using fixed exposure imaging. Afterwards, the analysis suite within the Image Scope software was used for area above threshold quantification of fluorescence intensity. Arbitrary cutoff was set at 20% of maximal signal, which accounted for all CCSP+ cells in uninjured mice without encompassing any background.

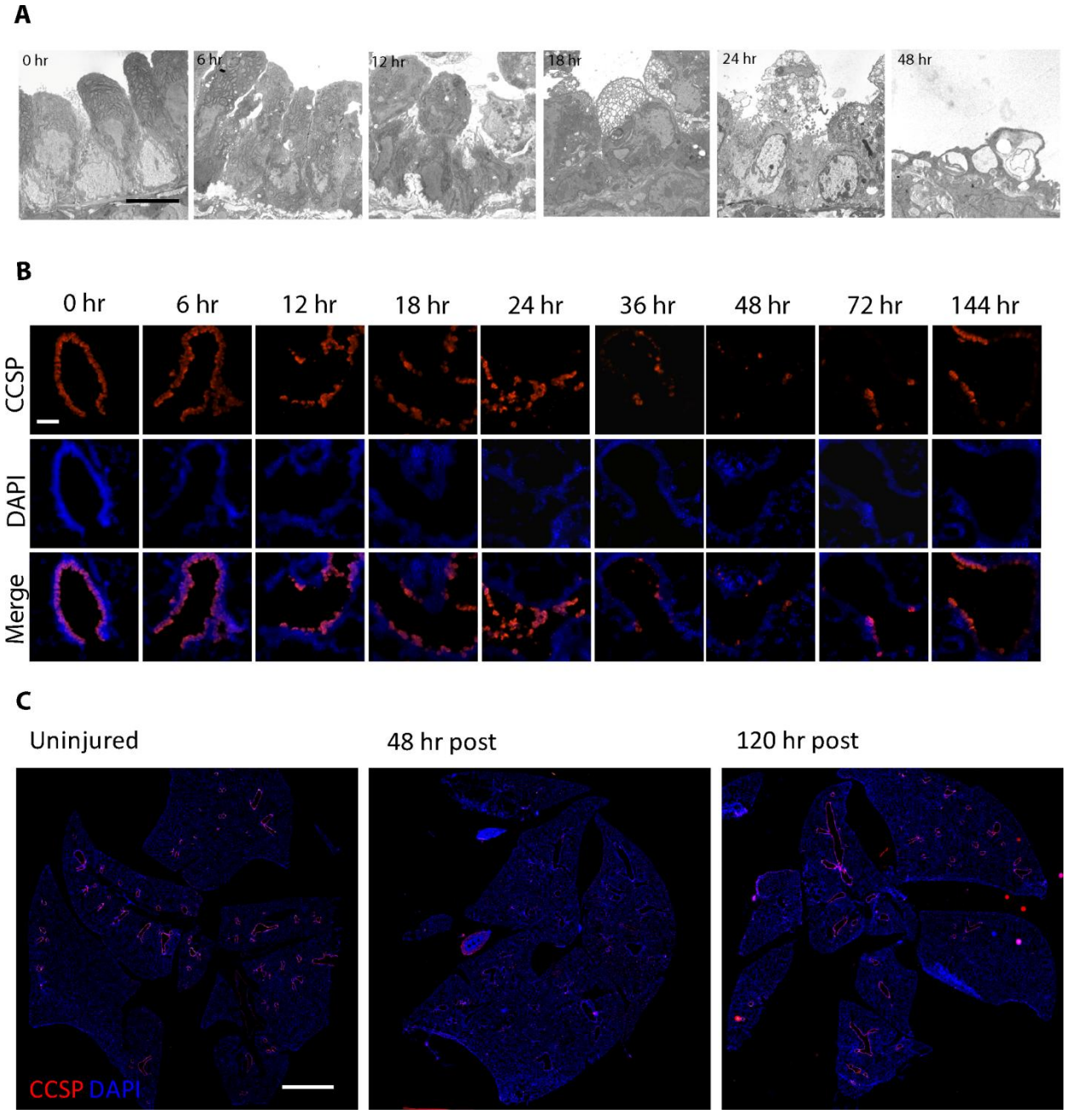

Figure 2.1 Naphthalene Causes Necrotic Exfoliation of Clara Cells. TEM of bronchial airways (A) from mice sacrificed at different times after naphthalene injection demonstrates cytological changes in Clara cells consistent with necrosis. Immunofluorescence microscopy of representative bronchioalveolar duct junctions (B) from mice during injury shows exfoliation of CCSP+ epithelium by 36 hours after injection. Lung wide CCSP+ cells levels (C) are greatly diminished by 48 hours after naphthalene administration but recover to near normal levels by 120 hours.

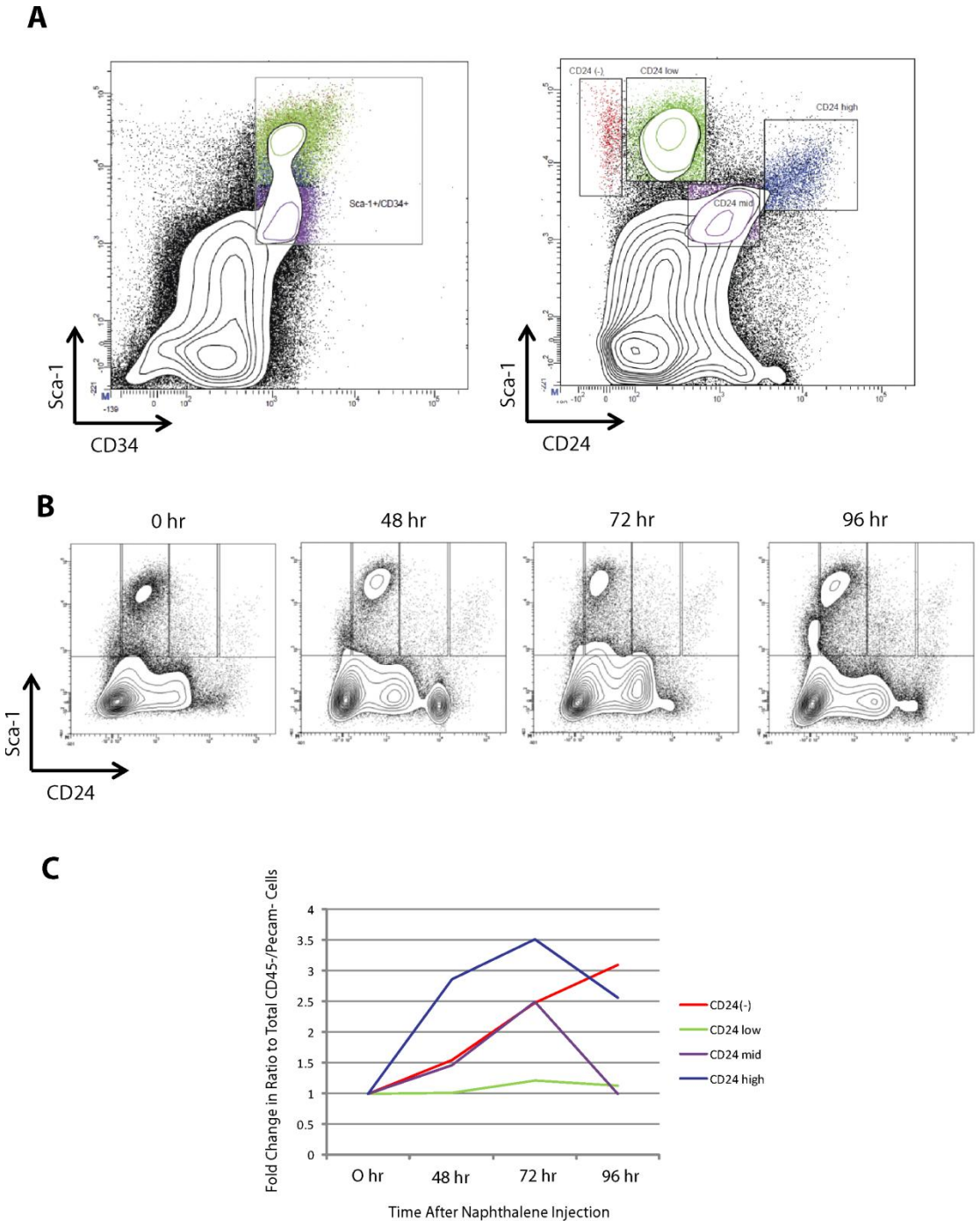

Figure 2.2 CD24 Subdivides the Sca-1+/CD34+/CD45-/Pecam- Fraction of the Lung. Flow cytometry analysis of lung cell suspension **(A)** shows that multiple populations identified by different levels of CD24 staining are present in the Sca-1+/CD34+/CD45-/Pecam- fraction of the lung. Gates set on the Sca-1 vs. CD24 axis color data points on the Sca-1 vs. CD34 axis. These CD24 subfractions are dynamic with time after naphthalene injury **(B)** as shown by flow cytometry of mice at defined points after injection. Quantification **(C)** of fold change from established baseline values shows the greatest relative increase in the CD24high cell group.

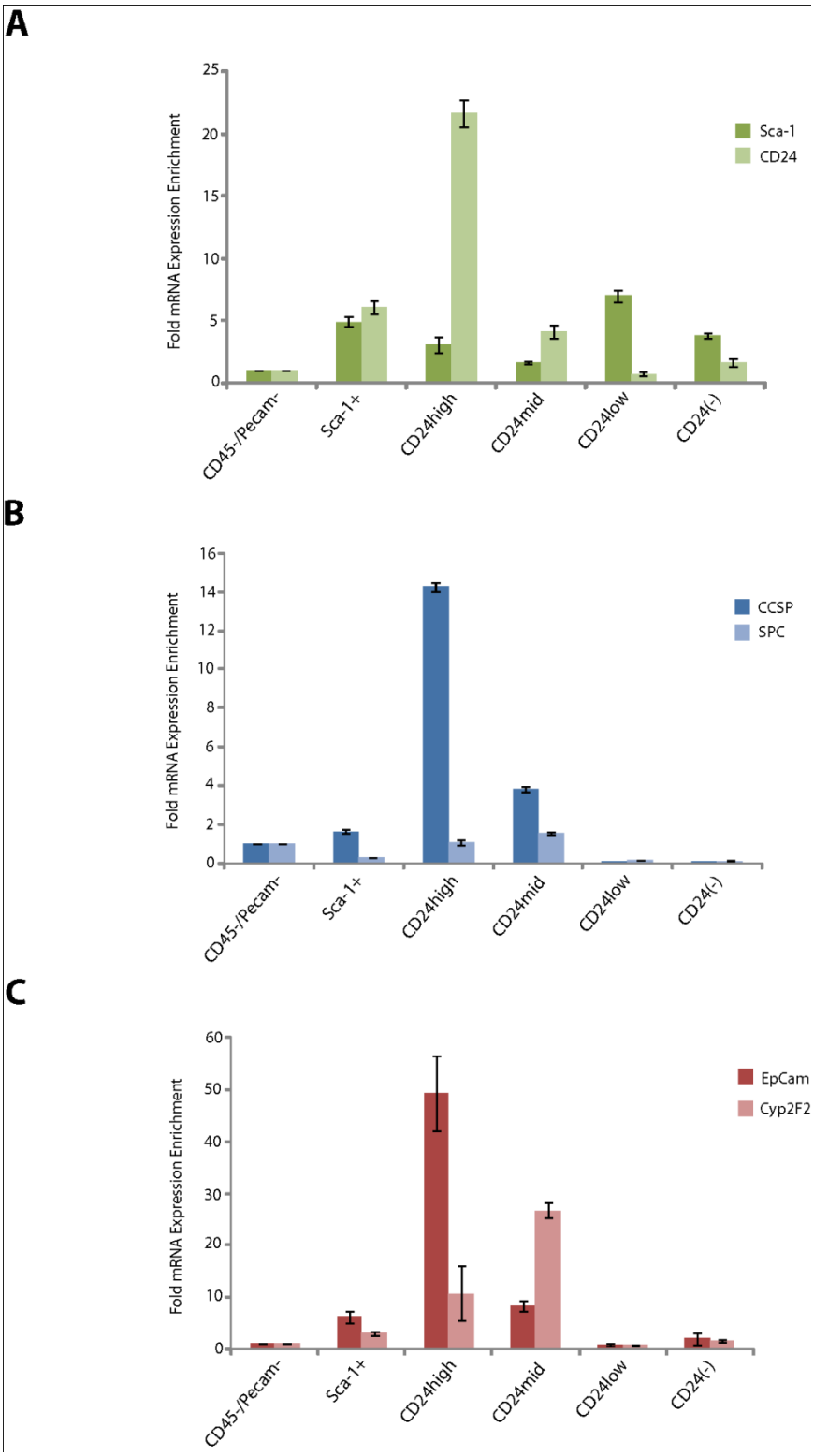

Figure 2.3 QPCR Analysis of Cells Sorted from the CD24 Sub-Fractions. Cells were sorted by FACS using the algorithm outlined in Figure 2.2 then tested for expression of: **(A)** markers used for sorting, **(B)** cytological markers of BASCs, and **(C)** markers of epithelial and Clara cell lineages by QPCR.

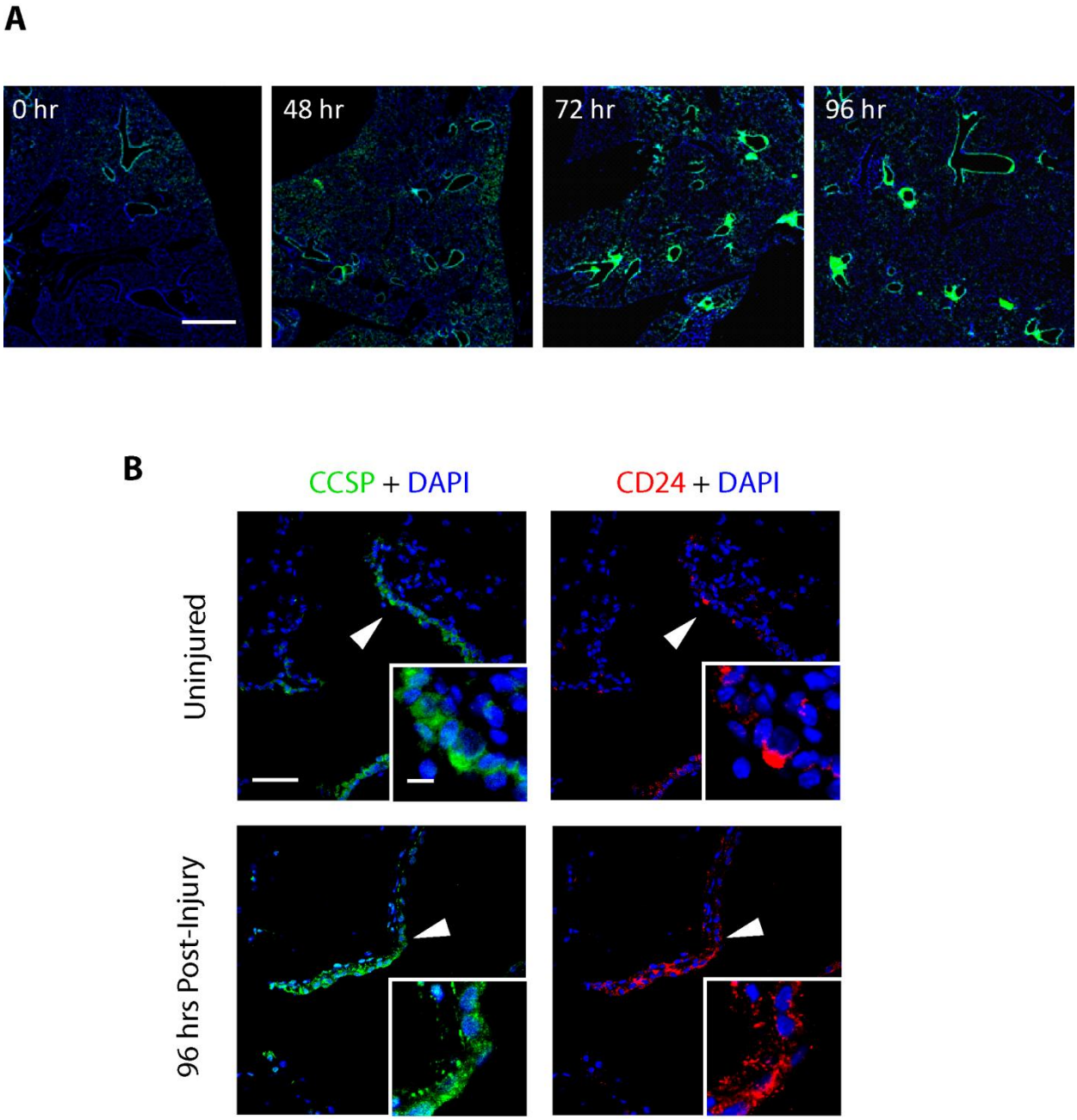

Figure 2.4 Immunofluorescence of Lungs Reveals CD24 Expression in Bronchial Epithelium. Lungs prepared from mice after naphthalene injury **(A)** display increasing levels of CD24 in bronchial structures and the peri-bronchial region (Scale bar is 1 mm). These CD24+ cells are CCSP+ **(B)** in both the uninjured and injured animal (Scale bar is 80 micron, inset, 10 micron).

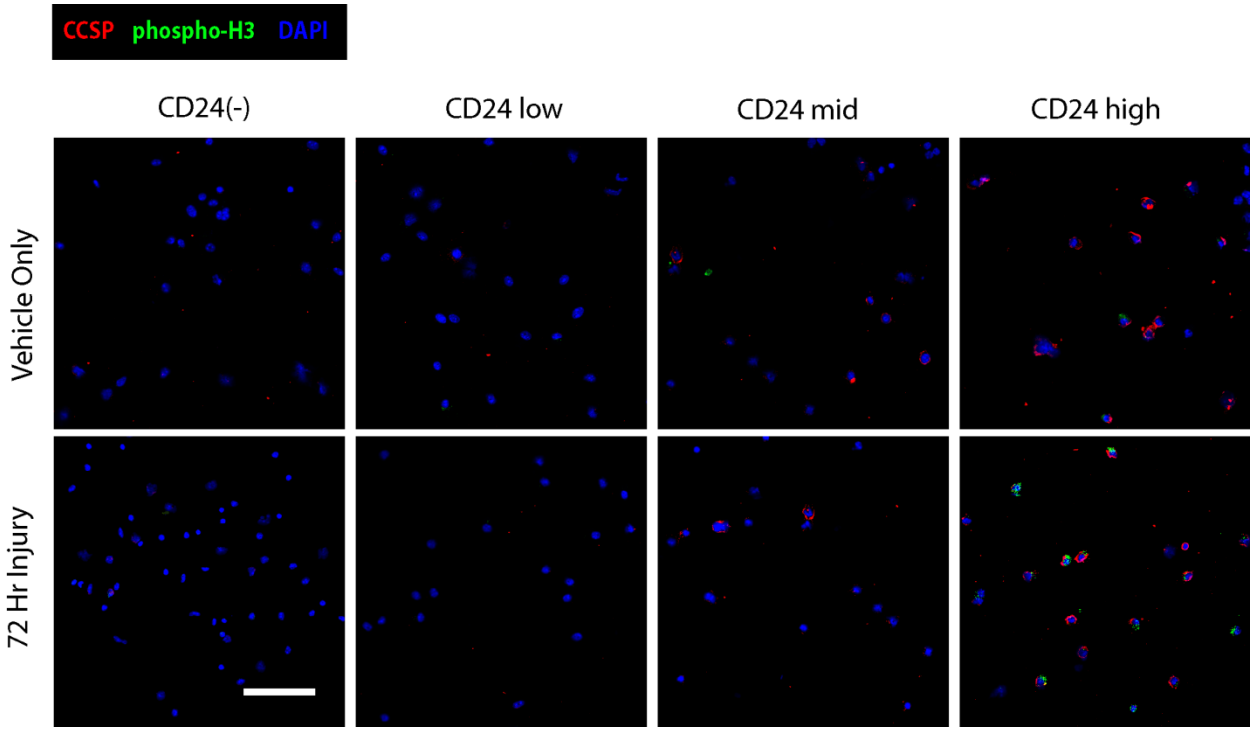

Figure 2.5 Staining of Sorted Cells for Purity and Response to Injury. CD24 subfractions of Sca-1+/CD45-/Pecam- cells were sorted from uninjured or 72 hour post naphthalene injection animals and stained for CCSP+ and phospho-Histone H3 (Scale bar = 50 micron). The majority of CCSP+ cells are located in the CD24high fraction in both injured and uninjured animals. Detection of mitosis in uninjured animals is rare but increases dramatically 72 hours after injury.

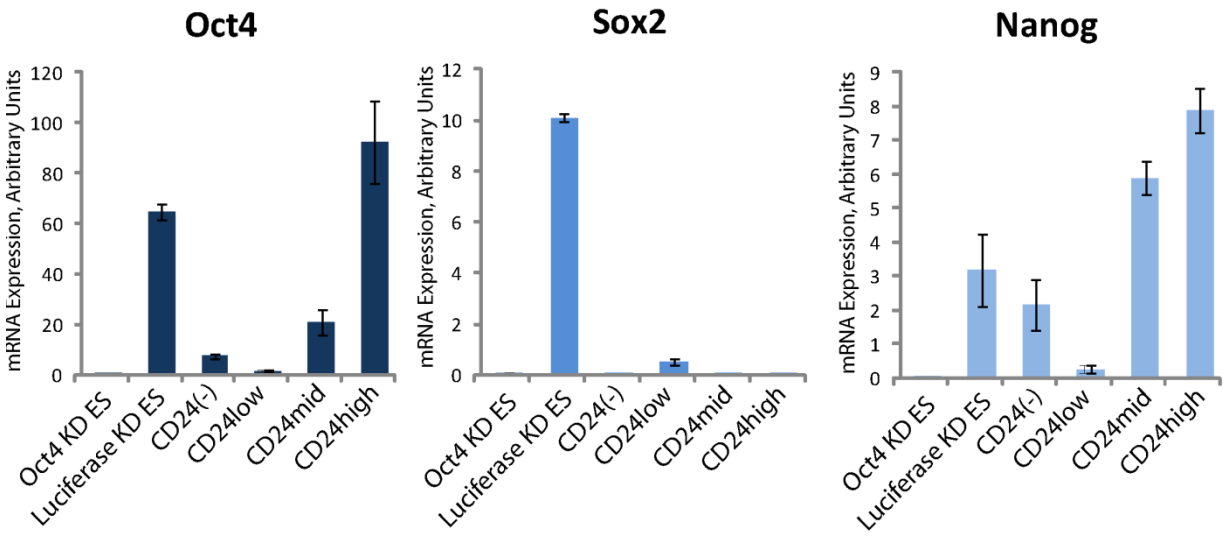

Figure 2.6 QPCR of Transcripts Associated with Pluripotency. Sorted cells were compared to either Oct4 KD (differentiated) or Luciferase KD (undifferentiated) embryonic stem cells for relative expression levels of pluripotency factors Oct4, Sox2 and Nanog. Both CD24high and CD24mid display elevated levels of Oct4 and Nanog but not Sox2.

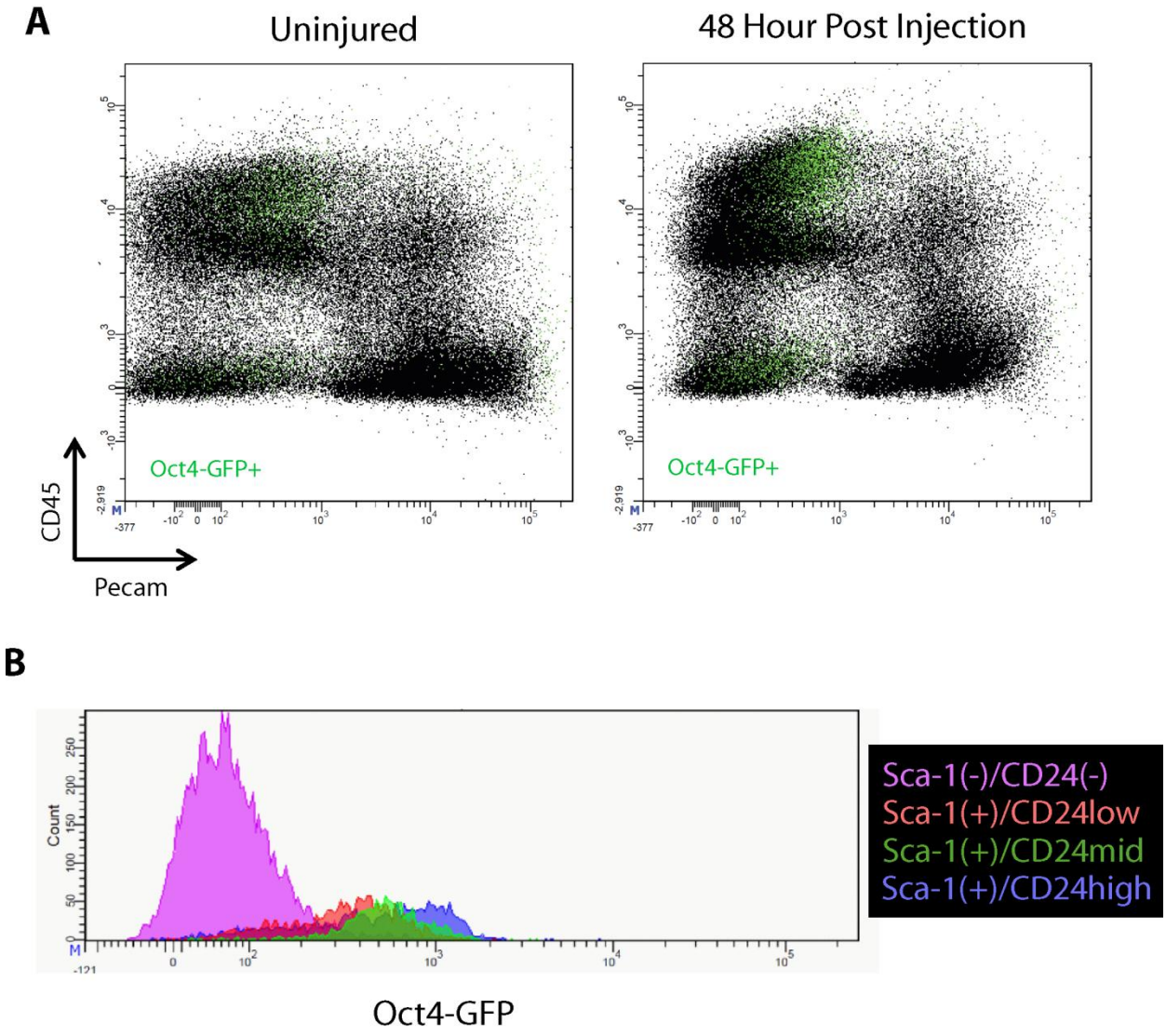

Figure 2.7 Flow Cytometry Analysis of Oct4-GFP Reporter Mouse Lungs. Cells gated positive for Oct4-GFP reporter construct expression **(A)** are displayed in green on plots for their relative expression of CD45 and Pecam. GFP+ cells exist in both marrow derived and non-marrow derived fractions. No reporter activity was detected in Pecam+ endothelial cells. Oct4-GFP expression was increased in response to injury. CD24 subfractions of Sca-1+/CD45-/Pecam- cells **(B)** are plotted for their relative expression of the Oct4-GFP reporter construct in comparison to the Sca-1- population.

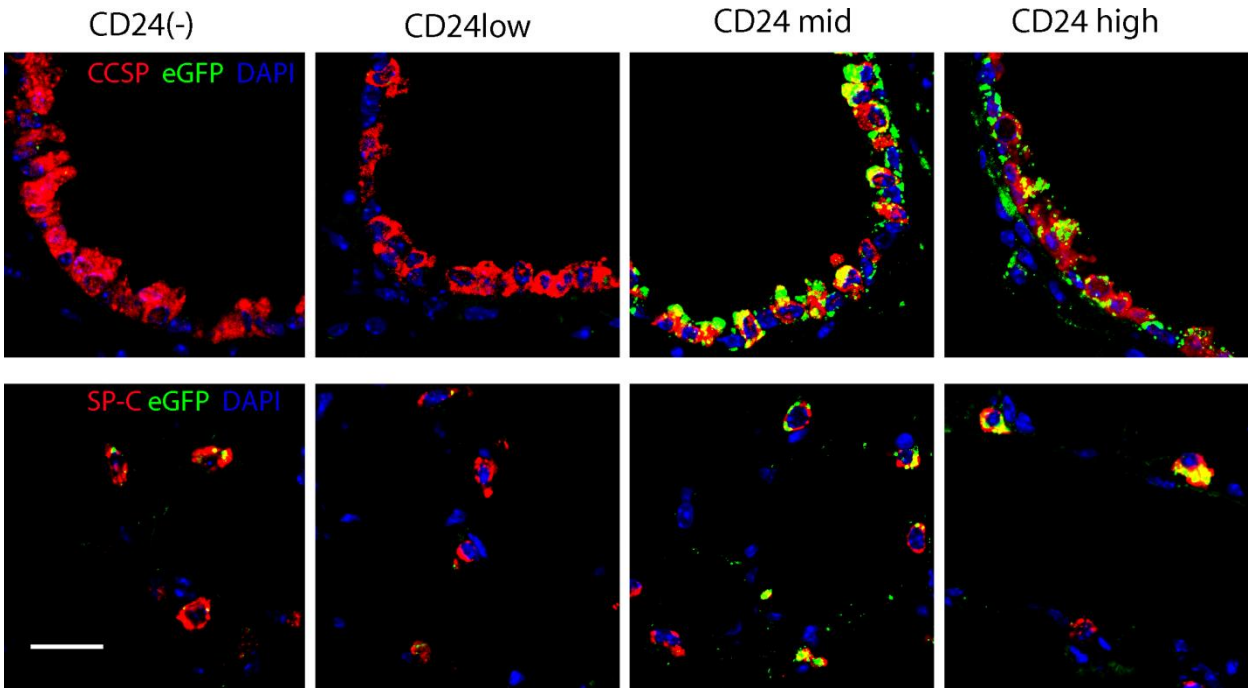

Figure 2.8 Detection of Donor Derived Cells In Transplant Recipient Mice. Lungs of transplant recipient mice were stained for GFP to detect engraftment of donor cells as well as lineage markers CCSP and SPC to detect differentiation of Clara cells and type II pneumocytes, respectively (Scale bar = 50 micron).

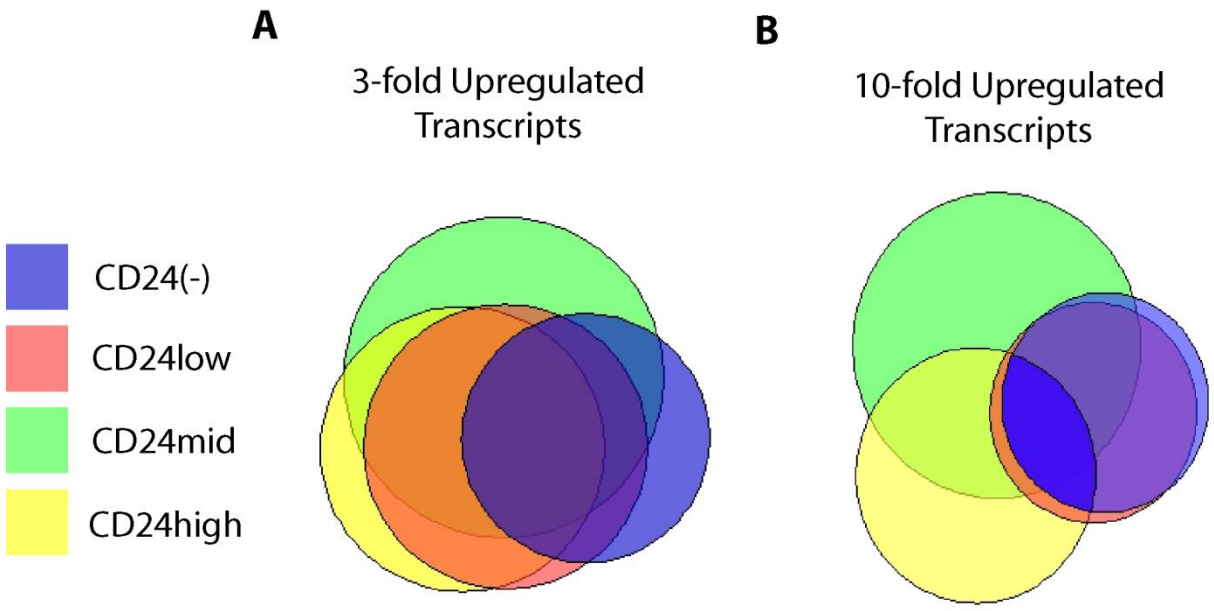

Figure 2.9 Comparison of Transcriptomes From Putative Progenitor Populations. Venn diagram depiction of overlap between genes found **(A)** 3-fold and **(B)** 10-fold upregulated compared to baseline minimum value.

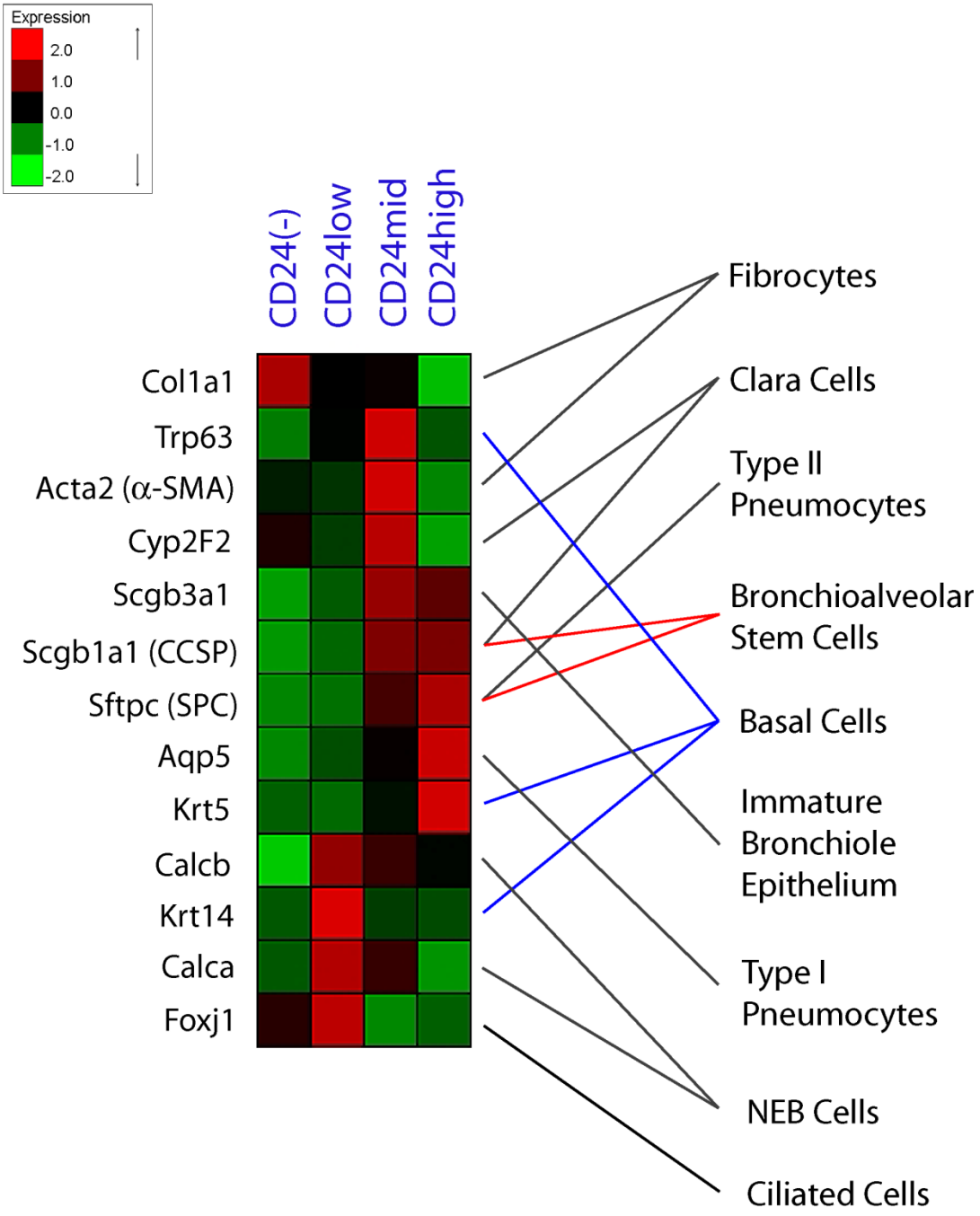

Figure 2.10 Heatmap of Lung Epithelium Lineage Markers. Expression of lineage markers from cells harvested 48 hours after injury. Identifiers are to the left of the heat map, cell types reported as expressing them to the right. Markers of putative stem cell populations as reported in the literature are colored red and blue. CD24high cells display an expression pattern consistent with that of a lower airway bronchial progenitor cell.

Gene Set Name	# Genes in Gene Set (K)	CD24high Genes in Overlap (k)	k/K	p value	CD24mid Genes in Overlap (k)	k/K	p value	CD24low Genes in Overlap (k)	k/K	p value	CD24(-) Genes in Overlap (k)	k/K	p value
BENPORATH_ES_WITH_H3K27ME3	1117	341	0.3053	0.00E+00	457	0.4091	0.00E+00	NS	NS	NS	NS	NS	NS
BENPORATH_SUZ12_TARGETS	1037	306	0.2951	1.28E-13	416	0.4012	4.44E-16	NS	NS	NS	NS	NS	NS
BENPORATH_NANOG_TARGETS	988	288	0.2915	3.29E-12	410	0.415	0.00E+00	213	0.2156	1.73E-09	356	0.3603	0.00E+00
BENPORATH_EED_TARGETS	1062	302	0.2844	2.24E-11	NS	NS	NS	NS	NS	NS	NS	NS	NS
BENPORATH_SOX2_TARGETS	734	221	0.3011	4.75E-11	NS	NS	NS	164	0.2234	1.07E-08	256	0.3488	0.00E+00
BENPORATH_PRC2_TARGETS	652	200	0.3067	6.88E-11	NS	NS	NS	NS	NS	NS	NS	NS	NS
DOUGLAS_BMI1_TARGETS_UP	512	NS	NS	NS	227	0.4434	2.04E-14	132	0.2578	2.14E-11	185	0.3613	0.00E+00
MUELLER_PLURINET	299	NS	NS	NS	146	0.4883	1.18E-13	NS	NS	NS	NS	NS	NS
YKH_HEMATOPOIESIS_STEM_CELL_QTL_T	984	NS	NS	NS	NS	NS	NS	210	0.2134	5.42E-09	289	0.2937	0.00E+00

Figure 2.11 MSigDB Detected Overlap with Stem Cell Gene Sets. Significant overlap between curated gene sets and 10-fold upregulated genes from each identified CD24 subfraction is listed. NS denotes no significant overlap.

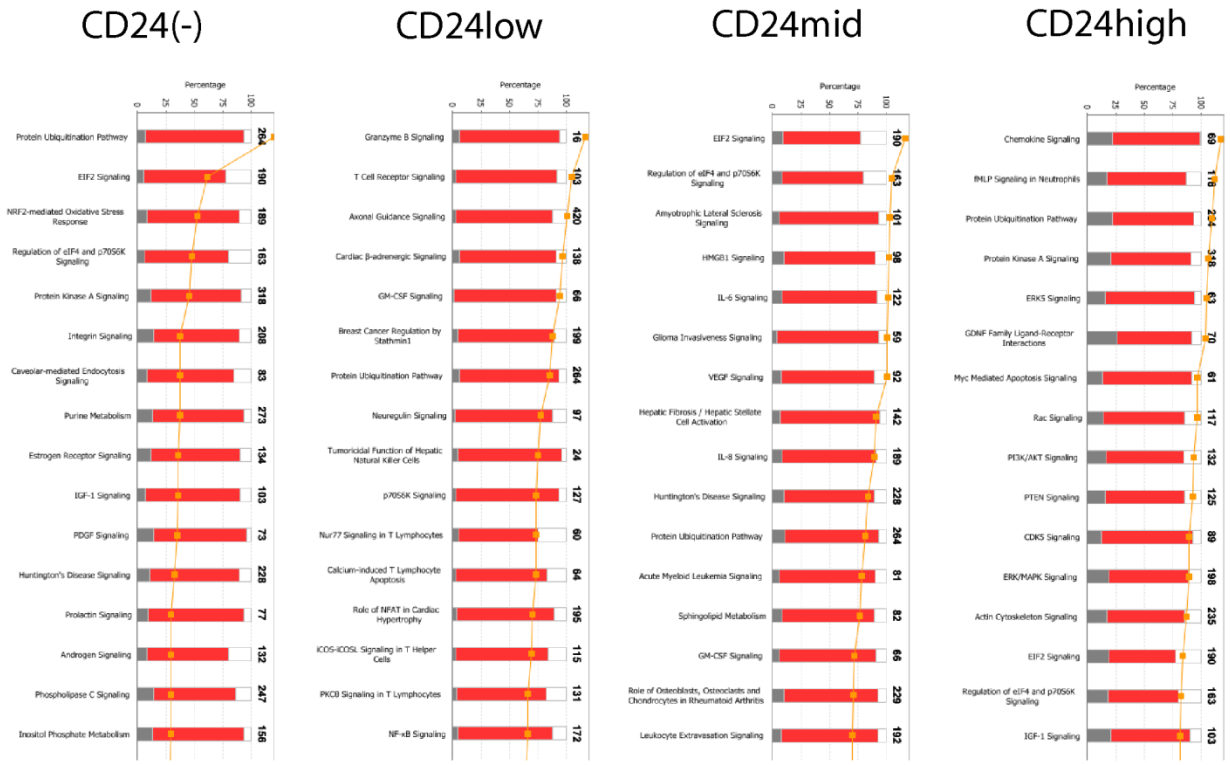

Figure 2.12 Ingenuity Pathway Analysis of CD24 Subfractions. Shown are canonical pathways detected by core analysis on the Ingenuity platform using 10-fold upregulated transcript sets. Red area indicates relative overlap of annotated pathway with the interrogated expression data.

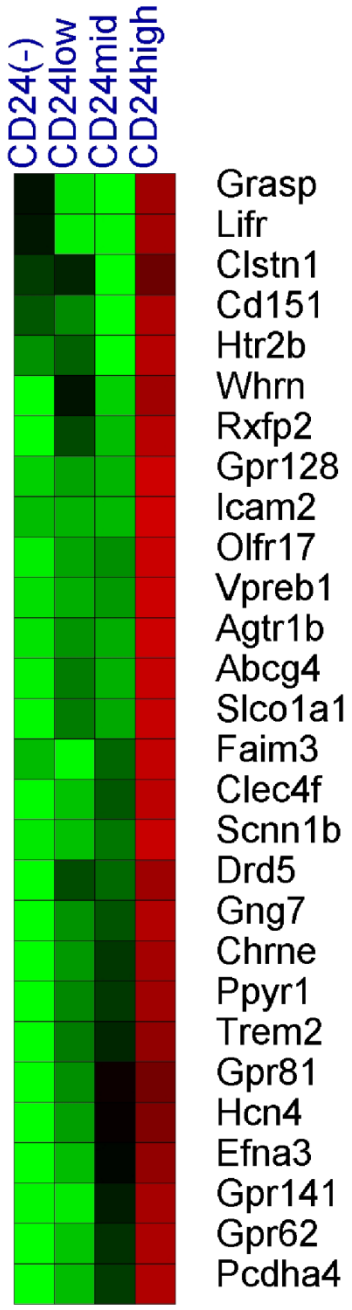

Figure 2.13 Heatmap of Surface Markers Labeling CD24high/Sca-1+/CD45-/Pecam- Cells. Color depicts relative expression. All genes shown were in the top quartile of expression by microarray.

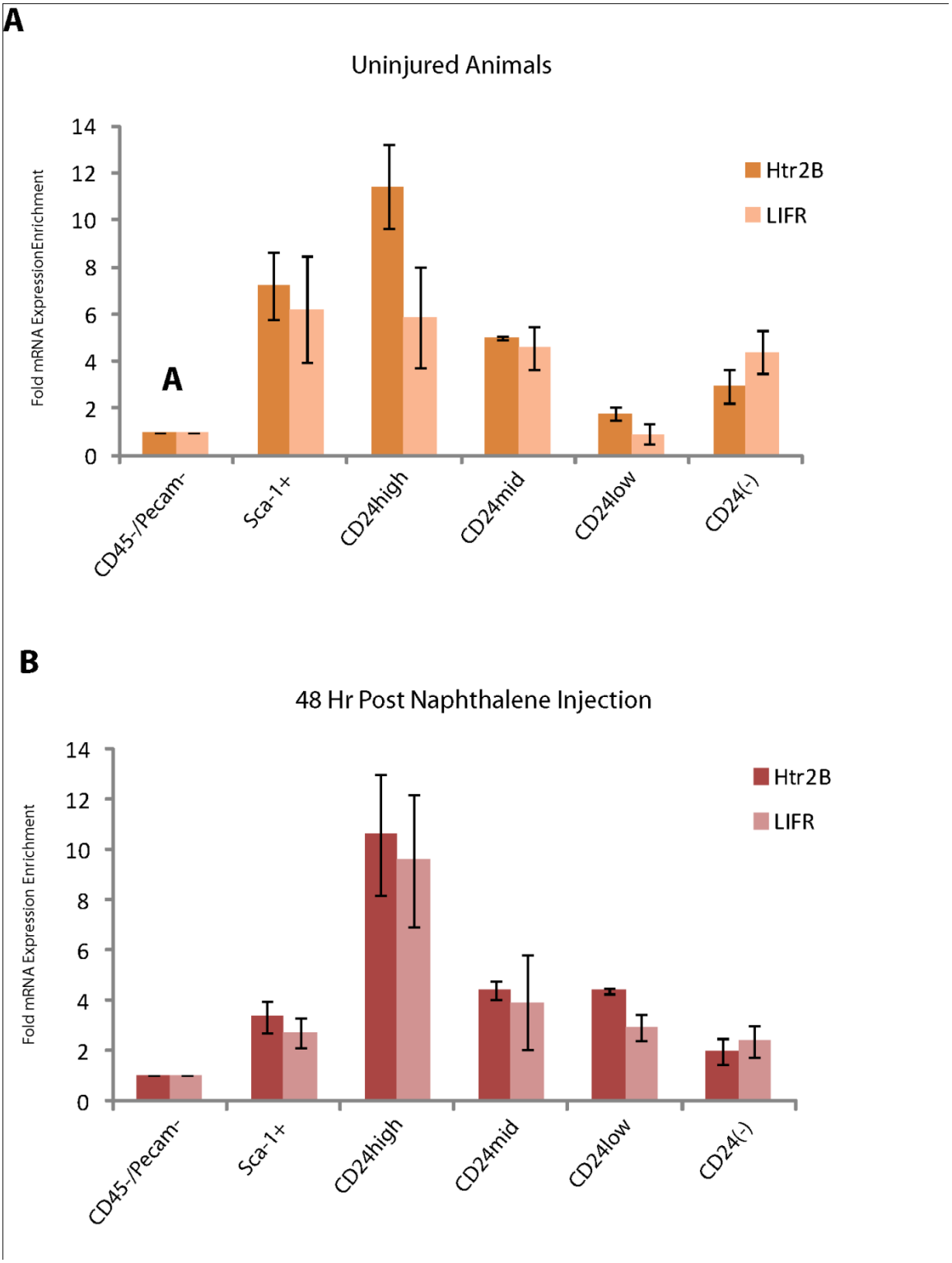

Figure 2.14 Validation of Selected Surface Markers by QPCR. Cells were sorted and tested for expression of HTR2B and LIFR in both uninjured **(A)** and 48 hour post injection **(B)** animals by QPCR. Samples are normalized to CD45-/Pecam- populations harvested at their respective time points.

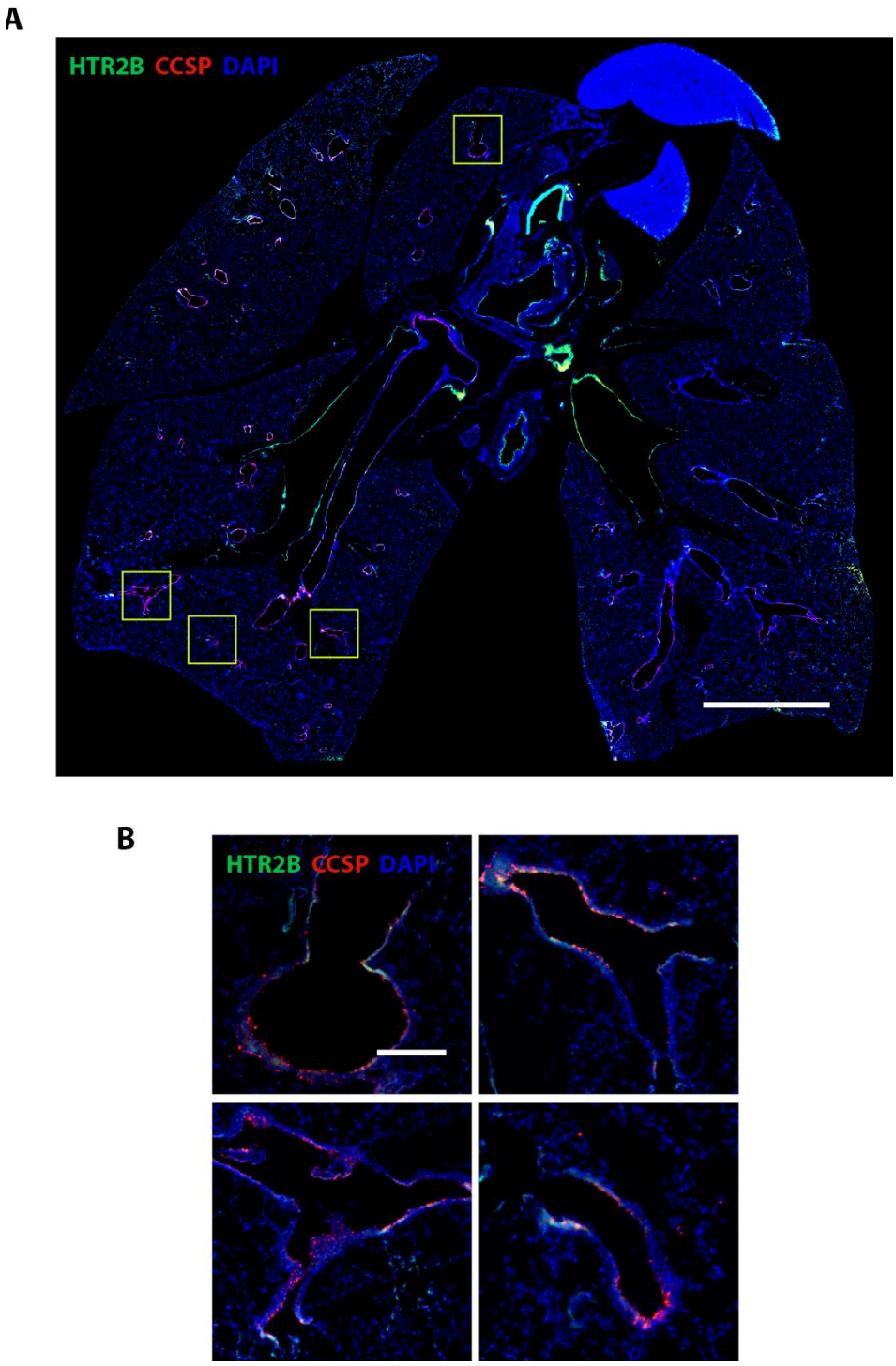

Figure 2.15 HTR2B Localizes to CCSP+ Epithelium at the BADJ. Immunofluorescence of the lung for CCSP and HTR2B shows expression relegated to large blood vessels **(A)** and some CCSP+ cells **(B)** of the bronchial epithelium (Scale bar in A is 1.5 cm, in B, 100 micron).

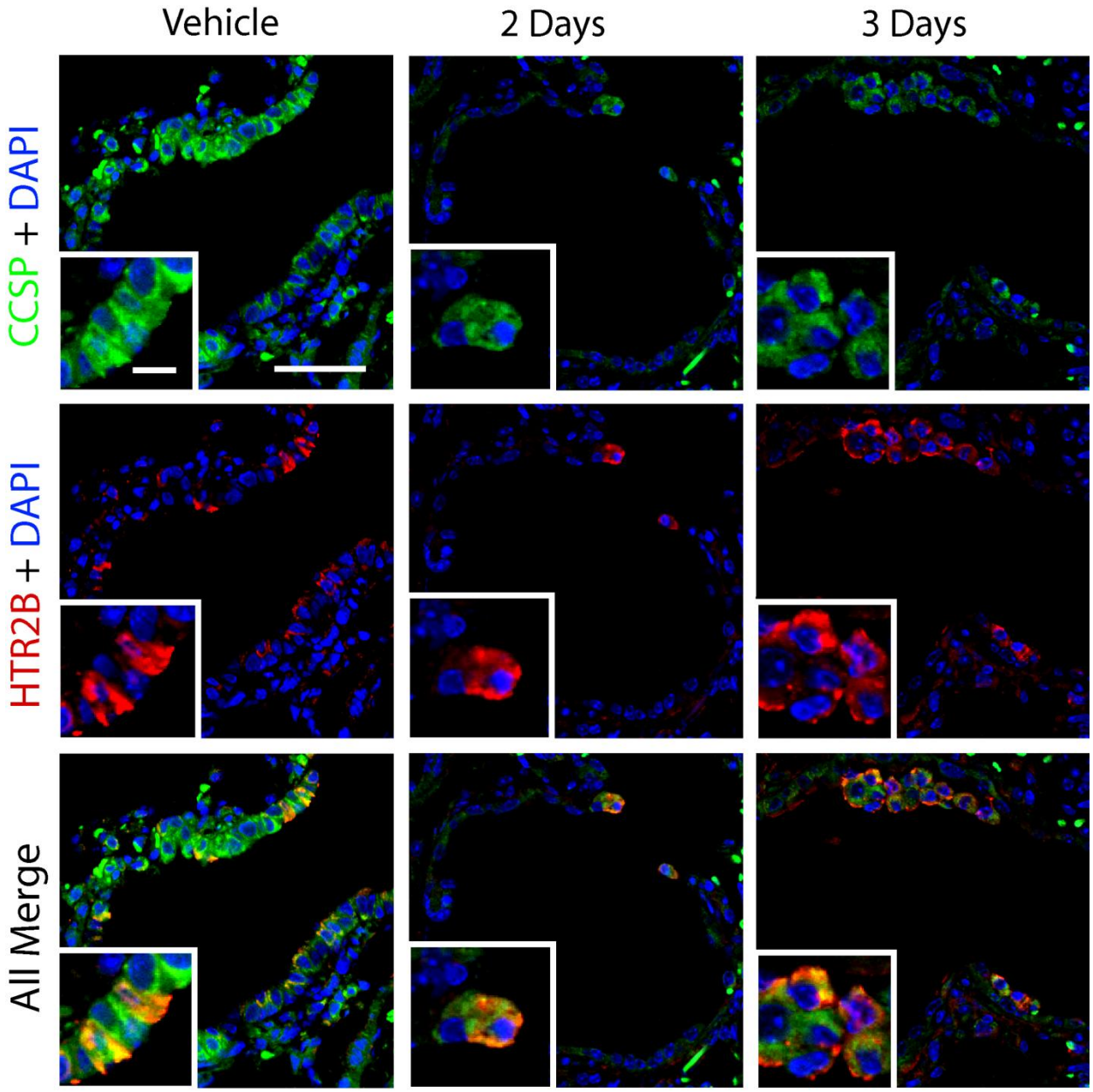

Figure 2.16 HTR2B+ Clara Cells at the BADJ Persist Through Naphthalene Injury. Immunofluorescence of the lung for CCSP and HTR2B at varying times post injection or without injury (Scale bar is 80 micron, inset is 10 micron). Dual positive cells persist through injury and increase in number during re-epitheliazation.

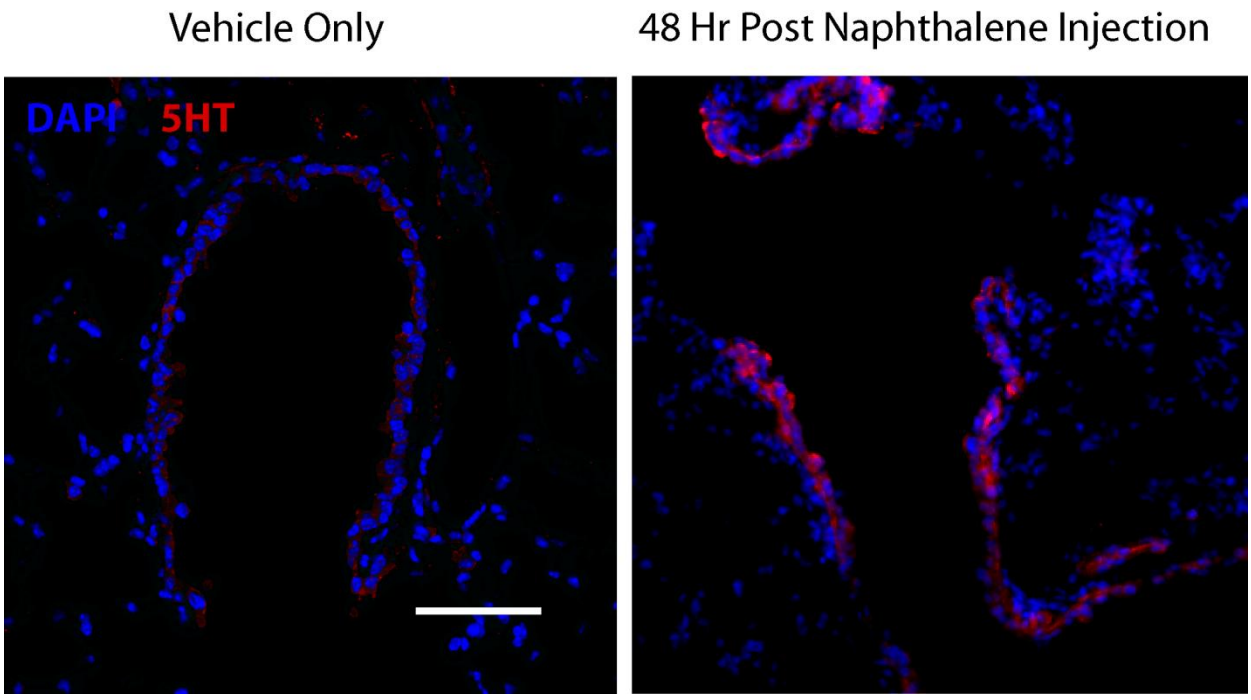

Figure 2.17 Detection of Serotonin in Bronchial Epithelium. Representative fields of BADJs stained for serotonin (5HT) before and 48 hours after naphthalene injury (Scale bar is 80 micron). Reactivity is low in the uninjured bronchial epithelium but increases dramatically at the BADJ after injury.

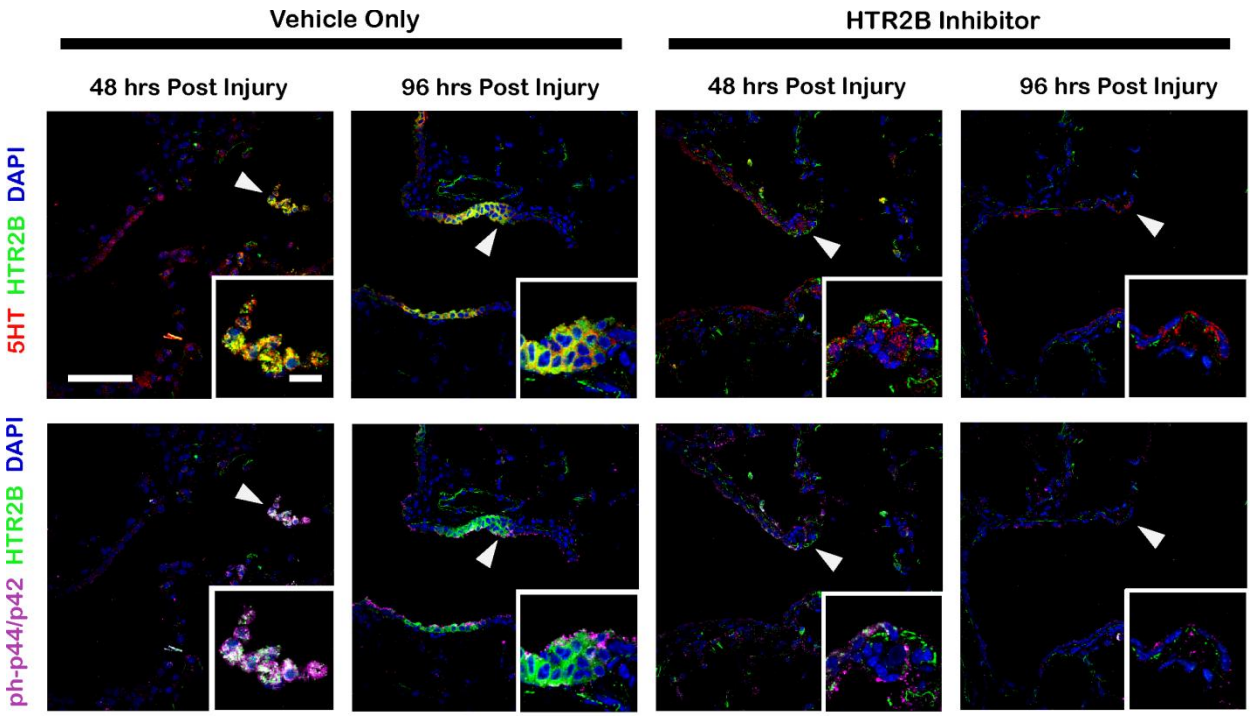

Figure 2.18 HTR2B Inhibition Impacts MAPK Phosphorylation and 5HT Production During Injury. Mice treated with SB-204741 (HTR2B inhibitor) or vehicle alone were sacrificed at the indicated times after naphthalene injury and stained for 5HT, HTR2B and phosphor-p44/p42 MAPK (Scale bar is 80 micron, inset 10 micron). Vehicle treated animals show robust 5HT production in HTR2B+ cells, with concomitant phosphorylation of MAPK. SB-204741 treatment greatly decreased 5HT production and MAPK phosphorylation in bronchial epithelium at the BADJ at both early and late time points after injury.

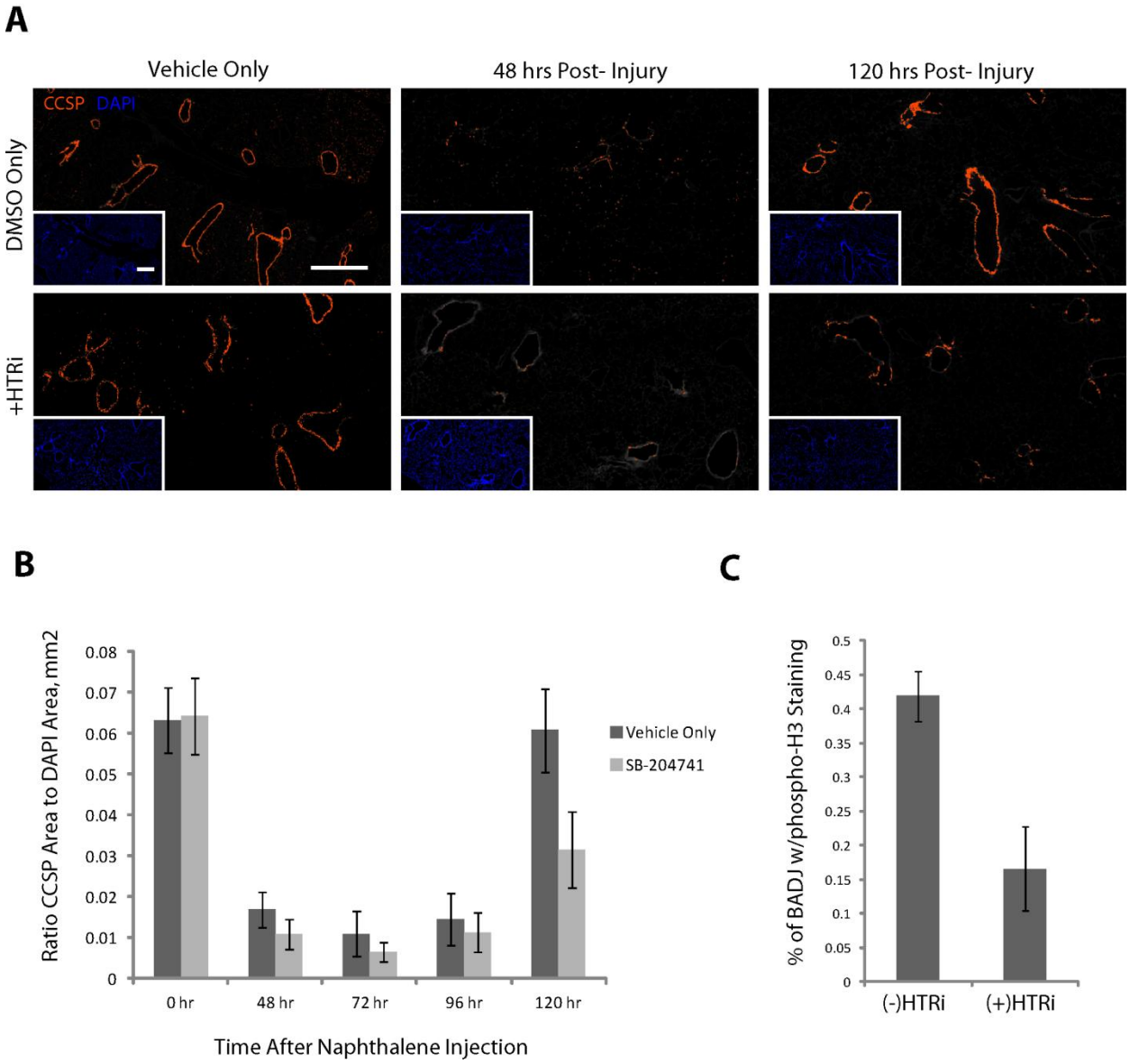

Figure 2.19 HTR2B Inhibition Abrogates CCSP+ Cell Regeneration after Injury. Mice treated with SB-204741 (HTR2B inhibitor) or vehicle alone were sacrificed at the indicated times after naphthalene injury. Slides were made from three planes of sectioning per mouse and stained for CCSP. Whole lungs were scanned for fluorescence (A) and area above threshold for CCSP and DAPI was calculated (Scale bar is 200 micron in main figure and inset). Ratio of CCSP to DAPI fluorescence (B) was calculated at varying times after injury. Decrease in CCSP+ cells was reflected in lower number of phospho-histone h3 (C) staining at the BADJ of mice treated with SB-204741.

Chapter 3

Regulatory Mechanisms Underlying the Migratory and Metastatic Phenotype of Non-Small Cell Lung Cancer Cells

Chapter 3: Regulatory Mechanisms Underlying the Migratory and Metastatic Phenotype of Non-Small Cell Lung Cancer Cells

Summary

While activation of tissue resident progenitor cells and proliferative response is necessary for proper wound resolution, it is not sufficient to accomplish this process. Cells must also migrate to sites of damage. Experimental evidence has shown that upon injury, epithelial cells acquire mesenchymal like features. This process, known as epithelial-to-mesenchymal transition (EMT), is accompanied by increased motility and secretion of defined cytokines and ECM components (Kalluri & Weinberg, 2009). Here we provide evidence indicating that in addition to environmental factors, transition between these different cell states can be accomplished by epigenetic regulation. As tumors have been often looked upon as "wounds that never heal," we sought to explore the role these mechanisms may play in metastatic behavior of certain non-small cell lung carcinomas (NSCLCs) (Schafer & Werner, 2008).

Highlights

- Cells with mesenchymal like features, characterized by high expression of CD44 and low CD24, are present within the lung and expand upon injury
- Cells with similar features are present in lung tumors and tumor derived cell lines
- $CD44^{high}/CD24^{low}$ cells are derived from the conversion of epithelial cells through cell autonomous and non-cell autonomous mechanisms.
- TGF-β signaling is an important paracrine and autocrine modality of EMT induction
- Upstream epigenetic regulation of mir335 controls this cell state transition

Introduction

The maintenance of epithelial barriers is of critical significance in protecting human beings from harmful agents in the external environment. Compromise to their integrity could mean invasion by pathogenic microbes or exposure to noxious chemicals. In some organs of the body, such as the skin or intestine, a rapid steady state turnover is established to ensure a constant renewal of cell mass within

epithelium. Other organs remain relatively quiescent. In both cases, tissue injury can trigger compensatory responses aimed at clearing out harmful agents and producing new epithelium. While some elements of this process may be dependent on the tissue in which it occurs, there are certain aspects of wound healing that are broadly conserved (Lawrence, 1998).

To compensate for tissue lost to injury, de novo cell mass must be generated. This can be accomplished through a variety of methods, as discussed in Chapters 1 and 2. Regardless of the source of the progenitor/stem cells, migration into the denuded area is a near universal feature of cells responding to wounding (Weber, Li, Wai, & Kuo, 2012). This process involves the acquisition of increased motility and the expression of extracellular matrix remodeling factors as part of large scale changes in cell state. One pathway responsible for the migratory phenotype of epithelial cells is epithelial-to-mesenchymal transition (EMT).

EMT is characterized by loss of polarity, cytoskeletal reorganization, transition to spindle shaped morphology, and changes in gene expression program (Kalluri & Weinberg, 2009). These changes in gene expression include loss of epithelial markers such as E-cadherin, cytokeratins and zonula occludens-1 with concomitant increase of mesenchymal marker expression including TGF-beta, CD44, α-SMA and vimentin and secretion of define cytokines such as Il-6 and CCL5. The activation of the TGF-β and Il-6 pathways have been shown critical for promoting motility of these cells as well as in mediating injury resolution within the lung upon naphthalene treatment (Kida et al., 2008).

The generation of cells baring characteristics of those observed in wound healing has been observed in tumors as well (Gomes et al., 2011). These findings are particularly interesting in that they support the notion that tumors maintain physiologic response to regulatory pathways governing the tissue from which they are derived. As such, disorganized and abnormal growth may essentially be considered a state of continuous tissue injury (Schafer & Werner, 2008). In 1986, Dvorak famously referred to tumors as “wounds that do not heal” (Dvorak, 1986). We have found that cells with the immunophenotype of $CD44^{high}/CD24^{low}$ are present in a variety of cancers as well as during lung wound healing. Gene expression profile of $CD44^{high}/CD24^{low}$ cells derived from injured lungs and from tumors show these cells to be highly homologous (Data not shown). Hence we hypothesized that a common mechanism regulating the ontogeny of $CD44^{high}/CD24^{low}$ cells could be in place in both injury repair of the adult lung as well as in cancer.

We found that both autonomous (e.g. epigenetic) and non-cell autonomous (e.g. paracrine) events may precipitate the emergence of $CD44^{high}/CD24^{low}$ cells within a tumor cell population. As such, we are currently investigating the significance of the TGF-β as well as its upstream regulators in cell fate determination under normal physiologic conditions as well as pathological states such as cancer and pulmonary fibrosis.

Results

Identification of Mesenchymal Subpopulations of Epithelial Cells

While studying molecular mechanisms of resistance to cancer therapies we identified a spontaneously arising $CD44^{high}CD24^{low}$ cell subpopulation from human-derived lung adenocarcinoma cell lines that, unlike the parental epithelial cells, stably adopt a mesenchymal state characterized by increased motility, invasion, and metastatic potential as well as resistance to EGFR inhibition (Yao et al., 2010). These mesenchymal like cells were pre-existing in the parental epithelial line H1650, such that sorting for the $CD44^{high}CD24^{low}$ population yielded cells with elongated morphology and differential expression of epithelial lineage markers (Figure 3.5). Other tested NSCLC cell lines showed differential distribution on the CD44/CD24 axis (Figure 3.4).

When we interrogated a large collection of NSCLC tumors for the presence of $CD44^{high}CD24^{low}$ cells both by flow cytometry and immunofluorescence microscopy, we found that while all tumors possessed $CD44^{high}CD24^{low}$ population, the relative number of cells baring this immunophenotype was often low—on the order of 1% (Figures 3.1 and 3.2). Yet in approximately 1 out of 5 tumors, we observed a much greater representation of $CD44^{high}CD24^{low}$ cells (Figures 3.2 and 3.3). Consistent with these cells harboring features associated with an increased metastatic potential, study of outcome from an annotated cancer tissue microarray set of 233 NSCLC patients suggests that this cytology is associated with decreased disease free survival time (Figure 3.6).

Molecular characterization of these cells showed increased expression of genes reported to play a critical role in regulating wound healing responses such as TGF-beta, IL-6, and Collagen V (Crosby & Waters, 2010). We thus became interested whether similar cells could play a role in physiologic wound healing in the lung.

To test for the emergence of a similar population during lung wounding, we employed the naphthalene injury paradigm described in Chapter 1. Administration of naphthalene causes rapid necrotic change within Clara cells of the terminal and respiratory bronchioles due to conversion of the drug into a toxic form by the cell specific microsomal enzyme Cyp2F2. To appreciate the role that $CD44^{high}/CD24^{low}$ epithelial cells may play in post-naphthalene lung regeneration, we administered the drug by intra-peritoneal injection to a cohort of mice and sacrificed them at 1 week intervals afterwards.

Results obtained from flow cytometry analysis of lung homogenates indeed revealed enrichment for cells baring the surface markers of EMT during the time after lung injury (Figure 3.7). These cells are negative for expression of CD31 or CD45, are in the lowest 10% of CD24 expression, and are several folds higher for CD44 surface staining than the remaining population. Their presence in the lung increases in a time dependant manner after injury, from near undetectable levels in the vehicle treated animal to almost 6% of non-endothelial, non-marrow derived cells by day 24. $CD44^{high}/CD24^{low}$/CD31-/CD45- cells sorted from injured animals on day 18 post injection showed decreased levels of E-cadherin and increased levels of vimentin expression compared to the CD31-/CD45- reference population, suggesting they had indeed undergone EMT.

In order to determine how similar these injury derived cells are to those observed in tumors, we sorted the $CD44^{high}/CD24^{low}$/EpCam+/CD31-/CD45- population from day 18 post injection injured animals as well as from tumors generated by a mouse model of lung cancer with functional silencing of the ARF tumor suppressor and constituitively active oncogenic Kras (described further in Chapter 4). We also purified the $CD44^{low}$/EpCam+/CD31-/CD45- fractions as reference populations. We observed high level of similarity among these cells. Ongoing work is aimed at further exploring these initial findings.

Paracrine Regulation of $CD44^{high}/cD24^{low}$ Cell State

As previous studies have underscored the importance of the canonical SMAD dependant TGF-β signaling axis on the $CD44^{high}/CD24^{low}$ state, we next set out to test its role in paracrine EMT induction (Scheel et al., 2011). We treated H1650 cells with TGF -β1 and 2 and saw a time dependant increase in mesenchymal marker expression as well as decrease in epithelial marker expression. Interestingly, this also correlated with a change in surface marker staining of CD24 and CD44 as measured by flow cytometry (Figure 3.8).

Although we have shown TGF –β capable of inducing the $CD44^{high}/CD24^{low}$ phenotype, comparison of gene expression profile between mouse sample groups and cell line models of EMT has suggested that this cytokine is not itself sufficient to induce a complete transition in cell state. Rather, it is likely a modular component of the process which regulates certain aspects of a larger constellation of phenotypes that make up the metastasis initiating cell.

Recent work has suggested that signaling via the serotonin receptor 2B (HTR2B) lies upstream of TGF-β signaling in animal models of fibrosis(Ebrahimkhani et al., 2011) . We were interested in surveying the effects of this pathway on NSCLC cells. To do so, we selected pharmacologic modulators that targeted both HTR2B and C receptors, as the two share common downstream effectors (B. Li et al., 2010). H1650 cells were plated at clonogenic density in two dimensional culture and treated a day later with the mixed HTR2B/C agonist mCPP or antagonist SB-206553 (Figure 3.9)(Gommans, Hijzen, Maes, & Olivier, 1998; Kennett et al., 1996). Colonies grown in the presence of mCPP showed jagged edges with poorly organized elongated cells. On the other hand, those grown with receptor antagonist SB-206553 displayed tight edges, small apparent cell volume and close contact with neighboring cells. Quantification of this effect proves an increased number of colonies baring mesenchymal morphology when cells are cultured in the presence of HTR2B/C agonist and a decrease when grown with antagonist (Figure 3.9).

Although this data is very preliminary, we would like to speculate that HTR2B could regulate secretory components of the cell state transition that foster autocrine and paracrine induction of EMT. Clearly, further experiments are needed to validate this intriguing hypothesis.

Identification of Epigenetic Regulators of the Mesenchymal Phenotype

When the NSCLC derived cell line H1650 was sorted based on expression of CD44 and CD24 and plated at clonogenic density, we observed that while certain colonies maintained their phenotypic characteristic during time others reverted to an epithelial like state (Figure 3.10). Unsorted cells as well as $CD24^{high}/CD44^{low}$ populations displayed primarily epithelial colony morphology at both 2 and 6 days post plating. In both cases only 2-5% of colonies scored were purely mesenchymal. On the other hand, $CD44^{high}/CD24^{low}$ sorted cells gave rise to a far greater number of mesenchymal colonies at both early and late time points. At 6 days, almost 35% of colonies plated were purely mesenchymal. Interestingly,

over half the colonies of $CD44^{high}/CD24^{low}$ were of mixed morphology—also a notable increase over unsorted and $CD24^{high}/CD44^{low}$ sorted cells.

We interpreted this data to signify that certain cells had stably acquired the mesenchymal phenotype, while others may either stochastically transit into it or be induced by outside signaling to acquire those properties. To test this hypothesis, we performed serial sorting of cells from the $CD44^{high}/CD24^{low}$ fraction of H1650 followed by single colony isolation to generate monoclonal lines (Figure 3.11). Many of these cell lines displayed mesenchymal morphology that was stable for up to 20 passages. Importantly, they also displayed differential relative CD24 and CD44 compositions by flow cytometry. Generation of stably mesenchymal cell lines by this strategy was also possible using H1299 and H1975 NSCLC cell lines (Date not shown). These data suggest that cell-autonomous signals could play a role in fostering the mesenchymal phenotype.

A large body of evidence has indicated that microRNAs (miRNAs) play a significant role in regulating cell identity (Howe, Cochrane, & Richer, 2012; Medrano, Monteagudo, Sequeira-Lopez, Pentz, & Gomez, 2012; Y. C. Wu, Chen, Mercer, & Sokol, 2012). Hence we hypothesize that a miRNA based mechanism could participate in the ontogeny of these cells. miRNAs are small (~22 nt) non-coding RNAs that constitute a novel class of gene regulators, able to post-transcriptionally repress gene expression by initiating the degradation or blocking translation of target mRNAs (Pillai, 2005). More than 1000 unique mature miRNAs have been identified in the human genome, each potentially regulating up to 200 mRNAs (Griffiths-Jones, Grocock, van Dongen, Bateman, & Enright, 2006). It is speculated that roughly 30% of all human gene transcripts may be targeted by miRNA regulation, involving them in virtually every cellular process. miRNAs have also been proposed as modulators of signaling processes, either potentiating or dampening them to limit stochastic fluctuations of biological systems. As such, they are attractive candidates for the regulation of cell-state transitions.

To investigate whether specific miRNA could play a role in the ontogeny of $CD44^{high}/CD24^{low}$ cells, we generated miRNA expression profiles of the epithelial NSCLC cell line H1650 as well as the EMT-derived H1650-M3 by constructing small RNA libraries (Data not shown). These libraries were subjected to deep sequencing using the Illumina platform and reads were mapped to the genome using a customized bioinformatics pipeline. Reads were annotated by BLAT to a unified database containing entries for small human RNAs from miRBase, NONCODE as well as tRNAs from the RNA modification Database and rRNAs from the Entrez Nucleotide Database. Comparative analysis was carried out with an arbitrary cut-off of a minimum of 1000 reads and >2 fold differential expression. Based on these

criteria, we identified 20 miRNAs that were up-regulated and 19 downregulated in $CD44^{high}/CD24^{low}$ cells (Data not shown).

To determine whether these identified miRNAs were regulated by paracrine mechanisms previously shown to induce EMT, or were upstream regulators, we examined their expression in response to manipulation of TGF-β signaling. Intriguingly, of the miRNAs identified by sequencing, only levels of mir-335 were unaffected by perturbations to this signaling pathway (Data not shown).

Since its initial report as a metastasis suppressing miRNA, a number of works have implicated mir335 as a central factor in suppressing motility, invasiveness and seeding capacity of tumor cells (Png et al., 2011; Tavazoie et al., 2008). As such, expression appears to abrogate a number of processes associated with the metastatic phenotype. Evidence from studies of normal mesenchymal stem cells (MSCs) indicates that mir-335 expression may be a conserved means of interfering with processes such as motility and self renewal (Tome et al., 2011). On-going work in the lab is aimed at demonstrating the role that mir-335 plays in epigenetic determination of cell fate.

The Use of an Alternative Promoter Regulates mir335 Expression

The mir-335 encoding sequence resides within the second intron of the mesoderm-specific transcript homolog (MEST)/paternally expressed 1 (PEG1) gene located on chromosome 7q32. In humans, usage of two alternative promoters yields distinct MEST pre-mRNA isoforms (Huntriss et al., 2012). Transcription starting from a promoter in exon 1 is favored in tissues of mesodermal origin and yields isoform 1 of the transcript. Usage of a promoter within exon A, on the other hand, is favored within tissue of endo-/ectodermal lineages and generates isoform 2.

Because intronic miRNAs are often coordinately expressed with the gene they are nested in, we investigated the relationship between MEST and mir335 expression level (Farh et al., 2005). RT-PCR analysis of total MEST transcripts in multiple tumor derived cell lines revealed a decrease in MEST expression within cells possessing low levels of mir-335 (Data not shown). Use of isoform specific primers revealed an associated between high MEST transcript level and utilization of the promoter within exon A to generate isoform 2. To corroborate this evidence, probes flanking the isoform specific junction between 5' UTR and first exon were designed for RNA fluorescence in situ hybridization (FISH).

To validate the efficacy of the different probes in detecting isoform specific transcripts, three breast cancer cell lines were chosen based on known variation in their CD24/CD44 status, gene expression pattern and relative MEST level by RT-PCR: MCF7, MDA-MB-231 and HS578. Progressing from former to latter, these cells represent epithelial/CD44low, intermediate/CD44mid and mesenchymal/CD44high populations, respectively (Figure 3.12). Hybridization of probes against isoforms 1 and 2 as well as a control oligo targeting an exon junction present in all reported ESTs (total MEST) of the gene showed reliable recapitulation of RT-PCR data (Figure 3.13).

RNA FISH analysis of the breast cancer cell lines revealed high total MEST mRNA levels in the epithelial/CD44^{low} MCF7 cells, with preferential detection of isoform 2. Observation of the mesenchymal/CD44^{high} HS578T cells, however, revealed lower levels of total MEST and an increase in the relative amount of isoform 1 transcript. MDA-MB-231 cells, which are CD44^{mid} and possess characteristics of both epithelial and mesenchymal cells, showed staining with both isoform 1 and 2 specific probes.

We next sought to evaluate use of fluorescently conjugated mir335 LNA probe for FISH studies using the same breast cancer cell lines (Figure 3.14). In the MEST high MCF7 cells, high levels of mir335 were apparent by fluorescent microscopy. In the lower MEST expressing HS578T cells, mir335 was nearly undetectable by this method. Again MDA-MB-231 showed an intermediate phenotype with milder levels of mir335 expression than MCF but markedly more than HS578T.

Satisfied with the performance of our labels for isoform specific mRNA and mir335 transcript levels, we next turned toward analysis of human primary tumors. Our data set consisted of tumor cores obtained from patients receiving surgical resection for lung cancer and was annotated for stage, grade, disease free survival and other measures of clinical outcome. RNA FISH was performed using the isoform specific probes as well as the mir335 LNA (Figure 3.15). Multiple tumors displayed a mixture of isoform 1 and 2 expressing cells, while others were characterized by predominant expression of one or the other. Isoform 2, which is typically expressed in cells of endo- or ectodermal origin, was localized predominantly to polarized epithelium. Isoform 1, which is found in normal mesodermal lineage cells, was expressed in the polarized epithelium of some tumors, but also within regions showing little differentiation or organization. Expression of MEST isoform 2 was correlated to mir335 levels and anti-correlated to CD44 status, as tumors with prominent CD44 staining were typically low or negative for the transcript by RNA FISH (Figure 3.16).

Distinct CpG islands have been identified in the promoters of both isoform 1 and isoform 2 of MEST. The CpG island in the promoter of isoform 1 is imprinted with expression only form the paternal allele, whereas the isoform 2 promoter CpG island is bi-allelicaly expressed (Huntriss et al., 2012). To determine whether the observed isoforms switch was due to hyper-methylation of the isoform 2 promoter, we quantified *MEST* CpG island methylation by methylation-specific PCR and by sequencing of bisulfite-treated DNA (Data not shown). All $CD44^{high}CD24^{low}$ cells examined displayed an increase in methylation of the CpG island in the promoter of isoform 1 relative to the parental $CD44^{low}$ cells, decreased expression of total *MEST* and miR-335, and augmented *MEST* isoform 1 levels. Together our data indicate that miR-335 and *MEST* isoform 2 are transcriptionally co-regulated and suggest that hyper-methylation of the *MEST* isoform 2 promoter silences miR-335 and *MEST* expression in $CD44^{+}CD24^{-}$ cells. Interestingly we also found that, in $CD44^{high}CD24^{low}$ cells an increased binding of NRSF leads to increased local DNA-methylation and silencing of both *MEST* and miR-335 expression.

In summary, these studies provide novel insights into key mechanisms that regulate the transition towards the acquisition of a $CD44^{high}CD24^{low}$ cell state. Current work is aimed at validating these findings in vivo and in determining their importance in pathologic conditions.

Discussion

In effort to maintain the barrier function of epithelium in the face of injury, cells must undergo a series of changes that net an increase in motility. The adoption of this migratory phenotype appears to be a broadly conserved aspect of wound healing that has function in a number of organs and tissues. One pathway that may lead to this is epithelial-to-mesenchymal transition (EMT), which involves loss of epithelial polarity, cytoskeletal reorganization, changes in morphology and gene expression program.

Cells displaying the properties of EMT have been shown to have the $CD44^{high}/CD24^{low}$ immunophenotype in a number of different cell culture and primary tissue studies. Here, we show the presence of these cells in NSCLC derived cell lines and primary tumors. We also illustrate the emergence of a similar population after lung injury, suggesting that transformed and normal epithelium may both respond to the signals governing EMT in the proper context. Ongoing experiments are aimed at determining whether these cells are derived from the CD24high progenitors described in Chapter 2. Importantly, signaling via the Il6-Stat3 pathway has been shown required for post naphthalene injury lung re-epitheliazation. As this pathway has also been shown critical for the survival of EMT derived

NSCLC cells, it appears that cells of a lung tumor maintain “memory” of the tissue from which they are derived in regulating key cell fate events .

Our studies indicate that both autonomous and non-cell autonomous pathways may govern the adaptation of the migratory phenotype in NSCLC derived cells. We reinforce the importance of TGF-β signaling and suggest that serotonin signaling via the HTR2B and C receptors may also impact EMT. Increased HTR2B expression has been detected in idiopathic pulmonary fibrosis patients (Konigshoff et al., 2010). Rat models of have suggested that TGF-β pathway activation is crucial for inducing the hallmark changes of the disease (Sime et al., 1997). HTR2B inhibition has shown to promote liver regeneration and prevent fibrosis in response to chemical injury by decreasing TGF-β secretion by stellate cells (Ebrahimkhani et al., 2011). As cellular EMT is considered a prominent contributor to fibrosis, it suggests that the HTR2B and C receptors may regulate key events in pro-fibrotic EMT signaling.

In addition to these paracrine/autocrine signaling modalities, we demonstrate that cell-autonomous, epigenetic changes may underlie cell fate decisions. One such epigenetic event may be precipitated at the MEST locus. Ongoing work from our group has indicated that differential methylation of the locus underlies the isoform switching process, and this event may be precipitated by actions of the chromatin regulator neuron-restrictive silencer factor (NRSF). The actions of NRSF in causing methylation induced silencing of the promoter used to generate the more abundantly expressed MEST isoform, thus effectively reducing mir335 dosage, may be an a critical event in the ontogeny of $CD44^{high}/CD24^{low}$ cells. These cells may then exploit paracrine signaling to propagate this fate choice to proximal epithelium.

Understanding the interplay between factors such as micro-environment derived inductive signals and tumor cell intrinsic determinants will be crucial in tailoring therapeutic interventions able to effect long term clinical remission of a cancer. We provide evidence that both may play a role in the ontogeny of cells displaying the mesenchymal phenotype caused by EMT. Importantly, we cannot rule out the reciprocal relationship that may exist between the two. Stochastic epigenetic events resulting in the stable adoption of stem-like phenotypes within populations of cancer cells could lead to the secretion of soluble factors such as TGF-β, WNT5a and Il-6. These cytokines and growth factors could then have profound effect on neighboring cells, resulting in emergent diversity within a tumor.

Experimental Procedures

Cell culture

H1650, H1299, H1975, MCF7, MDA-MB-231 and HS578T cells were obtained from the American Type Culture Collection (ATCC) repository. H1650, H1299 and H1975 were maintained in with 5% FBS, glutamine, penicillin, and streptomycin. MCF7, MDA-MB-231 and HS578T were maintained in similarly supplemented DMEM.

FACS Analysis of CD44+CD24- Cells

Cells were cultured in RPMI or DMEM supplemented with penicillin-streptomycin and 5% fetal bovine serum. After dissociation, cells were washed with cold PBS containing 5% serum, pelleted and resuspended. After filtering through 40 micron mesh to generate single cell suspension, samples were incubated with directly conjugated fluorescent antibodies to the desired antigens for 20 minutes on ice. Cells were then washed 3 times with cold PBS pH 7.2. Flow cytometry was perfomed using the LSRII running FACS Diva software, while sorting was accomplished with use of the Aria II (BD Bioscience).

For the in vivo experiments, mice were sacrificed at defined points after injury. Exsanguination was performed by severing of the brachial arteries. Lungs were flushed with cold PBS via intra-tracheal instillation, followed by incubation with collagenase and hyaluronidase to generate a single cell suspension. Remaining red blood cells were lysed with hypotonic ammonium chloride buffer, and cells were incubated with directly fluorescent conjugated antibodies to the desired antigens. Flow cytometry was perfomed using the LSRII running FACS Diva software. Single channel gating eliminated all cells expressing the surface antigen CD31, which labels endothelial cells, and CD45, which labels marrow-derived cells. Sorting experiments were performed using the BD Aria II.

FISH

Tissue sections were prepared, sectioned, cleared and rehydrated as described above. Slides were washed with PBS containing ribonucleoside vanadyl complex (New England Biolabs) to inhibit RNAse activity and treated with H2O2 to limit autofluorescence. Mild proteinase K treatment was used to expose mRNA for hybridization. After washing in 2x SSC, slides were hybridized overnight in heated,

humidified chambers. After hybridization, slides were washed in 2x SSC, followed by 1x PBS. Post hybridization fixation was accomplished by treatement with 3% formaldehyde for 10 minutes at room temperature. Slides were washed and permeabilized with 0.5% triton x-100 in PBS for 5 minutes on ice. Blocking was performed with 1% BSA in PBS. Detection of digoxigenin labeled probes was accomplished using rabbit anti-digoxigenin Fab fragments directly conjugated to rhodamine (Roche) incubated for 1 hour at room temperature. Immunofluoresent staining was performed by incubation for 1 hour at room temperature with the appropriate antibodies. Counterstaining with DAPI was performed to visualize nuclei. Imaging was done on a Zeiss Axio Observer inverted fluorescent microscope running Axiovision software.

Immunostaining of Tissue Slides

Slides were heated to 65 degree Celsius for 30 minutes to remove excess paraffin then cleared using Histoclear and rehydrated in stepwise graded alcohol. After washing in PBS, slides were treated with H2O2 to limit autofluorescence. Following another round of washes, slides were boiled in citrate antigen retrieval buffer for 20 minutes. Permeabilization was accomplished with 0.5% triton x-100 in PBS with 2% BSA, followed by washing with 1% BSA in PBS. Slides were incubated with primary antibody at 4 degrees Celsius overnight. Secondary antibody labeling was performed with the species appropriate fluorescent conjugate for one hour at room temperature the next day. DAPI was used to label nuclei. All slides were mounted using p-Phenylenediamine anti-fade media. Imaging was performed on the Zeiss 710 confocal microscrope running Zen software.

RNA Extraction and RT-PCR

Total RNA was collected from cultured cells and tissues purified using SV Total RNA Isolation System following the manufacturer's instructions (promega). Total RNA (200 ng) was subjected to a reverse transcriptase reaction using the Improm-II Reverse Transcriptase kit (Promega). cDNA corresponding to approximately 1% of the RNA was used in three replicates for quantitative PCR with the SYBR GREEN (Applied Biosystems) labeling or for standard PCR. Indicated Taqman gene expression assays (Applied Biosystems) and the Taqman universal PCR master mix (Applied Biosystems) were used

to quantify gene expression. Quantitative expression data were acquired and analyzed using an ABI (Applied Biosystems) Sequence Detection System.

Patients and Cancer Tissue Microarray

The NSCL tissue microarray was constructed by Dr. Robert Wagner from tissue obtained during surgical resections performed by Dr. Brendon Stiles, Dr. Alice Walsh, Dr. Matthew Lazzara, Dr. Anatoly Starkov and Dr. Nasser Altork in the Thoracic Department at Weill Cornell Medical School. Patients aged 18 years or older with histologically or cytologically confirmed lung cancer were enrolled in this study. Written informed consent was obtained from each study subject. The study was approved by the governing institutional review boards. Slides were prepared as detailed above.

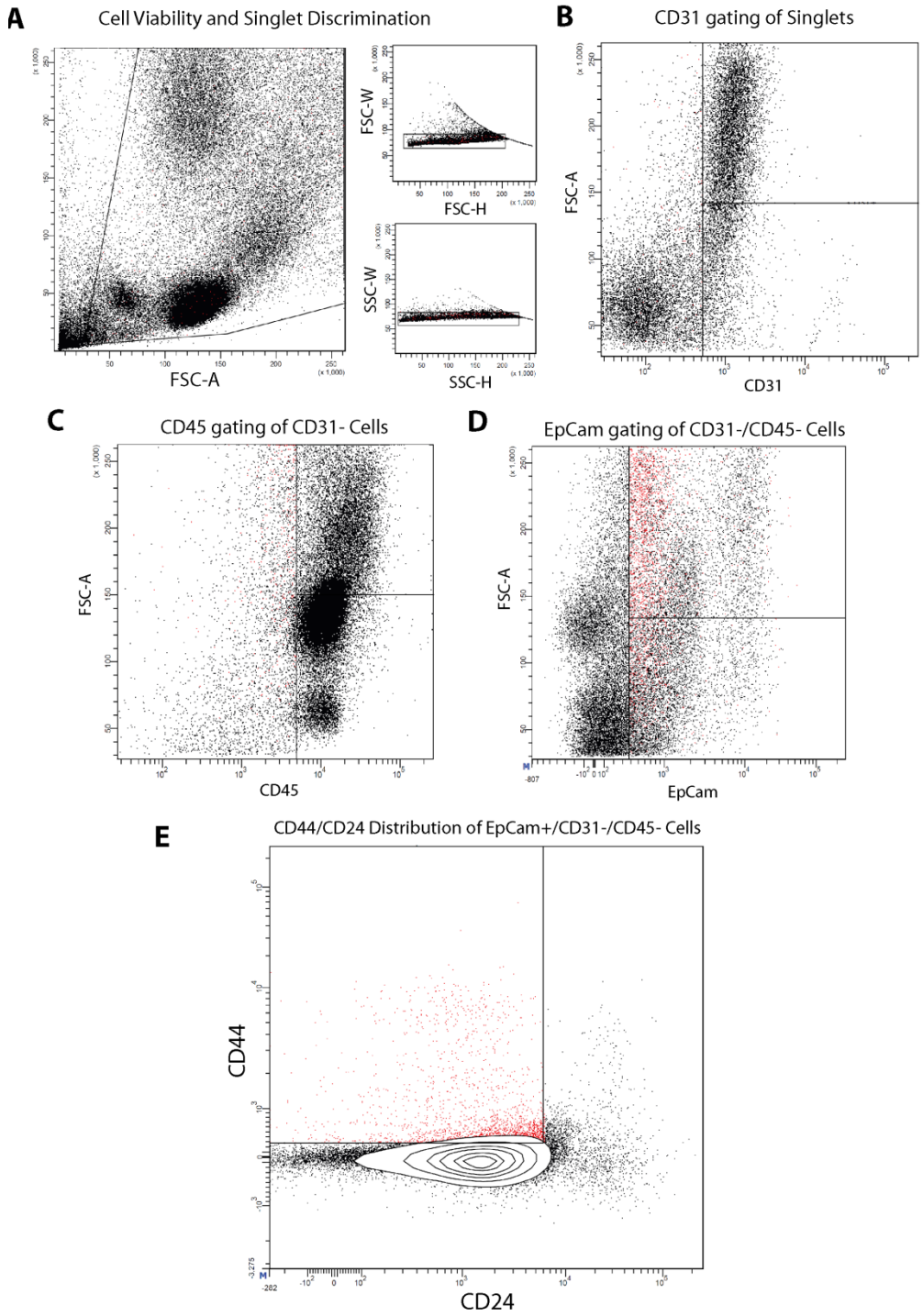

Figure 3.1 FACS Analysis of Human Tumor Samples. **(A)** Samples were gated for cell viability and singlet discrimination. **(B)** Viable singlets were then selected for negative CD31 staining, **(C)** negative CD45 staining **(D)** and positive EpCam staining. **(E)** Cells meeting this criteria were then plotted for relative CD44 and CD24 expression.

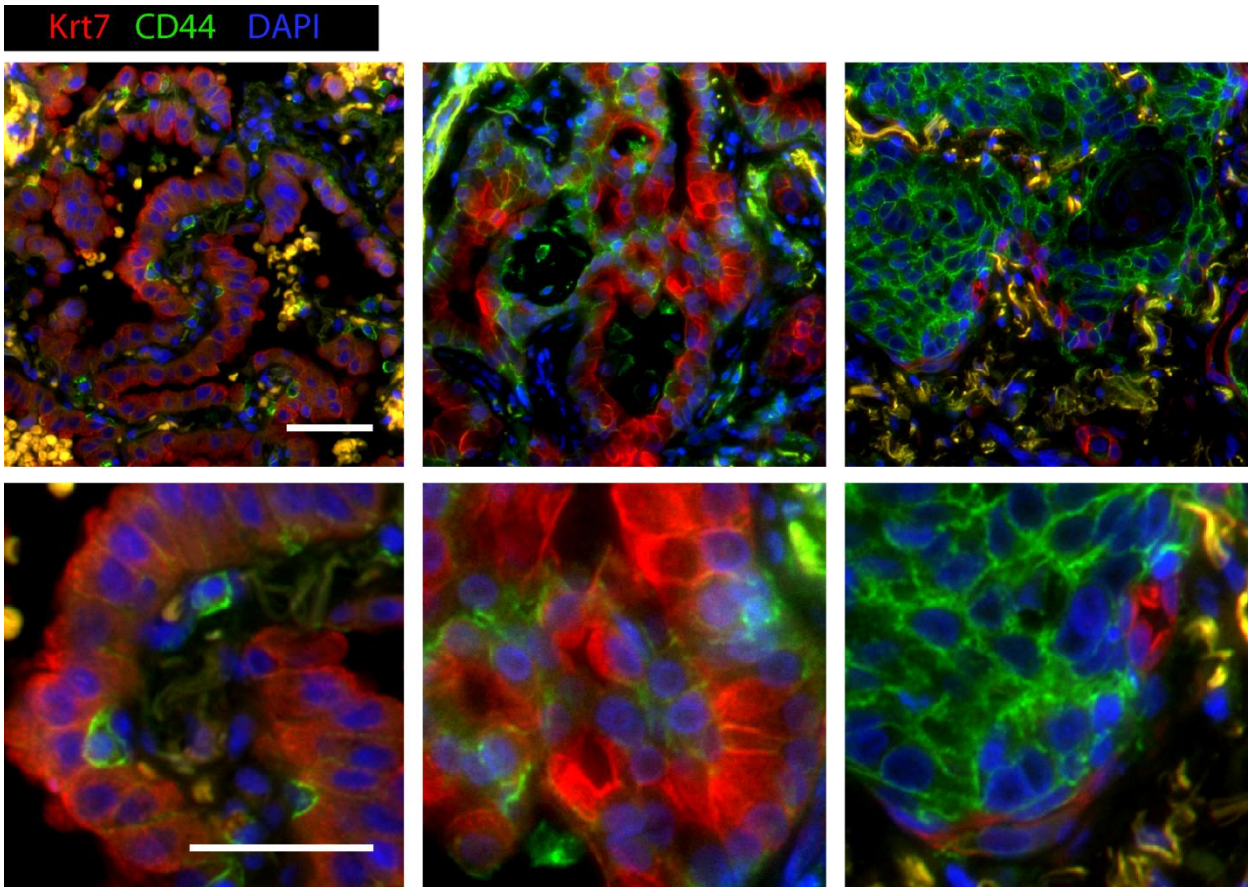

Figure 3.2 Human Tumors Show Varying Levels of CD44 Expression in Epithelium. Primary tumor samples were stained for the markers CD44 and Keratin 7. Number, orientation and morphology of CD44+ cells varied between samples. Representative fields of different staining patterns are shown (Scale bar is 50 micron).

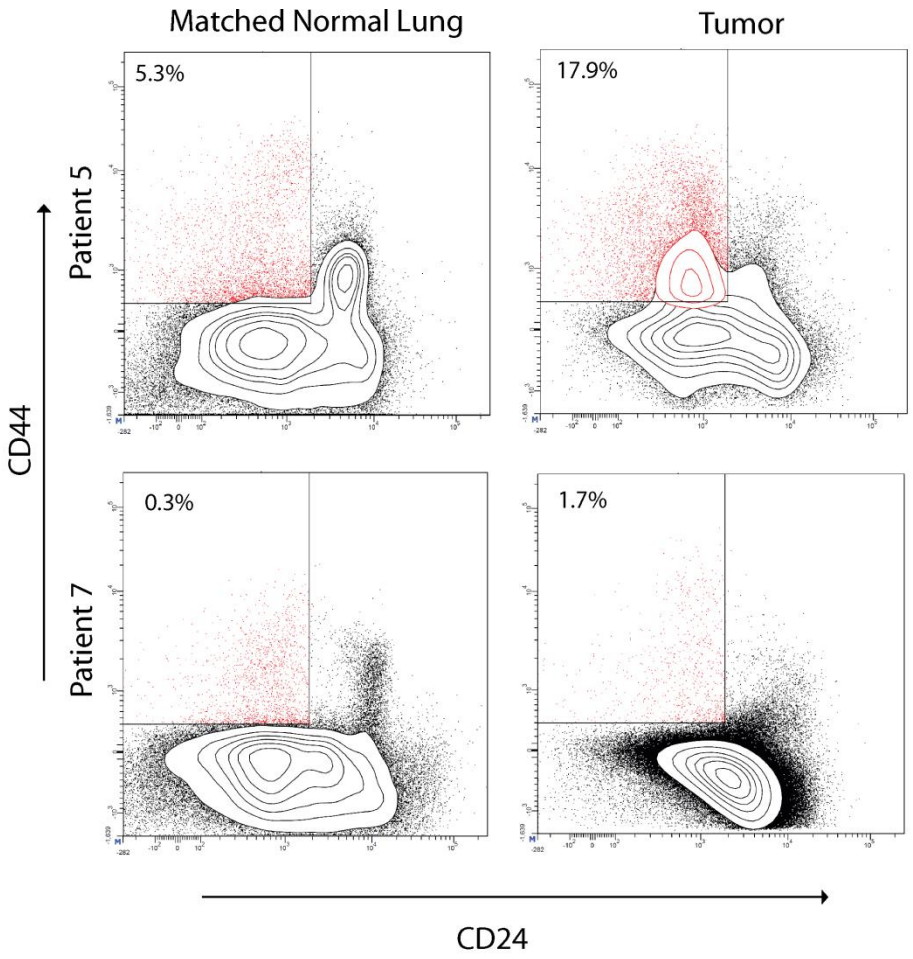

Figure 3.3 Flow Cytometry Confirms Differential CD44 Content of Human Tumors. Cells with the immunophenotype CD44high/CD24low were quantified as detailed in Figure 3.1. While the majority of tumors showed around 1% of epithelium with these characteristics, this number grew substantially in a subset of patients. Matched normal lung tissue was also quantified.

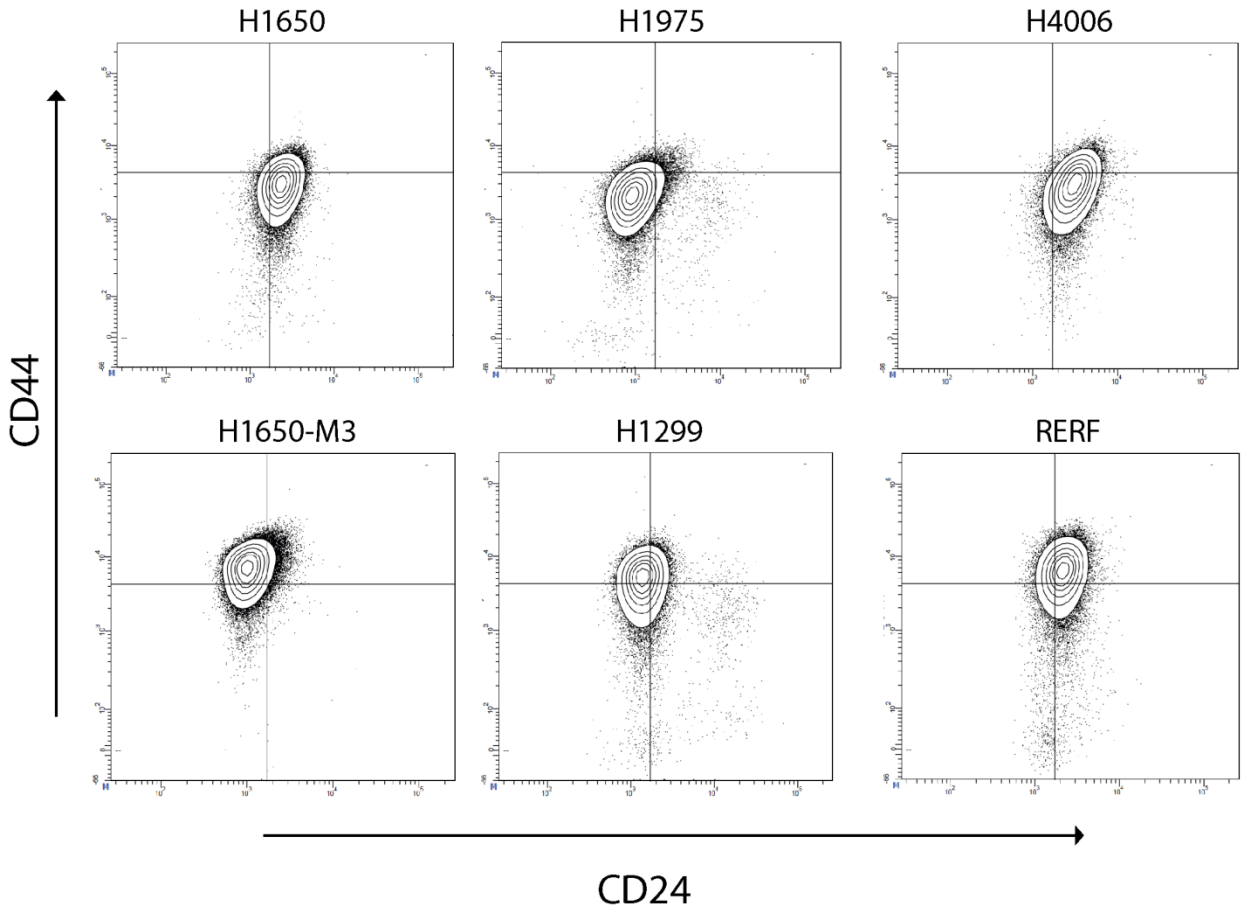

Figure 3.4 NSCLC Derived Cell Lines Mirror the Diversity of Human Tumors. Similar to primary tissue samples, NSCLC cell lines display heterogeneous expression of CD44 and CD24 as measured by flow cytometry. Values ranged from ~80% CD44high/CD24low in H1650-M3 to >1% in H4006.

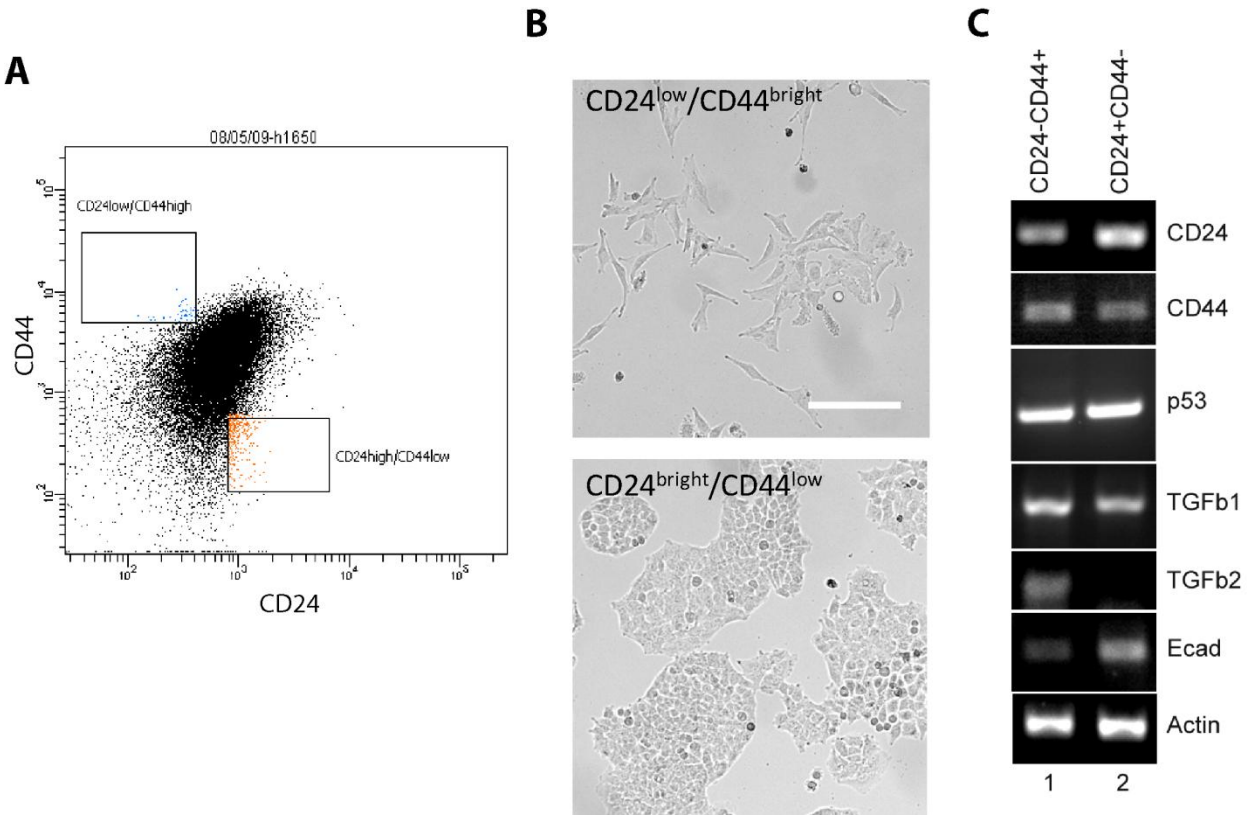

Figure 3.5 Mesenchymal-Like Cells are Pre-Existing in NSCLC Cell Lines. FACS sorting of the NSCLC cell line H1650 for the CD44high/CD24low population **(A)** yielded cells with mesenchymal morphology **(B)** when compared to CD24high/CD44low H1650 (Scale bar is 50 micron). These cells displayed molecular characteristics of EMT **(C)** including decreased Ecadherin expression and increased TGF-β expression.

A

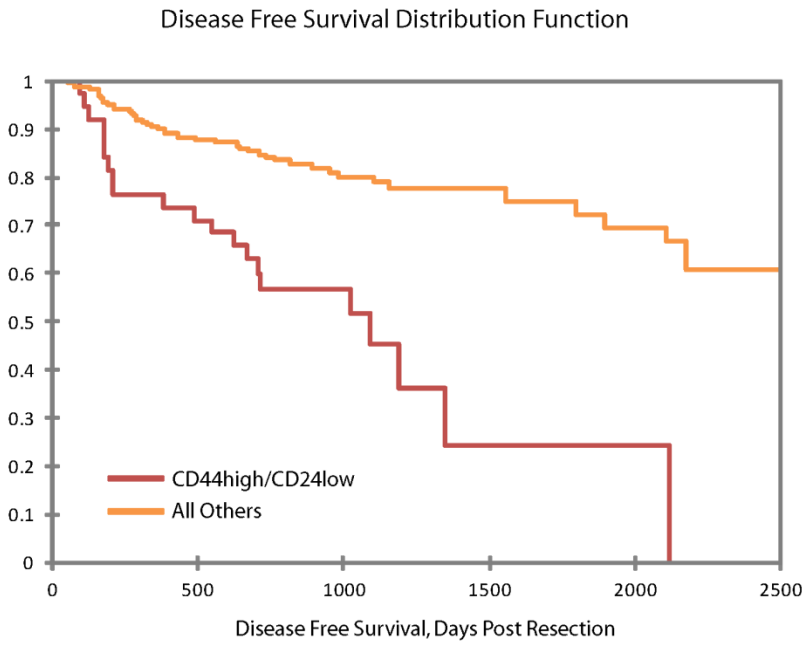

B

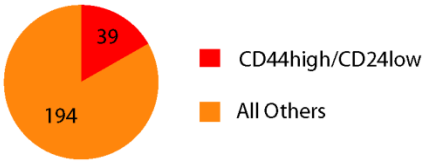

C

	Mean DFS Time (days)	StDev	Mean Survival Time (days)	StDev
CD44high /CD24low	1058.628	151.287	1687.835	136.387
All Others	2479.993	119.296	3080.171	202.226

Figure 3.6 The CD44high/CD24low Immunophenotype is Correlated with Poor Patient Outcome. Interrogation of cancer tissue microarray for expression of CD44 and CD24 followed by univariate Kaplan-Meier analysis of disease free survival post surgical resection of tumor **(A)** showed CD44high/CD24low immunophenotype to be correlated with poor prognosis. These tumors constituted ~17% of cases **(B)** and showed significant decrease in DFS and overall survival **(C).**

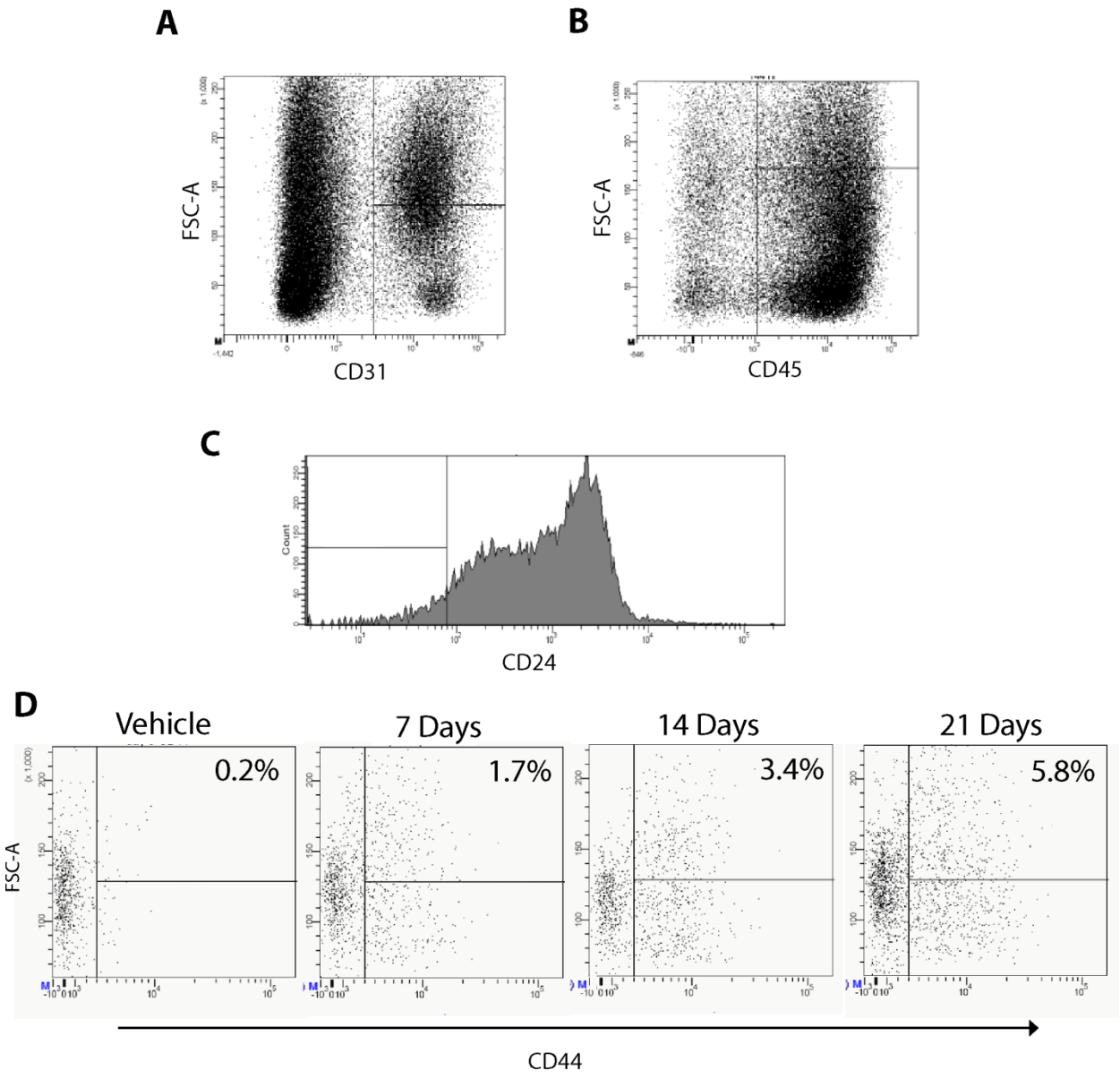

Figure 3.7 CD44high/CD24low Cells Increase In Number After Lung Injury. Animals treated with naphthalene to induce lung injury were sacrificed and prepared for flow cytometry. CD31 and CD45 negative selection **(A and B)** were used to deplete endothelial cells and marrow derived cells, respectively. The lowest 10% of CD24 expressing cells **(C)** were gated for CD44 expression **(D)**. Number of these cells increased dramatically over time, from near undetectable levels to a significant portion of lung epithelium.

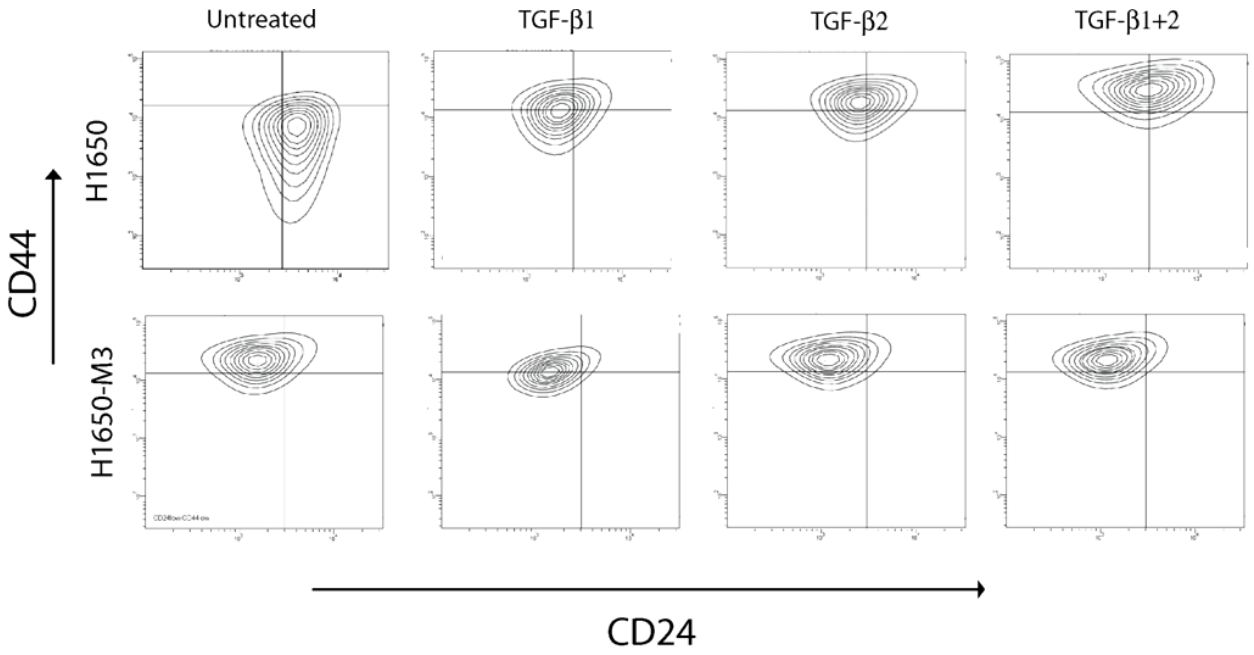

Figure 3.8 TGF-β Treatment Induces the CD44high/CD24low Immunophenotype in H1650. Cells treated with either TGF-β1, TGF-β2, or TGF-β1 and 2 for 16 days were analyzed by flow cytometry for relative CD44 and CD24 expression compared to untreated cells. For comparison, H1650-M3, which are already CD44high/CD24low, were prepared in the same manner.

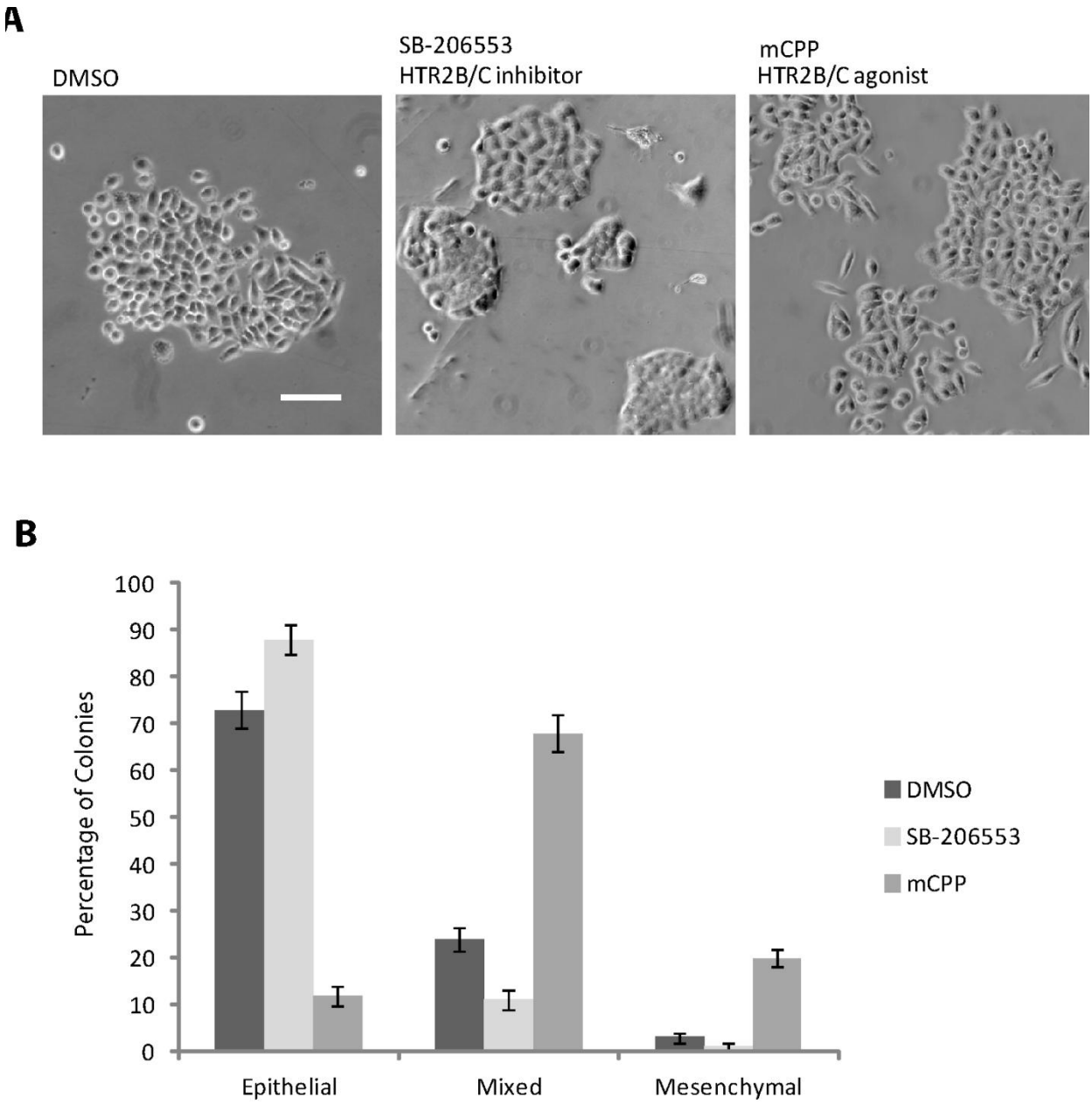

Figure 3.9 Pharmacological Modulation of HTR2B/C Signaling Affects Cell State. Treatment of H1650 plated at clonogenic density with vehicle only, SB-206553 (HTR2B/C inhibitor) or mCPP (HTR2B/C agonist) resulted in morphological changes **(A)** evocative of EMT in mCPP treated cells (Scale bar is 50 micron). Inhibitor treatment gave colonies of small cells with tight borders. Quantification of the effect **(B)** was carried out by scoring each colony as epithelial, mixed or mesenchymal. Experiment performed in 3 replicates.

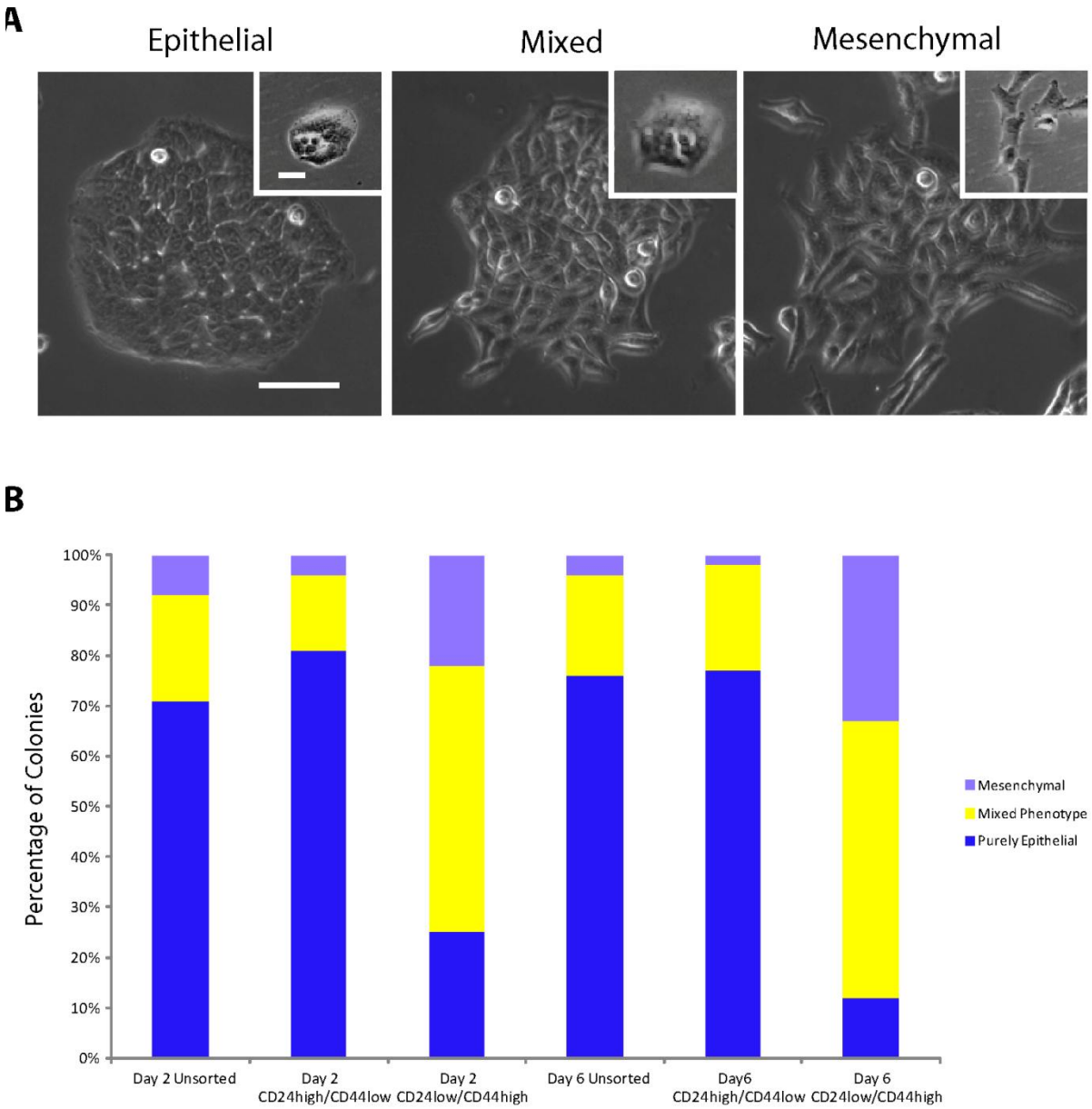

Figure 3.10 CD44high/CD24low Sorted Cells Show Stable Mesenchymal Phenotype. Clonogenic plating of unsorted as well as CD44high/CD24low and CD24high/CD44low H1650 cells sorted by FACS gave colonies with stable phenotype over time **(A)** between day 2 (inset) and day 6 (main figure)(Scale bar is 50 micron, inset is 10 micron). Quantification of this effect **(B)** showed increased number of mixed and mesenchymal colonies in CD44high/CD24low sorted cells but not other groups.

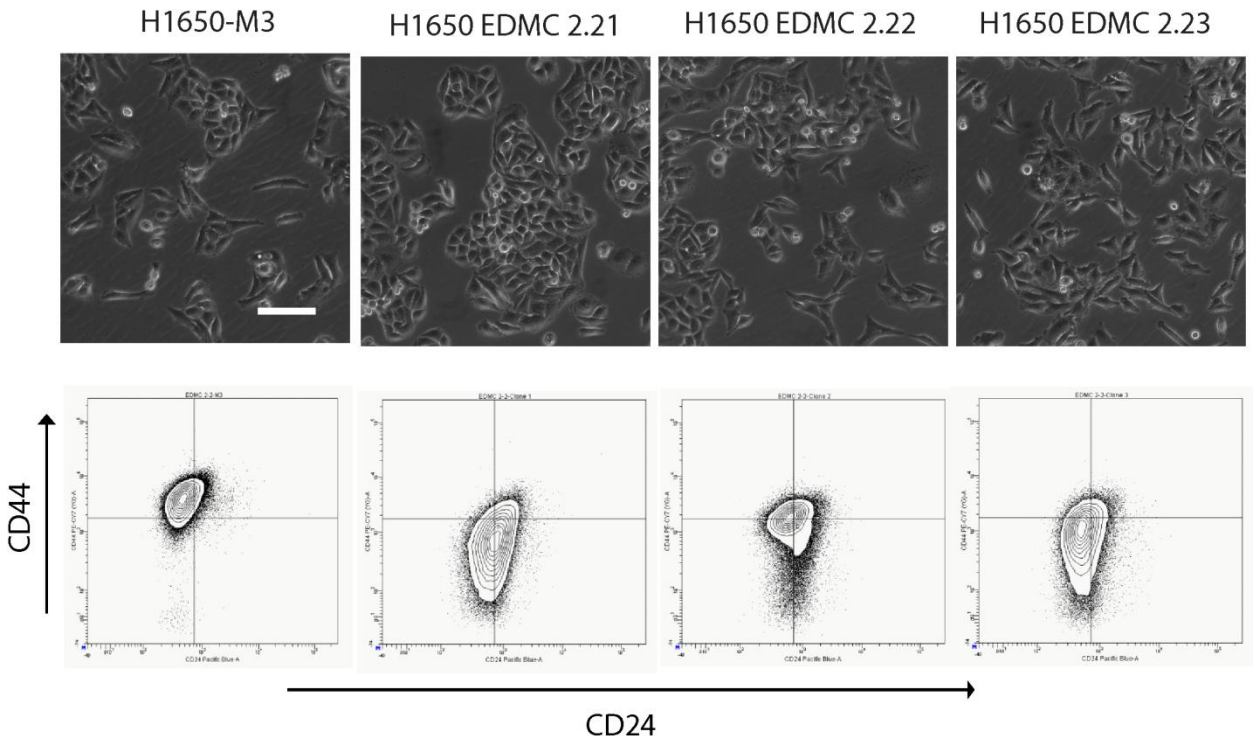

Figure 3.11 Generation of Stable Epithelially-Derived Mesenchymal Cells (EDMCs). Serial sorting of H1650 followed by colony isolation allow for the establishment of cells with stable mesenchymal morphology **(A).** This is reflected in differential CD44 and CD24 content measured by flow cytometry **(B).** The EMT derived cell line H1650-M3 is included for comparison.

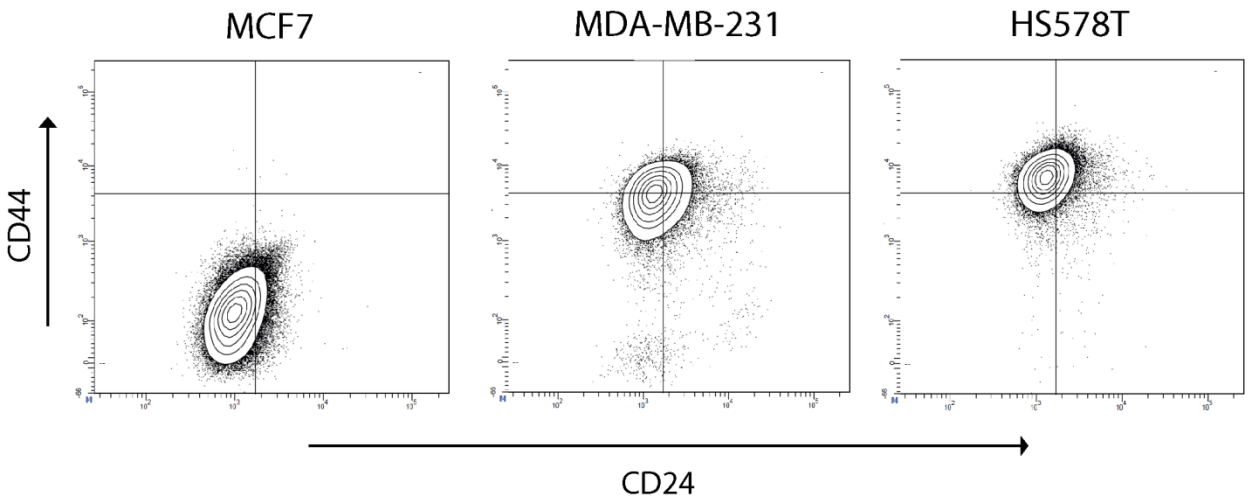

Figure 3.12 Breast Cancer Derived Cell Lines Display Differential CD44/CD24 Staining Levels. Similar to NSCLC cell lines, breast cancer cell lines display unique CD44/CD24 signatures by flow cytometry. MCF7 are CD44low, while MDA-MB-231 cells are intermediate and HS578T have a CD44high/CD24low immunophenotype.

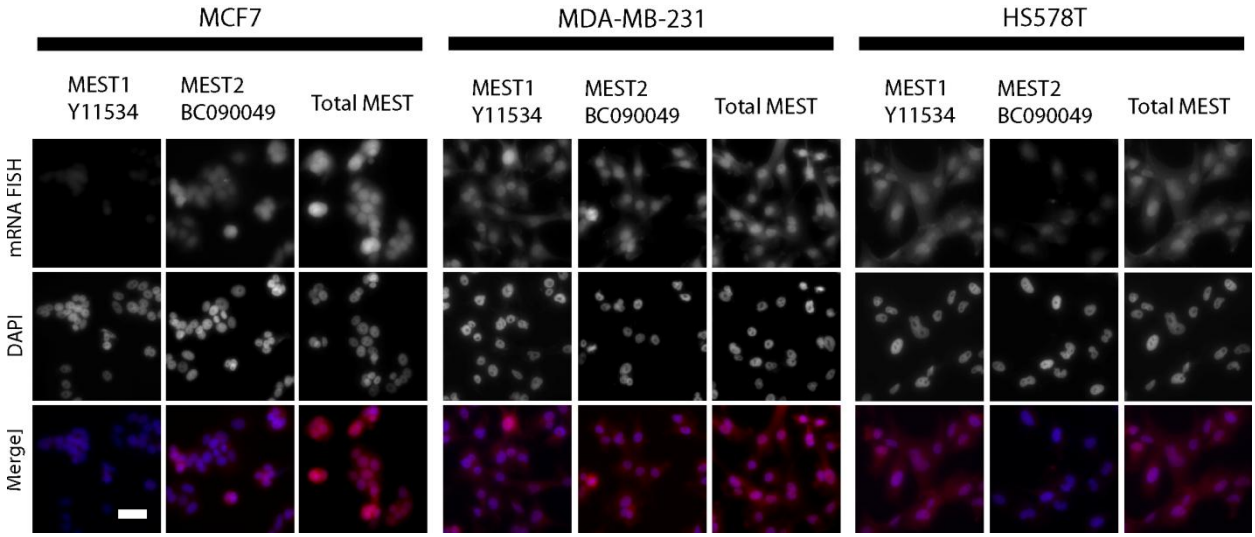

Figure 3.13 Detection of MEST Isoforms by RNA FISH. Breast cancer cell lines characterized for CD44/CD24 content in Figure 3.12 were tested for variation in MEST isoform expression levels using specific exon junction probes. MCF7 showed greatest levels of total MEST and preferential production of isoform 2, while HS578 showed lowest levels and relative increase in isoform 1. MDA-MB-231 showed production of both transcripts and intermediate total MEST levels (Scale bar is 40 micron).

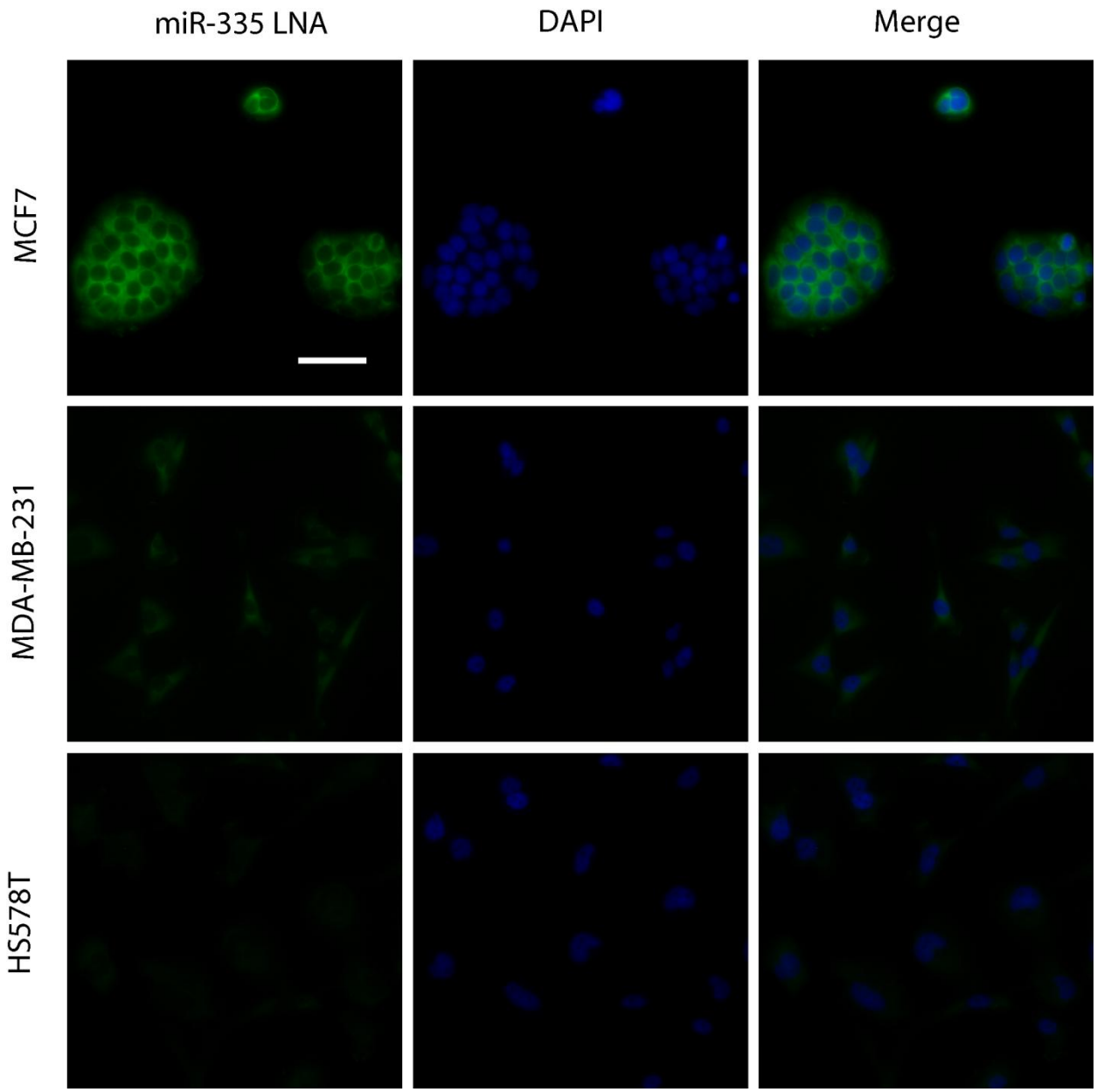

Figure 3.14 mir335 LNA Detection in Breast Cancer Cell Lines. FISH using mir335 specific LNA showed increased levels in MCF7 cells, which express high levels of MEST and preferentially produce isoform 3. Mir335 was nearly undetectable in HS578T, which express low levels of MEST. Intermediate levels of mir335 were apparent in MDA-MB-231 (Scale bar is 50 micron).

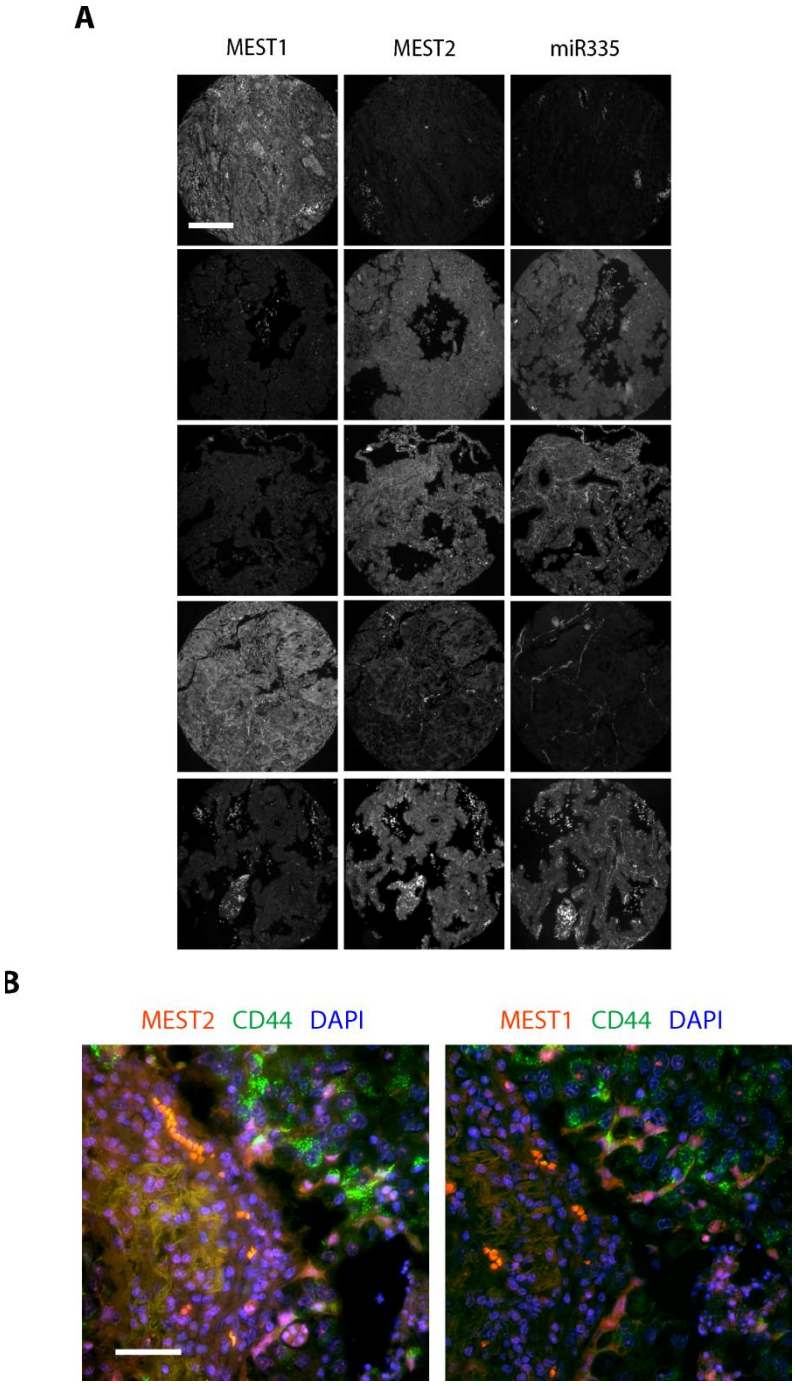

Figure 3.15 Staining of Human Tumors Correlates MEST Isoform Switching and mir335 Levels. FISH of human tumor samples using isoform specific probes shows differential staining for each isoform in the same tumor **(A)**. High isoform 1 expression is found in samples with low isoform 2 and mir335 expression, while samples with high isoform 2 expression typically have high mir335 expression and low isoform 1 expression (Scale bar is 300 micron). Comparison with CD44 staining **(B)** in a tumor displaying regions of both MEST1 and 2 staining show MEST1 to be localized to areas of CD44 immune-reactivity (Scale bar is 60 micron).

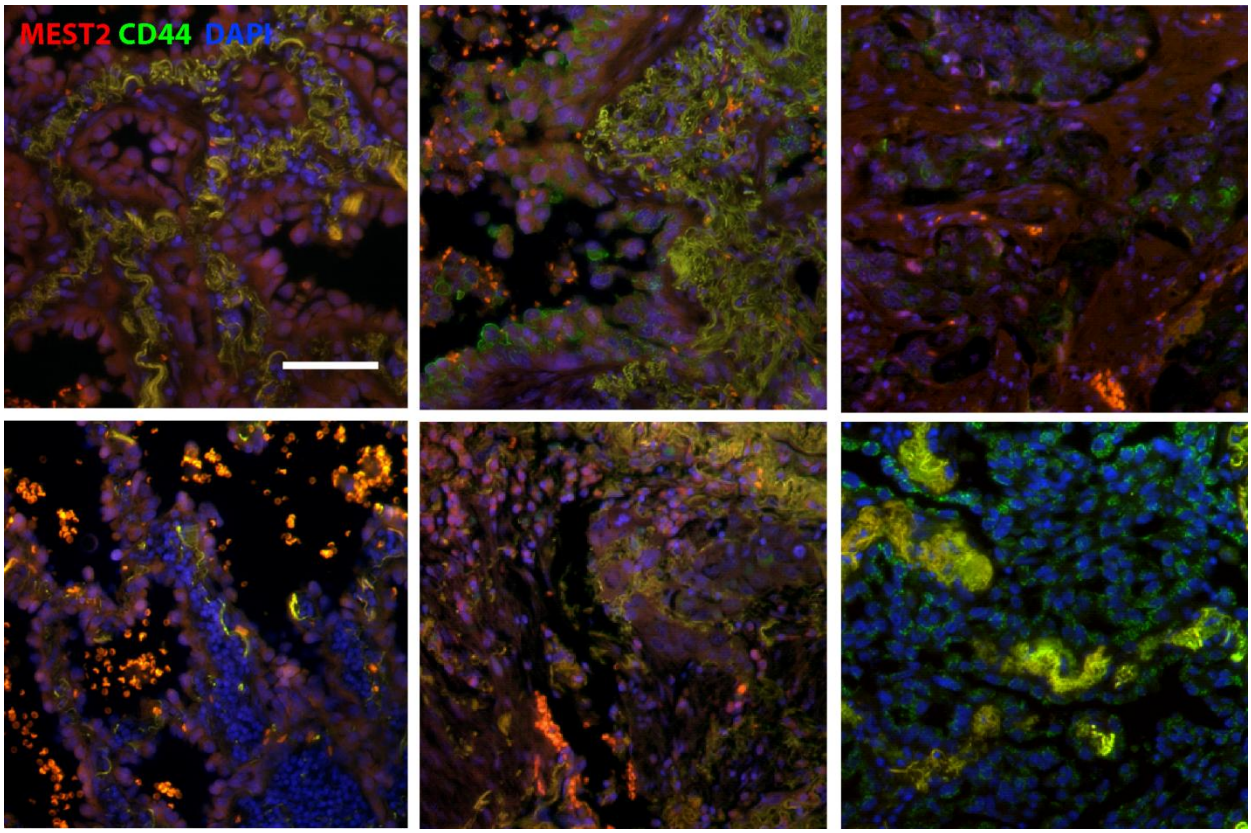

Figure 3.16 MEST2 Expression is Anti-Correlated with CD44 Expression. Co-labeling of human tumors for MEST2 mRNA and CD44 protein show a diversity of staining patterns. CD44 is typically not seen in MEST2+ polarized epithelium, with rare exception.

Chapter 4

P53-Ψ is a Neomorphic P53 Isoform that Lacks a Canonical P53 Tumor Suppressor Response

Chapter 4: P53-Ψ is a Neomorphic P53 Isoform that Lacks a Canonical P53 Tumor Suppressor Response

Summary

Transcriptional analysis of $CD44^{high}CD24^{low}$ cells revealed a decrease in the expression of p53. The p53 tumor suppressor plays a critical role in genome surveillance, suppression of oncogenic transformation, and regulation of many fundamental aspects of reversible and irreversible cellular stress responses (Vousden & Lane, 2007). p53 mutations, through loss of p53 function and putative gain-of-function activities, disable these effects and are associated with aggressive cancers and poor patient prognosis. Although much is known about the underlying mechanisms of p53 regulation and activity, the factors that influence the diversity and duration of p53 responses are not well understood. By studying the regulation of p53 expression in $CD44^{high}CD24^{low}$ populations, we uncovered a novel, evolutionarily conserved, mode of p53 regulation involving alternative splicing of the Tp53 gene. The use of an alternative 3' splice site in intron 6 generates a previously uncharacterized p53 isoform, dubbed p53Ψ (Wei, Zaika, & Zaika, 2012). At the molecular level, p53Ψ lacks major portions of the DNA-binding domain, the nuclear-localization sequence, and the tetramerization domain and as such is incapable of sequence-specific DNA binding and target trans-activation. Yet in a manner similar to certain p53 gain-of-function mutants, expression of p53Ψ attenuated expression of E-cadherin, induced expression of markers associated with EMT and enhanced motility and invasiveness (Adhikari & Iwakuma, 2009). Consistent with these contributions to a metastatic phenotype, expression of p53Ψ is a negative prognostic factor of disease free survival in non-small cell lung carcinoma patients. We describe a novel mechanism for the effects of p53Ψ involving the activation of ROS by cyclophilin D, a mitochondrial matrix peptidyl-prolyl isomerase known to modulate opening of the mitochondrial permeability transition pore (Schinzel et al., 2005).

Highlights

- Sequencing of p53 cDNA from EMT derived cells revealed a novel transcript that utilizes a conserved 3' splice site within intron 6 to generate a truncated molecule lacking complete DNA binding, nuclear localization and oligomerization domains

- Expression of this isoform, which we termed p53 Ψ, is correlated with poor outcome in human lung adenocarcinoma, fibrotic cells in animal models of injury and TGF-β signaling
- p53 Ψ is unable to activate the canonical p53 transcriptional response but causes increase in the expression of known markers of EMT
- Cellular EMT induced by p53 Ψ is dependent upon mitochondrial ROS generated by interaction between cyclophillin D and p53 Ψ

Introduction

The human TP53 gene spans a 20 kb region located on the short arm of chromosome 17 (17p13.1). The protein product encoded by this region, p53, is responsible for sensing a diverse number of cellular stresses and responding by inducing cell cycle arrest, apoptosis, sensescence, DNA repair or changes in metabolism (Vousden & Lane, 2007). Many of these functions have been ascribed to its ability to stimulate sequence specific DNA transcriptional activation of genes that inhibit growth or invasion (Kruse & Gu, 2009).

Because of its central role in growth arrest, p53 represents a significant hurdle towards a cell entering a state of immortal growth. It should come as no surprise that mutations disabling p53 stimulation of anti-proliferative down-stream effectors are common occurrences in human tumors (Rodin & Rodin, 2000). Many of these mutations occur at recurrent loci, or hotspots, within the DNA binding domain of the molecule. The fact that hotspots in the p53 gene show intensive positive selection, occur in highly conserved and functionally important regions and are distinct among different tumor types have led investigators to suggest that loss of function is not the only consequence of these frequent point mutations (van Oijen & Slootweg, 2000).

The vast majority of cancer-associated p53 mutations lead to the production of full length proteins, typically with only a single amino acid substitution, that are able to accumulate in tumor cells to levels in great excess of wtp53 in noncancerous cells (Rotter, 1983). Studies have suggested that these mutant proteins may confer gain-of-function properties to the cells in which they are expressed. This concept has been supported by the demonstration of a number of novel phenotypes caused by mutant p53 expression when compared to p53 null animals, including increased tumor incidence and the broadened variety of cancer types (Duan et al., 2002; Hingorani et al., 2005; Olive et al., 2004). *In*

vitro studies have corroborated the notion of p53 gain-of-function mutations by demonstrating increased motility and changes to integrin dynamics in response to expression of hotspot mutants in p53 null cells (Muller et al., 2009).

In addition to genomic mutation, multiple p53 variants generated by alternative promoter usage or alternative pre-mRNA splicing have been recorded (Marcel et al., 2011). These events lead to translation of distinct protein isoforms with differing effect on p53 transcriptional activity (Wei et al., 2012). We report the identification of a novel p53 isoform generated by the usage of an alternative 3' splice acceptor site within intron 6 of the TP53 gene. This transcript encodes a previously uncharacterized p53 isoform, dubbed p53Ψ. At the molecular level, p53Ψ lacks major portions of the DNA-binding domain, the nuclear-localization sequence, and the tetramerization domain and as such is incapable of sequence-specific DNA binding and target trans-activation. Unlike other reported splice variants of p53, we provide evidence of physiological expression during wound response in animal injury models and gain-of-function activity.

Intriguingly, expression of p53Ψ attenuated expression of E-cadherin, induced expression of markers associated with EMT and enhanced motility and invasiveness in a manner similar to certain p53 gain-of-function mutants (Dong et al., 2007). Consistent with these contributions to a metastatic phenotype, expression of p53Ψ is a negative prognostic factor of disease free survival in non-small cell lung carcinoma patients. We also provide evidence that p53 Ψ cooperates with the TGF-β signaling axis in promoting these phenotypes. Finally, we describe a novel mechanism for the effects of p53Ψ involving the activation of ROS by cyclophilin D, a mitochondrial matrix peptidyl-prolyl isomerase known to modulate opening of the mitochondrial permeability transition pore (Vaseva et al., 2012).

Results

We recently described a spontaneously occurring sub-population of cells present in non-small cell lung cancer (NSCLC) tumors and tumor-derived cell lines (Yao et al., 2010). These cells display mesenchymal morphology, increased motility and invasion, as well as differential expression of the cell-surface markers CD44 and CD24, compared to the parental cells. Gene expression profiling of these CD44high/CD24low cells revealed a substantial decrease in the expression of p53. When we measured p53 mRNA levels using RT-PCR in the $CD44^{high}/CD24^{low}$ cell line H1650-M3, we observed a less intense and slower migrating band (Figure 4.1). Further studies using multiple primers spanning the entire TP53

gene suggested that the mRNA species that we observed is a unique alternatively spliced TP53 transcript (Data not shown). Sequence analysis confirmed the existence of a novel p53 mRNA variant generated by the usage of an alternative 3' splice acceptor site within intron 6 that is highly conserved across species (Figure 4.1). The use of this alternative splice site leads to a frame shift that places a stop codon 19 amino acids downstream of the splice junction. Hence, ectopic expression of the novel p53 isoform resulted in a protein that runs more rapidly in SDS-PAGE gels than does full-length p53 (p53FL) and that co-migrates with a protein of similar size in $CD44^{high}/CD24^{low}$ -derived cell extracts. We will refer to the shorter p53 variant as p53Ψ.

To rule out the possibility that p53Ψ expression was unique to H1650-M3 cells or that it was a cell culture artifact, p53Ψ transcript levels were determined in multiple cancer-derived cells and in a large collection of lung tumors, by RT-PCR analysis and using a p53Ψ-specific RNA-FISH probe respectively (Figures 4.2, 4.3 and 4.4). Because initially we observed that p53Ψ expression was increased in $CD44^{high}/CD24^{low}$ cells, we specifically determined the expression of p53Ψ transcript in this cell population relative to all others. In all cases, enrichment of p53Ψ was observed in $CD44^{high}/CD24^{low}$ cells.

Aside from its well-established roles in tumorigenesis, the tumor suppressor p53 has been implicated in the pathogenesis of non-cancer-related conditions such as insulin resistance, cardiac failure, and fibrosis. To determine whether p53Ψ expression could also occur as part of a physiological response, we probed for p53Ψ expression in tissues after pro-fibrotic insults using RT-PCR and RNA FISH (Figures 4.8, 4.5 and 4.6). Within naphthalene injured lungs, we detected a robust increase in p53Ψ mRNA. Using exon6-intron6 specific FISH probes, we localized this expression to the bronchial epithelium, which is damaged after naphthalene administration (Figure 4.5). We saw similar increase in liver expression of p53Ψ in mice treated with carbon tetrachloride (CCL4). RNA FISH showed p53Ψ signal localized to regions of peri-sinusoidal fibrosis, demarcated by alpha-smooth muscle actin (α-SMA) expression (Figure 4.6).

During the tissue repair process, certain α-SMA+ cells up-regulate CD44, a surface marker associated with invasive and motile cancer cells. Because the $CD44^{high}/CD24^{low}$ population of tumors and tumor derived cell lines express p53Ψ, we sought to see if p53Ψ expression was relegated to a similar population in the injury repair process. As such, we sorted $CD44^{high}/CD24^{low}$/CD45-/Pecam- cells from naphthalene-injured lung tissue and evaluated the expression of p53Ψ by RT-PCR analysis (Figure 4.7). We indeed found p53Ψ expression restricted to the CD44highCD24low cells.

Functional and molecular studies have indicated that TGF-β plays a pivotal role in regulating the ontogeny of CD44high/CD24low cells. Hence, we hypothesized that increased activation of the TGF-β pathway observed across our studies in CD44high/CD24low cells was required for the regulation of the alternative splicing event that creates p53Ψ. Indeed, knocking-down the expression of either TGF-β1 or 2 resulted in the restoration of control levels of p53FL (Data not shown). To determine whether TGF-β treatment was per se sufficient to induce expression of p53Ψ, we next treated cells with TGF-β1 and TGF-β2. This resulted in an increased expression of p53Ψ (Figure 4.8). To rule out a specific role of TGF-β in regulating p53Ψ beyond the simple induction of a mesenchymal-like state we silenced snai1 expression; snai1 is a transcription factor regulated by TGF-β and known to mediate TGF-β-induced epithelial-mesenchymal transition (EMT) in $CD44^{high}/CD24^{low}$ cells (Mani et al., 2008). Snai1 silencing did not alter levels of p53Ψ but did revert the EMT (Data not shown). Hence, these observations indicate a causative role for TGF-β in regulating p53Ψ expression and in principle explain the restriction of p53Ψ expression to CD44high/CD24low cells.

Beyond the impact of an early stop codon on p53 expression levels, the p53Ψ isoform encodes a p53 protein devoid of its oligomerization domain, nuclear-localization-sequence (NLS), and critical residues required for DNA binding (Chang, Imam, & Wilkinson, 2007). Because these structural elements are critical for p53 transcriptional activity, we reasoned that p53Ψ would be neither able to induce canonical p53 transcription targets nor elicit a typical anti-proliferative response. Hence, the alternative splicing of p53 mRNA to generate p53Ψ encoding transcript could represent a novel mechanism in limiting canonical p53 activity and coordinating the TGF-β and p53 axis. Of note, deregulation of TGF-beta and p53 mediated signaling has been shown to play a critical role in tissue injury/repair and fibrotic conditions (K. K. Kim et al., 2006).

To provide experimental evidence supporting the lack of transcriptional activity of p53Ψ, we compared levels of expression of canonical p53 transcriptional targets in cells expressing the p53Ψ and p53FL isoforms (Figure 4.9). In all cases, we consistently observed a decreased expression of known constitutively expressed and DNA-damage-induced (e.g., by doxorubicin treatment) p53 targets. In addition, unlike expression of p53FL, expression of p53Ψ in p53-null H1299 cells caused no change in the viability of cells upon doxorubicin treatment, a DNA damaging agent known to activate p53FL (Data not shown). To more directly assess whether p53 Ψ was lacking transcriptional activity, we compared the activation of a p53-responsive promoter in cells ectopically expressing either p53FL or p53Ψ. Luciferase reporter assays using a synthetic p21CIP1 promoter demonstrated that p53Ψ was transcriptionally

inactive (Data not shown). Although it seemed possible that p53 Ψ could affect transcription by acting in a dominant negative fashion (e.g. titrating p53 interaction proteins), we found no evidence that p53 Ψ over-expression could impact levels of p53 transcriptional targets in cells expressing wild-type, full length p53 (Weisz, Oren, & Rotter, 2007). This was true in both basal conditions and upon stimulation with the DNA damaging agent doxorubicin.

$CD44^{high}/CD24^{low}$ cells are characterized not only by decreased expression of p53 targets, but also by mesenchymal-like morphology, expression of genes involved in epithelial-to-mesenchymal transition (EMT), and increased motility and invasiveness. These attributes were evocative of the phenotype caused by expression of certain p53 mutants (i.e., R273H and R249S), which led us to wonder if p53Ψ could contribute to the manifestation of these features (Adhikari & Iwakuma, 2009). Ectopic expression of even low levels of p53Ψ resulted in morphological and molecular changes typical of cells undergoing EMT (Figure 4.10). This included increased cell motility in standard scratch assays and enhanced invasive capability in reconstituted basal-membrane trans-well assays when compared to cells expressing p53FL in multiple cell lines (H1650, H1299, MCF7) independent of their original p53 status.

Interestingly, we found that p53Ψ was not only sufficient to induce phenotypic features associated with the $CD44^{high}/CD24^{low}$ state but it was also required for their maintenance. Knockdown of p53Ψ reduced the invasiveness of these cells and increased E-cadherin levels (Data not shown). This observation was of particular interest because autocrine secretion of TGF-β was necessary and sufficient to repress E-cadherin and increase invasiveness of $CD44^{high}/CD24^{low}$ cells. Thus, our data suggest p53Ψ to likely to be required for TGF-β mediated signaling. To test whether p53Ψ cooperates with TGF-β, we determined the activation of two synthetic reporter constructs measuring the activity of the TGF-beta axis (SBE4-luc and 3TP-lux) in p53-null cells ectopically expressing p53FL and p53Ψ. We found that p53Ψ ectopic expression was able to potentiate the activation of TGF-β-mediated transcription to a greater extent than did expression of p53FL (Data not shown).

This observation parallels recent findings reporting the unexpected identification of p53 as a partner of TGF-β in inducing EMT (Adorno et al., 2009). In addition, it implies that the expression of a truncated p53 isoform incapable of transcriptional activation is required/ sufficient for the cooperation with TGF-β. In principle this suggests that the alternative splicing event that creates p53Ψ results in a separation of p53 function activity—although it restricts p53 tumor suppressive activities, it allows for p53-mediated EMT, motility and invasion, and functional interaction with the TGF-β axis.

Epithelial to mesenchymal transition, increased motility and cell invasion are important hallmarks of metastatic cells and have all been linked to increased cell metastatic potential. Hence, having shown increased expression of p53Ψ in certain NSCLC cell lines, we evaluated whether p53Ψ expression could be indicative of an increased probability of tumor relapse in patients with early stage NSCLC. Univariate Kaplan-Meier survival analysis indicated that tumors expressing high levels of p53Ψ displayed a significant higher probability of disease recurrence or death from cancer when compared to the p53Ψ low group (p values ranged from 0.02 to 3 x 10-5 depending on the datasets) (Figure 4.11). The decreased average disease free and survival time in patients with tumors high in p53Ψ content therefore supports a general relevance of p53Ψ in reprogramming cells towards the acquisition of pro-metastatic features.

Due to the similarities of p53Ψ and gain-of-function p53 mutants and in order to elucidate the underpinnings of the p53Ψ-mediated phenotypes, we next determined whether molecular mechanisms proposed to explain p53 gain-of-function activities could be active in p53Ψ expressing cells. P53 mutations are proposed to have gain-of-function activities because of (1) a physical interaction with p53-related proteins such as p63 that negatively regulates their pro-apoptotic and anti-mesenchymal functions or (2) interactions with transcription factors that positively or negatively modulate their transcriptional output (Y. Li & Prives, 2007). In addition it has also been shown that gain-of-function p53 mutations may increase the invasive capabilities of cells by promoting the recycling of EGFR and integrin at the membrane as well as increasing the expression of certain microRNAs (Dong et al., 2012). However, none of these mechanisms appears to explain the biological activities of p53Ψ as p53Ψ is not localized in the nucleus, p63 and mir-128-2 are not expressed in H1650-M3 cells (Data not shown) and ectopic expression of p53Ψ did not change the internalization rate of EGFR when expressed in p53-deficient cells or cells expressing wild-type p53 (Data not shown).

A growing body of evidence highlights the importance of p53 localization to mitochondria in mediating some of the p53 transcription–independent activities . Interestingly, immunostaining and biochemical evidence indicated a distinct sub-cellular localization of p53Ψ compared to p53FL (Figure 4.12). In fact, in expression experiments we observed that p53FL exhibited a predominantly nuclear staining, whereas p53Ψ was mostly observed in a punctuate pattern in the cytoplasm. By co-expressing p53FL and p53Ψ with a GFP family protein that is targeted exclusively to mitochondria (mCherry) we found that a portion of p53Ψ localizes to mitochondria (Figure 4.13). Biochemical fractionation

experiments examining the sub-cellular distribution of endogenous as well as ectopically expressed p53Ψ corroborated this observation (Data not shown).

It has been previously shown that p53 binds to BAX and BCL2 at the mitochondrial outer membrane and to SOD2 and cyclophilin D (CpD) at the inner membrane and within the mitochondrial matrix (Chipuk et al., 2004). Immuno-precipitation experiments indicated that p53Ψ was not able to bind to BAX or SOD2 but reproducibly interacted with CpD (Data not shown). In light of this finding we tested whether the interaction with CpD was required for p53Ψ-dependent EMT and increased motility. To this end we transfected cells with siRNAs targeting CpD or treated cells with cyclosporine A (CsA), a pharmacological inhibitor of CpD. Inhibiting CpD restored the expression of E-cadherin and decreased the expression of EMT markers as well as reduced the motility of cells to levels similar to the ones observed in control (Data not shown). Interestingly, similar effects were also observed in cells expressing p53 mutants. Hence, we concluded that CpD is part of a novel transcription-independent mechanism that mediates activities elicited by p53Ψ and certain p53 gain-of-function mutants.

CpD, encoded by the Ppif gene, is a mitochondrial matrix peptidyl-prolyl isomerase that modulates the opening of the mitochondrial permeability transition pore (MPTP) (Schinzel et al., 2005). Hence we hypothesized that interaction of p53Ψ with CpD could modify MPTP permeability and reactive oxygen species (ROS) production. Consistent with this hypothesis, we observed increased mitochondria permeability and increased mitochondrial oxygen superoxide production in cells expressing p53Ψ compared to cells that expressed p53FL (Figure 4.14 and 4.15). To further establish a role for CpD in mediating MPTP increased opening and ROS generation in p53Ψ-expressing cells, we then measured mitochondrial ROS production and mitochondrial membrane permeability in cells treated with CsA (Figure 4.16). CpD inactivation in p53Ψ-expressing cells decreased permeability and ROS production to levels comparable to those observed in cells expressing p53FL.

Although initially considered to be detrimental for cells, recent studies suggest that ROS are necessary for the activation of multiple cellular pathways and for the induction of different cell states. Specifically, increased ROS has been shown to induce EMT and to increase the metastatic competence of cells (W. S. Wu, 2006). To determine whether ROS have a causative role in mediating p53Ψ-induced phenotypes, we modulated ROS levels in cells and determined their effects on expression of EMT markers and cell invasion (Data not shown). Inhibition of ROS production in H1650-M3 cells as well as in cells ectopically expressing p53Ψ with N-acetyl cysteine (NAC) and tempol, two well-known ROS scavengers, augmented expression of E-cadherin and decreased invasive capabilities of p53Ψ-expressing

cells compared to control cells. In contrast, low doses of H2O2 decreased the expression of E-cadherin without compromising the cells viability (Data not shown).

To exclude the possibility that the increased ROS production in p53Ψ-expressing cells was due to the activation of a parallel pathway, we performed epistasis experiments (Figure 4.17). Specifically we measured E-cadherin expression upon manipulation of ROS levels (e.g., by NAC treatment) in cells ectopically expressing p53Ψ in the presence and absence of CpD. We reasoned that if CpD and p53Ψ act on parallel pathways we would observe an additive effect of CpD silencing and ROS inhibition but that if p53Ψ acts solely through CpD, CpD silencing would be sufficient to reduce ROS levels and no additive effect would be observed. Notably, NAC did not result in increased E-cadherin expression in cells in which CpD was silenced, corroborating the conclusion that CpD is responsible for ROS-induced EMT by p53Ψ.

Discussion

In summary, we provide evidence describing a novel, evolutionarily conserved, mode of p53 regulation involving alternative splicing of the TP53 mRNA. The use of an alternative 3' splice site in intron 6 generates a previously uncharacterized p53 isoform that is incapable of sequence-specific DNA binding and trans-activation of canonical p53 target genes. Yet expression of this isoform, p53Ψ, decreased expression of E-cadherin, induced markers of EMT and promoted phenotypes associated with metastasis through a novel mechanism involving ROS generation via CpD binding. Although it was previously shown that p53 controls ROS levels through multiple mechanisms, the fact that ectopic expression of p53Ψ in p53FL cells was unable to modify the expression of Tigar, Sens1, Sens2, Gpx1, Bax, Puma strongly support the existence of a novel transcription-independent mechanism of ROS production by p53Ψ.

Consistent with these observations, we found that increased expression of p53Ψ in tumors correlated with poor prognosis and its expression was increased in CD44high/CD24low cells both in tumors and in injured tissues. In these cells, the expression of p53Ψ at the expense of p53FL acts to mitigate activation of canonical p53 tumor suppressor activities thus potentially facilitating proliferation of cells and invasion into damaged tissue.

The observation that p53Ψ is expressed highly in both metastatic cells and during tissue injury/repair supports previous findings that suggest tumors retain physiologic responses intrinsic to the tissue from which they are derived. Thus one may view the metastatic program as an abnormal activation of damage reparation mechanisms. In this regard, tumors are truly "wounds that never heal."

Current work in the lab aims at characterizing the role of p53Ψ in lung wound healing. Based on the pioneering work of Dr. Lowe's laboratory, we hypothesize that the alternative splicing event that generates this novel p53 isoform could represent a way to delay the occurrence of p53 induced senescence during tissue injury/repair. Interestingly, we find that although the $CD44^{high}/CD24^{low}$ population of tumor derived cell lines express the majority of SASP proteins, they are able to grow happily *in vitro*. Yet the expression of full length p53 rapidly induces senescence, suggesting these cells are primed in a pre-senescent state. Given the role of SASP in repairing damaged epithelium, this could indicate that premature clearance of the $CD44^{high}/CD24^{low}$ population would result in deficits of re-epitheliazation. Conversely, persistence of these cells may be linked to fibrosis. As such, the mechanistic understanding of factors governing the balance between production of p53 FL and p53Ψ mRNA could potentially be translated to novel therapeutics for the treatment of fibrotic conditions.

As decreased p53 expression or loss of transcriptional activity has been shown to lead to increased genomic instability, we are also interested in exploring whether restoring p53 FL expression in wounded epithelium may reduce tumor burden or delay tumor onset in models of carcinoma (Hingorani et al., 2005). This could be particularly relevant to lung cancer, as chronic inflammatory conditions such as COPD have shown strong association with the disease.

Lastly, the remarkably similar activities of p53Ψ with certain p53 "gain-of-function" mutants, which also reduce E-cadherin expression and facilitate invasion, suggests that these p53 mutations "highjack" a regulated and reversible program that coordinates the tissue damage response in normal tissues. The direct role of p53Ψ in precipitating neoplasm has not yet been explored, but we feel there is strong indication that p53 alternative splicing, similar to p53 hot spot mutation, will promote tumorigenesis. These similarities between the molecular mechanisms of p53Ψ and p53 mutant gain of function suggest a physiological origin for the phenomena that has been conserved through much evolutionary space.

Experimental Procedures

Cell culture

H1650 (H1650), H1299 (NCI-H1299), MCF7, Phoenix-AMPHO cells were obtained from the American Type Culture Collection (ATCC) repository. CpD +/+ and CpD -/- mouse embryo fibroblasts (MEF) cells were a gift of Dr. Ute Moll. The H1650-M3 cell line was generated as described previously1. All the cell lines except for HEK293T cells and MEFs were cultured in RPMI supplemented with 5% FBS, glutamine, penicillin, and streptomycin. The retroviral packaging cell line Phoenix-AMPHO and MEF were cultured in DMEM containing 10% FBS, penicillin, streptomycin, and sodium pyruvate.

Immunoblots and Immunoprecipitation

Cells were washed with PBS before collection and lysed directly in RIPA buffer containing 0.2% SDS. Proteins were separated by SDS-PAGE, transferred to nitrocellulose membranes (Bio-Rad), and blotted with antibodies as indicated.

In immune-preciptation experiments, protein extracts were incubated with 50ul protein A/G beads (#20423, Thermo Scientific) for 1h at 4°C to be pre-cleared. Beads wee then spin down and the supernatants were transferred to new tubes and incubated with primary antibodies (2ug/ml) for 4h. The complexes were further precipitated by binding to sepharose conjugated protein A/G beads for 2h. The pulled down proteins were eluted with laemmli buffer and subjected to western blot analysis.

Immunostaining of Cultured Cells and Tissue Slides

Cells were cultured in 24-well chamber slides. After washing once with phosphate-buffered saline (PBS), cells were fixed in 4% paraformaldehyde and permeabilized in 0.1% Triton X-100 in PBS for 10 min. Fixed cells were washed three times in PBS and blocked with 3% bovine serum albumin in PBS for 30 min. After washing three times with PBS, cells were incubated with the primary antibody for 1 h at room temperature. Immune complexes were then stained with donkey anti-mouse immunoglobulin G conjugated with rhodamine antibodies (Invitrogen). DAPI was used for nuclear staining. Stained cells

were mounted with Vectashield Mounting medium (Vector Laboratories) and analyzed under an inverted microscope.

Whole tissue sections were prepared from animals sacrificed and exsanguinated using PBS flushing. Livers and lungs were removed, washed and fixed in 4% formaldehyde/PBS overnight. Processing and embedding was performed by RADIL (University of Missouri) and the CSHL histology core facility, sections were cut at a thickness of 5 um. Slides were heated to 65 degree Celsius for 30 minutes to remove excess paraffin then cleared using Histoclear and rehydrated in stepwise graded alcohol. After washing in PBS, slides were treated with H2O2 to limit autofluorescence. Following another round of washes, slides were boiled in citrate antigen retrieval buffer for 20 minutes. Permeabilization was accomplished with 0.5% triton x-100 in PBS with 2% BSA, followed by washing with 1% BSA in PBS. Slides were incubated with primary antibody at 4 degrees Celsius overnight. Secondary antibody labeling was performed with the species appropriate fluorescent conjugate for one hour at room temperature the next day. DAPI was used to label nuclei. All slides were mounted using p-Phenylenediamine anti-fade media. Imaging was performed on the Zeiss 710 confocal microscrope running Zen software.

siRNA-Based Gene Knockdown

Commercially prepared siRNAs against p53 were obtained (I) HSS186391 from Invitrogen and (II) 115182 from Ambion; siRNAs against Cyclophilin D is from Dharmacon smart pool. siRNAs were transfected into cells using Lipofectamine 2000 (Invitrogen) as per the manufacturer's instructions. mRNA levels were determined by RT-PCR and Western Blot.

Retroviral-Based Tet-on Expression System

The retroviral-based inducible expression system was kindly provided by Dr. Scott Lowe. The regulatory vector pMSCV-rtTA3-PGK-Hygro expresses an optimized tetracycline-controlled transactivator and the response plasmids TtIGP-MluEX contains an improved tetracycline response element (TRE) within the promoter that controls expression of p53 or p53ψ. These were transfected along with a viral env expression vector (e.g. pVSV-G) into Phoenix-AMPHO cells to generate retrovirus stocks that are then titrated to determine virus content. Cells were co-infected by both retroviruses and

selected simultaneously with puromycin and hygromycin to produce the desired double-stable cell lines. The expression of p53 or p53ψ in these cells was induced by doxycycline treatment and confirmed by immunoblotting with anti-p53 antibody.

Invasion Assays

The invasion assays were performed in 24-well 6.5-mm diameter inserts (Corning, 8.0-mm pore size) coated with a layer of growth factor reduced Matrigel (BD Transduction Laboratories). The cells were plated in the upper well in 0.2% serum and incubated with 5% FBS and 100 ng/ml fibronectin in the lower chambers. After 24 hours, cells in the upper chamber were removed with a cotton swab. Cells that had migrated into the lower chamber were fixed in 4% PFA and stained with 0.5% Crystal Violet. Filters were photographed and the total number of cells was quantified using the Odyssey Imaging System. Every experiment was repeated in quadruplicate.

RNA Extraction and RT-PCR

Total RNA was collected from cultured cells and tissues purified using SV Total RNA Isolation System following the manufacturer's instructions (promega). Total RNA (200 ng) was subjected to a reverse transcriptase reaction using the Improm-II Reverse Transcriptase kit (Promega). cDNA corresponding to approximately 1% of the RNA was used in three replicates for quantitative PCR with the SYBR GREEN (Applied Biosystems) labeling or for standard PCR. Indicated Taqman gene expression assays (Applied Biosystems) and the Taqman universal PCR master mix (Applied Biosystems) were used to quantify gene expression. Quantitative expression data were acquired and analyzed using an ABI (Applied Biosystems) Sequence Detection System.

Sub-Cellular Fractionation

Cultured cells were trypsinized, pelleted and washed with PBS. 107 ~108 cells were then resuspended in 2ml pre chilled buffer A (20mM HEPES, 250mM Sucrose, 1.5Mm MgCl2, 10mM KCl, 1mM EDTA, 1mM EGTA, 0.5mM DTT, proteases inhibitors cocktail). Cells were kept on ice for 5 minutes and then broken with a pre-chilled Dounce homogenizer (10 strokes with tight pestle). The nuclei were

then centrifuged out at 228G for 10 minutes at 4°C, the pellet (Nucleia) was then washed with buffer A and re-suspended in RIPA buffer. The supernatant was centrifuged again at 10,000G for 20 minutes at 4°C to pellet the crude mitochondrial. Next, the membrane were separated from supernatant with a further centrifuge at 100,000G for 1h. The clear supernatant in this case represents the cytosolic fraction. The crude mitochondrial was washed again and lysed in RIPA buffer to extract mitochondrial proteins.

MTT Assay

A total of 3,000 cells were plated in 0.2 ml in 96-well flat bottom plates and then exposed to erlotinib as indicated. At the indicated times, 20 µl of 5 mg/ml MTT solution (Sigma) in PBS was added to each well. After 3-4 h, medium was removed and 200 µl of DMSO was added to each well to dissolve the formazan crystals. The absorbance at 540 nm was determined using a plate reader (SpectraMax 190, Molecular Devices, Inc.). Experiments were conducted in octuplicate.

Luciferase Reporter Assay

p21-luciferase reporter plasmid was obtained from B. Vogelstein (Johns Hopkins Oncology Center, Baltimore, Md.). SBE4-Luc and were obtained from Adgene. The luciferase reporter assay was performed using the Dual-Luciferase Reporter assay system according to the manufacturer's instructions (Promega). The quantification of luciferase activities and calculation of the relative ratios in intensity were carried out with the Synergy™ H4 Multi-Mode Microplate Reader (BioTek). Transfection efficiency was normalized with respect to Renila luciferase activity.

FACS Analysis of CD44+CD24- Cells

Cells were cultured in RPMI or DMEM supplemented with penicillin-streptomycin and 5% fetal bovine serum. After dissociation, cells were washed with cold PBS containing 5% serum, pelleted and resuspended. After filtering through 40 micron mesh to generate single cell suspension, samples were incubated with directly conjugated fluorescent antibodies to the desired antigens for 20 minutes on ice.

Cells were then washed 3 times with cold PBS pH 7.2. Flow cytometry was perfomed using the LSRII running FACS Diva software, while sorting was accomplished with use of the Aria II (BD Bioscience).

For the in vivo experiments, mice were sacrificed at defined points after injury. Exsanguination was performed by severing of the brachial arteries. Lungs were flushed with cold PBS via intra-tracheal instillation, followed by incubation with collagenase and hyaluronidase to generate a single cell suspension. Remaining red blood cells were lysed with hypotonic ammonium chloride buffer, and cells were incubated with directly fluorescent conjugated antibodies to the desired antigens. Flow cytometry was perfomed using the LSRII running FACS Diva software. Single channel gating eliminated all cells expressing the surface antigen CD31, which labels endothelial cells, and CD45, which labels marrow-derived cells. Sorting experiments were performed using the BD Aria II.

FISH

Tissue sections were prepared, sectioned, cleared and rehydrated as described above. Slides were washed with PBS containing ribonucleoside vanadyl complex (New England Biolabs) to inhibit RNAse activity and treated with H2O2 to limit autofluorescence. Mild proteinase K treatment was used to expose mRNA for hybridization. After washing in 2x SSC, slides were hybridized overnight in heated, humidified chambers. After hybridization, slides were washed in 2x SSC, followed by 1x PBS. Post hybridization fixation was accomplished by treatement with 3% formaldehyde for 10 minutes at room temperature. Slides were washed and permeabilized with 0.5% triton x-100 in PBS for 5 minutes on ice. Blocking was performed with 1% BSA in PBS. Detection of digoxigenin labeled probes was accomplished using rabbit anti-digoxigenin Fab fragments directly conjugated to rhodamine (Roche) incubated for 1 hour at room temperature. Immunofluoresent staining was performed by incubation for 1 hour at room temperature with the appropriate antibodies. Counterstaining with DAPI was performed to visualize nuclei. Imaging was done on a Zeiss Axio Observer inverted fluorescent microscope running Axiovision software.

Mitochondrial Reactive Oxygen Species and Mitochondrial Permeability Measurement

Measurement of reactive oxygen species was performed using Mitosox Red staining (Invitrogen M36008). Rotenone (Sigma-Aldrich R8875) incubation was performed for two hours prior to cell harvest

using a concentration of 500 nM in complete RPMI media. Cyclosporin A treatment was carried out for 12 hours at a concentration of 2 μM in complete RPMI media.

For flow cytometry analysis, samples were prepared as previously described. Mitosox Red was prediluted into Hank's Buffered Saline Solution (HBSS) and added to cell suspensions, which were incubated at 37 degrees Celsius for the time indicated. Afterwards, ten times the reaction volume of ice cold HBSS was added, samples placed on ice and spun down to remove buffer containing Mitosox. Cells were washed two additional times with ice cold HBSS and passed through a 40 micron filter to ensure single cell suspension. Data acquisition was performed using an LSR II cytometer (BD Bioscience).

For microscopy experiments, cells were seeded onto sterile #1.5 coverslips (Corning) and allowed to attach for 24 hours in complete media before drug treatment (e.g. rotenone or cylcosporin A). Drug treatments were performed at concentrations previously described. Mitosox was delivered to cells in serum and antibiotic free RPMI and incubated for the time indicated. Afterwards, coverslips were washed with ice cold HBSS and fixed using 3% paraformaldehyde in PBS for ten minutes at room temperature. Afterwards, coverslips were washed three times for five minutes in PBS, counterstained with DAPI and mounted in anti-fade media. Imaging was performed using the 710 Confocal LSM (Zeiss, Germany) outfitted with 40X and 63X objectives and set to excite at 510 nm and acquire at 580 nm to observe Mitosox staining.

Mitochondrial loading was measured using Mitotracker Green FL (Invitrogen M-7514). Cells were stained by incubation with serum and antibiotic free RPMI containing 100 nM dye for 30 minutes at 37 degrees Celsius. Afterwards, they were prepared for flow cytometry as previously described.

For mitochondrial permeability measurement, cells were stained using the Mitoprobe transition pore assay kit (Invitrogen M34153). Treatment with cyclosporine A was performed as previously described. Staining with Calcein AM was performed at a concentration of 10 nM in HBSS for 15 minutes at 37 degrees Celsius. Cytoplasmic signal quenching was accomplished via concomitant treatment of cells with $CoCl_2$. Quenching of mitochondrial signal was accomplished via concomitant treatment with 50 nM ionomycin. Suspensions or cultured cells were then washed 3 times with fresh HBSS. Imaging was performed on living cells using the Observer inverter fluorescence microscope (Zeiss, Germany) outfitted with 63x objectives and appropriate bandpass filters. Flow cytometry was carried out using the LSRII set to acquire in the Alexa 488 range. For quantitative measures of fluorescence, Calcein AM

only controls were used as reference to a cell lines maximal fluorescence and Calcein/ionomycin/$CoCl_2$ treated cells as basal fluorescence.

Patients and Cancer Tissue Microarray

The NSCL tissue microarray was constructed by Dr. Robert Wagner from tissue obtained during surgical resections performed by Dr. Brendon Stiles, Dr. Alice Walsh, Dr. Matthew Lazzara, Dr. Anatoly Starkov and Dr. Nasser Altork in the Thoracic Department at Weill Cornell Medical School. Patients aged 18 years or older with histologically or cytologically confirmed lung cancer were enrolled in this study. Written informed consent was obtained from each study subject. The study was approved by the governing institutional review boards. Slides were prepared as detailed above. Imaging was carried out with either the Zeiss Observer microscope or the Aperio ScanScope FL outfitted with Image Scope processing software.

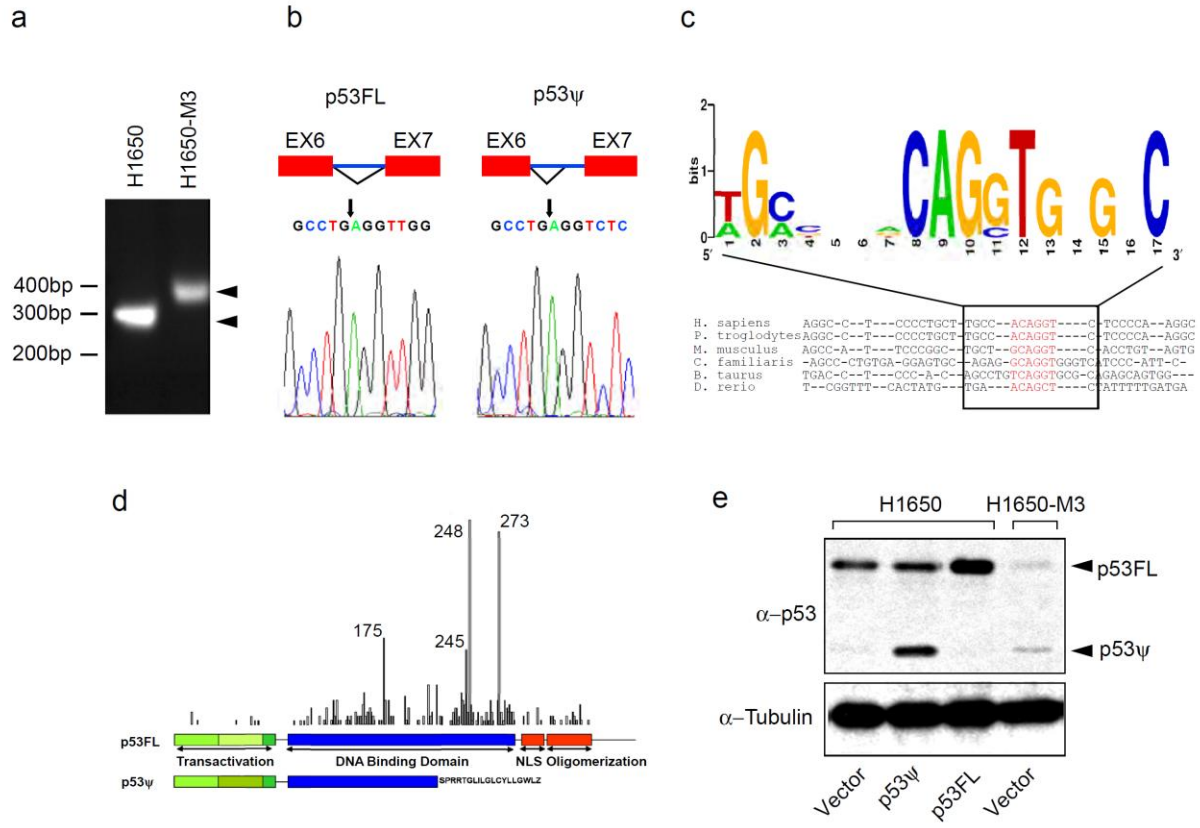

Figure 4.1 p53ψ is a Novel p53 Isoform Generated by the Use of an Alternative 3' Splice Site in Intron 6 in CD44^{high}/CD24^{low} Cells. (a) RT-PCR analysis of H1650 cells and of CD44^{high}/CD24^{low}-derived cells (H1650-M3) for *p53* mRNA revealed amplification products of approximately 300 and 350 base pairs (bp), respectively. **(b)** Sequence analysis of these two PCR products indicated use of a novel splice junction in the shorter *p53* transcript between exon 6 and exon 7 in the H1650-M3 cells. **(c)** Cross-species comparison of *TP53* genomic sequence revealed high homology at the alternative splicing site. **(d)** Schematic representation of p53FL and p53ψ isoforms. Functional domains and peptides unique to p53ψ are indicated in the diagram. Vertical lines represent the frequency of known missense p53 mutations. **(e)** Western blot analysis indicated that ectopic expression of the novel *p53* isoform in H1650 cells generated a protein that co-migrated with a band of similar size observed in H1650-M3 cells

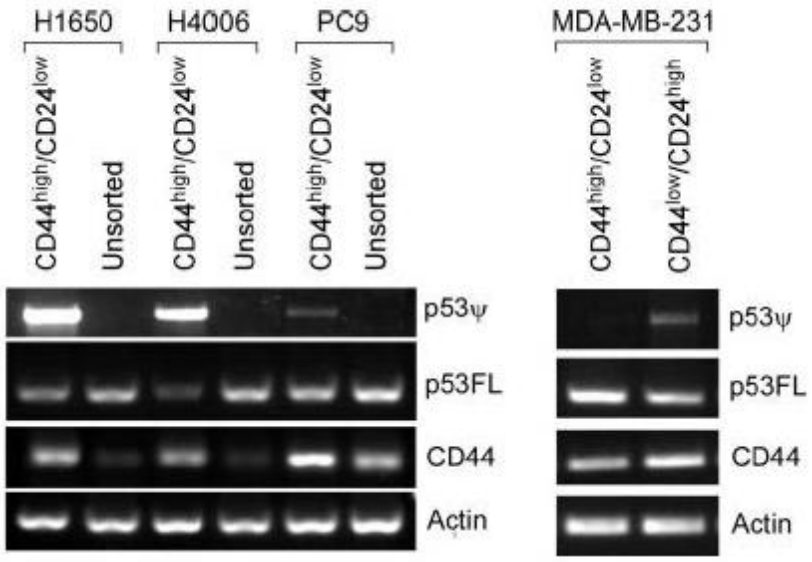

Figure 4.2 p53Ψ is Expressed by CD44high/CD24low Cells in Multiple Tumor Derived Cell Lines. Cells sorted for CD44/CD24 expression as described in Chapter 3 were interrogated for p53 expression using specific primers for full length (p53FL) and p53Ψ splicing isoforms. p53Ψ was preferentially detected in the CD44high/CD24low fraction compared to unsorted. This coincided with a decrease in p53FL transcript level.

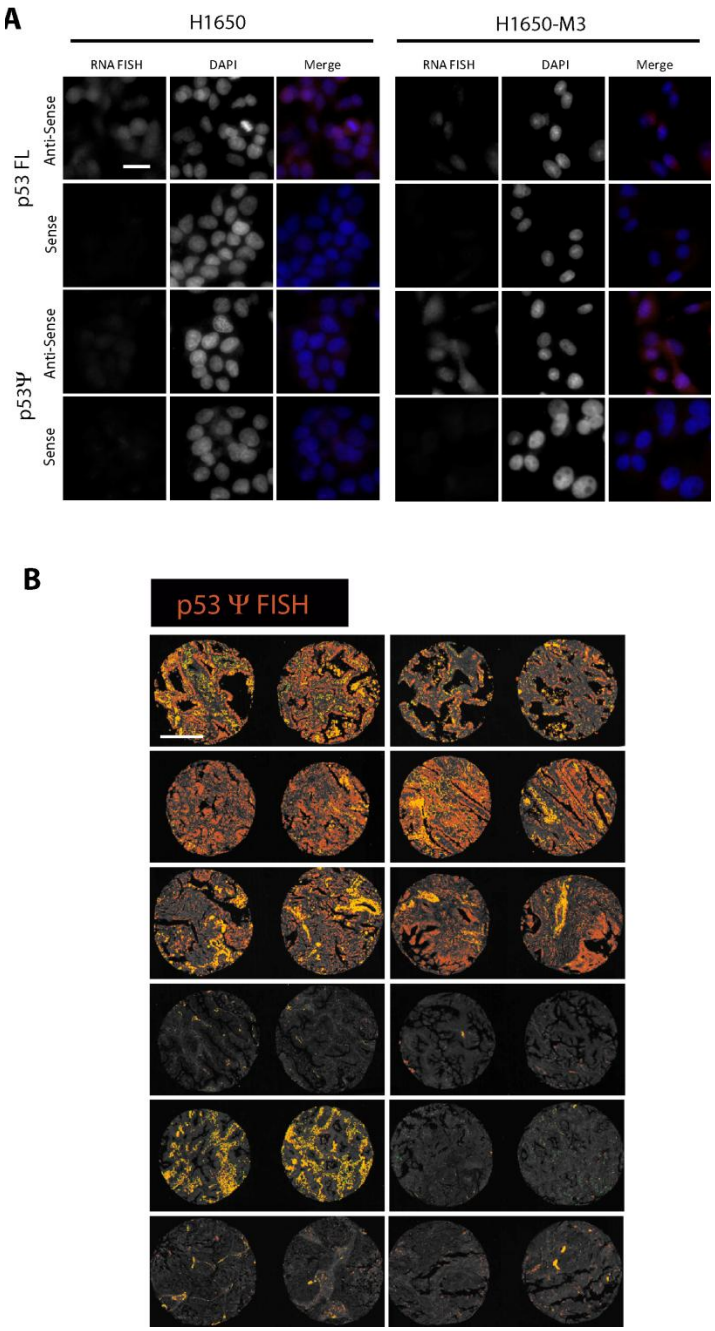

Figure 4.3 Detection of p53Ψ in NSCLC Cell Lines and Human Primary Tumors Using Exon Junction FISH. DNA oligo probe was designed to hybridize to the region spanning the exon6-intron6 splice site of p53Ψ or the exon6-exon7 splice site of p53 FL. Staining was validated using cell lines known to express differential levels of the two splice isoforms **(A)** (Scale bar is 20 micron). Primary human tumors were then hybridized with probe and scanned for fluorescence **(B)**. Area over threshold as determined by Aperio Image Scope analysis is pseudocolored red. Yellow denotes near channel autofluorescence. Expression of p53Ψ in polarized epithelium was detectable in a subset of adenocarcinomas of varying stage (Scale bar is 500 micron).

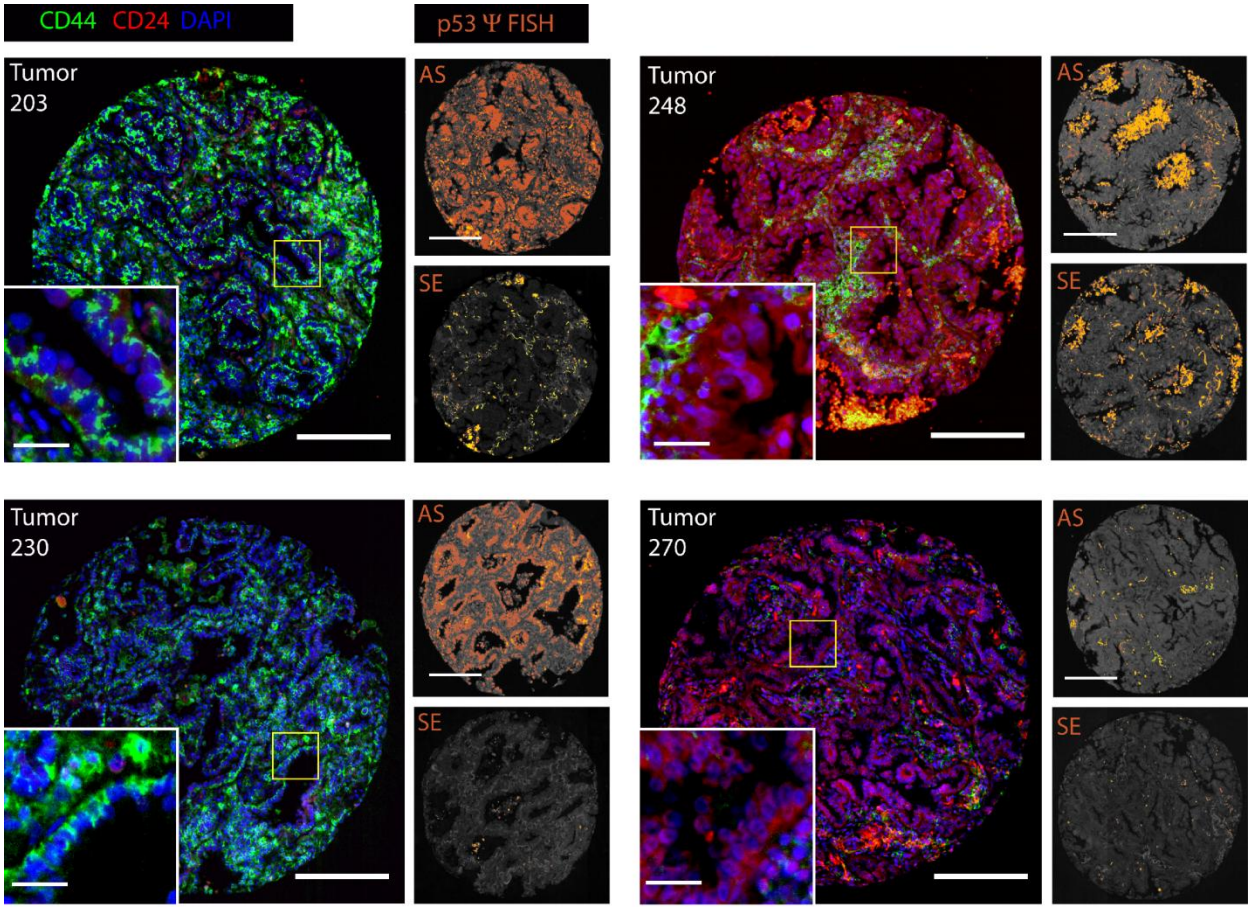

Figure 4.4 p53Ψ Expression is Found in Tumors with CD44high/CD24low Epithelium. Cancer tissue microarray was co-stained for CD44 and CD24 and compared to p53Ψ RNA FISH. Slides were hybridized with anti-sense (AS) and sense (SE) oligos to verify specificity of signal. Tumors expressing p53Ψ in polarized epithelium were predominantly CD44high/CD24low. Conversely, cores that showed CD24 immune-reactivity but not CD44 had little detectable p53Ψ expression. Scale bar is 250 micron in large IF pictures, 20 micron in IF inset, and 300 micron in FISH images.

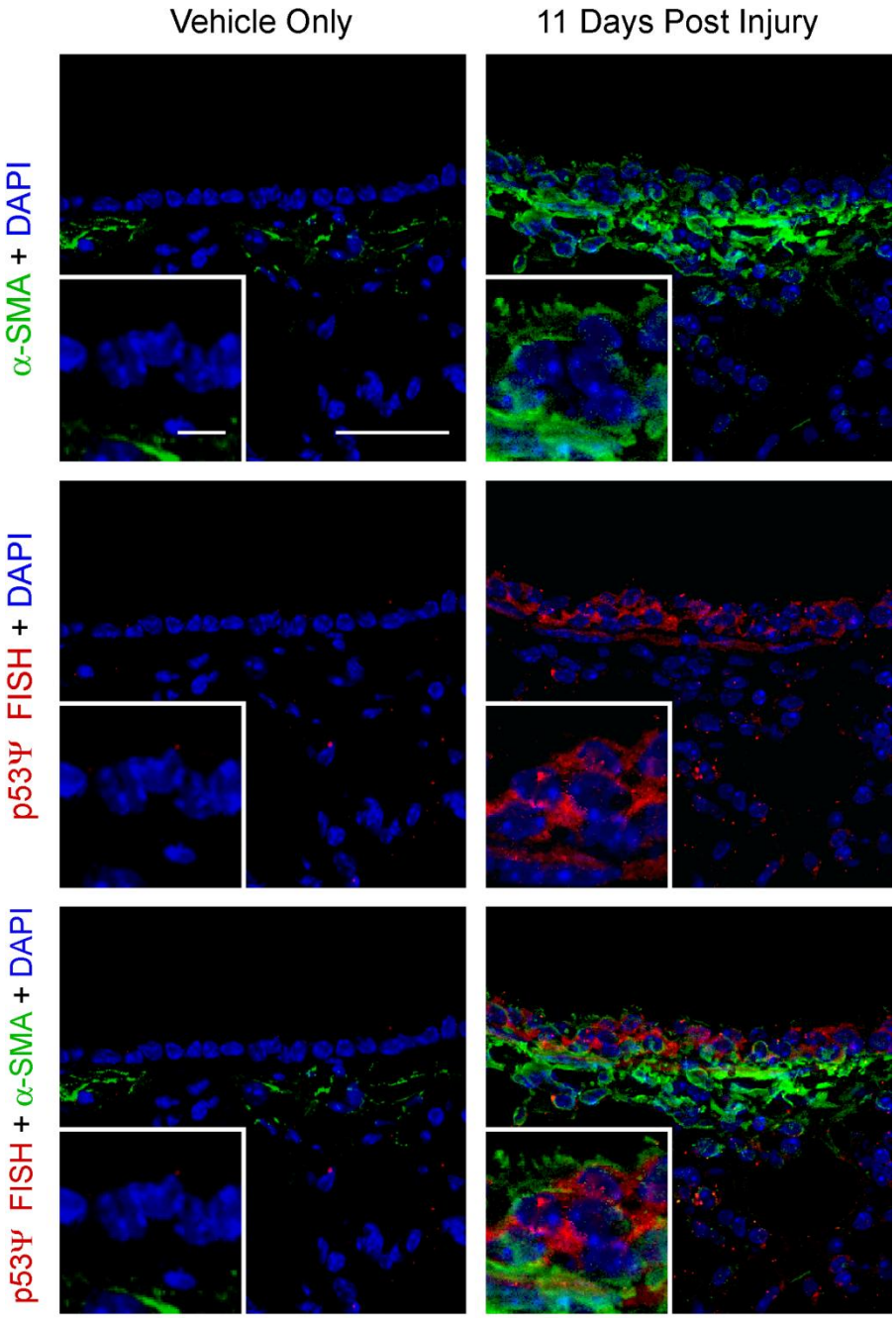

Figure 4.5 p53Ψ Expression Occurs During Recovery of Injured Bronchial Epithelium. RNA FISH using p53Ψ specific probes hybridized to tissue prepared from vehicle only or naphthalene injured mice shows p53Ψ expression to occur in the injured bronchial epithelium during repair. These cells also gain expression of α-SMA (Scale bar is 100 micron in main image, 20 micron in inset).

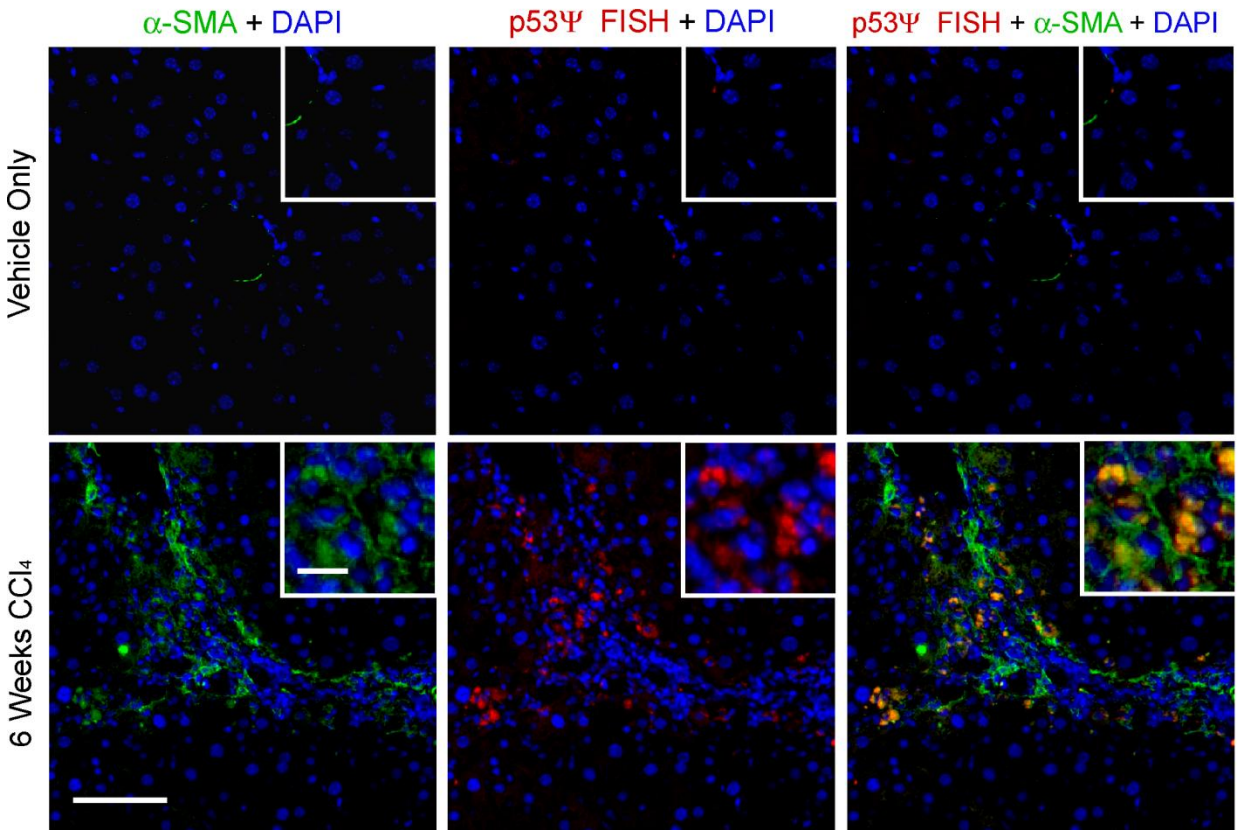

Figure 4.6 Injury Induced Fibrotic Liver Tissue Expresses p53Ψ. RNA FISH using p53Ψ specific oligo detects mRNA expression within the α-SMA+ cells of peri-sinusoidal scarring in livers from carbon tetrachloride treated animals (Scale bar is 150 micron in main figure, 30 micron in inset).

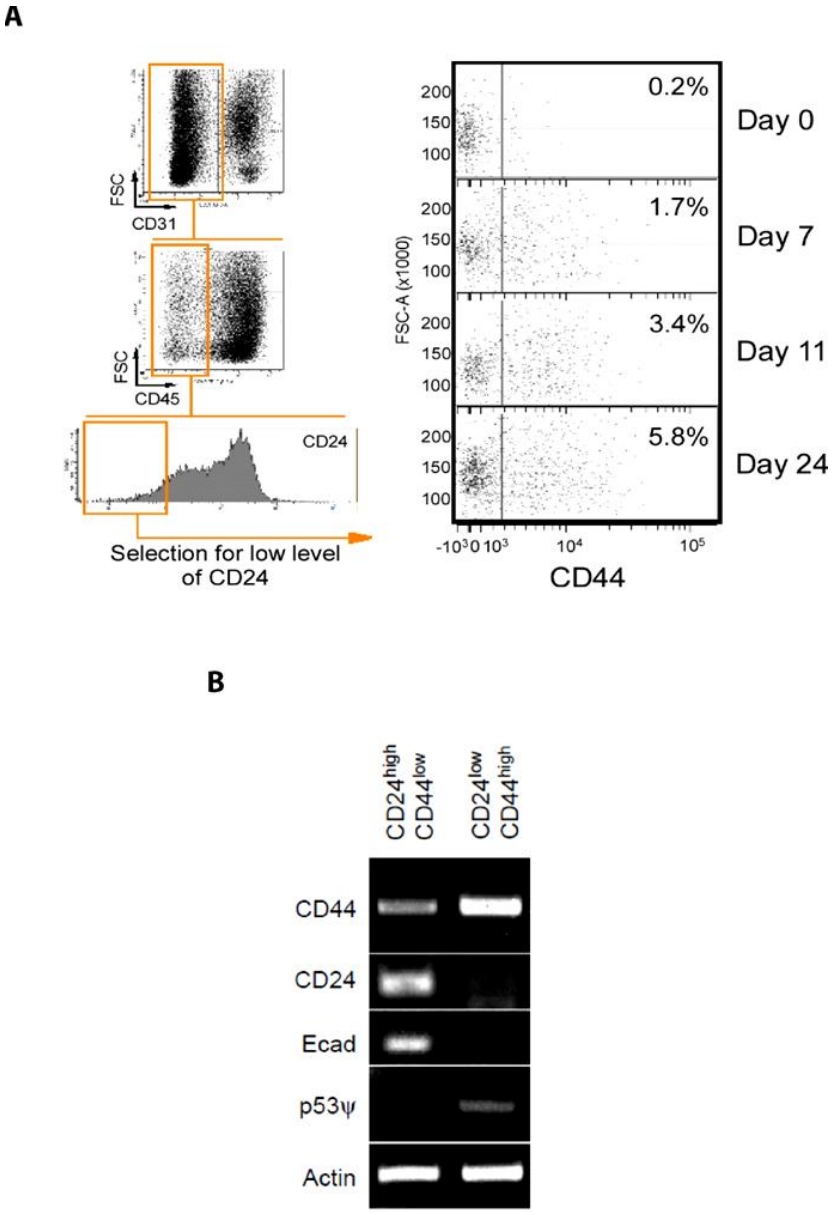

Figure 4.7 p53Ψ Expression Occurs in CD44high/CD24low Cells Induced During Lung Injury. As described in Figure 3.7, naphthalene induced injury to the murine lung causes emergence of CD44high/CD24low cells with characteristics of EMT. These cells were sorted and compared to CD24high/CD44low reference population of expression of epithelial marker E-Cadherin and p53Ψ. p53Ψ expression was detected exclusively within CD44high/CD24low cells, which expressed decreased levels of E-Cadherin compared to control.

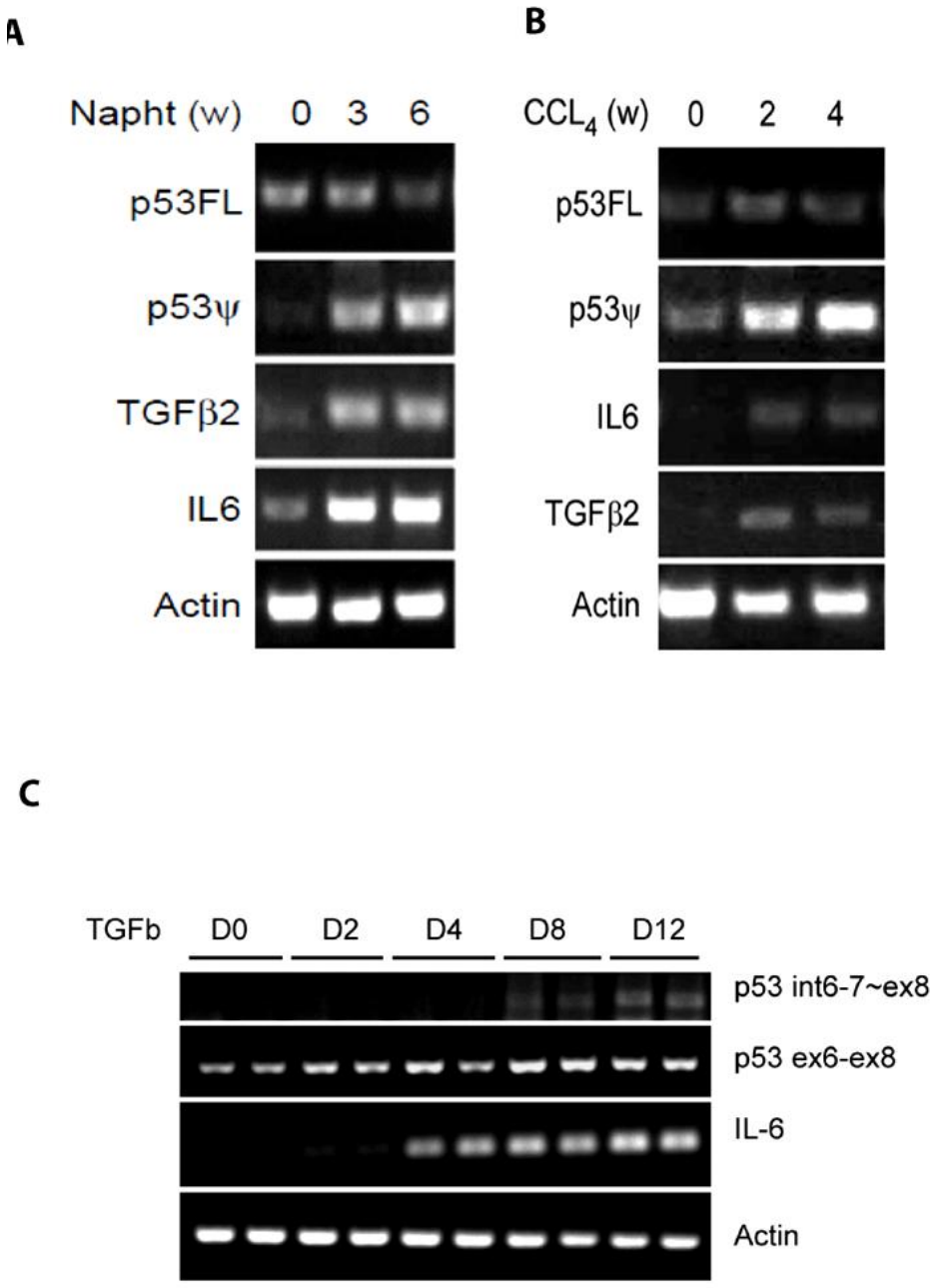

Figure 4.8 TGF-β Expression is Increased During Injury and is Able to Induce Alternative Splicing of p53. RT-PCR of **(A)** lung tissue prepared from animals injured with naphthalene or **(B)** liver tissue from animals injured with carbon tetrachloride shows increased expression of TGF-β2 and Il-6 in injured versus uninjured samples. Increased p53Ψ expression is also seen in a time dependant manner, suggesting a link. **(C)** Treatment of H1650 with TGF-β induces expression of Il-6 and alternative splicing of the p53 pre-mRNA to yield increasing amounts of p53.

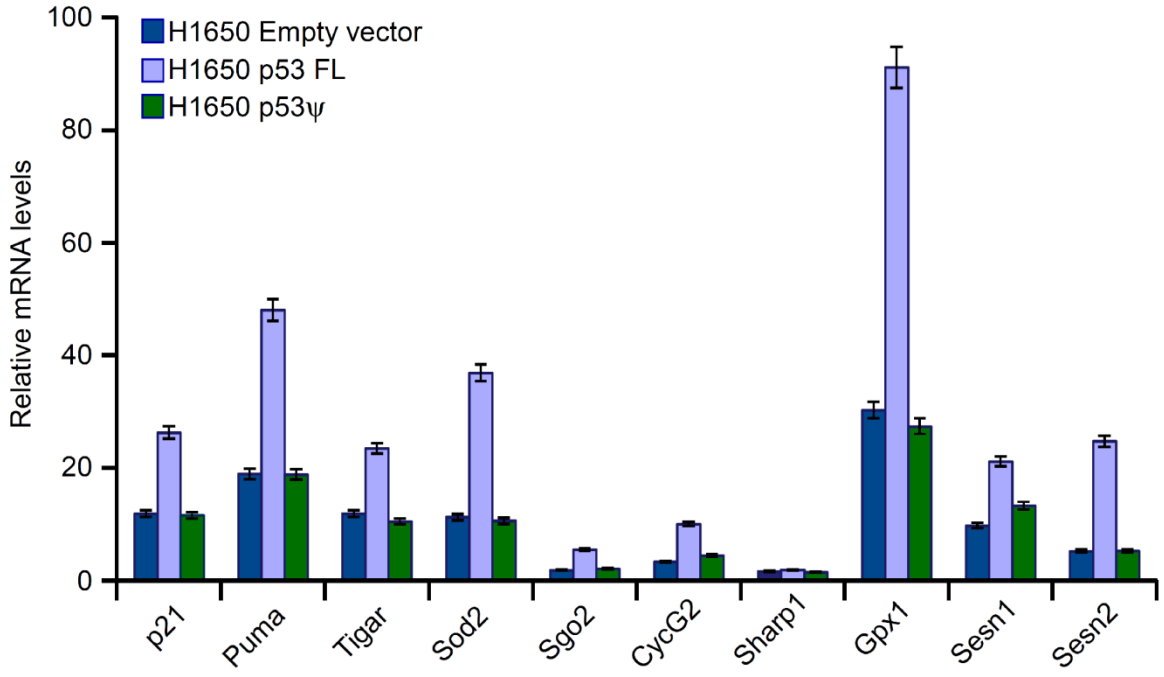

Figure 4.9 p53ψ is Unable to Modify the Transcriptional Activity of p53. Ectopic expression of p53Ψ in cells expressing p53FL did not induce the expression of known p53 targets even in the presence of a DNA damaging agent (doxorubicin) as measured by QPCR.

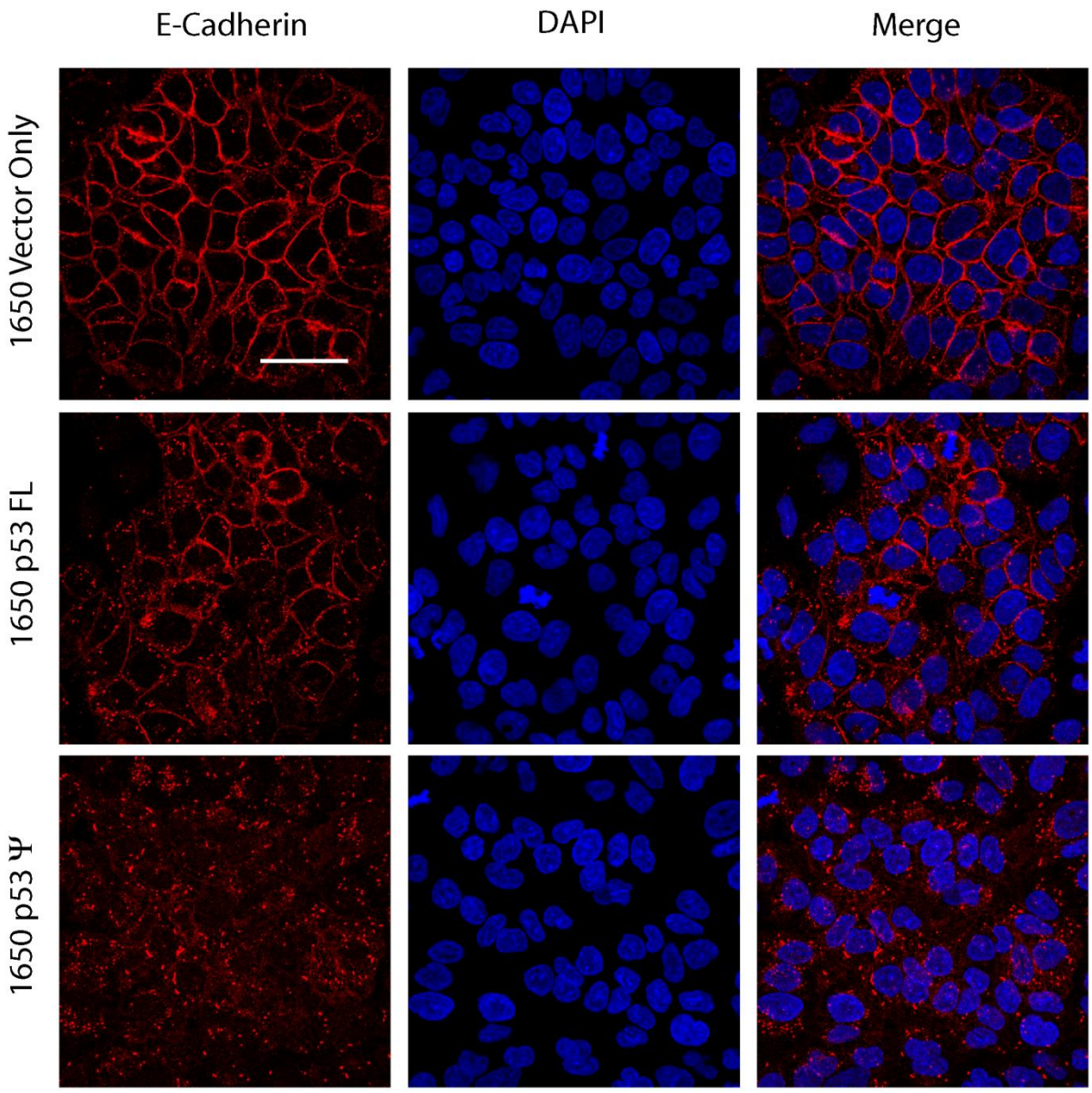

Figure 4.10 p53Ψ Lowers E-Cadherin Levels and Alters Cadherin Junctions. Expression of either vector control or p53FL constructs in H1650 cells did not appreciably affect Cadherin intercellular junctions. p53Ψ expression, however, lowered E-Cadherin levels and disrupted the organization of intercellular junctions.

A

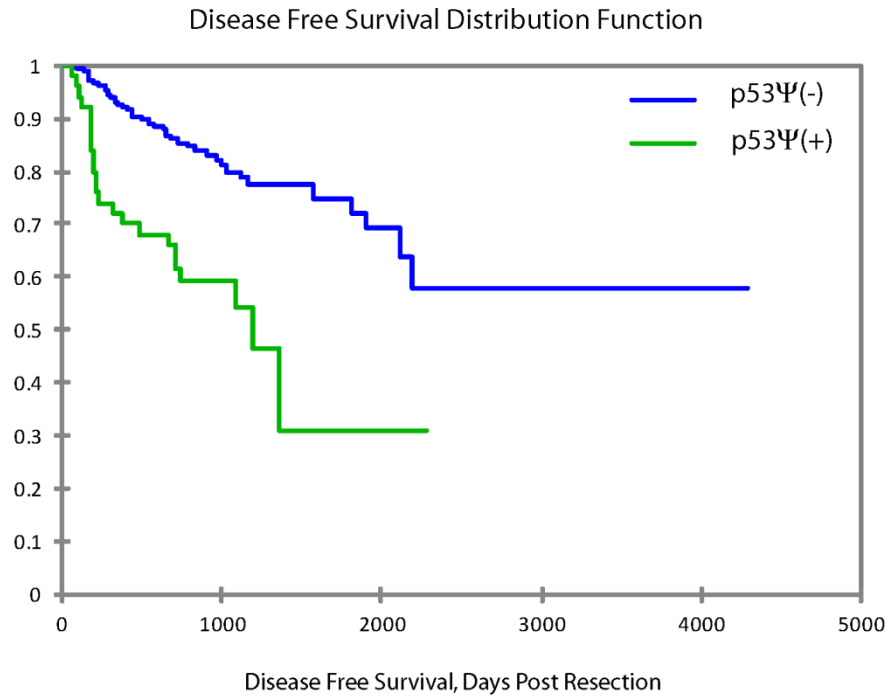

B

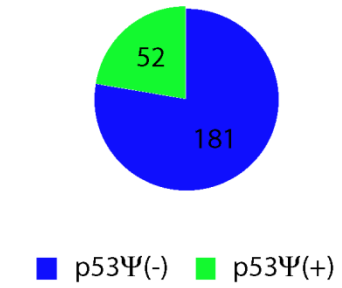

C

	Mean DFS Time (days)	StDev	Mean Survival Time (days)	StDev
p53Ψ(-)	2437.84	119.24	3053.81	203.32
p53Ψ(+)	903.29	75.851	1643.12	110.85

Figure 4.11 p53Ψ Expression is a Negative Prognostic Factor for Disease Free Survival in Lung Adenocarcinoma. Interrogation of cancer tissue microarray for expression p53Ψ followed by univariate Kaplan-Meier analysis of disease free survival post surgical resection of tumor **(A)** showed expression p53Ψ to be correlated with poor prognosis. These tumors constituted ~22% of cases **(B)** and showed significant decrease in DFS and overall survival **(C)**.

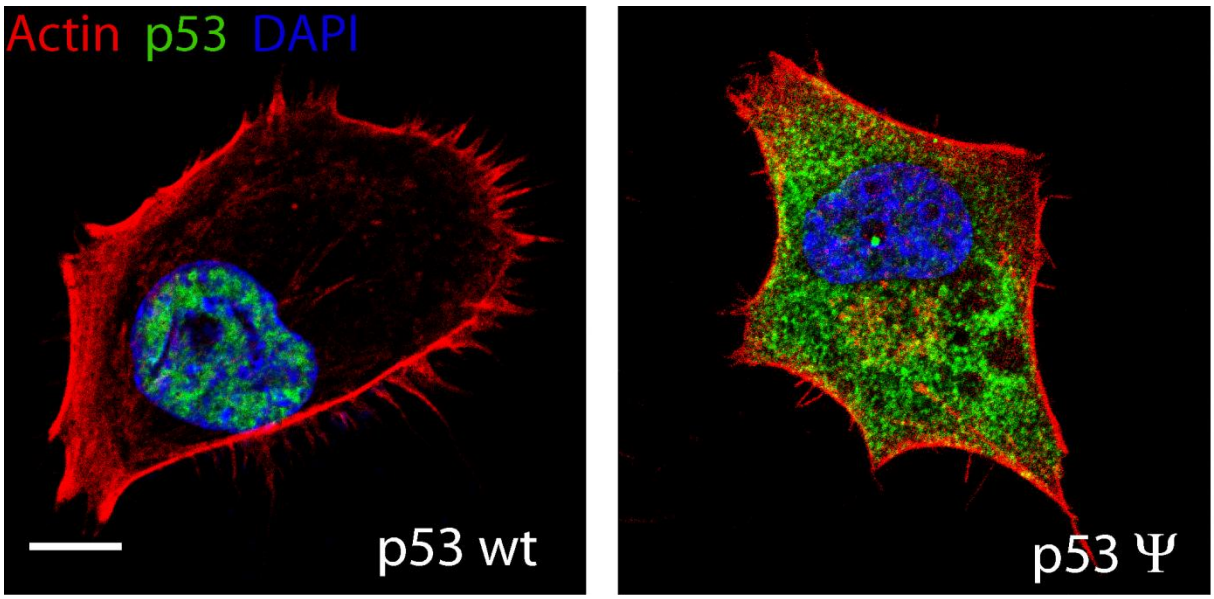

Figure 4.12 p53Ψ is Relegated to the Cytoplasm an Appears in Discrete Foci. Immunofluorescence of p53 null H1299 cells expressing either wt p53 FL or p53Ψ counterstained with phalloidin to delineate cytoplasm and DAPI to show the nucleus of cells. Unlike full length protein, p53Ψ is found in the cytoplasm of cells in discrete foci (Scale bar is 1 micron). Images are maximum intensity projections of 5 microns z-coverage.

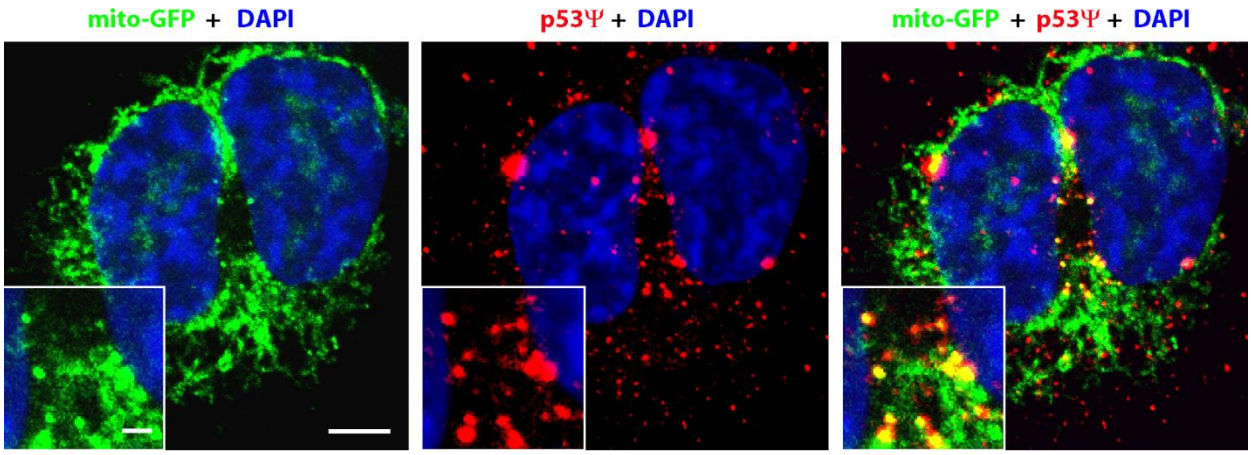

Figure 4.13 A Fraction of p53Ψ has Mitochondrial Localization. H1299 cells expressing mitochondrially localized GFP variant mCherry as well as p53Ψ were imaged for colocalization. Overlap was reliably detected in peri-nuclear mitochondria (Scale bar is 2 micron in main figure, 200 nm in inset). Images are maximum intensity projections of 2 microns z-coverage.

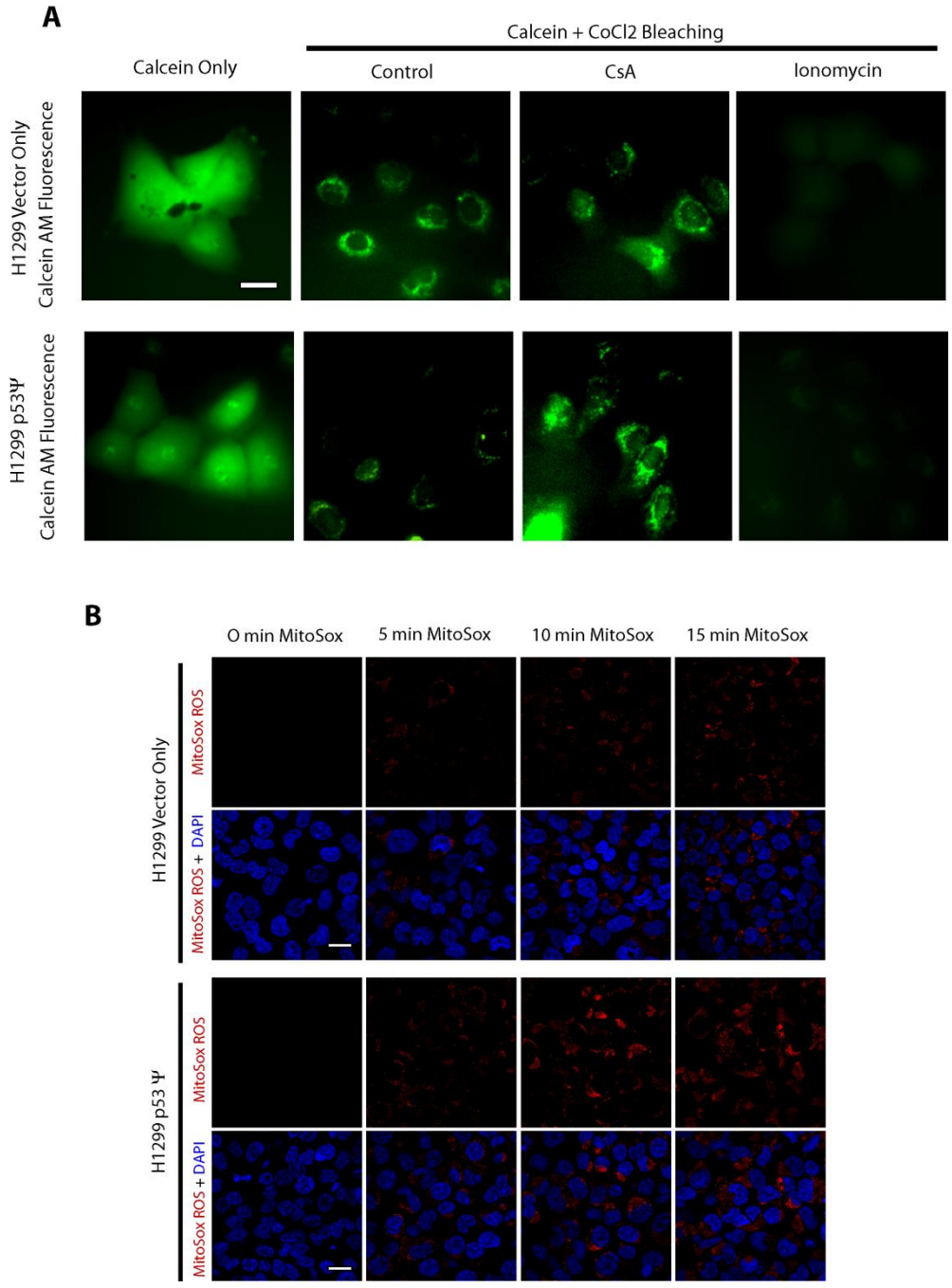

Figure 4.14 p53Ψ Increases Mitochondrial Permeability and ROS generation. Calcein transition pore assay **(A)** of H1299 cells expressing vector only or p53Ψ. P53Ψ renders mitochondria more permeable to CoCl2 (calcein quencer). The pictures depict representative images by fluorescence microscopy. Ionomycin treatment is showed as control. Time course evaluation of ROS production **(B)** in H1299 cells expressing vector only or p53Ψ measured by Mitosox fluorescence microscopy. P53Ψ causes increase ROS generation.

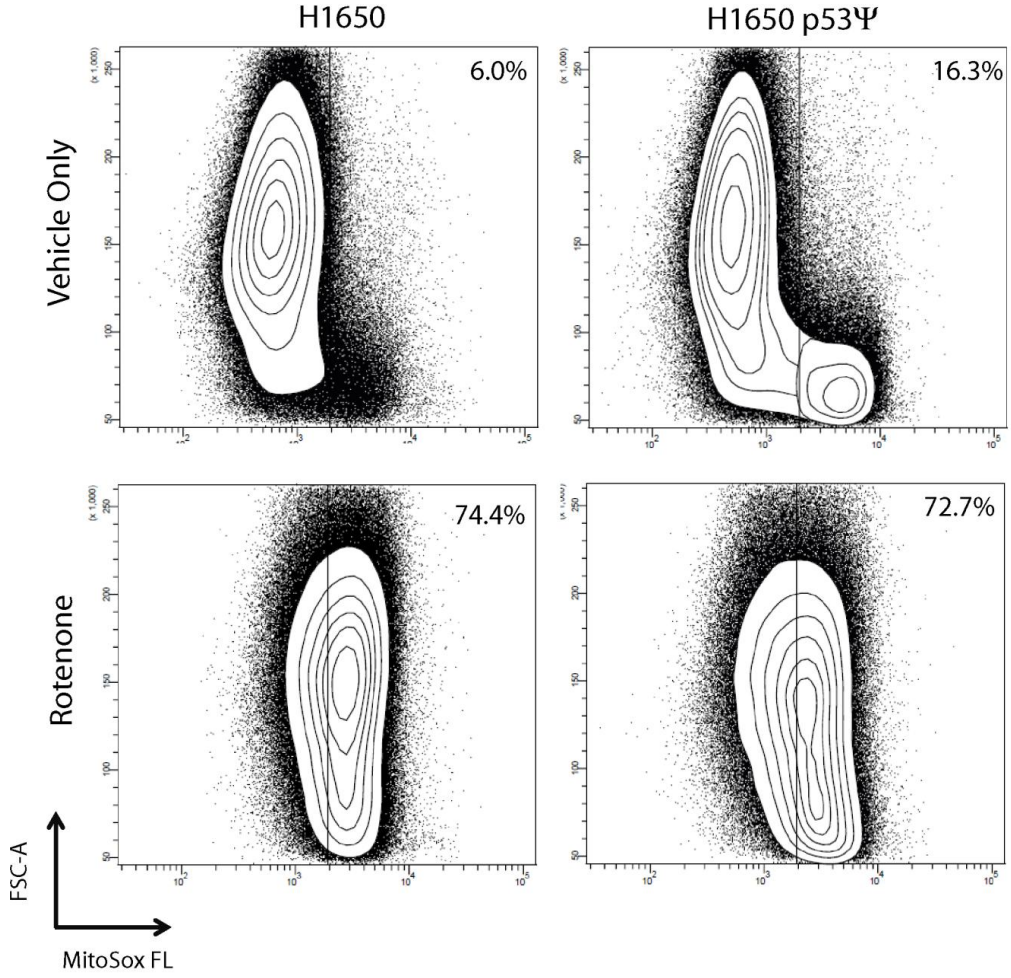

Figure 4.15 Expression of p53Ψ Increases Steady State ROS Production. Expression of p53Ψ increases the percentage of cells positive for high levels of ROS compared to vector only by flow cytometry analysis of H1650 stained with Mitosox ROS indicator. p53Ψ does not impact ROS generation in response to electron transport chain complex I poison rotenone (100 nM).

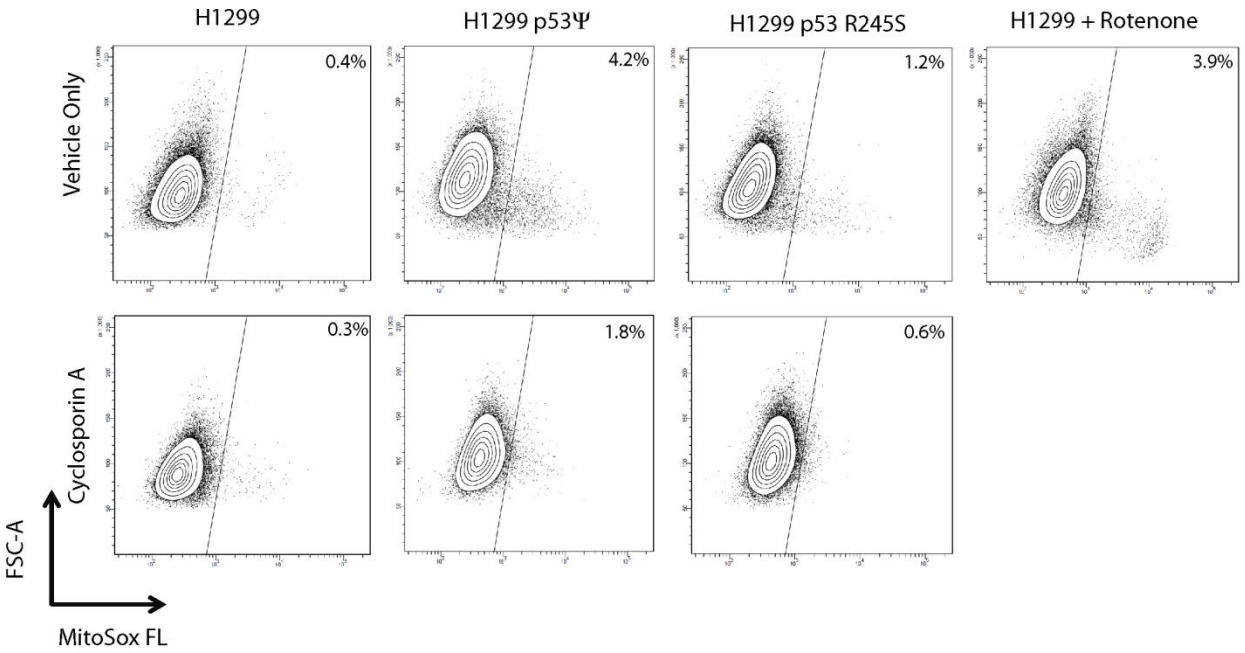

Figure 4.16 p53Ψ and p53 R245S Dependant ROS Generation is Blocked by Cyclophillin D Inhibition. Flow cytometry of Mitosox staining of H1299 cells expressing either vector control, p53Ψ or p53 R245S shows that both p53Ψ and p53 R245S are able to stimulate ROS generation at levels comparable to short term rotenone treatment (1 hour). This effect is Cyclophillin D dependant, as inhibitor cyclosporin A abrogates the elevated ROS levels. Representative plots for triplicate experiments shown.

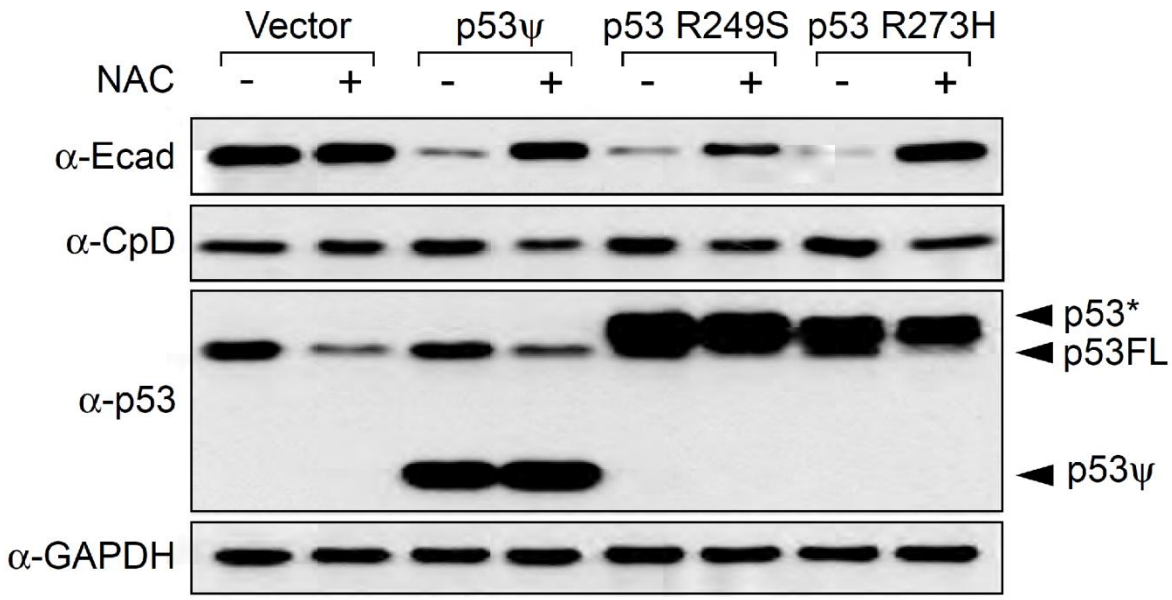

Figure 4.17 Treatment of Cells with ROS Scavenger Blocks p53ψ or Gain-of-function p53 Mutant Induced EMT. Treatment of H1650 cells expressing p53ψ or gain-of-function p53 mutants with 10 mM N-acetyl cysteine (NAC), a ROS scavenger, for 7 days restores E-cadherin to levels observed in parental or vector-transduced cells.

Chapter 5

Lung Slice Culture Preparation and Ex Vivo Imaging to Study Cell Fate Determination in Lung Injury Models and Tumors

Chapter 5: Lung Slice Culture Preparation and *Ex Vivo* Imaging to Study Cell Fate Determination in Lung Injury Models and Tumors

Summary

Imaging has proven an invaluable tool during the course of my thesis work. However, there have been times when standard fixed tissue microscopy was insufficient for gaining full appreciation of the system we were observing. Intra-vital imaging offers tremendous insight into the localized biology of structures in the context of a whole living animal but requires specialized equipment and training (Chambers, 1995; Funakoshi, 2000; Gavins & Chatterjee, 2004; Hak, Reitan, Haraldseth, & de Lange Davies, 2010; Vajkoczy, Ullrich, & Menger, 2000). We report a simple procedure for the generation of viable, living lung tissue slices that maintain proper morphology for up to a week in culture. We apply *ex vivo* lung culture to observe the events of bronchial injury in living epithelium. In addition, we use a modified immunofluorescence protocol to study the biology of tumorigenesis in multiple mouse models of lung cancer and demonstrate intra-tumor heterogeneity for markers of metastasis initiating cells.

Highlights

- Vibratome sectioning of lung can yield slices ranging from 50 micron to 1 mm in depth that maintain lung architecture and viability for up to a week in culture
- Imaging analysis with concomitant detection of transgenenic fluorescent proteins and antibody labeled endogenous proteins can be accomplished with depths of field exceeding 200 microns
- Application of these techniques to mouse models of cancer allow us to demonstrate both inter- and intra-tumoral heterogeneity

Introduction

Microscopy has long been crucial in developing our understanding of cell biology. As technology continues to advance, investigators have begun using time lapse imaging studies of dynamically changing systems to appreciate things not captured by static observation. Perhaps some of the most intriguing applications of live cell imaging have come from studies of tissues within whole organisms.

This so called intra-vital microscopy (IVM) has yielded fascinating advances in our knowledge of innate and adaptive immune response, tumor angiogenesis, and nervous system connectivity (Padera, Stoll, So, & Jain, 2002; Vajkoczy et al., 2000).

While IVM represents an impressive tool for asking and answering biological questions, it requires expensive and potentially custom-made equipment not available to everyone (Sumen, Mempel, Mazo, & von Andrian, 2004). In addition, application to study of the lung presents a particularly daunting challenge, as access to the thoracic cavity threatens the negative pressure that prevents airway collapse. To circumvent these problems, we have written a protocol for the preparation of *ex vivo* lung slices.

The production of lung slices requires little unique reagents or tools beyond a standard vibratome. The process is quick, easy to perform and reproducible. It yields living lung tissue that remains viable for up to a week in culture. Slices processed this way maintain the diversity of structural features normally found within the organ without artifacts of processing that might be generated during snap freezing or paraffin embedding. As such, vibratome sectioning provides an attractive alternative to conventional preparations for immunofluorescence microscopy.

The lung slice model can also be used to appreciate the 3D organization of a tissue. To demonstrate the utility of this method for imaging studies we utilized mouse models of lung cancer developed on campus. We report observations from the characterization of these mice, and demonstrate intra-tumoral heterogeneity for expression of the surface marker CD44 and activation of the TGF-β pathway.

Results

Lung Slice Preparation Protocol

One of the main problems encountered with sectioning the lungs is their intrinsic elasticity. We found that instillation of high rigidity agarose at 3% agarose wt/vol provided adequate resistance to the sectioning blade. The volume of agarose solution required for sectioning varies but typically falls between 1 and 2 mL. For ease of clearance afterwards, low melting temperature agarose is advisable. We currently use Type IX agarose, available from Sigma-Aldrich, suspended in Hank's buffered saline solution (HBSS).

Mice should be sacrificed according to institutionally approved guidelines. After sacrifice, specimens should be dissected cleanly to allow access to the thoracic cavity. To avoid contact with lung tissue during the process, reflect the xiphoid process upwards and enter the thoracic cavity just below the junction of rib cage and diaphragm. Be sure to maintain contact with the internal side of the rib cage at all times to minimize chance of accidental damage to the lung.

To exsanguinate the mouse lung, sever the brachial arteries within the axilla as well as the descending aorta at the level of the diaphragm. A peristaltic pump fitted with a small bore veterinary catheter is suitable for pushing sterile PBS through the right ventricle and into pulmonary circulation to clear the remaining blood. Successful flushing will turn the lungs from a light pink to white.

Once the rib cage was cleanly removed and the mouse exsanguinated, the exterior of the lungs should be rinsed with cold PBS and access to the trachea established by dissecting away the superficial tissue between the mandibular margin and the clavicles. At this point the thyroid is removed and an incision within the muscular surroundings of the trachea should be made. The best site for instillation is just below the vocal folds, which appear as the thickest set of cartilaginous rings.

Using a dulled syringe, the lungs are filled with agarose until back pressure forces fluid out from the trachea. To avoid perforation, remain as shallow in the airway as possible. Clamp off the lumen of the trachea with a hemostat before removing the syringe completely. To solidify the agarose and prevent leaking, apply dry ice to the trachea. Contact with parenchymal lung tissue should be avoided as it will result in damage.

The lungs are then removed by reflecting the trachea upwards and severing its connection to the rest of the body. Gentle upwards pressure should be maintained on the trachea while muscles and connective tissue are severed from the posterior aspect of the lung. Afterwards, the sample should be rinsed with ice cold PBS briefly and placed at 4 degrees Celsius for 10 minutes to harden. Specimens prepared in this manner do not require agarose casing for sectioning.

To facilitate blade entry and limit pulling, clean sharp scissors should be used to trim the edges of the lung where the convergence of pleura make sectioning difficult. The sectioning chamber should be maintained as cold as possible to ensure the rigidity of the lungs as they are cut. Slices were collected into HBSS on ice and subsequently placed into LHC9 cell media or an equivalent serum free growth media. Incubation overnight in normal cell culture conditions (37 degrees Celsius, 5% CO_2) was

sufficient to remove the agarose. Clearing is complete when trapped air bubbles are no longer seen within the lumen of peripheral air spaces.

Once the slices were cleared, they were then transfer into fresh culture media or alternatively, lung slices fixed for immunofluorescence.

Characterization of Lung Slices

One hypothetical advantage to the generation of slice cultures of primary lung cells is the ability to study a specimen with intact local microenvironment and intracellular interactions. To verify our sectioning procedure was maintaining the intrinsic features of the lung, we studied their morphology by phase contrast and DIC microscopy (Figure 5.1). We found conservation of structure in both alveolar and bronchial airspace. Testing for viability with trypan blue exclusion proved that 96% of cells survived the sectioning process (data not shown). 7-Aminoactinomycin D (7-AAD), a fluorescent compound that binds DNA with high affinity but cannot pass through intact cell membranes, was used to confirm viability of lung slices (Figure 5.1). As control, slices were fixed and permeabilized, then subsequently re-stained with 7-AAD to verify binding of nuclear DNA.

Many genetically engineered mouse models utilize regulatable systems to spatially and temporally control transgene expression. A popular model in lung biology utilizes the rat Clara cell secretory protein (CCSP) promoter to drive targeted expression within bronchiole epithelium. Combining this cell specificity with a chemical induction system such as tetracycline-controlled transcriptional activation allows for precise manipulation of a subset of lung cells. Using the CCSP promoter to drive reverse tetracycline-controlled transactivator (rtTA) expression, it is possible activate transgenes under control of a tet-responsive element (TRE) within bronchiole epithelium by doxycycline addition (Premsrirut et al., 2011).

To determine if cells in the lung slices were still alive and able to respond to induction, we tested the efficacy of *ex vivo* doxycycline (dox) administration in stimulating GFP expression within epithelium of TRE-GFP-shLuciferase/rCCSP-rtTA transgenic mice (Figure 5.2). We prepared slices from mice maintained on doxycycline containing food as positive control, as well as slices from non-transgenic animals as negative control. Induction of expression as measured by GFP fluorescence occurred rapidly,

as signal was detected in bronchial epithelium 6 hours after doxycycline administration to slices harvested from drug naïve animals.

The use of air-liquid interface (ALI) culture has proven a valuable tool for generating epithelial layers mimicking the morphology of those found endogenously within lung. Adaptation of this culture method for *ex vivo* lung slices involved tissue trimming to fit within a transwell insert. A defined volume of media is then applied to the sample as to allow the basolateral surface to remain in contact but the apical surface to have access to environmental gas. To test the effect that this culture method would have on maintaining lung slices, we compared ALI using either serum free LHC9, serum free DMEM or serum supplemented DMEM to culture using those media with no physical constraint of the specimen (Data not shown).

In all cases, viability at the end of a one week period exceeded 80%. ALI was superior to unconstrained culture in maintaining morphology of bronchial airways, which in some cases saw accumulations of cells and alterations in structure. This effect was particularly pronounced in serum supplemented cultures. LHC9 fostered cell survival with minimal aberrant outgrowths. In cases of unconstrained culture, the presence of cells that hid migrated out of lung slices and were able to attach to tissue culture plastic was detectable as early as 4 days after sectioning. These cells displayed a diversity of morphological characteristics by microscopy. We determined that for the purpose of live cell microscopy on *ex vivo* slices, ALI culture with LHC9 media was most suitable.

Time-lapse Live Cell Microscopy

With suitable culture conditions worked out, we sought next to visualize living slice culture as proof of concept for future biological studies. Wild type C57Bl/6 mice were harvested and prepared as described. Immobilized slices in ALI culture with LHC9 media were imaged using the Zeiss Observer live cell microscope outfitted with environmental control chamber, stage heating elemental and CO_2 controller (Data not shown).

We next aimed to test how suitable our system was for observing processes involving mitosis, as study of is process in non-transformed primary cells can be difficult, particularly by live cell microscopy. To do so, we injured mice with naphthalene 48 hours before sacrifice. Naphthalene injury causes necrotic exfoliation of Clara cells from the bronchial airspace, leading to proliferation of injury resistant

progenitors. Imaging was conducted at five minute intervals for 36 hours and revealed a diversity of processes that could not be appreciated from fixed specimens (Movie 5.3). Previous reports have demonstrated that mitotically active injury resistant progenitors reside at the bronchioalveolar duct junction (BADJ) and bifurcation of the bronchioles. We provide evidence of this occurring within *ex vivo* slices. Surprisingly, migration both into and out of the BADJ is apparent in tissue taken from injured animals. Remodeling of the peri-bronchial region is much more complex than previously appreciated, as spontaneous contraction of airspaces and changes in gross morphology occurred consistently during the 36 hour imaging window.

Having previously shown the efficacy of visualizing fluorescent transgene expression with our culture system, we next attempted long term time lapse microscopy of mice engineered to harbor a reporter construct for the let-7 microRNA (Wakiyama & Yokoyama, 2010). The let-7 family is highly conserved across species in sequence and function, and its misregulation leads to a less differentiated cellular state and development of diseases such as cancer (Boyerinas, Park, Hau, Murmann, & Peter, 2010). The reporter mouse, generated by Greg Hanon's group, utilizes tandem repeats of the let-7 seed sequence in the 3' UTR of a GFP reporter construct to sense miRNA levels in a cell. Imaging of the let-7 reporter mouse revealed heterogeneous GFP intensity in various regions of the lung. Cells were particularly bright around structures reported to take part in mitotic regeneration in response to injury, indicating low levels of let-7 miRNA. We chose to image the bifurcation of the bronchioles using the naphthalene injury paradigm previously described (Movie 5.4). Cells in this region demonstrated mitotic activity over the 24 hour imaging window. Although many remained clearly active by appearance on phase contrast, silencing of GFP signal began as early as two hours into the imaging window and continued throughout. Cells with the lowest GFP signal were the first to turn dark. Those that underwent mitosis as well as others proximal to them maintained high levels of GFP and thus low levels of let-7 throughout the experiment. This suggests that proliferative response to naphthalene injury is related to low let-7 expression.

Detection of Rare Cell Populations

Evaluation of rare cell populations by traditional histology can be time consuming and expensive, particularly for a large tissue such as the lung. Typical histology deals with sectioning thickness of around 5 micron. Efficient detection of fluorescent markers is possible with vibratome

sections up to 400 microns. Because vibratome slicing of the lung maintains morphology and allows for visual inspection without use of stains or processing, rapid surveillance of tissue to identify rare cells of interest is much more efficient.

While optimizing conditions for the transplant procedures performed in Chapter 2, vibratome sectioning and slice evaluation proved an invaluable tool for detecting engraftment. The orthotopic transplant of lung epithelial progenitors allows for determination of lineage contribution as well as integration efficiency and site of homing. When optimizing delivery conditions, it was necessary to have a robust imaging modality to ensure we were not limited by detection.

Our early studies employed the usage of Carboxyfluorescein succinimidyl ester (CFSE) to fluorescently label donor cells. Upon uptake, this dye is converted by cytosolic esterases to a membrane impermeable form that becomes trapped within a cell. CFSE then covalently couples with intracellular molecules in a stable and long lasting manner and is passed down to daughter cells during mitosis. As such, it is suitable for tracking populations over a fairly long period and allows for discerning relative mitotic activity as a measure of dye dilution.

We first determined the effect of animal pre-injury on engraftment efficiency using syngenic whole lung homogenate cell suspensions (Figure 5.5). Tissue was digested, cleared of blood cells, stained with CFSE and introduced into recipient mice. We tested the effect of donor pre-injury with naphthalene, recipient pre-injury with naphthalene, and pre-injury of both donor and recipient before instillation. Recipient pre-injury improved engraftment efficiency both with and without donor pre-treatment. However, animals had far worse post-instillation outcome (30% vs. 90%) when receiving naphthalene before surgery to denude the airway of existing Clara cells. Surprisingly, injury of donor animals also had a beneficial effect on grafting efficiency. To limit accidental mortality we decided to use donor pre-injury, but not recipient, going forward.

With a reasonable transplant protocol worked out, we began work trying to characterize putative stem cell populations identified by flow cytometry in Chapter 2. Briefly, we discovered the existence of 4 sub-groups within the Sca-1+/CD45-/Pecam- lung population that varied on their expression of key markers associated with lower airway bronchial stem cells. These subgroups were demarcated by their differential expression of the surface protein CD24. To biologically characterize the different potential progenitors, we purified them using fluorescence assisted cell sorting (FACS), labeled them with CFSE and instilled them into the tracheas of syngenic recipients (Figure 5.5). It is worth

noting when interpreting the data from these experiments that the instillation technique used was different than the trans-thyroidal survival surgery described in Chapter 2. Tracheal instillation utilized a non-invasive approach that while effective, was less efficient and more variable than surgery.

A week after instillation, animals were sacrificed and the whole lungs were sectioned by vibratome at 300 micron intervals. Performance of the four different donor cell populations was quantified as number of slices with at least one integration site identified by CFSE fluorescence. In three individual experiments we were able to successfully find engraftment by at least one putative progenitor candidate. In all replicates, the CD24high donor population was most effective at integrating into the host airway (Figure 5.5). Areas of integration showed cells of different dye intensity, indicating both retention and dilution. As staining control, freshly dissociated and stained cells were fixed onto coverslips to measure fluorescence.

Interestingly, while CFSE+ cells were found in both central and peripheral airways, the colonies were very different in nature. Peripherally located grafts were typically dye bright, and present alone or in aggregates of a few cells within the alveoli. Grafts within the bronchioles, however, were typically larger in size and had both weakly and intensely staining CFSE labeled cells (Figure 5.5). Our findings further support the idea that the CD24high population, which express cytological markers of stem cells at the bronchioalveolar duct junction, are the progenitors to Clara cells lost during naphthalene injury.

Fixed Tissue Imaging

As already illustrated, the use of this tissue preparation technique was not relegated to studies requiring live cell microscopy. In fact, it proved extremely useful for fixed specimen immunofluorescence studies for a number of reasons. Firstly, the lack of dehydration or freezing prevents morphological alteration to the structures of the lung. Secondly, tissue prepared in this manner has lower intrinsic autofluorescence properties that paraffin embedded sample. Finally, because fixation is light and no further processing occurs, antigenecity is well maintained without steps to reverse cross linking.

To accomplish antibody staining of vibratome prepared sections, tissue must be cleared of agarose, rinsed with PBS and fixed with neutral buffered formalin. Preparation for immunofluorescence proceeds with components similar to other staining—as with all preparations, cells are permeabilized,

blocked with exogenous protein, and stained with appropriate antibodies. Special considerations for vibratome slices must account for the thickness and non-adherence of the tissue. Suspension in relevant buffers and mild agitation is sufficient to compensate for these things in samples of thickness up to 300 micron.

Because of the mild nature of tissue preparation, signal from intrinsically fluorescent, GFP expressing populations is well maintained. As such, antibody detection may not be necessary and should be screened on a case-by-case basis. As mentioned earlier, chemical transgene induction is possible during the post-sectioning, pre-fixation interval. Imaging of lung slices for multicolor immunofluorescence does not require use of a confocal microscope. Acquisition of 20X fields was readily accomplished using standard inverted fluorescent light microscopes. However, for higher power reconstructions, or for deeper tissue access, confocal microscopy is absolutely necessary.

Genomic analysis of patient populations has proven extremely successful in identifying molecules that may contribute to pathological states in human beings. For obvious reasons, validation and mechanistic studies must be conducted using alternative means. Genetically engineered mouse models provide a powerful tool to analyze the impact that candidates may have on an intact mammalian organism. We employed our imaging techniques to characterize the biology of two novel models of lung cancer engineered by the Lowe lab (Premsrirut et al., 2011). These models employ reversible tumor suppressor loss directed at specific cells of the lung by utilizing the CCSP-rTTA cassette mentioned earlier in this chapter to drive tet-inducible hairpins to either the p53 or p19ARF tumor suppressors . These genotypes were bred into a pre-existing mouse strain harboring a latent oncogenenic Kras (G12D) allele that can be activated by intranasal injection of adenoviral Cre (adeno-Cre).

To approach our characterization studies, we began by comparing rat-CCSP driven rtTA induction of the eGFP reporter in sh-p53/KrasG12D mice with endogenous murine CCSP production. Previous work has indicated that the scgb1a1 locus (which produces the CCSP protein) becomes silenced in human and mouse adenocarcinoma. We found robust eGFP expression in the lungs of animals maintained on doxycycline (dox) diets (Figure 5.6). In Kras G12D transduced mice, eGFP expression within tumors was easily detectable in over 95% of discrete nodules. However, in both cancerous and non-cancerous tissue of animals maintained on dox, overlap between endogenous CCSP and reporter activity was a rare event.

The initial reports utilizing the rat-CCSP locus to drive transgene expression noted RNA production in both central and peripheral airways. It was assumed that peripheral staining represented expression by type II pneumocytes. We tested this in shP53/Kras animals maintained on dox diets after Kras transduction. Surprisingly, while many tumors did indeed show robust expression of the type II pneumocyte marker surfactant protein-C (SPC), the signals only rarely coincided in hyperplastic or untransformed regions (Figure 5.7).

Characterization of the Kras G12D model of lung cancer described hyperplastic foci at the bronchioalveolar duct junction (BADJ) that proceeds to papillary adenoma and then adenocarcinoma. These different lesions were apparent within individual lungs of shp53/Kras mice kept on dox before sacrifice. Interestingly, hyperplasia was not relegated to the BADJ and could also be seen infiltrating the distal alveolar airspace (Figure 5.8). These regions were characterized by diffuse septal thickening, with GFP+ cells interspersed at regular intervals. These GFP+ cells were negative for both CCSP and SPC. Often times, these regions of diffuse septal thickening could be linked to an area of bronchiole airspace demonstrating poor differentiation and drastic epithelial overgrowth.

Within certain regions of the peripheral airways, the regular staining pattern of transgene expressing cells gave way to more cellular and less organized morphology. While it's possible these changes represent the early stages of adenoma, there were other areas with a more clearly defined papillary morphology, making them better candidates for early stage or precursor lesions to adenocarcinoma (Figure 5.8). Instead, these poorly organized, hypertrophic lesions more closely resembled bronchio-alveolar carcinoma (BAC), in which the tumor grows along pre-existing airway structures without detectable invasion or destruction of underlying tissue. In human patients, non-mucinous BAC is thought to be derived from a transformed cell in the distal airways and terminal respiratory units, often displaying features of Clara cell or type II pneumocyte differentiation.

Detection of a frank nodule always occurred within a region displaying dysplastic growth, whether it be well differentiated septal thickening or poorly differentiated, irregular hyperplasia. Nodules varied in size and apparent morphology, with some possessing easily discernable papillary fronds and others showing marked disorganization (Figure 5.8). Taken together, the histological appearance of lung tissue from these mice suggests a model of cancer initiation and progression where bronchial epithelium becomes transformed, expand in number and migrate outward towards peripheral airspaces. Once there, they experience subsequent alteration and form frank neoplasia within regions of pre-malignant hypercellularity.

One of the attractive features of the shp53/Kras mouse is the ability to discontinue the inducible gene silencing and thus restore p53 protein levels. Studies have suggested that restoring p53 function to tumors which have either lost the corresponding genomic coding region or experienced hypermethylation and promoter silencing may be a viable therapeutic modality (Krizhanovsky, Xue, et al., 2008). Cessation of doxycycline treatment resulted in a decrease in GFP expression and a reduction in cellularity of the lungs after 3 weeks. Interestingly, at the one and two week post cessation time points, an increase in colocalization between endogenous CCSP and GFP signals was seen in bronchial airways as well as adenomas and adenocarcinomas. GFP signal reduction was not complete, and even at 4 week post cessation time points, some tumors had interspersed GFP+ cells (Figure 5.9). In a number of cases, there was even notable expansion of GFP+ cells within a tumor that had otherwise largely silenced transgene expression. This may be due to mutational uncoupling of the tet-induction system via rtTA or TRE mutation.

Flow cytometry studies of tumor tissue derived from dox treated, adeno-cre transduced shARF/Kras mice suggested an enrichment of CD44high/CD24low/CD45-/Pecam- tumor epithelium (Figure 5.10). Levels of these cells were comparable to extreme cases found from profiling of human primary tumors. As this signature identifies cells with increased metastatic potential in vitro and poor prognostic outcome according to our tissue microarray data set, the shARF/Kras mouse might represent an interesting model of aggressive adenocarcinoma. Indeed, studies comparing this mouse strain to Kras only and shRenilla/Kras controls proved markedly increased tumor burden, with gains in both tumor size and number of nodules, as well as significantly reduced survival (Premsrirut et al., 2011).

We next looked at tissue from shARF/Kras mice to observe the distribution of CD44high cells in primary tumors. There was a surprising amount of inter-tumoral heterogeneity with respect to number and distribution of CD44+ epithelium (Figure 5.11). This was found to be independent of tumor size, indicating that intrinsic factors unique to each neoplasm may have dictated the emergence of this subpopulation. In many but not all tumors, CD44+ cells were located at the periphery and were positive for nuclear phosphor-SMAD2, a marker of active TGF-β signaling (Figure 5.12). CD44+ cells were located primarily at the interface between tumor and local environment, suggesting a potential role of foreign body immune reaction in inducing the cell state.

Studies suggest that hypermethylation of the ARF tumor suppressor occurs in approximately 30% of human non-small lung carcinoma. Drugs inhibiting DNA methyltransferases (DNMTI) and histone deacetylase (HDACI) have been put forward as therapeutic strategies to reactivate tumor suppressors

and may have benefit to patients with silenced ARF loci. To test the "on-target" effect of these drugs, we withdrew dox from shARF/Kras animals with detectable disease (as measured by Luciferase imaging). After two weeks, ARF reactivation coincided with a massive induction of cleaved-caspase 3 suggesting that p19ARF reactivation induced apoptosis can promote tumor regression in KRasG12D driven lung cancer (Figure 5.13).

Discussion

We report a simple and inexpensive tissue preparation procedure that allows for *ex vivo* imaging of lung biology and imaging analysis of whole mount samples with ~100 times the spatial information (5 microns vs 500 microns). We have demonstrated a number of valuable applications, including live-cell study of wounding, detection of rare cell populations and comprehensive biological characterization of mouse models of lung disease.

Our studies employing genetically engineered models of lung cancer produced interesting findings regarding tumor biology. In particular, the increased depth of sectioning allowed us to compare peripheral vs. central areas for intra-tumoral heterogeneity. The increased presence of CD44high cells in many shARF/Kras tumors suggests a genotype specific intrinsic factor that may promote the development of these cells. Because many, but not all of these tumors showed high CD44+ cell content, it would be interesting to perform serial transplant to determine whether the ability to generate cells with metastatic properties was maintained. Perhaps some tumors would maintain CD44 status (and as such, have cell autonomous determination) while others would revert to a mostly CD44 negative histology.

Having shown the utility of lung slice culture for both detection of rare events and live cell microscopy, it would be interesting to utilize this technique for real time fate mapping of cells grafted into a host lung. Transplant of genetically or chemically labeled progenitor populations, followed by subsequent naphthalene injury and slice generation would allow for definitive proof of replication during the injury process. Additionally, a host of reporter gene constructs could be used in conjunction with this technique to study diverse processes such as epithelial to mesenchymal transition and induction of cellular differentiation.

Experimental Procedures

Agarose Preparation

To avoid clumping, preheat the required volume of HBSS to a boil then mix the agarose in by vortexing. Rest the solution at 42 degrees Celsius for one hour. During this time, warm the syringes that will hold the agarose to 37 degrees Celsius. Load the agarose into syringes and keep them at 37 degrees until mice are ready for instillation. Maintaining the agarose at this temperature is important for limiting thermal damage to lung tissue during preparation.

Lung Sectioning

In order to section the lungs we utilized a Leica vibratome .To facilitate blade entry and limit pulling, clean sharp scissors should be used to trim the edges of the lung where the convergence of pleura make sectioning difficult. The sectioning chamber should be maintained as cold as possible to ensure the rigidity of the lungs as they are cut. Slices were collected into HBSS on ice and subsequently placed into LHC9 cell media or an equivalent serum free growth media. Incubation overnight in normal cell culture conditions (37 degrees Celsius, 5% CO_2) was sufficient to remove the agarose. Clearing is complete when trapped air bubbles are no longer seen within the lumen of peripheral air spaces.

Once the slices were cleared, they were then transfer into fresh culture media or alternatively, lung slices fixed for immunofluorescence.

Immunofluorescence

Permeabilization was accomplished with 0.5% triton x-100 in PBS with 2% BSA, followed by washing with 1% BSA in PBS. Slides were incubated with primary antibody at 4 degrees Celsius overnight. Secondary antibody labeling was performed with the species appropriate fluorescent conjugate for one hour at room temperature the next day. DAPI was used to label nuclei. All slides were mounted using p-Phenylenediamine anti-fade media. Imaging was performed on the Zeiss 710 confocal microscrope running Zen software.

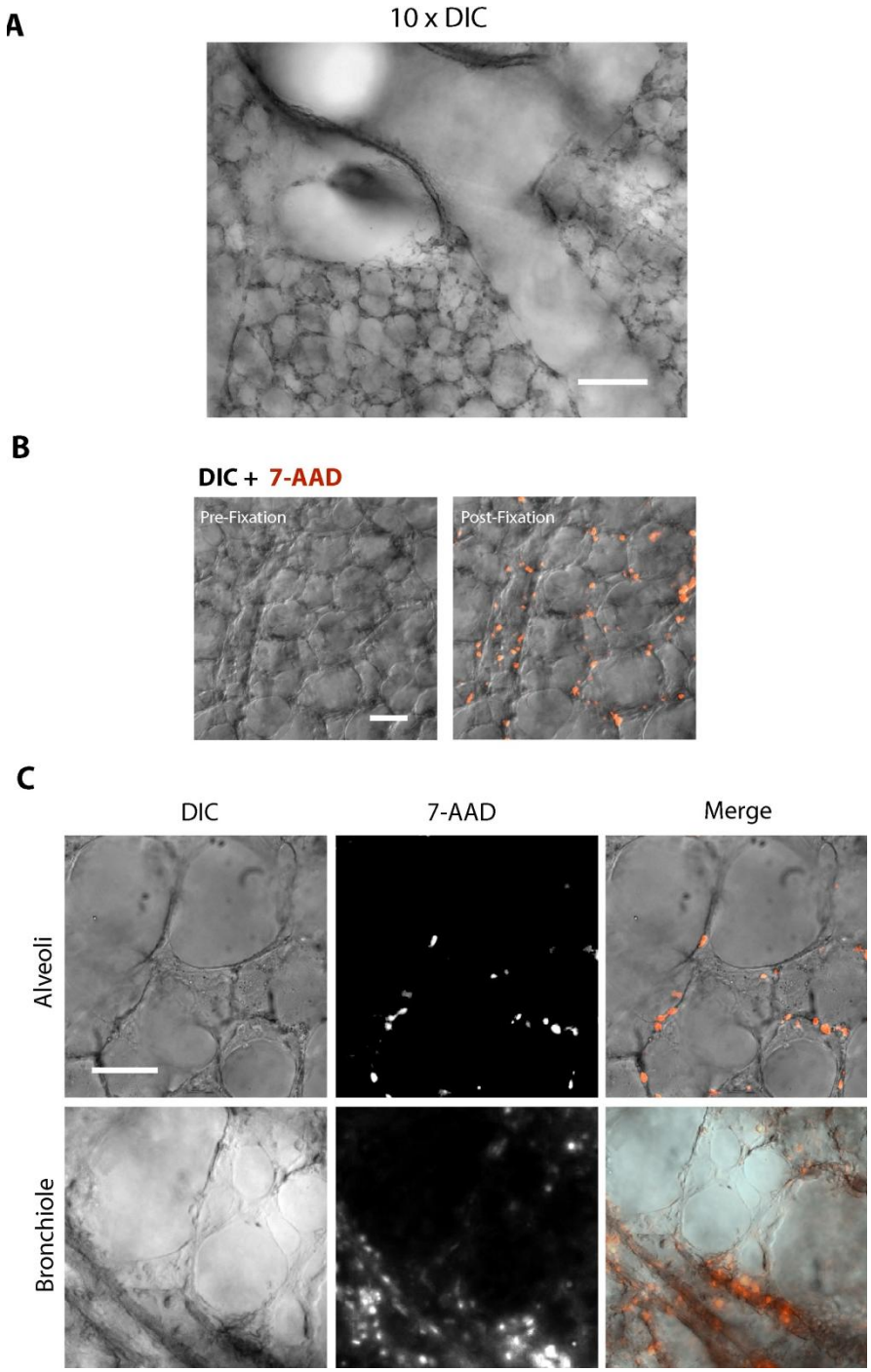

Figure 5.1 Characterization of Lungs Maintained in *Ex vivo* Culture. **(A)** Lung slices prepared by vibratome sectioning maintain diverse morphological characteristics (Scale bar 200 micron). **(B)** Slices prepared and cultured for 3 days are still viable as measured by 7-AAD exclusion before fixation (Scale bar 80 micron). **(C)** After one week in culture, structures of the alveolar and bronchial airways remain intact. Tissue was fixed and counterstained with 7-AAD to demonstrate persistence of nucleated cells in culture (Scale bar 50 micron).

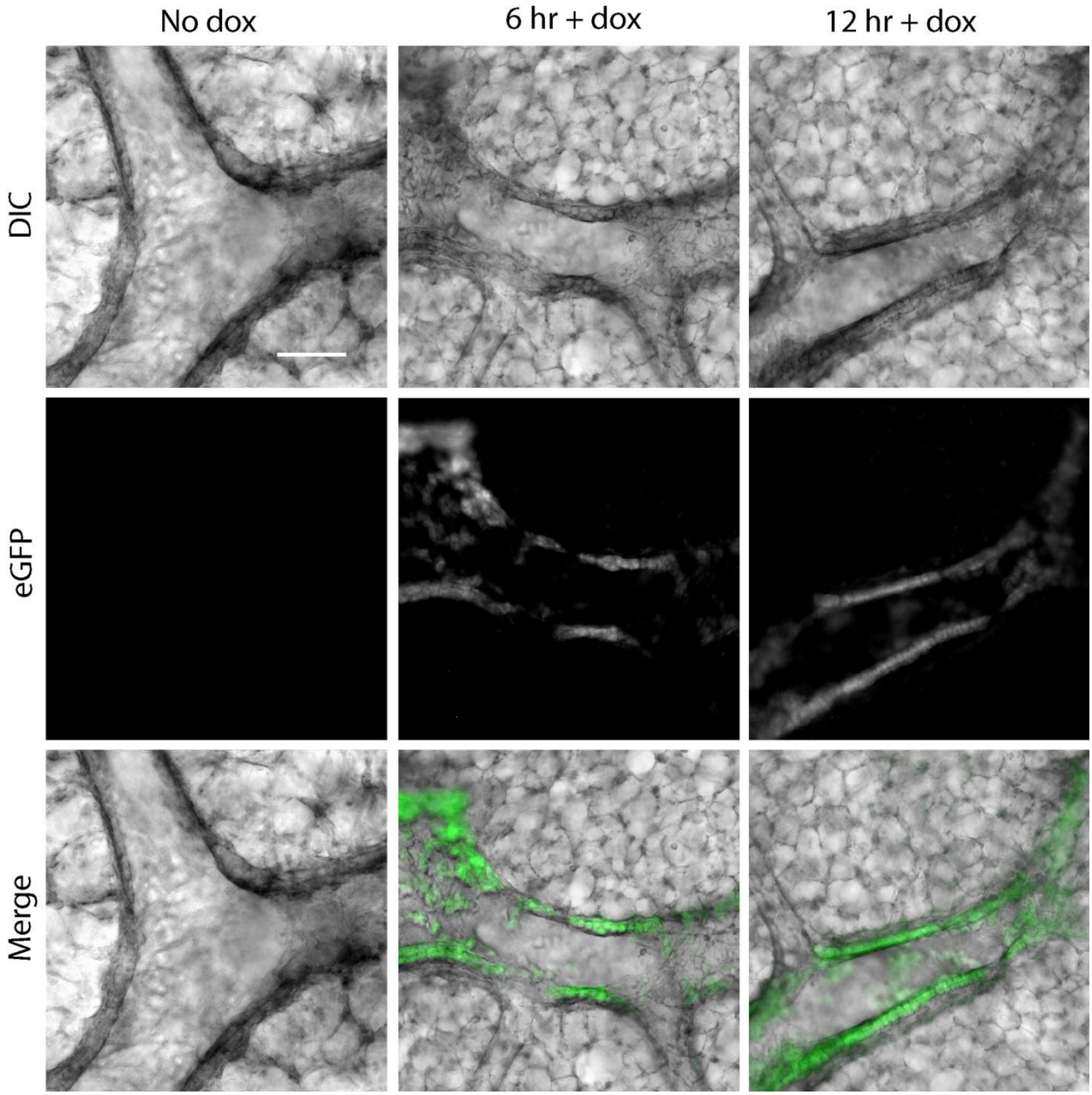

Figure 5.2 *Ex vivo* Induction and Detection of Transgenes. Slices harvested from mice with doxycycline inducible transgene under control of the CCSP promoter show rapid activation and spatially correct expression of GFP reporter (Scale bar is 150 micron).

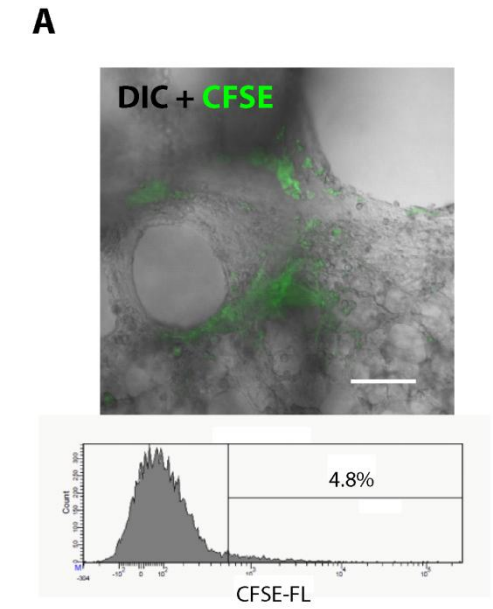

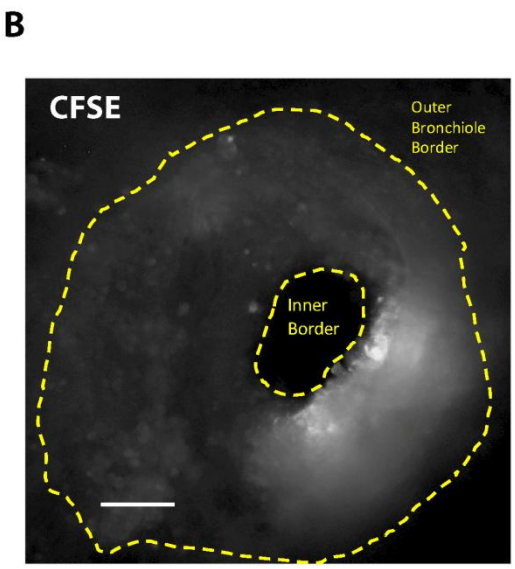

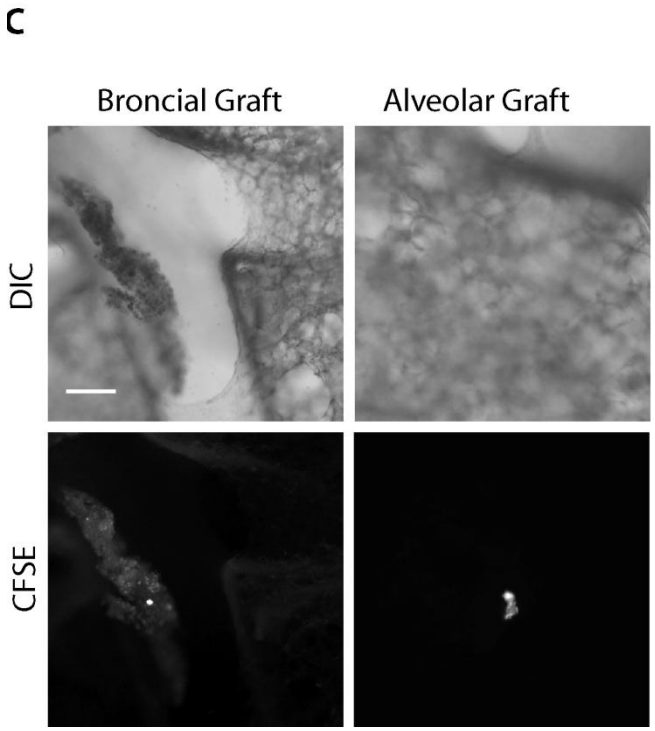

D

Transplanted Population	300 uM Slices w/CFSE Staining	Bronchial Grafts	Respiratory Airway Grafts
CD24 (-)	5/43	0	5
CD24 low	3/42	2	1
CD24 mid	12/42	8	4
CD24 high	26/43	18	8

Figure 5.5 Detection of CFSE Stained Lung Grafts. **(A)** Whole lung homogenate was harvested from syngenic mice, labeled with CFSE and transplanted into non-fluorescent recipients. Fluorescent microscopy showed similar efficacy of detection as flow cytometry (Scale bar is 100 microns). **(B)** CD24high donor cells, described in detail in Chapter 2, integrated into host airways and displayed dye dilution and retention properties (Scale bar is 100 microns). **(C)** Grafts detected in the bronchial airways showed much more apparent growth 1 week after transplant than those found in peripheral airspaces (Scale bar is 200 microns). **(D)** Use of lung slice preparation allowed for the quantification of grafting efficiency even at short time intervals after transplant.

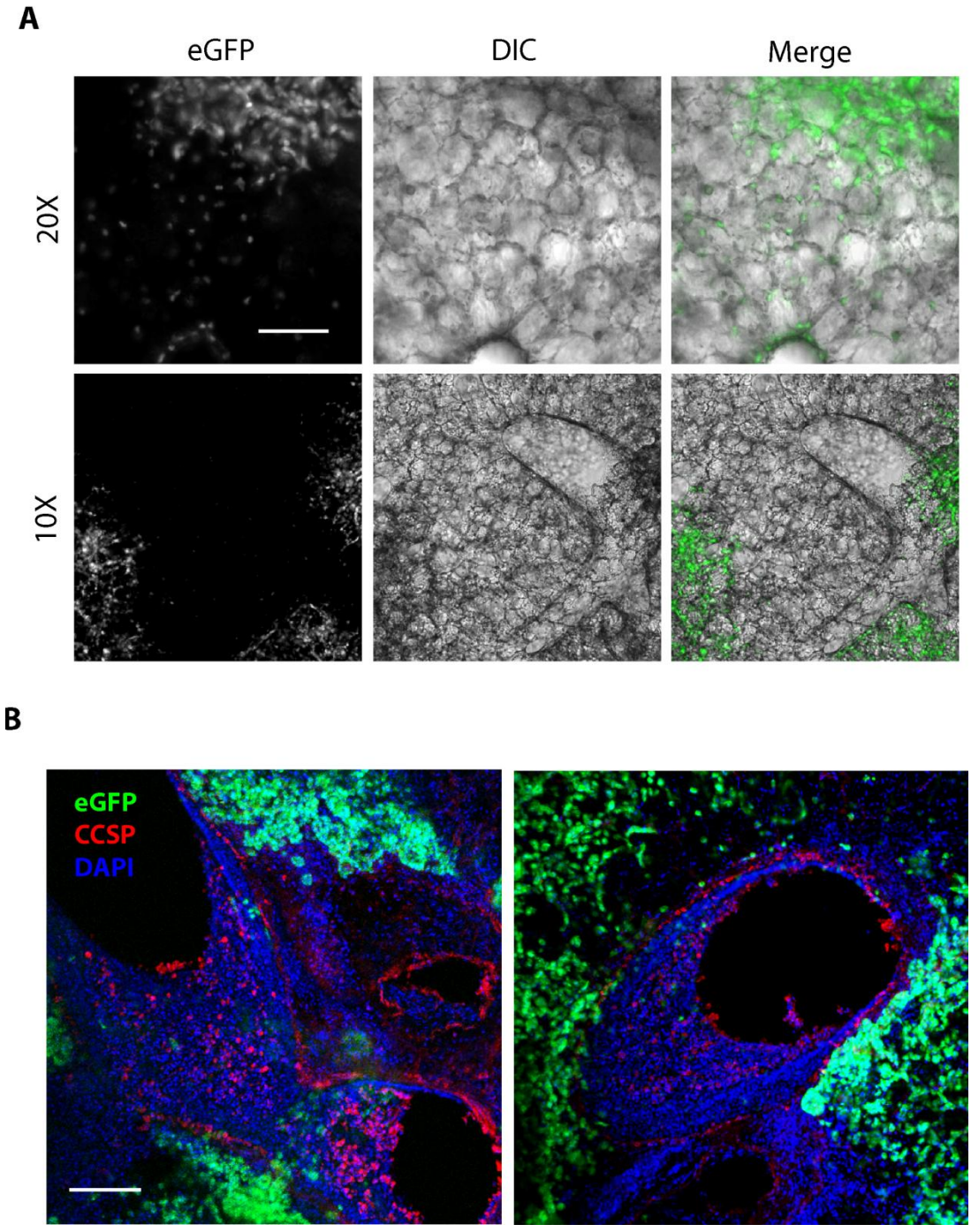

Figure 5.6 Characterization of GFP Expression in Transgenic Murine Models of Lung Cancer. (A) GFP+ cells were readily observable in freshly prepared lung slices of shp53/KRAS G12D mice. Expression was apparent non-transformed cells of peripheral airways as well as hyperplastic foci (Scale bar is 200 microns). **(B)** Co-staining of lungs with CCSP antibody showed only rare CCSP+/GFP+ cells, suggesting that p53 knockdown may result in a de-differentiation phenotype. Large hyperplastic foci of densely packed cells occurred around many medium sized bronchioles (Scale bar is 100 microns).

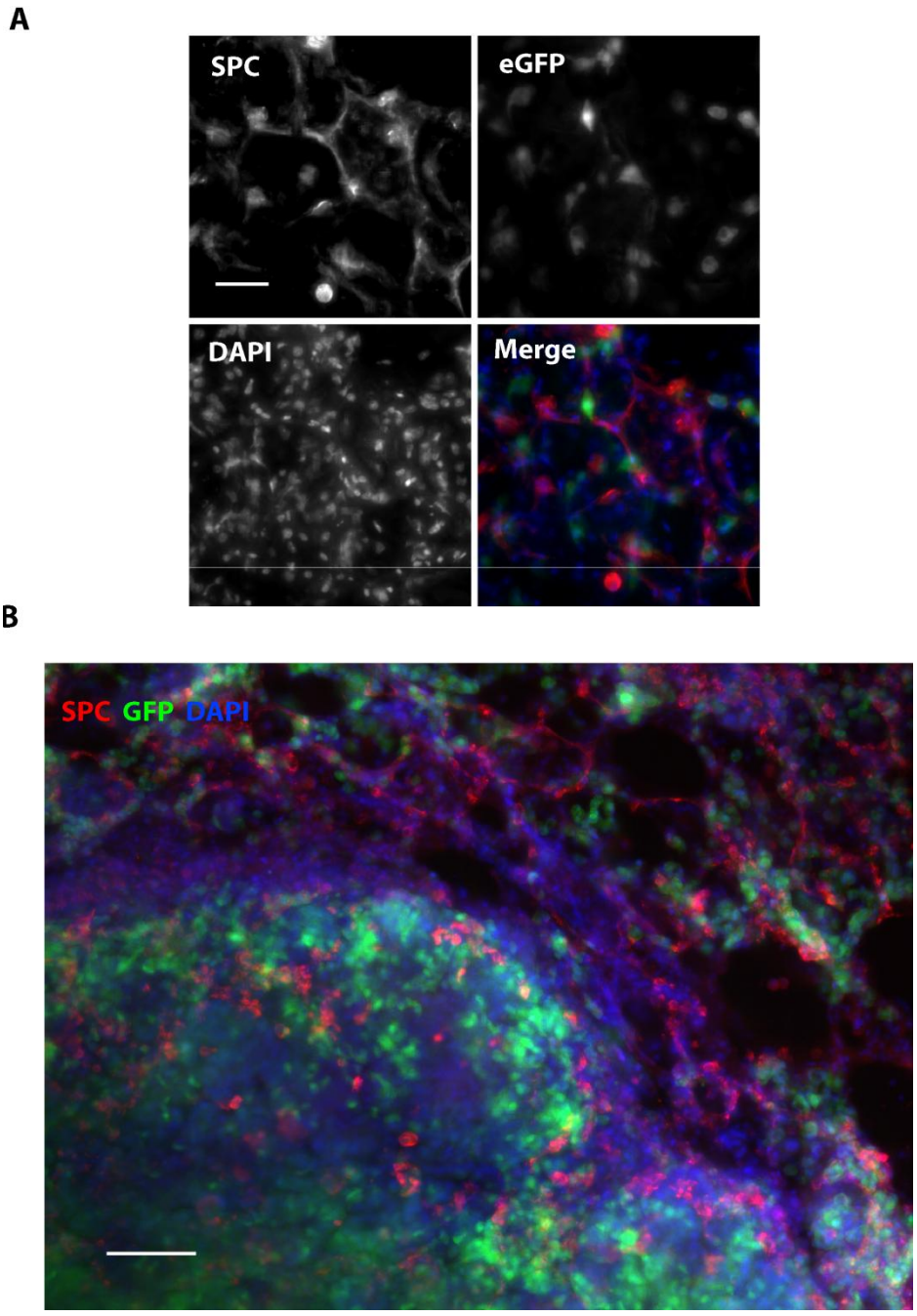

Figure 5.7 Identifying GFP+ Cells in Alveolar Airways. The presence of GFP+ cells in the alveolar airways has suggested to be due to transgene expression in type II pneumocytes. **(A)** Co-labeling with type II pneumocyte marker SPC revealed the two populations are distinct from one and other (Scale bar is 50 microns). **(B)** SPC expression was present in tumors and hyperplastic foci (Scale bar is 100 microns).

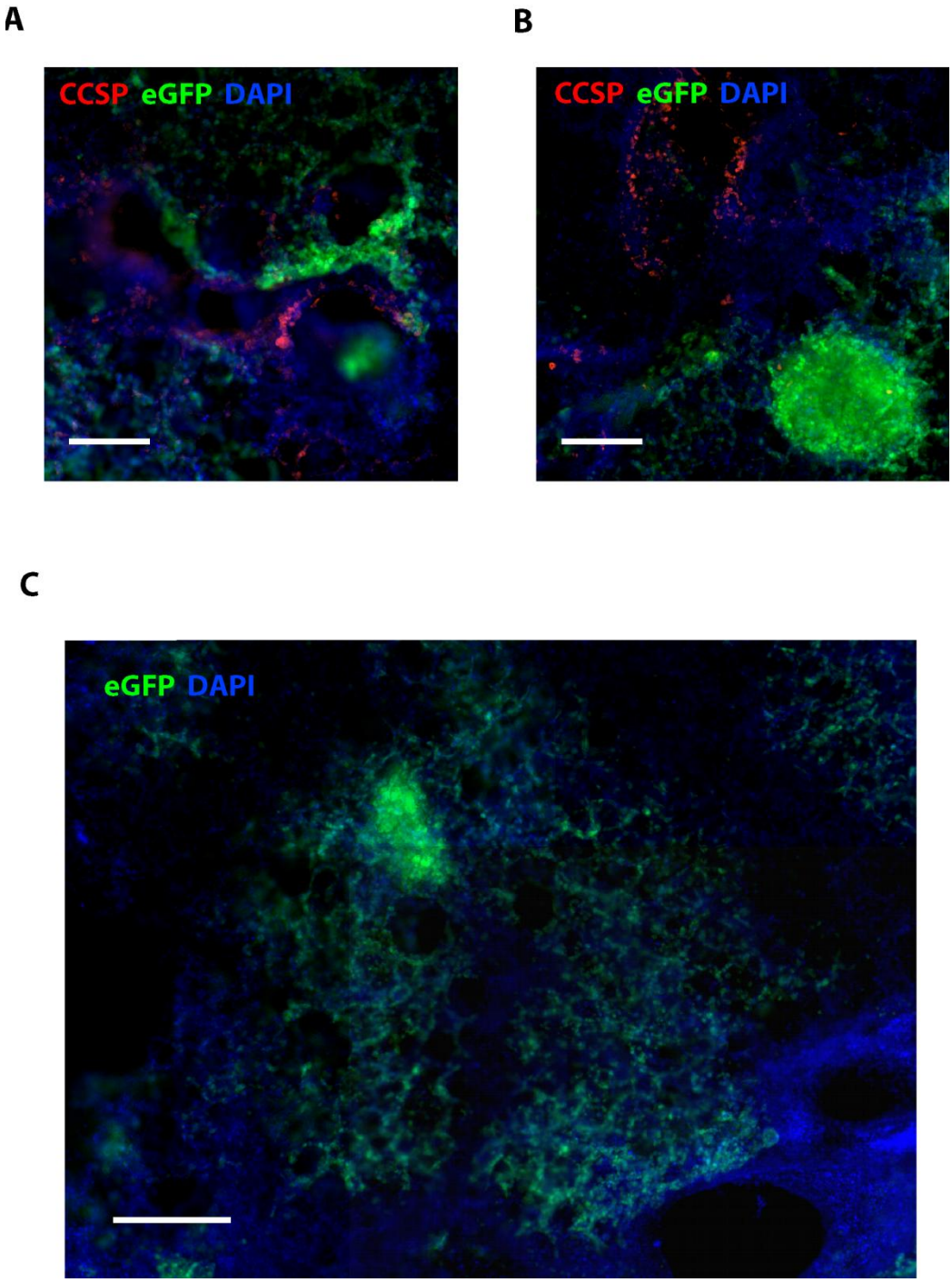

Figure 5.8 Apparent Progression of Dysplastic Growth in shp53/KRAS G12D Lungs. (A) Regions of densely packed dysplastic cells often bordered on CCSP bronchiole airways. Adjacent to these spaces were diffusely hyperplastic regions of GFP+ cells (Scale bar is 200 microns). **(B)** Within these regions of hyperplasia, large nodular growths frequently occurred (Scale bar is 200 microns). **(C)** Mosaic imaging of an entire region, from bronchiole to nodule (Scale bar is 500 micron).

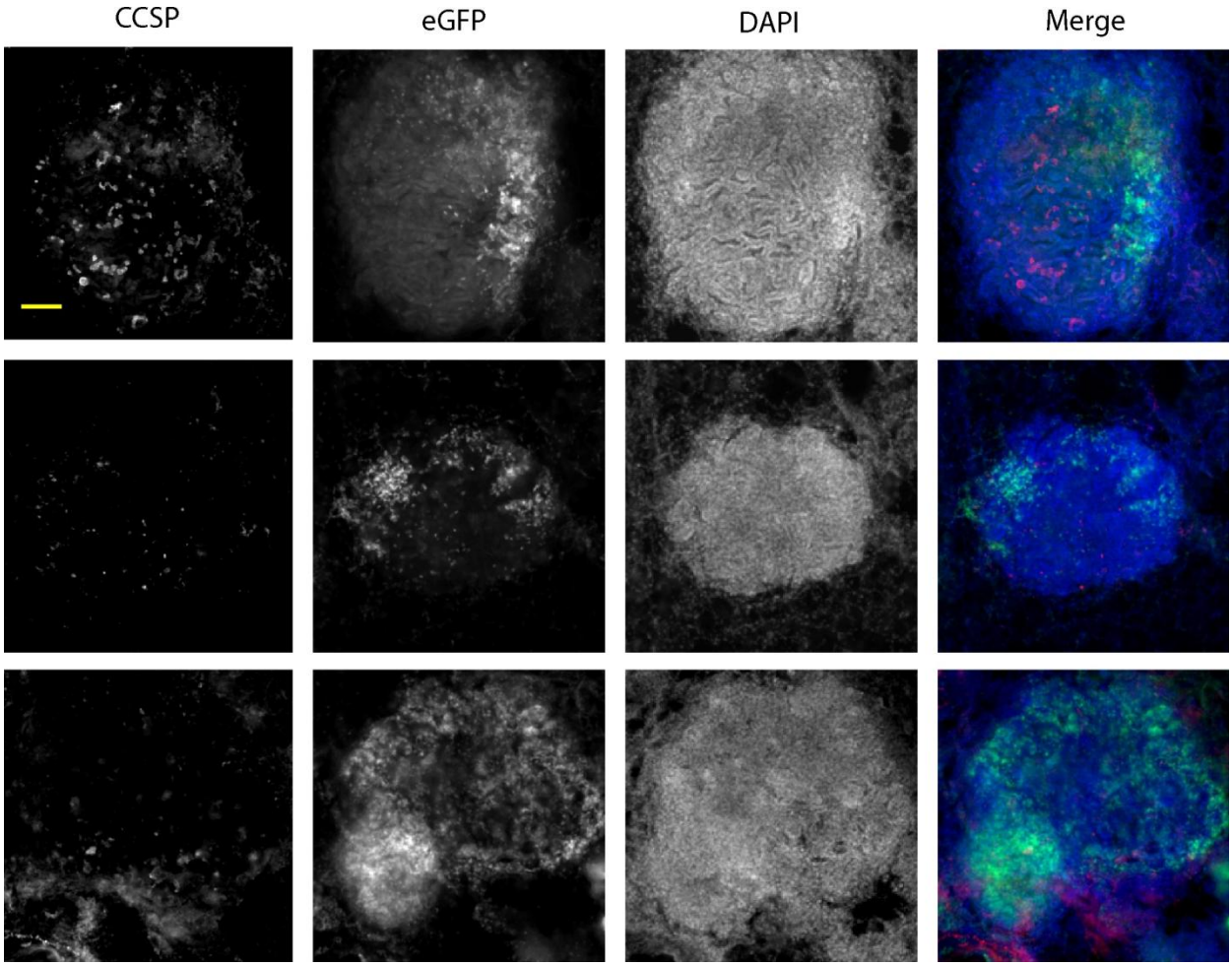

Figure 5.9 Doxycycline Cessation Restores CCSP Expression. Animals taken off dox for four weeks prior to sacrifice show dramatic decrease in number of GFP+ cells. In many cases, CCSP expression was apparent even within tumors. This was never seen in animals maintained on dox. Some tumors showed localized outgrowth of GFP+ populations, possibly attributable to a genomic event causing uncoupling of the tet-regulatable system.

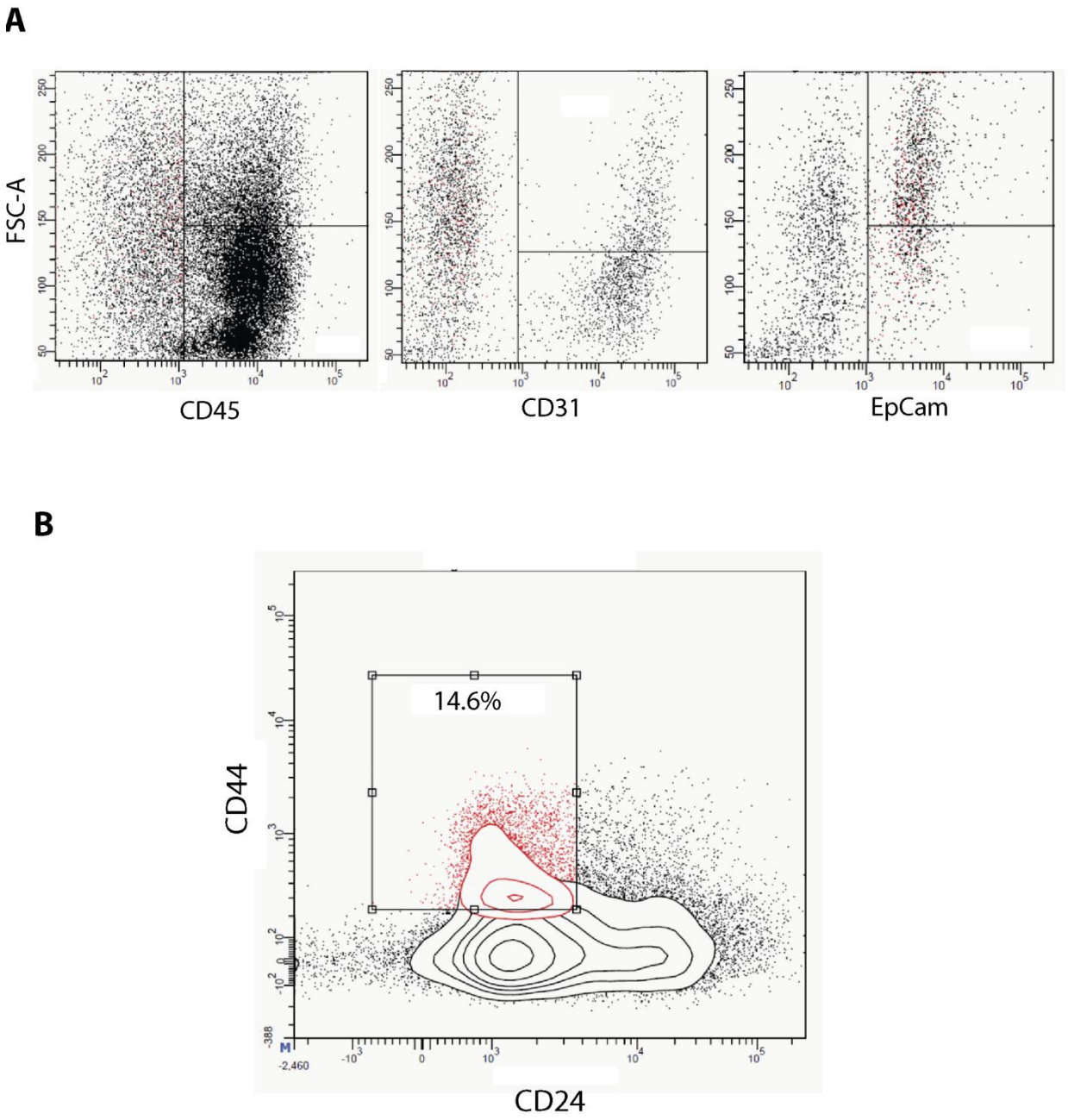

Figure 5.10 Tumors from shARF/KRAS G12D Mice Have Increased Number of CD44high/CD24low Cells. Nodules harvested from the lungs of shARF/KRAS G12D kept on dox were dissected and prepared for flow cytometry. **(A)** Epithelial cells were identified as CD45-/CD31-/Epcam+. **(B)** Relative distribution of cells on the CD44/CD24 axis frequently revealed tumors with CD44high/CD24low cell content comparable to the highest levels seen in human patients.

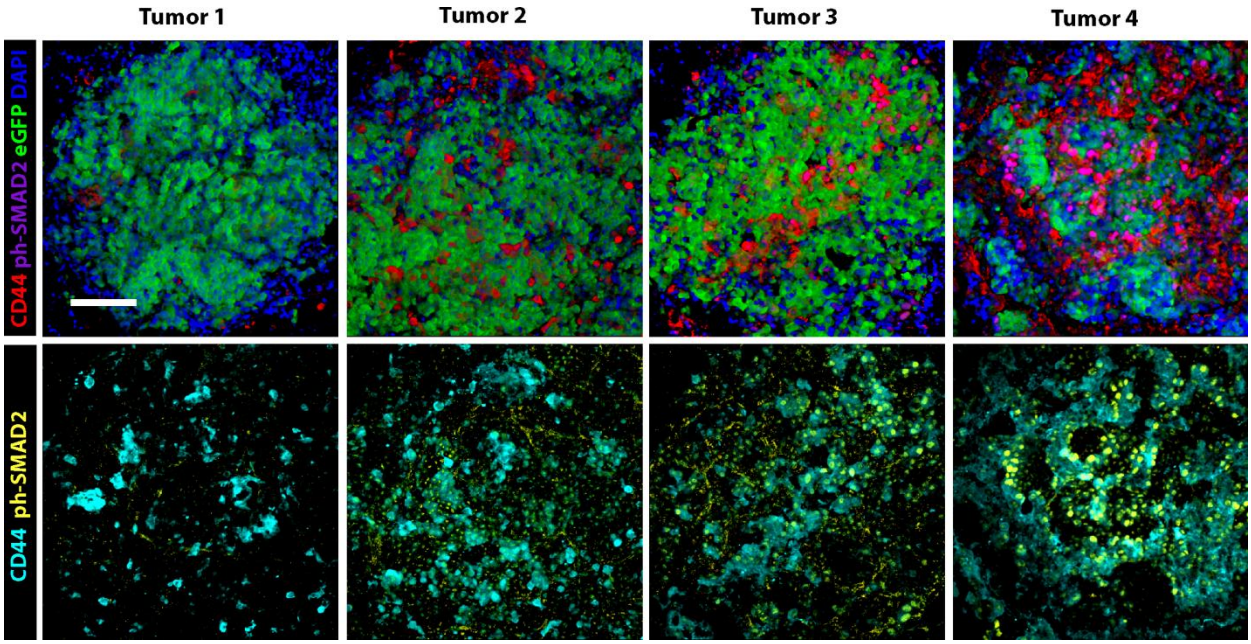

Figure 5.11 Inter-tumoral Heterogeneity for CD44 Cell Content in the Lungs of shARF/KRAS G12D Mice. Tumors identified as the same approximate diameter and volume in slice culture were imaged for the presence of CD44+ cells. High levels of CD44+ cells were detectable in tumors with increased phosphor-SMAD2 staining, confirming the role of TGF-β in the ontogeny of these cells. Images shown are 3D reconstructions of 200 micron coverage z-stacks taken at 2 micron intervals made with the Zeiss Zen software (Scale bar is 100 microns).

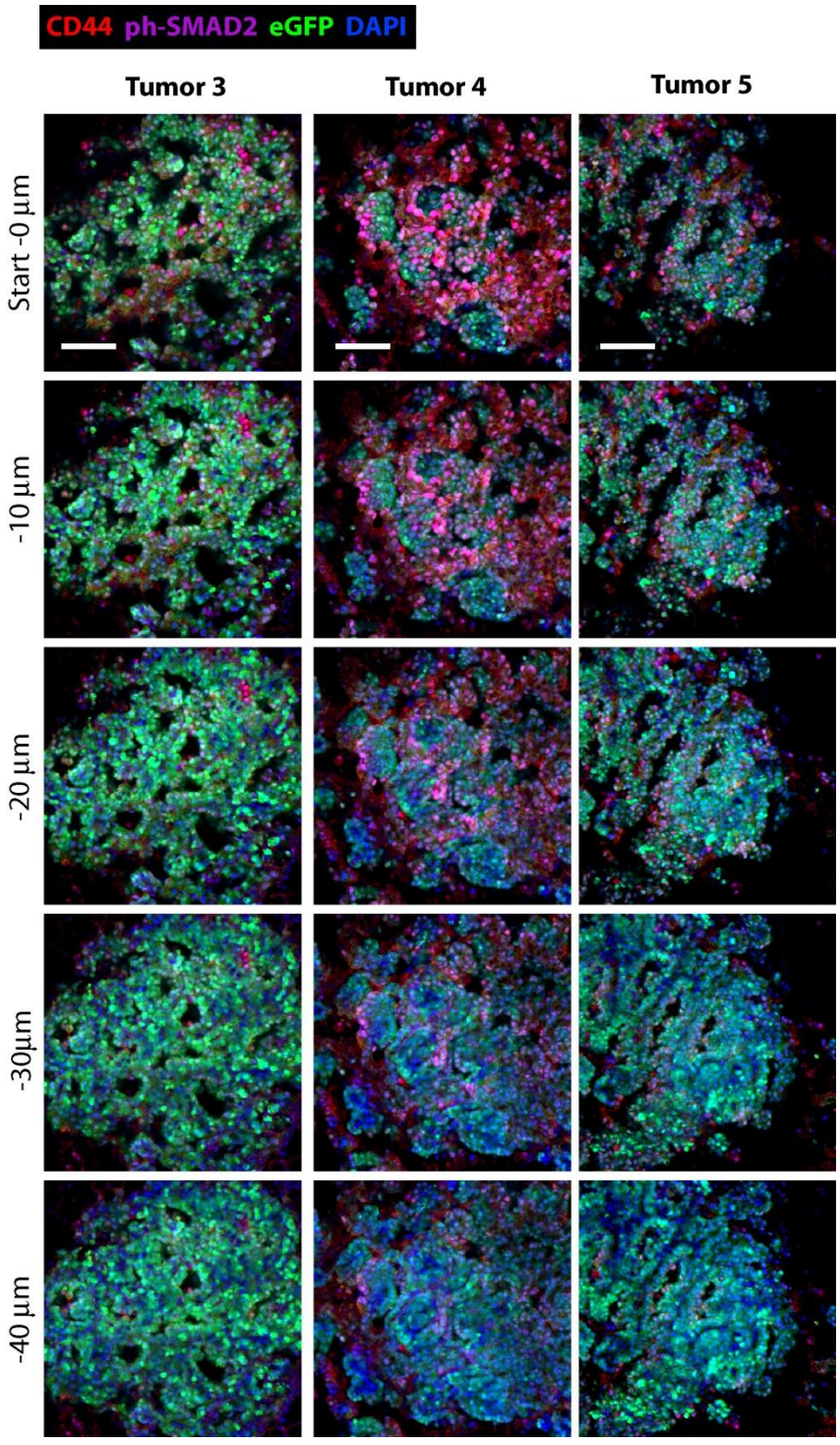

Figure 5.12 Spatial Localization of CD44+ Cells within shARF/KRAS G12D Tumors. Imaging of tumors prepared as tissue slices allowed for discernment of the location of CD44+ cells within a give neoplasm. Each tumor was imaged in its entirety. "Start" denotes the outermost apex of the mass. Subsequent images are shown at 10 micron intervals. CD44+ cells are located primarily at the periphery of the tumor (Scale bar is 150 microns).

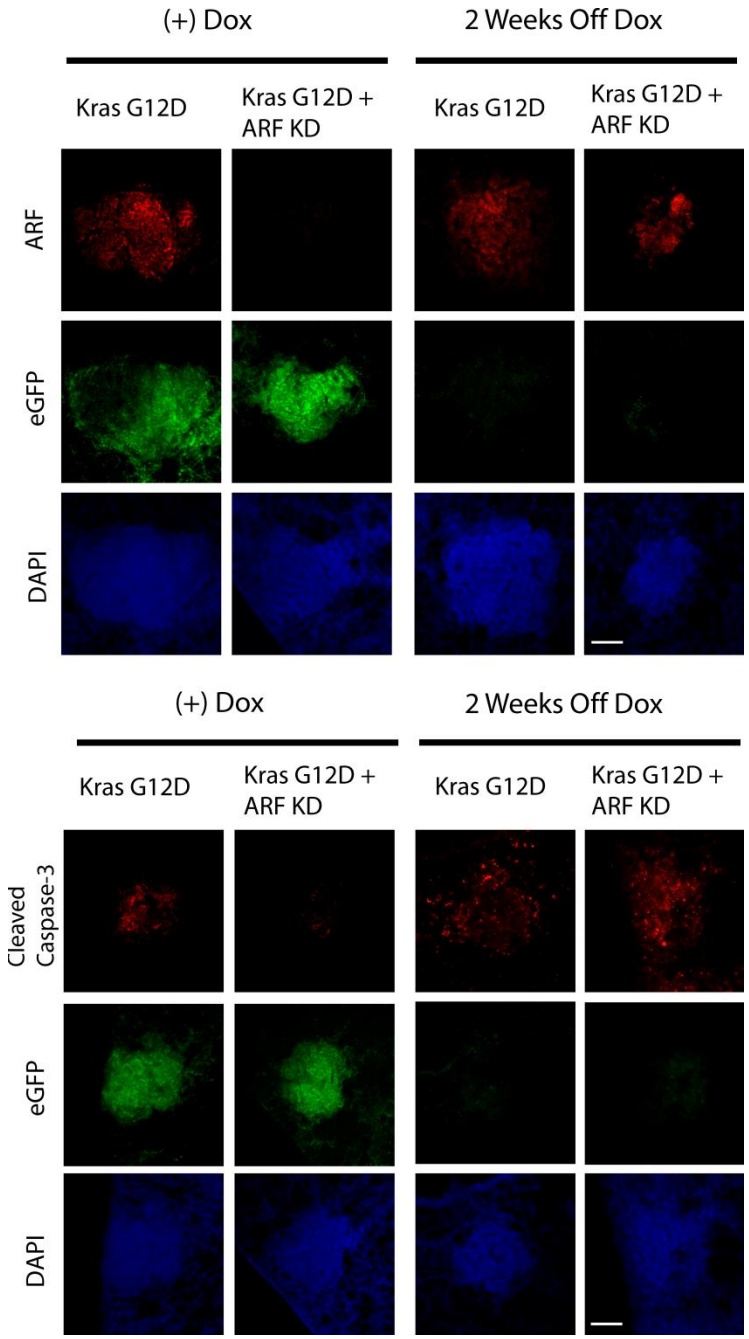

Figure 5.13 Reactivation of the ARF Tumor Suppressor Induces Apoptosis in KRAS Mutant Lung Carcinoma. Animals previously maintained on dox were withdrawn from treatment to cease expression of the shARF construct in shARF/KRAS G12D mice. Mice were sacrificed two weeks later. ARF reactivation coincided with a massive induction of cleaved-caspase 3, indicating robust induction of apoptosis (Scale bar is 100 microns).

Chapter 6

Discussion and Closing Remarks

Chapter 6: Discussion and Closing Remarks

Proper repair of wounded tissue requires the concerted effort of a myriad different cells working together to return homeostasis to their local environment. Over the past few chapters, processes crucial to recovery from injury have been discussed. These include activation of latent epithelial progenitors, the acquisition of the migrating phenotype, and the molecular pathways that play a role in promoting survival of injury responsive cells through evasion of senescence and apoptosis. The lessons learned from these studies highlight a compelling cross talk between the processes governing wound healing and those of tumor initiation, promotion and evolution.

The activation of cells baring the functional characteristics of adult stem cells is critically important to epithelial regeneration within the lung. A number of classical studies have demonstrated by way of labeled nucleotide retention that progenitors for particular regions lie at distinct anatomic sites. Current thinking has defined a number of niches that serve to supply cells to nearby tissue. The interrelation between progenitors at these points along the proximal-distal axis of the lung remains a question of interest. Could these cells be of common origin? To what extent are regional progenitors fate specified?

Tools to evaluate progenitor populations within the lung are still in their infancy when compared to other, more characterized systems. Particularly in the distal airways, cellular components of epithelial regeneration are still under much dispute. Prior to our study, a prominent role for a CCSP+/SPC+ distal bronchiole progenitor had been described in a number of settings pertaining to wounding and tumorigenesis. However, works aimed at in vitro culture of these cells using the FACS purification scheme published in their initial report produced data that called their existence and significance into question. Here we resolve these issues by illustrating the existence of CCSP+ cells as a subfraction of Sca-1+/CD45-/Pecam- cells in the lung.

The surface glycoprotein CD24 was shown to effectively stratify the Sca-1+ population of lung cells into subgroups with very divergent gene expression programs. The functional significance of this molecule and how it may pertain to progenitor biology in the lung has not yet been addressed. CD24 is known to be the receptor for p-selectin, the molecule that lines endothelium and activated platelets (Aigner et al., 1997). It is tempting to postulate that tissue resident progenitors capable of responding to injury express CD24 as means of attracting platelets and coordinating wound healing. Corroborating this idea is our discovery that serotonin signaling appears to play a role in fostering proliferation of lung

adult stem cells at the bronchioalveolar duct junction (BADJ). Serotonin is found in large quantities within circulating platelets, and this relationship may explain the initial impetus for subsequent autocrine secretion of the molecule by these cells.

Our engraftment studies utilizing transplant between littermate animals allowed for lineage tracing and grafting efficiency determination of the different CD24 subfractions of Sca-1+ cells. These results expanded on previously published data illustrating that a CCSP expressing cell served as progenitor to bronchial epithelium by providing a precise immunophenotype to the cell demonstrating this ability. While this algorithm for purification of distal bronchial progenitors cannot be used for human studies due to its dependence on Sca-1, it could be potentially valuable for a number of applications in mouse studies. In particular, using this knowledge for transplantable models of lung carcinoma seems a natural extension of our work, as a wealth of data has implicated hyperplasia of cells at the BADJ in oncogenesis.

The fact that our purified progenitors homed back to the anatomic site from which they were harvested suggests a regional specificity that is encoded in a cell-autonomous fashion. There also appears to be a fair amount of lineage specificity to these cells. Paradoxically, this population appears to express factors associated with embryonic pluripotency. The role that Oct4 and Nanog may play in maintaining adult stem cells in the lung is as of now completely unknown. Previous work has demonstrated that Oct4 expression was not necessary for maintenance of somatic tissue. However this work did not employ use of a lung injury paradigm requiring activation of quiescent bronchial progenitors. Further studies aimed at longer term integration after adult stem cell transplant may demonstrate a wider lineage contribution. Additionally, use of different injury paradigms after transplantation may elucidate cellular contributions we have not yet appreciated.

The increased presence of CD45- and CD45+ cells displaying Oct4-GFP reporter activity at just 48 hours after naphthalene injection suggests a role for locus activation in endogenous lung cells as well as homing of marrow derived cells expressing Oct4 to the lung. The relationship between these marrow derived and non-marrow derived Oct4+ cells may be of tremendous interest going forward. CCSP+ cells able to generate bronchial epithelium have recently been reported to exist in the murine bone marrow (Wong, Keating, Lu, et al., 2009). This finding suggests that lung progenitors may arise from stem cell populations in the bone marrow and hone to the lung after entering systemic circulation where they take up permanent residence in distinct anatomic niches.

Evidence has implicated serotonin signaling in a diverse number of pathological processes in the lung including chronic obstructive pulmonary disease. In this disease, abnormal thickening of the bronchial airspaces cause problems with expiration. We show that bronchial progenitors express the serotonin receptor 2B and produce serotonin in response to naphthalene induced injury. Chemical inhibition of the receptor results in deficits in epithelial regeneration after chemical wounding, suggesting a critical role for subsequent downstream signaling in progenitor activation or proliferation. Interestingly, serotonin producing cells have been reported within the lung neuro-epithelial bodies of a number of species. These structures lie at the bifurcation of the bronchioles, one of two sites reported to harbor naphthalene resistant Clara cell progenitors.

Recent work described an important relationship between lung epithelial progenitors and signals derived from nearby endothelium. The link between the two compartments may represent a physiological coupling to ensure that regions of the lung that are oxygenated receive adequate blood supply and vice versa. Studies of HTR2B null animals have suggested a role for the receptor in endothelial remodeling in response to hypoxia. The expression of the receptor on epithelial progenitors as well may represent a common modality for injury signaling.

A role for HTR2B in the fibrotic response has been described in a number of organs. Increased staining for the receptor is apparent in human patients with idiopathic pulmonary fibrosis. In addition, inhibition of HTR2B attenuated fibrotic response to bleomycin treatment in animal lung injury models. Blockade of HTR2B was also shown to mitigate liver fibrosis by preventing expression of downstream pro-fibrotic cytokines and growth factors (e.g. Il-6 and TGF-β). Taken together, these data illustrate a role for this serotonin receptor in both fate selection and proliferation. Given that Il-6 dependant activation of Stat3 was shown to be required for epithelial regeneration after naphthalene, the proliferation of progenitors and migration of daughter cells may be mechanistically coupled. As such, certain mitogenic signaling events in adult stem cells may stimulate their secretion of pro-inflammatory cytokines which promote epithelial to mesenchymal transition of daughter cells that then migrate to sites of wounding.

The TGF-β signaling axis represents one arm of the mechanisms we have investigated underlying the acquisition of mesenchymal-like phenotypes by cells of epithelial origin. We have demonstrated that certain human non-small cell lung carcinoma derived cells lines, when exposed to this growth factor, will adopt the characteristics of metastasis initiating cells. Paracrine signaling is not, however,

the only means by which cells may adopt a mesenchymal-like fate. We also provide evidence of stable, cell-autonomous changes that may influence the immuno-phenotype of a cell.

The presence of cells displaying mesenchymal characteristics within epithelial populations has important consequence for the diagnosis and treatment of cancer as they are inherently dependant on different pathway activation for survival and imbued with properties associated with heighted cancer morbidity and mortality. Evidence from cultured breast cancer cells has indicated that inter-conversion between immunophenotypically distinct subpopulations can account for heterogeneity. This work, however, has not definitively ruled out the occurrence of multiple stable, non-transiting phenotypes within monogenomic tumors. Nor does it address the possibility of multiple stable clones with divergent but symbiotic phenotypes within polygenomic tumors.

Understanding the interplay between factors such as micro-environment derived inductive signals and tumor cell intrinsic determinants will be crucial in tailoring therapeutic interventions able to effect long term clinical remission of a cancer. We provide evidence that both may play a role in the ontogeny of cells displaying the mesenchymal phenotype caused by EMT. Importantly, we cannot rule out the reciprocal relationship that may exist between the two. Stochastic epigenetic events resulting in the stable adoption of stem-like phenotypes within populations of cancer cells could lead to the secretion of soluble factors such as TGF-β, WNT5a and Il-6. These cytokines and growth factors could then have profound effect on neighboring cells, resulting in emergent diversity within a tumor. One such epigenetic event may be precipitated at the MEST locus. Data from our group has indicated that differential methylation of the promoter region may in fact be responsible for the isoform switching process, and that this event may be governed by the chromatin regulator NRSF.

It is clear from studies of lung cancer tissue microarray that the epithelium of some cancers is largely if not entirely CD44+. This data has been corroborated by flow cytometry of human tumors, showing that large portions of cells staining positive for the epithelial lineage marker EpCam can have the CD44high/CD24 low immunophenotype, and that this percentage varies greatly between individual cancers. This observation fosters the conclusion that some tumors experience a genomic or stable epigenetic event early on in growth that can either induce this state or prevent transitioning back from it to a less motile, more traditional epithelial phenotype. It will be of great interest to define genomic lesions that favor the $CD44^{high}/CD24^{low}$, as this is a suitable explanation to why a certain number of early stage cancers are prone to dissemination despite small apparent primary tumor volume and early diagnosis.

Studies of genetically engineered mouse models of cancer harboring oncogenic Kras and functional disabling of the p19ARF tumor suppressor suggested that certain elements intrinsic to these tumors may hold clues as to what factors govern the emergence of $CD44^{high}/CD24^{low}$ cells in a lung adenocarcinoma. Flow cytometry analysis of animal derived primary tumors illustrated a relative distribution of $CD44^{high}/CD24^{low}$ cells consistent with the highest levels detected in surgically resected human specimens. Microscopy studies of 300 micron lung slice specimens demonstrated that CD44+ cells occurred primarily at the periphery of tumors, and that these cells existed in tumors both with and without prominent TGF-β pathway activation as measured by nuclear phospho-SMAD2.

To further elucidate the ontogeny of the mesenchymal-like phenotype within non-small cell lung carcinoma, we provide evidence of an alternative splicing event of the TP53 gene that is both induced by and cooperates with TGF-β signaling in fostering the $CD44^{high}/CD24^{low}$ cell state. This transcript encodes a previously uncharacterized p53 isoform, dubbed p53Ψ, that lacks major portions of the DNA-binding domain, nuclear localization sequence and tetramerization domain and as such is incapable of sequence-specific DNA binding and target trans-activation. The 3' splice acceptor site within intron 6 of the gene is evolutionarily conserved, and evidence of p53Ψ generation in the context of primary human tumors, multiple cancer cell lines derived from different tissue of origin, as well animal models of epithelial injury was provided. These data provide a physiological context never before ascribed to an alternative splicing event of the TP53 gene.

Expression of p53Ψ decreased protein levels of E-cadherin , disorganized cadherin junctions and induced expression of markers for epithelial-to-mesenchymal transition. These pro-metastatic events appear to be mediated by a novel mechanism involving mitochondrial reactive oxygen species (ROS) production in a cyclophillin D (CpD) dependant manner. Although previous work has suggested that p53 is able to control ROS generation via multiple mechanisms, we show that regulation in our system is accomplished without transcription of downstream p53 targets. Recent work in the field has corroborated the purely cytosolic, non-transcriptional effects of the p53 molecule (T. Li et al., 2012).

The remarkable similarity between activities of p53Ψ and certain p53 "gain-of-function" mutants suggests these molecules may co-opt a regulated and reversible program that coordinates injury response in normal tissues. In both cases, abrogation of transcriptional response networks downstream of p53 allows for the purely cytosolic functions of the molecule to affect cell phenotype. In principle, this suggests a physiological origin for p53 "gain-of-function" mutants. The alternative splicing of p53 in settings of tissue injury may allow for the evasion of senescence by cells responding to

damage. The expression of p53Ψ at the expense of p53FL, while antagonizing p53 tumor suppressor activities, may act to facilitate the proliferation and invasion into damaged tissue to facilitate wound repair. The reversible nature of this change would then allow for the restoration of full length transcript and subsequent clearance of unnecessary cells.

The correlation between p53Ψ mRNA expression, CD44/CD24 status and disease free survival in primary human tumors further supports the concept that potentiation of the TGF-β signaling pathway may lead to the emergence of cells with intrinsic proclivity for invasion and metastasis. As gene expression profiles evocative of a wound healing signature are often ascribed to poor prognosis tumors, the fact that p53Ψ is detected in both settings points to an interesting convergence. The canonical TGF-β response in tumorigenesis is often referred to as biphasic, as the growth factor is initially anti-proliferative to epithelial cells but later becomes an integral part of tumor evolution and the acquisition of traits associated with high grade cancers. Given that TGF-β treatment of NSCLC derived cells was sufficient to induce alternative splicing of the TP53 gene, this event may represent part of the signal switching mechanism that changes TGF-β from a growth inhibitory signal to an EMT promoting one.

In summary, the work presented here illustrates a number of physiologic processes governing the tissue injury response. We detail mechanisms for identifying and purifying injury resistant progenitor cells within the lung. In addition, we have characterized HTR2B as a novel functional marker for cells responding to Clara cell ablation and uncovered a role for serotonin signaling in maintaining lung epithelium. Recent work has identified HTR2B as an upstream mediator of pro-inflammatory cytokine production, with many of the downstream signaling molecules governing the acquisition of a mesenchymal-like phenotype by epithelial cells. This acquisition of increased motility and invasiveness, also called EMT, is responsible for generating heterogeneity within tumor cell populations. Determination of cell fate along the epithelial to mesenchymal axis involves fate decisions governed not just by paracrine signaling, but also by epigenetic regulators such as mir335. Dosage of this molecule may be controlled by isoform switching at the MEST locus. The alternative splicing of p53 may also contribute to EMT by generating a novel form of the molecule that utilizes strictly cytosolic function to promote EMT by ROS generation in a CpD dependant manner. This truncated form of p53 is also seen during injury repair in epithelial structures, suggesting once again that aspects of tumor evolution may indeed represent abnormal activation of normal physiologic response to tissue damage.

Adamson, R. (2009). Role of macrophages in normal wound healing: an overview. *J Wound Care, 18*(8), 349-351.

Adhikari, A. S., & Iwakuma, T. (2009). Mutant p53 gain of oncogenic function: in vivo evidence, mechanism of action and its clinical implications. *Fukuoka Igaku Zasshi, 100*(6), 217-228.

Adorno, M., Cordenonsi, M., Montagner, M., Dupont, S., Wong, C., Hann, B., . . . Piccolo, S. (2009). A Mutant-p53/Smad complex opposes p63 to empower TGFbeta-induced metastasis. *Cell, 137*(1), 87-98. doi: 10.1016/j.cell.2009.01.039

Aigner, S., Sthoeger, Z. M., Fogel, M., Weber, E., Zarn, J., Ruppert, M., . . . Altevogt, P. (1997). CD24, a mucin-type glycoprotein, is a ligand for P-selectin on human tumor cells. *Blood, 89*(9), 3385-3395.

Akashi, T., Minami, J., Ishige, Y., Eishi, Y., Takizawa, T., Koike, M., & Yanagishita, M. (2005). Basement membrane matrix modifies cytokine interactions between lung cancer cells and fibroblasts. *Pathobiology, 72*(5), 250-259. doi: 10.1159/000089419

Albini, A., Adelmann-Grill, B. C., & Muller, P. K. (1985). Fibroblast chemotaxis. *Coll Relat Res, 5*(3), 283-296.

Almaraz, R. T., Mathew, M. P., Tan, E., & Yarema, K. J. (2012). Metabolic oligosaccharide engineering: implications for selectin-mediated adhesion and leukocyte extravasation. *Ann Biomed Eng, 40*(4), 806-815. doi: 10.1007/s10439-011-0450-y

American Thoracic Society/European Respiratory Society International Multidisciplinary Consensus Classification of the Idiopathic Interstitial Pneumonias. (2002). *American Journal of Respiratory and Critical Care Medicine, 165*(2), 277-304.

Ando, J., & Kamiya, A. (1993). Blood flow and vascular endothelial cell function. *Front Med Biol Eng, 5*(4), 245-264.

Armstrong, W. B., & Netterville, J. L. (1995). Anatomy of the larynx, trachea, and bronchi. *Otolaryngol Clin North Am, 28*(4), 685-699.

Arwert, Esther N., Hoste, Esther, & Watt, Fiona M. (2012). Epithelial stem cells, wound healing and cancer. *Nat Rev Cancer, 12*(3), 170-180.

Bakris, G. L., Mulopulos, G. P., Korchik, R., Ezdinli, E. Z., Ro, J., & Yoon, B. H. (1983). Pulmonary scar carcinoma. A clinicopathologic analysis. *Cancer, 52*(3), 493-497.

Barker, N., Bartfeld, S., & Clevers, H. (2010). Tissue-resident adult stem cell populations of rapidly self-renewing organs. *Cell Stem Cell, 7*(6), 656-670. doi: 10.1016/j.stem.2010.11.016

Barr, S., Thomson, S., Buck, E., Russo, S., Petti, F., Sujka-Kwok, I., . . . Haley, J. D. (2008). Bypassing cellular EGF receptor dependence through epithelial-to-mesenchymal-like transitions. *Clin Exp Metastasis, 25*(6), 685-693. doi: 10.1007/s10585-007-9121-7

Belvisi, M. G., & Bottomley, K. M. (2003). The role of matrix metalloproteinases (MMPs) in the pathophysiology of chronic obstructive pulmonary disease (COPD): a therapeutic role for inhibitors of MMPs? *Inflamm Res, 52*(3), 95-100.

Berg, J. S., & Goodell, M. A. (2007). An argument against a role for Oct4 in somatic stem cells. *Cell Stem Cell, 1*(4), 359-360. doi: 10.1016/j.stem.2007.09.007

Berger, A. H., Niki, M., Morotti, A., Taylor, B. S., Socci, N. D., Viale, A., . . . Pandolfi, P. P. (2010). Identification of DOK genes as lung tumor suppressors. *Nat Genet, 42*(3), 216-223. doi: 10.1038/ng.527

Besson, A., Hwang, H. C., Cicero, S., Donovan, S. L., Gurian-West, M., Johnson, D., . . . Roberts, J. M. (2007). Discovery of an oncogenic activity in p27Kip1 that causes stem cell expansion and a multiple tumor phenotype. *Genes Dev, 21*(14), 1731-1746. doi: 10.1101/gad.1556607

Bharti, A. C., & Aggarwal, B. B. (2002). Nuclear factor-kappa B and cancer: its role in prevention and therapy. *Biochem Pharmacol, 64*(5-6), 883-888.
Bhatia, M., Zemans, R. L., & Jeyaseelan, S. (2012). Role of chemokines in the pathogenesis of acute lung injury. *Am J Respir Cell Mol Biol, 46*(5), 566-572. doi: 10.1165/rcmb.2011-0392TR
Blatti, S. P., Foster, D. N., Ranganathan, G., Moses, H. L., & Getz, M. J. (1988). Induction of fibronectin gene transcription and mRNA is a primary response to growth-factor stimulation of AKR-2B cells. *Proc Natl Acad Sci U S A, 85*(4), 1119-1123.
Bobba, R. K., Holly, J. S., Loy, T., & Perry, M. C. (2011). Scar carcinoma of the lung: a historical perspective. *Clin Lung Cancer, 12*(3), 148-154. doi: 10.1016/j.cllc.2011.03.011
Boyer, A. S., Ayerinskas, II, Vincent, E. B., McKinney, L. A., Weeks, D. L., & Runyan, R. B. (1999). TGFbeta2 and TGFbeta3 have separate and sequential activities during epithelial-mesenchymal cell transformation in the embryonic heart. *Dev Biol, 208*(2), 530-545. doi: 10.1006/dbio.1999.9211
Boyerinas, B., Park, S. M., Hau, A., Murmann, A. E., & Peter, M. E. (2010). The role of let-7 in cell differentiation and cancer. *Endocr Relat Cancer, 17*(1), F19-36. doi: 10.1677/erc-09-0184
Bradfute, S. B., Graubert, T. A., & Goodell, M. A. (2005). Roles of Sca-1 in hematopoietic stem/progenitor cell function. *Exp Hematol, 33*(7), 836-843. doi: 10.1016/j.exphem.2005.04.001
Brockes, J. P., & Kumar, A. (2008). Comparative aspects of animal regeneration. *Annu Rev Cell Dev Biol, 24*, 525-549. doi: 10.1146/annurev.cellbio.24.110707.175336
Bucala, R., Spiegel, L. A., Chesney, J., Hogan, M., & Cerami, A. (1994). Circulating fibrocytes define a new leukocyte subpopulation that mediates tissue repair. *Mol Med, 1*(1), 71-81.
Buckpitt, A., Boland, B., Isbell, M., Morin, D., Shultz, M., Baldwin, R., . . . Plopper, C. (2002). Naphthalene-induced respiratory tract toxicity: metabolic mechanisms of toxicity. *Drug Metab Rev, 34*(4), 791-820. doi: 10.1081/dmr-120015694
Burgess, J. K. (2009). The role of the extracellular matrix and specific growth factors in the regulation of inflammation and remodelling in asthma. *Pharmacol Ther, 122*(1), 19-29. doi: 10.1016/j.pharmthera.2008.12.002
Callebert, J., Esteve, J. M., Herve, P., Peoc'h, K., Tournois, C., Drouet, L., . . . Maroteaux, L. (2006). Evidence for a control of plasma serotonin levels by 5-hydroxytryptamine(2B) receptors in mice. *J Pharmacol Exp Ther, 317*(2), 724-731. doi: 10.1124/jpet.105.098269
Campisi, J. (2005). Senescent cells, tumor suppression, and organismal aging: good citizens, bad neighbors. *Cell, 120*(4), 513-522. doi: 10.1016/j.cell.2005.02.003
Cardoso, Wellington V., & Lü, Jining. (2006). Regulation of early lung morphogenesis: questions, facts and controversies. *Development, 133*(9), 1611-1624.
Chambers, A. F. (1995). Steps in tumor metastasis: new concepts from intravital videomicroscopy. *Cancer Metastasis Rev., 14*, 279-301.
Chang, Y. F., Imam, J. S., & Wilkinson, M. F. (2007). The nonsense-mediated decay RNA surveillance pathway. *Annu Rev Biochem, 76*, 51-74. doi: 10.1146/annurev.biochem.76.050106.093909
Chen, Felicia, Desai, Tushar J., Qian, Jun, Niederreither, Karen, Lü, Jining, & Cardoso, Wellington V. (2007). Inhibition of Tgfβ signaling by endogenous retinoic acid is essential for primary lung bud induction. *Development, 134*(16), 2969-2979.
Chen, H., Matsumoto, K., Brockway, B. L., Rackley, C. R., Liang, J., Lee, J. H., . . . Stripp, B. R. (2012). Airway Epithelial Progenitors are Region-Specific and Show Differential Responses to Bleomycin-Induced Lung Injury. *Stem Cells*. doi: 10.1002/stem.1150
Chen, H., Matsumoto, K., & Stripp, B. R. (2009). Bronchiolar progenitor cells. *Proc Am Thorac Soc, 6*(7), 602-606. doi: 10.1513/pats.200907-078RM
Chen, W., Li, Z., Bai, L., & Lin, Y. (2011). NF-kappaB in lung cancer, a carcinogenesis mediator and a prevention and therapy target. *Front Biosci, 16*, 1172-1185.

Chilosi, M., Poletti, V., & Rossi, A. (2012). The pathogenesis of COPD and IPF: distinct horns of the same devil? *Respir Res, 13*, 3. doi: 10.1186/1465-9921-13-3

Chipuk, J. E., Kuwana, T., Bouchier-Hayes, L., Droin, N. M., Newmeyer, D. D., Schuler, M., & Green, D. R. (2004). Direct activation of Bax by p53 mediates mitochondrial membrane permeabilization and apoptosis. *Science, 303*(5660), 1010-1014. doi: 10.1126/science.1092734

Cho, M. I., Lin, W. L., & Genco, R. J. (1995). Platelet-derived growth factor-modulated guided tissue regenerative therapy. *J Periodontol, 66*(6), 522-530.

Colby, T. V. (1995). Malignancies in the lung and pleura mimicking benign processes. *Semin Diagn Pathol, 12*(1), 30-44.

Cole, B. B., Smith, R. W., Jenkins, K. M., Graham, B. B., Reynolds, P. R., & Reynolds, S. D. (2010). Tracheal Basal cells: a facultative progenitor cell pool. *Am J Pathol, 177*(1), 362-376. doi: 10.2353/ajpath.2010.090870

Colwell, A. S., Longaker, M. T., & Lorenz, H. P. (2003). Fetal wound healing. *Front Biosci, 8*, s1240-1248.

Conti, J. A., Kendall, T. J., Bateman, A., Armstrong, T. A., Papa-Adams, A., Xu, Q., . . . Iredale, J. P. (2008). The desmoplastic reaction surrounding hepatic colorectal adenocarcinoma metastases aids tumor growth and survival via alphav integrin ligation. *Clin Cancer Res, 14*(20), 6405-6413. doi: 10.1158/1078-0432.ccr-08-0816

Coppe, J. P., Patil, C. K., Rodier, F., Sun, Y., Munoz, D. P., Goldstein, J., . . . Campisi, J. (2008). Senescence-associated secretory phenotypes reveal cell-nonautonomous functions of oncogenic RAS and the p53 tumor suppressor. *PLoS Biol, 6*(12), 2853-2868. doi: 10.1371/journal.pbio.0060301

Costa, J. L. (1977). In situ observation of dense-body release from hydrated human platelets. *Biophys J, 19*(3), 307-313. doi: 10.1016/s0006-3495(77)85590-2

Cottam, D. R., Mattar, S. G., Barinas-Mitchell, E., Eid, G., Kuller, L., Kelley, D. E., & Schauer, P. R. (2004). The chronic inflammatory hypothesis for the morbidity associated with morbid obesity: implications and effects of weight loss. *Obes Surg, 14*(5), 589-600. doi: 10.1381/096089204323093345

Cristofalo, V. J., & Pignolo, R. J. (1993). Replicative senescence of human fibroblast-like cells in culture. *Physiol Rev, 73*(3), 617-638.

Crosby, L. M., & Waters, C. M. (2010). Epithelial repair mechanisms in the lung. *Am J Physiol Lung Cell Mol Physiol, 298*(6), L715-731. doi: 10.1152/ajplung.00361.2009

Curtis, S. J., Sinkevicius, K. W., Li, D., Lau, A. N., Roach, R. R., Zamponi, R., . . . Kim, C. F. (2010). Primary tumor genotype is an important determinant in identification of lung cancer propagating cells. *Cell Stem Cell, 7*(1), 127-133. doi: 10.1016/j.stem.2010.05.021

Derynck, Rik, & Zhang, Ying E. (2003). Smad-dependent and Smad-independent pathways in TGF-[beta] family signalling. *Nature, 425*(6958), 577-584.

Diaz, S. L., & Maroteaux, L. (2011). Implication of 5-HT(2B) receptors in the serotonin syndrome. *Neuropharmacology, 61*(3), 495-502. doi: 10.1016/j.neuropharm.2011.01.025

Ding, B. S., Nolan, D. J., Guo, P., Babazadeh, A. O., Cao, Z., Rosenwaks, Z., . . . Rafii, S. (2011). Endothelial-derived angiocrine signals induce and sustain regenerative lung alveolarization. *Cell, 147*(3), 539-553. doi: 10.1016/j.cell.2011.10.003

Dolberg, D. S., Hollingsworth, R., Hertle, M., & Bissell, M. J. (1985). Wounding and its role in RSV-mediated tumor formation. *Science, 230*(4726), 676-678.

Dong, P., Karaayvaz, M., Jia, N., Kaneuchi, M., Hamada, J., Watari, H., . . . Sakuragi, N. (2012). Mutant p53 gain-of-function induces epithelial-mesenchymal transition through modulation of the miR-130b-ZEB1 axis. *Oncogene*. doi: 10.1038/onc.2012.334

Dong, P., Tada, M., Hamada, J., Nakamura, A., Moriuchi, T., & Sakuragi, N. (2007). p53 dominant-negative mutant R273H promotes invasion and migration of human endometrial cancer HHUA cells. *Clin Exp Metastasis, 24*(6), 471-483. doi: 10.1007/s10585-007-9084-8

Duan, W., Ding, H., Subler, M. A., Zhu, W. G., Zhang, H., Stoner, G. D., . . . Villalona-Calero, M. A. (2002). Lung-specific expression of human mutant p53-273H is associated with a high frequency of lung adenocarcinoma in transgenic mice. *Oncogene, 21*(51), 7831-7838. doi: 10.1038/sj.onc.1205909

Duong, H. T., Erzurum, S. C., & Asosingh, K. (2011). Pro-angiogenic hematopoietic progenitor cells and endothelial colony-forming cells in pathological angiogenesis of bronchial and pulmonary circulation. *Angiogenesis, 14*(4), 411-422. doi: 10.1007/s10456-011-9228-y

Dupuit, F., Gaillard, D., Hinnrasky, J., Mongodin, E., de Bentzmann, S., Copreni, E., & Puchelle, E. (2000). Differentiated and functional human airway epithelium regeneration in tracheal xenografts. *Am J Physiol Lung Cell Mol Physiol, 278*(1), L165-176.

Dvorak, H. F. (1986). Tumors: wounds that do not heal. Similarities between tumor stroma generation and wound healing. *N Engl J Med, 315*(26), 1650-1659. doi: 10.1056/nejm198612253152606

Ebrahimkhani, M. R., Oakley, F., Murphy, L. B., Mann, J., Moles, A., Perugorria, M. J., . . . Mann, D. A. (2011). Stimulating healthy tissue regeneration by targeting the 5-HT(2)B receptor in chronic liver disease. *Nat Med, 17*(12), 1668-1673. doi: 10.1038/nm.2490

Egeblad, M., Nakasone, E. S., & Werb, Z. (2010). Tumors as organs: complex tissues that interface with the entire organism. *Dev Cell, 18*(6), 884-901. doi: 10.1016/j.devcel.2010.05.012

Eming, S. A., Hammerschmidt, M., Krieg, T., & Roers, A. (2009). Interrelation of immunity and tissue repair or regeneration. *Semin Cell Dev Biol, 20*(5), 517-527. doi: 10.1016/j.semcdb.2009.04.009

Evans, Martin. (2011). Discovering pluripotency: 30 years of mouse embryonic stem cells. *Nat Rev Mol Cell Biol, 12*(10), 680-686.

Farh, K. K., Grimson, A., Jan, C., Lewis, B. P., Johnston, W. K., Lim, L. P., . . . Bartel, D. P. (2005). The widespread impact of mammalian MicroRNAs on mRNA repression and evolution. *Science, 310*(5755), 1817-1821. doi: 10.1126/science.1121158

Ferbeyre, G., de Stanchina, E., Lin, A. W., Querido, E., McCurrach, M. E., Hannon, G. J., & Lowe, S. W. (2002). Oncogenic ras and p53 cooperate to induce cellular senescence. *Mol Cell Biol, 22*(10), 3497-3508.

Forbes, I. T., Jones, G. E., Murphy, O. E., Holland, V., & Baxter, G. S. (1995). N-(1-methyl-5-indolyl)-N'-(3-methyl-5-isothiazolyl)urea: a novel, high-affinity 5-HT2B receptor antagonist. *J Med Chem, 38*(6), 855-857.

Freund, A., Patil, C. K., & Campisi, J. (2011). p38MAPK is a novel DNA damage response-independent regulator of the senescence-associated secretory phenotype. *EMBO J, 30*(8), 1536-1548. doi: 10.1038/emboj.2011.69

Fuchs, E. (2009). The tortoise and the hair: slow-cycling cells in the stem cell race. *Cell, 137*(5), 811-819. doi: 10.1016/j.cell.2009.05.002

Funakoshi, N. (2000). A new model of lung metastasis for intravital studies. *Microvasc. Res., 59*, 361-367.

Garofalo, M., Romano, G., Di Leva, G., Nuovo, G., Jeon, Y. J., Ngankeu, A., . . . Croce, C. M. (2012). EGFR and MET receptor tyrosine kinase-altered microRNA expression induces tumorigenesis and gefitinib resistance in lung cancers. *Nat Med, 18*(1), 74-82. doi: 10.1038/nm.2577

Gavins, F. N., & Chatterjee, B. E. (2004). Intravital microscopy for the study of mouse microcirculation in anti-inflammatory drug research: focus on the mesentery and cremaster preparations. *J Pharmacol Toxicol Methods, 49*(1), 1-14. doi: 10.1016/s1056-8719(03)00057-1

Ghanei, M., & Harandi, A. A. (2011). Molecular and cellular mechanism of lung injuries due to exposure to sulfur mustard: a review. *Inhal Toxicol, 23*(7), 363-371. doi: 10.3109/08958378.2011.576278

Gharaee-Kermani, M., Gyetko, M. R., Hu, B., & Phan, S. H. (2007). New insights into the pathogenesis and treatment of idiopathic pulmonary fibrosis: a potential role for stem cells in the lung parenchyma and implications for therapy. *Pharm Res, 24*(5), 819-841. doi: 10.1007/s11095-006-9216-x

Giangreco, A., Arwert, E. N., Rosewell, I. R., Snyder, J., Watt, F. M., & Stripp, B. R. (2009). Stem cells are dispensable for lung homeostasis but restore airways after injury. *Proc Natl Acad Sci U S A, 106*(23), 9286-9291. doi: 10.1073/pnas.0900668106

Giangreco, A., Reynolds, S. D., & Stripp, B. R. (2002). Terminal bronchioles harbor a unique airway stem cell population that localizes to the bronchoalveolar duct junction. *Am J Pathol, 161*(1), 173-182. doi: 10.1016/s0002-9440(10)64169-7

Gilbert, L. A., & Hemann, M. T. (2010). DNA damage-mediated induction of a chemoresistant niche. *Cell, 143*(3), 355-366. doi: 10.1016/j.cell.2010.09.043

Gilmore, T. D. (2006). Introduction to NF-kappaB: players, pathways, perspectives. *Oncogene, 25*(51), 6680-6684. doi: 10.1038/sj.onc.1209954

Godwin, J. W., & Brockes, J. P. (2006). Regeneration, tissue injury and the immune response. *J Anat, 209*(4), 423-432. doi: 10.1111/j.1469-7580.2006.00626.x

Gomes, L. R., Terra, L. F., Sogayar, M. C., & Labriola, L. (2011). Epithelial-mesenchymal transition: implications in cancer progression and metastasis. *Curr Pharm Biotechnol, 12*(11), 1881-1890.

Gommans, J., Hijzen, T. H., Maes, R. A., & Olivier, B. (1998). Discriminative stimulus properties of mCPP: evidence for a 5-HT2C receptor mode of action. *Psychopharmacology (Berl), 137*(3), 292-302.

Gomperts, B. N., & Strieter, R. M. (2007). Fibrocytes in lung disease. *J Leukoc Biol, 82*(3), 449-456. doi: 10.1189/jlb.0906587

Griffiths-Jones, S., Grocock, R. J., van Dongen, S., Bateman, A., & Enright, A. J. (2006). miRBase: microRNA sequences, targets and gene nomenclature. *Nucleic Acids Res, 34*(Database issue), D140-144. doi: 10.1093/nar/gkj112

Grinnell, F. (1984). Fibronectin and wound healing. *J Cell Biochem, 26*(2), 107-116. doi: 10.1002/jcb.240260206

Grisham, M. B., Jourd'heuil, D., & Wink, D. A. (2000). Review article: chronic inflammation and reactive oxygen and nitrogen metabolism--implications in DNA damage and mutagenesis. *Aliment Pharmacol Ther, 14 Suppl 1*, 3-9.

Haigis, K. M., Wistuba, II, & Kurie, J. M. (2007). Lung premalignancy induced by mutant B-Raf, what is thy fate? To senesce or not to senesce, that is the question. *Genes Dev, 21*(4), 361-366. doi: 10.1101/gad.1532107

Hak, S., Reitan, N. K., Haraldseth, O., & de Lange Davies, C. (2010). Intravital microscopy in window chambers: a unique tool to study tumor angiogenesis and delivery of nanoparticles. *Angiogenesis, 13*(2), 113-130. doi: 10.1007/s10456-010-9176-y

Hayflick, L., & Moorhead, P. S. (1961). The serial cultivation of human diploid cell strains. *Exp Cell Res, 25*, 585-621.

Herzog, E. L., & Krause, D. S. (2006). Engraftment of marrow-derived epithelial cells: the role of fusion. *Proc Am Thorac Soc, 3*(8), 691-695. doi: 10.1513/pats.200605-109SF

Herzog, E. L., Van Arnam, J., Hu, B., & Krause, D. S. (2006). Threshold of lung injury required for the appearance of marrow-derived lung epithelia. *Stem Cells, 24*(8), 1986-1992. doi: 10.1634/stemcells.2005-0579

Hingorani, S. R., Wang, L., Multani, A. S., Combs, C., Deramaudt, T. B., Hruban, R. H., . . . Tuveson, D. A. (2005). Trp53R172H and KrasG12D cooperate to promote chromosomal instability and widely metastatic pancreatic ductal adenocarcinoma in mice. *Cancer Cell, 7*(5), 469-483. doi: 10.1016/j.ccr.2005.04.023

Hombach-Klonisch, S., Panigrahi, S., Rashedi, I., Seifert, A., Alberti, E., Pocar, P., . . . Los, M. (2008). Adult stem cells and their trans-differentiation potential--perspectives and therapeutic applications. *J Mol Med (Berl), 86*(12), 1301-1314. doi: 10.1007/s00109-008-0383-6

Hong, K. U., Reynolds, S. D., Giangreco, A., Hurley, C. M., & Stripp, B. R. (2001). Clara cell secretory protein-expressing cells of the airway neuroepithelial body microenvironment include a label-

retaining subset and are critical for epithelial renewal after progenitor cell depletion. *Am J Respir Cell Mol Biol, 24*(6), 671-681.
Hong, K. U., Reynolds, S. D., Watkins, S., Fuchs, E., & Stripp, B. R. (2004a). Basal cells are a multipotent progenitor capable of renewing the bronchial epithelium. *Am J Pathol, 164*(2), 577-588. doi: 10.1016/s0002-9440(10)63147-1
Hong, K. U., Reynolds, S. D., Watkins, S., Fuchs, E., & Stripp, B. R. (2004b). In vivo differentiation potential of tracheal basal cells: evidence for multipotent and unipotent subpopulations. *Am J Physiol Lung Cell Mol Physiol, 286*(4), L643-649. doi: 10.1152/ajplung.00155.2003
Howe, E. N., Cochrane, D. R., & Richer, J. K. (2012). The miR-200 and miR-221/222 microRNA families: opposing effects on epithelial identity. *J Mammary Gland Biol Neoplasia, 17*(1), 65-77. doi: 10.1007/s10911-012-9244-6
Hu, B., Wu, Z., & Phan, S. H. (2003). Smad3 mediates transforming growth factor-beta-induced alpha-smooth muscle actin expression. *Am J Respir Cell Mol Biol, 29*(3 Pt 1), 397-404. doi: 10.1165/rcmb.2003-0063OC
Huntriss, J. D., Hemmings, K. E., Hinkins, M., Rutherford, A. J., Sturmey, R. G., Elder, K., & Picton, H. M. (2012). Variable imprinting of the MEST gene in human preimplantation embryos. *Eur J Hum Genet*. doi: 10.1038/ejhg.2012.102
Hurd, Suzanne. (2000). The Impact of COPD on Lung Health Worldwide*Epidemiology and Incidence. *CHEST Journal, 117*(2_suppl), 1S-4S.
Idiopathic Pulmonary Fibrosis: Diagnosis and Treatment. (2000). *American Journal of Respiratory and Critical Care Medicine, 161*(2), 646-664.
Jackson, E. L., Willis, N., Mercer, K., Bronson, R. T., Crowley, D., Montoya, R., . . . Tuveson, D. A. (2001). Analysis of lung tumor initiation and progression using conditional expression of oncogenic K-ras. *Genes Dev, 15*(24), 3243-3248. doi: 10.1101/gad.943001
Jemal, Ahmedin, Bray, Freddie, Center, Melissa M., Ferlay, Jacques, Ward, Elizabeth, & Forman, David. (2011). Global cancer statistics. *CA: A Cancer Journal for Clinicians, 61*(2), 69-90.
Jones, C. P., & Rankin, S. M. (2011). Bone marrow-derived stem cells and respiratory disease. *Chest, 140*(1), 205-211. doi: 10.1378/chest.10-2348
Kajstura, J., Rota, M., Hall, S. R., Hosoda, T., D'Amario, D., Sanada, F., . . . Anversa, P. (2011). Evidence for human lung stem cells. *N Engl J Med, 364*(19), 1795-1806. doi: 10.1056/NEJMoa1101324
Kalinichenko, V. V., Lim, L., Stolz, D. B., Shin, B., Rausa, F. M., Clark, J., . . . Costa, R. H. (2001). Defects in pulmonary vasculature and perinatal lung hemorrhage in mice heterozygous null for the Forkhead Box f1 transcription factor. *Dev Biol, 235*(2), 489-506. doi: 10.1006/dbio.2001.0322
Kalluri, R., & Weinberg, R. A. (2009). The basics of epithelial-mesenchymal transition. *J Clin Invest, 119*(6), 1420-1428. doi: 10.1172/jci39104
Kefaloyianni, E., Gaitanaki, C., & Beis, I. (2006). ERK1/2 and p38-MAPK signalling pathways, through MSK1, are involved in NF-kappaB transactivation during oxidative stress in skeletal myoblasts. *Cell Signal, 18*(12), 2238-2251. doi: 10.1016/j.cellsig.2006.05.004
Kelly, M. (2002). Pathophysiology of COPD. *Thorax, 57*(6), 563-564.
Kennett, G. A., Wood, M. D., Bright, F., Cilia, J., Piper, D. C., Gager, T., . . . Blackburn, T. P. (1996). In vitro and in vivo profile of SB 206553, a potent 5-HT2C/5-HT2B receptor antagonist with anxiolytic-like properties. *Br J Pharmacol, 117*(3), 427-434.
Kida, H., Mucenski, M. L., Thitoff, A. R., Le Cras, T. D., Park, K. S., Ikegami, M., . . . Whitsett, J. A. (2008). GP130-STAT3 regulates epithelial cell migration and is required for repair of the bronchiolar epithelium. *Am J Pathol, 172*(6), 1542-1554. doi: 10.2353/ajpath.2008.071052
Kim, C. F., & Dirks, P. B. (2008). Cancer and stem cell biology: how tightly intertwined? *Cell Stem Cell, 3*(2), 147-150. doi: 10.1016/j.stem.2008.07.012

Kim, C. F., Jackson, E. L., Woolfenden, A. E., Lawrence, S., Babar, I., Vogel, S., . . . Jacks, T. (2005). Identification of bronchioalveolar stem cells in normal lung and lung cancer. *Cell, 121*(6), 823-835. doi: 10.1016/j.cell.2005.03.032

Kim, Jeong Beom, Zaehres, Holm, Wu, Guangming, Gentile, Luca, Ko, Kinarm, Sebastiano, Vittorio, . . . Scholer, Hans R. (2008). Pluripotent stem cells induced from adult neural stem cells by reprogramming with two factors. *Nature, 454*(7204), 646-650. doi: http://www.nature.com/nature/journal/v454/n7204/suppinfo/nature07061_S1.html

Kim, K. K., Kugler, M. C., Wolters, P. J., Robillard, L., Galvez, M. G., Brumwell, A. N., . . . Chapman, H. A. (2006). Alveolar epithelial cell mesenchymal transition develops in vivo during pulmonary fibrosis and is regulated by the extracellular matrix. *Proc Natl Acad Sci U S A, 103*(35), 13180-13185. doi: 10.1073/pnas.0605669103

Kimber, S. J., Sneddon, S. F., Bloor, D. J., El-Bareg, A. M., Hawkhead, J. A., Metcalfe, A. D., . . . Brison, D. R. (2008). Expression of genes involved in early cell fate decisions in human embryos and their regulation by growth factors. *Reproduction, 135*(5), 635-647. doi: 10.1530/rep-07-0359

King, T. E., Jr., Schwarz, M. I., Brown, K., Tooze, J. A., Colby, T. V., Waldron, J. A., Jr., . . . Cherniack, R. M. (2001). Idiopathic pulmonary fibrosis: relationship between histopathologic features and mortality. *Am J Respir Crit Care Med, 164*(6), 1025-1032.

Konigshoff, M., Dumitrascu, R., Udalov, S., Amarie, O. V., Reiter, R., Grimminger, F., . . . Eickelberg, O. (2010). Increased expression of 5-hydroxytryptamine2A/B receptors in idiopathic pulmonary fibrosis: a rationale for therapeutic intervention. *Thorax, 65*(11), 949-955. doi: 10.1136/thx.2009.134353

Krause, D. S. (2008). Bone marrow-derived lung epithelial cells. *Proc Am Thorac Soc, 5*(6), 699-702. doi: 10.1513/pats.200803-031AW

Krizhanovsky, V., Xue, W., Zender, L., Yon, M., Hernando, E., & Lowe, S. W. (2008). Implications of cellular senescence in tissue damage response, tumor suppression, and stem cell biology. *Cold Spring Harb Symp Quant Biol, 73*, 513-522. doi: 10.1101/sqb.2008.73.048

Krizhanovsky, V., Yon, M., Dickins, R. A., Hearn, S., Simon, J., Miething, C., . . . Lowe, S. W. (2008). Senescence of activated stellate cells limits liver fibrosis. *Cell, 134*(4), 657-667. doi: 10.1016/j.cell.2008.06.049

Kruse, J. P., & Gu, W. (2009). Modes of p53 regulation. *Cell, 137*(4), 609-622. doi: 10.1016/j.cell.2009.04.050

Kuilman, T., Michaloglou, C., Mooi, W. J., & Peeper, D. S. (2010). The essence of senescence. *Genes Dev, 24*(22), 2463-2479. doi: 10.1101/gad.1971610

Kumar, M. S., Hancock, D. C., Molina-Arcas, M., Steckel, M., East, P., Diefenbacher, M., . . . Downward, J. (2012). The GATA2 transcriptional network is requisite for RAS oncogene-driven non-small cell lung cancer. *Cell, 149*(3), 642-655. doi: 10.1016/j.cell.2012.02.059

Laiho, M., DeCaprio, J. A., Ludlow, J. W., Livingston, D. M., & Massague, J. (1990). Growth inhibition by TGF-beta linked to suppression of retinoblastoma protein phosphorylation. *Cell, 62*(1), 175-185.

Lama, V. N., Smith, L., Badri, L., Flint, A., Andrei, A. C., Murray, S., . . . Thannickal, V. J. (2007). Evidence for tissue-resident mesenchymal stem cells in human adult lung from studies of transplanted allografts. *J Clin Invest, 117*(4), 989-996. doi: 10.1172/jci29713

Lau, W. K., Chan-Yeung, M. M., Yip, B. H., Cheung, A. H., Ip, M. S., & Mak, J. C. (2012). The role of circulating serotonin in the development of chronic obstructive pulmonary disease. *PLoS One, 7*(2), e31617. doi: 10.1371/journal.pone.0031617

Launay, J. M., Herve, P., Peoc'h, K., Tournois, C., Callebert, J., Nebigil, C. G., . . . Maroteaux, L. (2002). Function of the serotonin 5-hydroxytryptamine 2B receptor in pulmonary hypertension. *Nat Med, 8*(10), 1129-1135. doi: 10.1038/nm764

Lauweryns, J. M., de Bock, V., Verhofstad, A. A., & Steinbusch, H. W. (1982). Immunohistochemical localization of serotonin in intrapulmonary neuro-epithelial bodies. *Cell Tissue Res, 226*(1), 215-223.

Lawrence, W. T. (1998). Physiology of the acute wound. *Clin Plast Surg, 25*(3), 321-340.

Lee, Hong-Lyeol, Ryu, Jay H., Wittmer, Michael H., Hartman, Thomas E., Lymp, James F., Tazelaar, Henry D., & Limper, Andrew H. (2005). Familial Idiopathic Pulmonary Fibrosis*Clinical Features and Outcome. *CHEST Journal, 127*(6), 2034-2041. doi: 10.1378/chest.127.6.2034

Lengner, C. J., Camargo, F. D., Hochedlinger, K., Welstead, G. G., Zaidi, S., Gokhale, S., . . . Jaenisch, R. (2007). Oct4 expression is not required for mouse somatic stem cell self-renewal. *Cell Stem Cell, 1*(4), 403-415. doi: 10.1016/j.stem.2007.07.020

Lengner, C. J., Welstead, G. G., & Jaenisch, R. (2008). The pluripotency regulator Oct4: a role in somatic stem cells? *Cell Cycle, 7*(6), 725-728.

Lewis, M. P., Lygoe, K. A., Nystrom, M. L., Anderson, W. P., Speight, P. M., Marshall, J. F., & Thomas, G. J. (2004). Tumour-derived TGF-beta1 modulates myofibroblast differentiation and promotes HGF/SF-dependent invasion of squamous carcinoma cells. *Br J Cancer, 90*(4), 822-832. doi: 10.1038/sj.bjc.6601611

Li, B., Zhang, S., Li, M., Hertz, L., & Peng, L. (2010). Serotonin increases ERK1/2 phosphorylation in astrocytes by stimulation of 5-HT2B and 5-HT2C receptors. *Neurochem Int, 57*(4), 432-439. doi: 10.1016/j.neuint.2010.04.017

Li, L., & Clevers, H. (2010). Coexistence of quiescent and active adult stem cells in mammals. *Science, 327*(5965), 542-545. doi: 10.1126/science.1180794

Li, T., Kon, N., Jiang, L., Tan, M., Ludwig, T., Zhao, Y., . . . Gu, W. (2012). Tumor suppression in the absence of p53-mediated cell-cycle arrest, apoptosis, and senescence. *Cell, 149*(6), 1269-1283. doi: 10.1016/j.cell.2012.04.026

Li, X., Wang, J., Xu, Z., Ahmad, A., Li, E., Wang, Y., . . . Wang, Q. (2012). Expression of sox2 and oct4 and their clinical significance in human non-small-cell lung cancer. *Int J Mol Sci, 13*(6), 7663-7675. doi: 10.3390/ijms13067663

Li, Y., & Prives, C. (2007). Are interactions with p63 and p73 involved in mutant p53 gain of oncogenic function? *Oncogene, 26*(15), 2220-2225. doi: 10.1038/sj.onc.1210311

Ling, T. Y., Kuo, M. D., Li, C. L., Yu, A. L., Huang, Y. H., Wu, T. J., . . . Yu, J. (2006). Identification of pulmonary Oct-4+ stem/progenitor cells and demonstration of their susceptibility to SARS coronavirus (SARS-CoV) infection in vitro. *Proc Natl Acad Sci U S A, 103*(25), 9530-9535. doi: 10.1073/pnas.0510232103

Little, Marie-Terese, & Storb, Rainer. (2002). History of haematopoietic stem-cell transplantation. *Nat Rev Cancer, 2*(3), 231-238.

Liu, Y., Sadikot, R. T., Adami, G. R., Kalinichenko, V. V., Pendyala, S., Natarajan, V., . . . Malik, A. B. (2011). FoxM1 mediates the progenitor function of type II epithelial cells in repairing alveolar injury induced by Pseudomonas aeruginosa. *J Exp Med, 208*(7), 1473-1484. doi: 10.1084/jem.20102041

Mackie, E. J., Halfter, W., & Liverani, D. (1988). Induction of tenascin in healing wounds. *J Cell Biol, 107*(6 Pt 2), 2757-2767.

Maeda, Yutaka, Davé, Vrushank, & Whitsett, Jeffrey A. (2007). Transcriptional Control of Lung Morphogenesis. *Physiological Reviews, 87*(1), 219-244.

Mani, S. A., Guo, W., Liao, M. J., Eaton, E. N., Ayyanan, A., Zhou, A. Y., . . . Weinberg, R. A. (2008). The epithelial-mesenchymal transition generates cells with properties of stem cells. *Cell, 133*(4), 704-715. doi: 10.1016/j.cell.2008.03.027

Marcel, V., Dichtel-Danjoy, M. L., Sagne, C., Hafsi, H., Ma, D., Ortiz-Cuaran, S., . . . Bourdon, J. C. (2011). Biological functions of p53 isoforms through evolution: lessons from animal and cellular models. *Cell Death Differ, 18*(12), 1815-1824. doi: 10.1038/cdd.2011.120

Marhaba, R., Klingbeil, P., Nuebel, T., Nazarenko, I., Buechler, M. W., & Zoeller, M. (2008). CD44 and EpCAM: cancer-initiating cell markers. *Curr Mol Med, 8*(8), 784-804.

Matsuda, A., Suzuki, Y., Honda, G., Muramatsu, S., Matsuzaki, O., Nagano, Y., . . . Sugano, S. (2003). Large-scale identification and characterization of human genes that activate NF-kappaB and MAPK signaling pathways. *Oncogene, 22*(21), 3307-3318. doi: 10.1038/sj.onc.1206406

McClatchey, A. I., & Yap, A. S. (2012). Contact inhibition (of proliferation) redux. *Curr Opin Cell Biol*. doi: 10.1016/j.ceb.2012.06.009

McDuff, F. K., & Turner, S. D. (2011). Jailbreak: oncogene-induced senescence and its evasion. *Cell Signal, 23*(1), 6-13. doi: 10.1016/j.cellsig.2010.07.004

McQualter, J. L., Brouard, N., Williams, B., Baird, B. N., Sims-Lucas, S., Yuen, K., . . . Bertoncello, I. (2009). Endogenous fibroblastic progenitor cells in the adult mouse lung are highly enriched in the sca-1 positive cell fraction. *Stem Cells, 27*(3), 623-633. doi: 10.1634/stemcells.2008-0866

Medrano, S., Monteagudo, M. C., Sequeira-Lopez, M. L., Pentz, E. S., & Gomez, R. A. (2012). Two microRNAs, miR-330 and miR-125b-5p, mark the juxtaglomerular cell and balance its smooth muscle phenotype. *Am J Physiol Renal Physiol, 302*(1), F29-37. doi: 10.1152/ajprenal.00460.2011

Meylan, E., Dooley, A. L., Feldser, D. M., Shen, L., Turk, E., Ouyang, C., & Jacks, T. (2009). Requirement for NF-kappaB signalling in a mouse model of lung adenocarcinoma. *Nature, 462*(7269), 104-107. doi: 10.1038/nature08462

Minoo, P., Su, G., Drum, H., Bringas, P., & Kimura, S. (1999). Defects in tracheoesophageal and lung morphogenesis in Nkx2.1(-/-) mouse embryos. *Dev Biol, 209*(1), 60-71. doi: 10.1006/dbio.1999.9234

Monaco, J. L., & Lawrence, W. T. (2003). Acute wound healing an overview. *Clin Plast Surg, 30*(1), 1-12.

Morgensztern, D., & McLeod, H. L. (2005). PI3K/Akt/mTOR pathway as a target for cancer therapy. *Anticancer Drugs, 16*(8), 797-803.

Morrisey, E. E., & Hogan, B. L. (2010). Preparing for the first breath: genetic and cellular mechanisms in lung development. *Dev Cell, 18*(1), 8-23. doi: 10.1016/j.devcel.2009.12.010

Muller, P. A., Caswell, P. T., Doyle, B., Iwanicki, M. P., Tan, E. H., Karim, S., . . . Vousden, K. H. (2009). Mutant p53 drives invasion by promoting integrin recycling. *Cell, 139*(7), 1327-1341. doi: 10.1016/j.cell.2009.11.026

Munger, J. S., Huang, X., Kawakatsu, H., Griffiths, M. J., Dalton, S. L., Wu, J., . . . Sheppard, D. (1999). The integrin alpha v beta 6 binds and activates latent TGF beta 1: a mechanism for regulating pulmonary inflammation and fibrosis. *Cell, 96*(3), 319-328.

Murray, P. J., & Wynn, T. A. (2011). Protective and pathogenic functions of macrophage subsets. *Nat Rev Immunol, 11*(11), 723-737. doi: 10.1038/nri3073

Nagaoka, T., Kaburagi, Y., Hamaguchi, Y., Hasegawa, M., Takehara, K., Steeber, D. A., . . . Sato, S. (2000). Delayed wound healing in the absence of intercellular adhesion molecule-1 or L-selectin expression. *Am J Pathol, 157*(1), 237-247. doi: 10.1016/s0002-9440(10)64534-8

Nanney, L. B., Magid, M., Stoscheck, C. M., & King, L. E., Jr. (1984). Comparison of epidermal growth factor binding and receptor distribution in normal human epidermis and epidermal appendages. *J Invest Dermatol, 83*(5), 385-393.

Navaratnam, V., Fleming, K. M., West, J., Smith, C. J., Jenkins, R. G., Fogarty, A., & Hubbard, R. B. (2011). The rising incidence of idiopathic pulmonary fibrosis in the U.K. *Thorax, 66*(6), 462-467. doi: 10.1136/thx.2010.148031

Nawshad, A., LaGamba, D., & Hay, E. D. (2004). Transforming growth factor beta (TGFbeta) signalling in palatal growth, apoptosis and epithelial mesenchymal transformation (EMT). *Arch Oral Biol, 49*(9), 675-689. doi: 10.1016/j.archoralbio.2004.05.007

Nielson, E. G., Phillips, S. M., & Jimenez, S. (1982). Lymphokine modulation of fibroblast proliferation. *J Immunol, 128*(3), 1484-1486.

Nimni, M. E. (1974). Collagen: Its structure and function in normal and pathological connective tissues. *Semin Arthritis Rheum, 4*(2), 95-150.

Nolen-Walston, R. D., Kim, C. F., Mazan, M. R., Ingenito, E. P., Gruntman, A. M., Tsai, L., . . . Hoffman, A. M. (2008). Cellular kinetics and modeling of bronchioalveolar stem cell response during lung regeneration. *Am J Physiol Lung Cell Mol Physiol, 294*(6), L1158-1165. doi: 10.1152/ajplung.00298.2007

Olive, K. P., Tuveson, D. A., Ruhe, Z. C., Yin, B., Willis, N. A., Bronson, R. T., . . . Jacks, T. (2004). Mutant p53 gain of function in two mouse models of Li-Fraumeni syndrome. *Cell, 119*(6), 847-860. doi: 10.1016/j.cell.2004.11.004

Ortiz, Luis A., Gambelli, Frederica, McBride, Christine, Gaupp, Dina, Baddoo, Melody, Kaminski, Naftali, & Phinney, Donald G. (2003). Mesenchymal stem cell engraftment in lung is enhanced in response to bleomycin exposure and ameliorates its fibrotic effects. *Proceedings of the National Academy of Sciences, 100*(14), 8407-8411.

Otrock, Z. K., Mahfouz, R. A., Makarem, J. A., & Shamseddine, A. I. (2007). Understanding the biology of angiogenesis: review of the most important molecular mechanisms. *Blood Cells Mol Dis, 39*(2), 212-220. doi: 10.1016/j.bcmd.2007.04.001

Pacheco-Pinedo, E. C., Durham, A. C., Stewart, K. M., Goss, A. M., Lu, M. M., Demayo, F. J., & Morrisey, E. E. (2011). Wnt/beta-catenin signaling accelerates mouse lung tumorigenesis by imposing an embryonic distal progenitor phenotype on lung epithelium. *J Clin Invest, 121*(5), 1935-1945. doi: 10.1172/jci44871

Padera, T. P., Stoll, B. R., So, P. T. C., & Jain, R. K. (2002). High-speed intravital multiphoton laser scanning microscopy of microvasculature, lymphatics, and leukocyte-endothelial interactions. *Mol. Imaging, 1*, 9-15.

Papetti, Michael, & Herman, Ira M. (2002). Mechanisms of normal and tumor-derived angiogenesis. *American Journal of Physiology - Cell Physiology, 282*(5), C947-C970.

Parimon, T., Chien, J. W., Bryson, C. L., McDonell, M. B., Udris, E. M., & Au, D. H. (2007). Inhaled corticosteroids and risk of lung cancer among patients with chronic obstructive pulmonary disease. *Am J Respir Crit Care Med, 175*(7), 712-719. doi: 10.1164/rccm.200608-1125OC

Pazolli, E., & Stewart, S. A. (2008). Senescence: the good the bad and the dysfunctional. *Curr Opin Genet Dev, 18*(1), 42-47. doi: 10.1016/j.gde.2007.12.002

Pei, X. H., Bai, F., Smith, M. D., & Xiong, Y. (2007). p18Ink4c collaborates with Men1 to constrain lung stem cell expansion and suppress non-small-cell lung cancers. *Cancer Res, 67*(7), 3162-3170. doi: 10.1158/0008-5472.can-06-4517

Phan, S. H. (2002). The myofibroblast in pulmonary fibrosis. *Chest, 122*(6 Suppl), 286S-289S.

Phan, S. H. (2012). Genesis of the myofibroblast in lung injury and fibrosis. *Proc Am Thorac Soc, 9*(3), 148-152. doi: 10.1513/pats.201201-011AW

Pillai, R. S. (2005). MicroRNA function: multiple mechanisms for a tiny RNA? *RNA, 11*(12), 1753-1761. doi: 10.1261/rna.2248605

Plichta, J. K., & Radek, K. A. (2012). Sugar-coating wound repair: a review of FGF-10 and dermatan sulfate in wound healing and their potential application in burn wounds. *J Burn Care Res, 33*(3), 299-310. doi: 10.1097/BCR.0b013e318240540a

Plouet, J., Schilling, J., & Gospodarowicz, D. (1989). Isolation and characterization of a newly identified endothelial cell mitogen produced by AtT-20 cells. *EMBO J, 8*(12), 3801-3806.

Png, K. J., Yoshida, M., Zhang, X. H., Shu, W., Lee, H., Rimner, A., . . . Tavazoie, S. F. (2011). MicroRNA-335 inhibits tumor reinitiation and is silenced through genetic and epigenetic mechanisms in human breast cancer. *Genes Dev, 25*(3), 226-231. doi: 10.1101/gad.1974211

Premsrirut, Prem K, Dow, Lukas E, Kim, Sang Yong, Camiolo, Matthew, Malone, Colin D, Miething, Cornelius, . . . Lowe, Scott W. (2011). A Rapid and Scalable System for Studying Gene Function in Mice Using Conditional RNA Interference. *Cell, 145*(1), 145-158. doi: 10.1016/j.cell.2011.03.012

Punturieri, Antonello, Szabo, Eva, Croxton, Thomas L., Shapiro, Steven D., & Dubinett, Steven M. (2009). Lung Cancer and Chronic Obstructive Pulmonary Disease: Needs and Opportunities for Integrated Research. *Journal of the National Cancer Institute, 101*(8), 554-559.

Raghu, Ganesh, Weycker, Derek, Edelsberg, John, Bradford, Williamson Z., & Oster, Gerry. (2006). Incidence and Prevalence of Idiopathic Pulmonary Fibrosis. *American Journal of Respiratory and Critical Care Medicine, 174*(7), 810-816.

Raiser, D. M., & Kim, C. F. (2009). Commentary: Sca-1 and Cells of the Lung: A matter of Different Sorts. *Stem Cells, 27*(3), 606-611. doi: 10.1002/stem.10

Raiser, D. M., Zacharek, S. J., Roach, R. R., Curtis, S. J., Sinkevicius, K. W., Gludish, D. W., & Kim, C. F. (2008). Stem cell biology in the lung and lung cancers: using pulmonary context and classic approaches. *Cold Spring Harb Symp Quant Biol, 73*, 479-490. doi: 10.1101/sqb.2008.73.036

Ramasamy, S. K., Mailleux, A. A., Gupte, V. V., Mata, F., Sala, F. G., Veltmaat, J. M., . . . Bellusci, S. (2007). Fgf10 dosage is critical for the amplification of epithelial cell progenitors and for the formation of multiple mesenchymal lineages during lung development. *Dev Biol, 307*(2), 237-247. doi: 10.1016/j.ydbio.2007.04.033

Raviv, Stacy, Hawkins, Keenan A., DeCamp, Malcolm M., & Kalhan, Ravi. (2011). Lung Cancer in Chronic Obstructive Pulmonary Disease. *American Journal of Respiratory and Critical Care Medicine, 183*(9), 1138-1146.

Rawlins, E. L., & Hogan, B. L. (2006). Epithelial stem cells of the lung: privileged few or opportunities for many? *Development, 133*(13), 2455-2465. doi: 10.1242/dev.02407

Rawlins, E. L., & Hogan, B. L. (2008). Ciliated epithelial cell lifespan in the mouse trachea and lung. *Am J Physiol Lung Cell Mol Physiol, 295*(1), L231-234. doi: 10.1152/ajplung.90209.2008

Rawlins, E. L., Okubo, T., Xue, Y., Brass, D. M., Auten, R. L., Hasegawa, H., . . . Hogan, B. L. (2009). The role of Scgb1a1+ Clara cells in the long-term maintenance and repair of lung airway, but not alveolar, epithelium. *Cell Stem Cell, 4*(6), 525-534. doi: 10.1016/j.stem.2009.04.002

Regala, R. P., Davis, R. K., Kunz, A., Khoor, A., Leitges, M., & Fields, A. P. (2009). Atypical protein kinase C{iota} is required for bronchioalveolar stem cell expansion and lung tumorigenesis. *Cancer Res, 69*(19), 7603-7611. doi: 10.1158/0008-5472.can-09-2066

Reynolds, S. D., Giangreco, A., Hong, K. U., McGrath, K. E., Ortiz, L. A., & Stripp, B. R. (2004). Airway injury in lung disease pathophysiology: selective depletion of airway stem and progenitor cell pools potentiates lung inflammation and alveolar dysfunction. *Am J Physiol Lung Cell Mol Physiol, 287*(6), L1256-1265. doi: 10.1152/ajplung.00203.2004

Reynolds, S. D., Giangreco, A., Power, J. H., & Stripp, B. R. (2000). Neuroepithelial bodies of pulmonary airways serve as a reservoir of progenitor cells capable of epithelial regeneration. *Am J Pathol, 156*(1), 269-278. doi: 10.1016/s0002-9440(10)64727-x

Reynolds, S. D., Hong, K. U., Giangreco, A., Mango, G. W., Guron, C., Morimoto, Y., & Stripp, B. R. (2000). Conditional clara cell ablation reveals a self-renewing progenitor function of pulmonary neuroendocrine cells. *Am J Physiol Lung Cell Mol Physiol, 278*(6), L1256-1263.

Reynolds, S. D., & Malkinson, A. M. (2010). Clara cell: progenitor for the bronchiolar epithelium. *Int J Biochem Cell Biol, 42*(1), 1-4. doi: 10.1016/j.biocel.2009.09.002

Reynolds, S. D., Reynolds, P. R., Snyder, J. C., Whyte, F., Paavola, K. J., & Stripp, B. R. (2007). CCSP regulates cross talk between secretory cells and both ciliated cells and macrophages of the

conducting airway. *Am J Physiol Lung Cell Mol Physiol, 293*(1), L114-123. doi: 10.1152/ajplung.00014.2007

Rock, J. R., Barkauskas, C. E., Cronce, M. J., Xue, Y., Harris, J. R., Liang, J., . . . Hogan, B. L. (2011). Multiple stromal populations contribute to pulmonary fibrosis without evidence for epithelial to mesenchymal transition. *Proc Natl Acad Sci U S A, 108*(52), E1475-1483. doi: 10.1073/pnas.1117988108

Rock, J. R., Gao, X., Xue, Y., Randell, S. H., Kong, Y. Y., & Hogan, B. L. (2011). Notch-dependent differentiation of adult airway basal stem cells. *Cell Stem Cell, 8*(6), 639-648. doi: 10.1016/j.stem.2011.04.003

Rodin, S. N., & Rodin, A. S. (2000). Human lung cancer and p53: the interplay between mutagenesis and selection. *Proc Natl Acad Sci U S A, 97*(22), 12244-12249. doi: 10.1073/pnas.180320897

Rossi, L., Challen, G. A., Sirin, O., Lin, K. K., & Goodell, M. A. (2011). Hematopoietic stem cell characterization and isolation. *Methods Mol Biol, 750*, 47-59. doi: 10.1007/978-1-61779-145-1_3

Rotter, V. (1983). p53, a transformation-related cellular-encoded protein, can be used as a biochemical marker for the detection of primary mouse tumor cells. *Proc Natl Acad Sci U S A, 80*(9), 2613-2617.

Sachlos, E., Risueno, R. M., Laronde, S., Shapovalova, Z., Lee, J. H., Russell, J., . . . Bhatia, M. (2012). Identification of drugs including a dopamine receptor antagonist that selectively target cancer stem cells. *Cell, 149*(6), 1284-1297. doi: 10.1016/j.cell.2012.03.049

Sajan, M. P., Standaert, M. L., Nimal, S., Varanasi, U., Pastoor, T., Mastorides, S., . . . Farese, R. V. (2009). The critical role of atypical protein kinase C in activating hepatic SREBP-1c and NFkappaB in obesity. *J Lipid Res, 50*(6), 1133-1145. doi: 10.1194/jlr.M800520-JLR200

Salminen, A., Kauppinen, A., & Kaarniranta, K. (2012). Emerging role of NF-kappaB signaling in the induction of senescence-associated secretory phenotype (SASP). *Cell Signal, 24*(4), 835-845. doi: 10.1016/j.cellsig.2011.12.006

Salminen, A., Suuronen, T., Huuskonen, J., & Kaarniranta, K. (2008). NEMO shuttle: a link between DNA damage and NF-kappaB activation in progeroid syndromes? *Biochem Biophys Res Commun, 367*(4), 715-718. doi: 10.1016/j.bbrc.2007.11.189

Santini, R., Vinci, M. C., Pandolfi, S., Penachioni, J. Y., Montagnani, V., Olivito, B., . . . Stecca, B. (2012). HEDGEHOG-GLI Signaling Drives Self-Renewal and Tumorigenicity of Human Melanoma-Initiating Cells. *Stem Cells*. doi: 10.1002/stem.1160

Scarpelli, E. M. (2003). Physiology of the alveolar surface network. *Comp Biochem Physiol A Mol Integr Physiol, 135*(1), 39-104.

Schafer, M., & Werner, S. (2008). Cancer as an overhealing wound: an old hypothesis revisited. *Nat Rev Mol Cell Biol, 9*(8), 628-638. doi: 10.1038/nrm2455

Schaible, B., Schaffer, K., & Taylor, C. T. (2010). Hypoxia, innate immunity and infection in the lung. *Respir Physiol Neurobiol, 174*(3), 235-243. doi: 10.1016/j.resp.2010.08.006

Scheel, C., Eaton, E. N., Li, S. H., Chaffer, C. L., Reinhardt, F., Kah, K. J., . . . Weinberg, R. A. (2011). Paracrine and autocrine signals induce and maintain mesenchymal and stem cell states in the breast. *Cell, 145*(6), 926-940. doi: 10.1016/j.cell.2011.04.029

Schinzel, A. C., Takeuchi, O., Huang, Z., Fisher, J. K., Zhou, Z., Rubens, J., . . . Korsmeyer, S. J. (2005). Cyclophilin D is a component of mitochondrial permeability transition and mediates neuronal cell death after focal cerebral ischemia. *Proc Natl Acad Sci U S A, 102*(34), 12005-12010. doi: 10.1073/pnas.0505294102

Schmuck, K., Ullmer, C., Engels, P., & Lubbert, H. (1994). Cloning and functional characterization of the human 5-HT2B serotonin receptor. *FEBS Lett, 342*(1), 85-90.

Schurch, W., Seemayer, T. A., & Gabbiani, G. (1998). The myofibroblast: a quarter century after its discovery. *Am J Surg Pathol, 22*(2), 141-147.

Scotti, M. L., Bamlet, W. R., Smyrk, T. C., Fields, A. P., & Murray, N. R. (2010). Protein kinase Ciota is required for pancreatic cancer cell transformed growth and tumorigenesis. *Cancer Res, 70*(5), 2064-2074. doi: 10.1158/0008-5472.can-09-2684

Shackleton, M., Vaillant, F., Simpson, K. J., Stingl, J., Smyth, G. K., Asselin-Labat, M. L., . . . Visvader, J. E. (2006). Generation of a functional mammary gland from a single stem cell. *Nature, 439*(7072), 84-88. doi: 10.1038/nature04372

Shu, W., Guttentag, S., Wang, Z., Andl, T., Ballard, P., Lu, M. M., . . . Morrisey, E. E. (2005). Wnt/beta-catenin signaling acts upstream of N-myc, BMP4, and FGF signaling to regulate proximal-distal patterning in the lung. *Dev Biol, 283*(1), 226-239. doi: 10.1016/j.ydbio.2005.04.014

Sime, P. J., Xing, Z., Graham, F. L., Csaky, K. G., & Gauldie, J. (1997). Adenovector-mediated gene transfer of active transforming growth factor-beta1 induces prolonged severe fibrosis in rat lung. *J Clin Invest, 100*(4), 768-776. doi: 10.1172/jci119590

Smith, M. K., Koch, P. J., & Reynolds, S. D. (2012). Direct and indirect roles for beta-catenin in facultative basal progenitor cell differentiation. *Am J Physiol Lung Cell Mol Physiol, 302*(6), L580-594. doi: 10.1152/ajplung.00095.2011

Snyder, Joshua C., Zemke, Anna C., & Stripp, Barry R. (2009). Reparative Capacity of Airway Epithelium Impacts Deposition and Remodeling of Extracellular Matrix. *American Journal of Respiratory Cell and Molecular Biology, 40*(6), 633-642.

Sorokin, Sergei P. (1970). The Cells of the Lungs. *Morphology of Experimental Respriatory Carcinogenesis*, 40.

Steffensen, B., Hakkinen, L., & Larjava, H. (2001). Proteolytic events of wound-healing--coordinated interactions among matrix metalloproteinases (MMPs), integrins, and extracellular matrix molecules. *Crit Rev Oral Biol Med, 12*(5), 373-398.

Stevens, T. (2011). Functional and molecular heterogeneity of pulmonary endothelial cells. *Proc Am Thorac Soc, 8*(6), 453-457. doi: 10.1513/pats.201101-004MW

Stevens, T. P., McBride, J. T., Peake, J. L., Pinkerton, K. E., & Stripp, B. R. (1997). Cell proliferation contributes to PNEC hyperplasia after acute airway injury. *Am J Physiol, 272*(3 Pt 1), L486-493.

Stiernberg, J., Redin, W. R., Warner, W. S., & Carney, D. H. (1993). The role of thrombin and thrombin receptor activating peptide (TRAP-508) in initiation of tissue repair. *Thromb Haemost, 70*(1), 158-162.

Stripp, B. R. (2008). Hierarchical organization of lung progenitor cells: is there an adult lung tissue stem cell? *Proc Am Thorac Soc, 5*(6), 695-698. doi: 10.1513/pats.200801-011AW

Sumen, C., Mempel, T. R., Mazo, I. B., & von Andrian, U. H. (2004). Intravital microscopy: visualizing immunity in context. *Immunity, 21*(3), 315-329. doi: 10.1016/j.immuni.2004.08.006

Sumitran-Holgersson, Suchitra, & Holgersson, Jan. (2001). Endothelial Cells: Immunological Aspects *eLS*: John Wiley & Sons, Ltd.

Takahashi, K., & Yamanaka, S. (2006). Induction of pluripotent stem cells from mouse embryonic and adult fibroblast cultures by defined factors. *Cell, 126*(4), 663-676. doi: 10.1016/j.cell.2006.07.024

Tavazoie, S. F., Alarcon, C., Oskarsson, T., Padua, D., Wang, Q., Bos, P. D., . . . Massague, J. (2008). Endogenous human microRNAs that suppress breast cancer metastasis. *Nature, 451*(7175), 147-152. doi: 10.1038/nature06487

Teisanu, Roxana M., Chen, Huaiyong, Matsumoto, Keitaro, McQualter, Jonathan L., Potts, Erin, Foster, W. Michael, . . . Stripp, Barry R. (2011). Functional Analysis of Two Distinct Bronchiolar Progenitors during Lung Injury and Repair. *American Journal of Respiratory Cell and Molecular Biology, 44*(6), 794-803.

Thomas, A. Q., Lane, K., Phillips, J., 3rd, Prince, M., Markin, C., Speer, M., . . . Loyd, J. E. (2002). Heterozygosity for a surfactant protein C gene mutation associated with usual interstitial

pneumonitis and cellular nonspecific interstitial pneumonitis in one kindred. *Am J Respir Crit Care Med, 165*(9), 1322-1328.

Thomson, Stuart, Buck, Elizabeth, Petti, Filippo, Griffin, Graeme, Brown, Eric, Ramnarine, Nishal, . . . Haley, John D. (2005). Epithelial to Mesenchymal Transition Is a Determinant of Sensitivity of Non–Small-Cell Lung Carcinoma Cell Lines and Xenografts to Epidermal Growth Factor Receptor Inhibition. *Cancer Research, 65*(20), 9455-9462.

Tome, M., Lopez-Romero, P., Albo, C., Sepulveda, J. C., Fernandez-Gutierrez, B., Dopazo, A., . . . Gonzalez, M. A. (2011). miR-335 orchestrates cell proliferation, migration and differentiation in human mesenchymal stem cells. *Cell Death Differ, 18*(6), 985-995. doi: 10.1038/cdd.2010.167

Tompkins, D. H., Besnard, V., Lange, A. W., Keiser, A. R., Wert, S. E., Bruno, M. D., & Whitsett, J. A. (2011). Sox2 activates cell proliferation and differentiation in the respiratory epithelium. *Am J Respir Cell Mol Biol, 45*(1), 101-110. doi: 10.1165/rcmb.2010-0149OC

Tsai, C. C., Su, P. F., Huang, Y. F., Yew, T. L., & Hung, S. C. (2012). Oct4 and nanog directly regulate dnmt1 to maintain self-renewal and undifferentiated state in mesenchymal stem cells. *Mol Cell, 47*(2), 169-182. doi: 10.1016/j.molcel.2012.06.020

Uchida, N., Buck, D. W., He, D., Reitsma, M. J., Masek, M., Phan, T. V., . . . Weissman, I. L. (2000). Direct isolation of human central nervous system stem cells. *Proc Natl Acad Sci U S A, 97*(26), 14720-14725. doi: 10.1073/pnas.97.26.14720

Ueha, Satoshi, Shand Francis, H. W., & Matsushima, Kouji. (2012). Cellular and molecular mechanisms of chronic inflammation-associated organ fibrosis. *Frontiers in Immunology, 3*.

Vajkoczy, P., Ullrich, A., & Menger, M. (2000). Intravital fluorescence videomicroscopy to study tumor angiogenesis and microcirculation. *Neoplasia, 2*, 53-61.

Van Arnam, J. S., Herzog, E., Grove, J., Bruscia, E., Ziegler, E., Swenson, S., & Krause, D. S. (2005). Engraftment of bone marrow-derived epithelial cells. *Stem Cell Rev, 1*(1), 21-27. doi: 10.1385/scr:1:1:021

van der Flier, L. G., & Clevers, H. (2009). Stem cells, self-renewal, and differentiation in the intestinal epithelium. *Annu Rev Physiol, 71*, 241-260. doi: 10.1146/annurev.physiol.010908.163145

van Oijen, M. G., & Slootweg, P. J. (2000). Gain-of-function mutations in the tumor suppressor gene p53. *Clin Cancer Res, 6*(6), 2138-2145.

Van Vranken, B. E., Romanska, H. M., Polak, J. M., Rippon, H. J., Shannon, J. M., & Bishop, A. E. (2005). Coculture of embryonic stem cells with pulmonary mesenchyme: a microenvironment that promotes differentiation of pulmonary epithelium. *Tissue Eng, 11*(7-8), 1177-1187. doi: 10.1089/ten.2005.11.1177

Varkey, M., Ding, J., & Tredget, E. E. (2011). Differential collagen-glycosaminoglycan matrix remodeling by superficial and deep dermal fibroblasts: potential therapeutic targets for hypertrophic scar. *Biomaterials, 32*(30), 7581-7591. doi: 10.1016/j.biomaterials.2011.06.070

Vaseva, A. V., Marchenko, N. D., Ji, K., Tsirka, S. E., Holzmann, S., & Moll, U. M. (2012). p53 Opens the Mitochondrial Permeability Transition Pore to Trigger Necrosis. *Cell, 149*(7), 1536-1548. doi: 10.1016/j.cell.2012.05.014

Veis, A., & Anesey, J. (1965). Modes of intermolecular cross-linking in mature insoluble collagen. *J Biol Chem, 240*(10), 3899-3908.

Ventura, J. J., Tenbaum, S., Perdiguero, E., Huth, M., Guerra, C., Barbacid, M., . . . Nebreda, A. R. (2007). p38alpha MAP kinase is essential in lung stem and progenitor cell proliferation and differentiation. *Nat Genet, 39*(6), 750-758. doi: 10.1038/ng2037

Vermeulen, L., De Wilde, G., Van Damme, P., Vanden Berghe, W., & Haegeman, G. (2003). Transcriptional activation of the NF-kappaB p65 subunit by mitogen- and stress-activated protein kinase-1 (MSK1). *EMBO J, 22*(6), 1313-1324. doi: 10.1093/emboj/cdg139

Vestweber, D. (2012). Novel insights into leukocyte extravasation. *Curr Opin Hematol, 19*(3), 212-217. doi: 10.1097/MOH.0b013e3283523e78
Vousden, K. H., & Lane, D. P. (2007). p53 in health and disease. *Nat Rev Mol Cell Biol, 8*(4), 275-283. doi: 10.1038/nrm2147
Wakiyama, M., & Yokoyama, S. (2010). MicroRNA-mediated mRNA deadenylation and repression of protein synthesis in a mammalian cell-free system. *Prog Mol Subcell Biol, 50*, 85-97. doi: 10.1007/978-3-642-03103-8_6
Walter, Nicholas, Collard, Harold R., & King, Talmadge E. (2006). Current Perspectives on the Treatment of Idiopathic Pulmonary Fibrosis. *Proceedings of the American Thoracic Society, 3*(4), 330-338.
Wang, H. M., Bodenstein, M., & Markstaller, K. (2008). Overview of the pathology of three widely used animal models of acute lung injury. *Eur Surg Res, 40*(4), 305-316. doi: 10.1159/000121471
Wang, X., Ouyang, H., Yamamoto, Y., Kumar, P. A., Wei, T. S., Dagher, R., . . . McKeon, F. (2011). Residual embryonic cells as precursors of a Barrett's-like metaplasia. *Cell, 145*(7), 1023-1035. doi: 10.1016/j.cell.2011.05.026
Warburton, D., El-Hashash, A., Carraro, G., Tiozzo, C., Sala, F., Rogers, O., . . . Jesudason, E. (2010). Lung organogenesis. *Curr Top Dev Biol, 90*, 73-158. doi: 10.1016/s0070-2153(10)90003-3
Weber, C. E., Li, N. Y., Wai, P. Y., & Kuo, P. C. (2012). Epithelial-mesenchymal transition, TGF-beta, and osteopontin in wound healing and tissue remodeling after injury. *J Burn Care Res, 33*(3), 311-318. doi: 10.1097/BCR.0b013e318240541e
Wei, J., Zaika, E., & Zaika, A. (2012). p53 Family: Role of Protein Isoforms in Human Cancer. *J Nucleic Acids, 2012*, 687359. doi: 10.1155/2012/687359
Weiss, D. J., Bertoncello, I., Borok, Z., Kim, C., Panoskaltsis-Mortari, A., Reynolds, S., . . . Prockop, D. J. (2011). Stem cells and cell therapies in lung biology and lung diseases. *Proc Am Thorac Soc, 8*(3), 223-272. doi: 10.1513/pats.201012-071DW
Weisz, L., Oren, M., & Rotter, V. (2007). Transcription regulation by mutant p53. *Oncogene, 26*(15), 2202-2211. doi: 10.1038/sj.onc.1210294
Willis, B. C., & Borok, Z. (2007). TGF-beta-induced EMT: mechanisms and implications for fibrotic lung disease. *Am J Physiol Lung Cell Mol Physiol, 293*(3), L525-534. doi: 10.1152/ajplung.00163.2007
Willis, B. C., Liebler, J. M., Luby-Phelps, K., Nicholson, A. G., Crandall, E. D., du Bois, R. M., & Borok, Z. (2005). Induction of epithelial-mesenchymal transition in alveolar epithelial cells by transforming growth factor-beta1: potential role in idiopathic pulmonary fibrosis. *Am J Pathol, 166*(5), 1321-1332.
Winbanks, C. E., Darby, I. A., Kelynack, K. J., Pouniotis, D., Becker, G. J., & Hewitson, T. D. (2011). Explanting is an ex vivo model of renal epithelial-mesenchymal transition. *J Biomed Biotechnol, 2011*, 212819. doi: 10.1155/2011/212819
Windoffer, R., Borchert-Stuhltrager, M., & Leube, R. E. (2002). Desmosomes: interconnected calcium-dependent structures of remarkable stability with significant integral membrane protein turnover. *J Cell Sci, 115*(Pt 8), 1717-1732.
Wong, A. P., Keating, A., Lu, W. Y., Duchesneau, P., Wang, X., Sacher, A., . . . Waddell, T. K. (2009). Identification of a bone marrow-derived epithelial-like population capable of repopulating injured mouse airway epithelium. *J Clin Invest, 119*(2), 336-348. doi: 10.1172/jci36882
Wong, A. P., Keating, A., & Waddell, T. K. (2009). Airway regeneration: the role of the Clara cell secretory protein and the cells that express it. *Cytotherapy, 11*(6), 676-687. doi: 10.3109/14653240903313974
Wu, W. S. (2006). The signaling mechanism of ROS in tumor progression. *Cancer Metastasis Rev, 25*(4), 695-705. doi: 10.1007/s10555-006-9037-8

Wu, Y. C., Chen, C. H., Mercer, A., & Sokol, N. S. (2012). let-7-Complex MicroRNAs Regulate the Temporal Identity of Drosophila Mushroom Body Neurons via chinmo. *Dev Cell, 23*(1), 202-209. doi: 10.1016/j.devcel.2012.05.013

Xiao, Q., & Ge, G. (2012). Lysyl Oxidase, Extracellular Matrix Remodeling and Cancer Metastasis. *Cancer Microenviron*. doi: 10.1007/s12307-012-0105-z

Yanagi, S., Kishimoto, H., Kawahara, K., Sasaki, T., Sasaki, M., Nishio, M., . . . Suzuki, A. (2007). Pten controls lung morphogenesis, bronchioalveolar stem cells, and onset of lung adenocarcinomas in mice. *J Clin Invest, 117*(10), 2929-2940. doi: 10.1172/jci31854

Yang, Y., Iwanaga, K., Raso, M. G., Wislez, M., Hanna, A. E., Wieder, E. D., . . . Kurie, J. M. (2008). Phosphatidylinositol 3-kinase mediates bronchioalveolar stem cell expansion in mouse models of oncogenic K-ras-induced lung cancer. *PLoS One, 3*(5), e2220. doi: 10.1371/journal.pone.0002220

Yang, Y., Xia, F., Hermance, N., Mabb, A., Simonson, S., Morrissey, S., . . . Kelliher, M. A. (2011). A cytosolic ATM/NEMO/RIP1 complex recruits TAK1 to mediate the NF-kappaB and p38 mitogen-activated protein kinase (MAPK)/MAPK-activated protein 2 responses to DNA damage. *Mol Cell Biol, 31*(14), 2774-2786. doi: 10.1128/mcb.01139-10

Yao, Z., Fenoglio, S., Gao, D. C., Camiolo, M., Stiles, B., Lindsted, T., . . . Sordella, R. (2010). TGF-beta IL-6 axis mediates selective and adaptive mechanisms of resistance to molecular targeted therapy in lung cancer. *Proc Natl Acad Sci U S A, 107*(35), 15535-15540. doi: 10.1073/pnas.1009472107

Yatabe, Y., Kosaka, T., Takahashi, T., & Mitsudomi, T. (2005). EGFR mutation is specific for terminal respiratory unit type adenocarcinoma. *Am J Surg Pathol, 29*(5), 633-639.

Yeager, M. E., Frid, M. G., & Stenmark, K. R. (2011). Progenitor cells in pulmonary vascular remodeling. *Pulm Circ, 1*(1), 3-16. doi: 10.4103/2045-8932.78095

Yoshida, T., Okamoto, I., Okamoto, W., Hatashita, E., Yamada, Y., Kuwata, K., . . . Nakagawa, K. (2010). Effects of Src inhibitors on cell growth and epidermal growth factor receptor and MET signaling in gefitinib-resistant non-small cell lung cancer cells with acquired MET amplification. *Cancer Sci, 101*(1), 167-172. doi: 10.1111/j.1349-7006.2009.01368.x

Zhang, K., Rekhter, M. D., Gordon, D., & Phan, S. H. (1994). Myofibroblasts and their role in lung collagen gene expression during pulmonary fibrosis. A combined immunohistochemical and in situ hybridization study. *Am J Pathol, 145*(1), 114-125.

Zhang, Y., Goss, A. M., Cohen, E. D., Kadzik, R., Lepore, J. J., Muthukumaraswamy, K., . . . Morrisey, E. E. (2008). A Gata6-Wnt pathway required for epithelial stem cell development and airway regeneration. *Nat Genet, 40*(7), 862-870. doi: 10.1038/ng.157